SOIL-WATER CHARACTERISITIC CURVES AND

SHRINKAGE BEHAVIOUR OF HIGHLY PLASTIC CLAYS:

AN EXPERIMENTAL INVESTIGATION

MOHD YUHYI MOHD TADZA

Geoenvironmental Research Centre

Cardiff School of Engineering

Cardiff University

Thesis submitted in candidature for the degree of Doctor of Philosophy at Cardiff University

July 2011

UMI Number: U585482

UMI

Dissertation Publishing

ProQuest

DECLARATION

This work has not previously been accepted in substance for any degree and is not concurrently submitted in candidature for any degree.

Signed .... (MOHD YUHYI MOHD TADZA)

Date ...... 29 JUNE 2011 ....

STATEMENT 1

This thesis is being submitted in partial fulfillment of the requirements for the degree of Doctor of Philosophy (PhD).
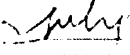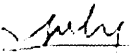
Signed .... (MOHD YUHYI MOHD TADZA)

Date ...... 29 JUNE 2011 ....

STATEMENT 2

This thesis is the result of my own independent work/investigation, except where otherwise stated. Other sources are acknowledged by explicit references.

Signed .... (MOHD YUHYI MOHD TADZA)

Date ...... 29 JUNE 2011 ....

STATEMENT 3

I hereby give consent for my thesis, if accepted, to be available for photocopying and for inter-library loan, and for the title and summary to be made available to outside organisations.

Signed .... (MOHD YUHYI MOHD TADZA)

Date ...... 29 JUNE 2011 ....

Knowledge is the most noble talent, the most magnificent degree, the most splendid object of pride, and the most valuable form of merchandise, since it is the means by which to arrive at the realization and affirmation of the Oneness of the Lord of All the Worlds [tawhid Rabb al- 'alamin], and belief in His Prophets and Messengers (may Allah's blessings be upon them all).

"No amount of guilt can change the past and no amount of worrying can change the future. Go easy on yourself, for the outcome of all affairs is determined by Allah's decree. If something is meant to go elsewhere, it will never come your way but if it is yours by destiny, then it cannot flee from you" [Sayyidina Umar Ibn al-Khattab r.a.]

ACKNOWLEDGEMENTS

Abstract

Highly plastic clays are increasingly used in many countries for various geotechnical and geoenvironmental applications. Bentonites are used as barrier and backfilling materials in high-level toxic waste repositories and as a key component of land-fill liner systems for the near surface storage of intermediate and low-level toxic wastes. In some cases, in an attempt to develop low cost technologies kaolinite-rich soils serve as the undisturbed clayey barrier and mineral liner. Studies concerning changes in the water content and the void ratio of clays as affected by a change in the soil suction are extremely crucial for long-term assessment of the engineering behaviour of clays. This thesis experimentally investigated the changes in the water content and the void ratio of initially slurried highly plastic clays under zero applied stress during the drying process, changes in the water content of compacted unsaturated clay specimens during the wetting process under zero applied stress for laterally confined and free swelling conditions, and the wetting behaviour of heavily compacted bentonite specimens under confined condition.

In total three clays were used, namely MX80 bentonite, Yellow bentonite, and Speswhite kaolin. Several laboratory techniques, namely centrifuge, axis-translation, vapour equilibrium, osmotic and chilled-mirror dew-point techniques were used to establish the suction-water content soil-water characteristic curves (SWCCs). The shrinkage paths of the clays were established from Clod tests and wax method. The suction-water content SWCCs in conjunction with the Clod test results enabled establishing the suction-degree of saturation SWCCs and determination of the air-entry values (AEVs). The AEVs of the clays were also determined based on the chemical analyses of Polyethylene Glycol (PEG) solutions and the applied suctions in the osmotic tests. Degradation of PEG molecules and semipermeable membranes were studied using Fourier Transform Infrared (FTIR) spectroscopy and Atomic Force Microscopy (AFM), respectively. Isochoric (constant volume) swelling pressure tests were carried out on compacted bentonite specimens using deionised water. Additionally, a newly developed suction controlled oedometer was used to study the swelling pressure and the water uptake capacities of heavily compacted bentonites under confined conditions. Microstructural changes of compacted bentonites were studied using Environmental Scanning Electron Microscope. X-Ray Diffraction technique was used to monitor the changes in the c-axis spacing of clay specimens equilibrated at several applied suctions. Applications of the Gouy-Chapman diffuse double layer theory and the van der Waals attractive pressure theory in predicting the drying and wetting suction-water content SWCCs were explored. One-dimensional wetting model (Richard's equation) was used to evaluate the elapsed time versus water content relationships for the clays.

Chemical analyses of PEG solutions after the osmotic tests showed a clear lack of equalisation of the osmotic suctions due to the expelled and the retained salts on either side of semipermeable membranes. A majority of the salts were found to be retained within the clays during the osmotic tests. The AEVs of the clays determined based on the suction-degree of saturation SWCCs and that from the total suction equilibrium in the osmotic tests were found to be similar. The FTIR studies did not indicate any degradation of PEG molecules. The AFM studies of membranes revealed alterations of the pore-size during the tests that possibly lead to an intrusion of PEG into the bentonite specimens. Both qualitative and in some cases quantitative agreements were noted between the experimental suction-water content SWCCs and those predicted from the physico-chemical theories.

[I]

TABLE OF CONTENTS

[III]

CHAPTER 4 – EXPERIMENTAL METHODS

CHAPTER 5 – DRYING SOIL-WATER CHARACTERISTIC CURVES FROM SLURRY CONDITION

CHAPTER 6 – OSMOTIC SUCTION EQUILIBRIUM IN OSMOTIC TESTS

CHAPTER 9 – SUCTION-WATER CONTENT SWCCs FROM THEORETICAL CONSIDERATIONS

LIST OF FIGURES

CHAPTER 4 – EXPERIMENTAL METHODS

CHAPTER 5 – DRYING SOIL-WATER CHARACTERISTIC CURVES

CHAPTER 6 – OSMOTIC SUCTION EQUILIBRIUM IN OSMOTIC TESTS

[XI]

CHAPTER 7 – AIR-ENTRY VALUES FROM DRYING SWCCs AND SHRINKAGE CURVES

CHAPTER 8 – EFFECTS OF COMPACTION DENSITY & CONFINING CONDITIONS ON WETTING BEHAVIOUR

CHAPTER 9 – SUCTION-WATER CONTENT SWCCs FROM THEORETICAL CONSIDERATIONS

[XIV]

LIST OF TABLES

CHAPTER 7 – AIR-ENTRY VALUES FROM DRYING SWCCs AND SHRINKAGE CURVES

CHAPTER 8 – EFFECTS OF COMPACTION DENSITY & CONFINING CONDITIONS ON WETTING BEHAVIOUR

CHAPTER 9 – SUCTION-WATER CONTENT SWCCs FROM THEORETICAL CONSIDERATIONS

LIST OF ABBREVIATIONS

AEV	Air-entry value
AFM	Atomic force microscope
BET	Brunauer-Emmett-Teller
CEC	Cation exchange capacity
EGME	Ethylene glycol monoethyl ether
ESEM	Environmental scanning electron microscope
FEG	Field emission gun
FTIR	Fourier transform infrared
GSE	Gaseous secondary electron detector
HLW	High level waste
ICP-OES	Inductively couple plasma – Optical emission spectroscopy
MEK	Methyl ethyl ketone
MWCO	Molecular weight cut-off
NMR	Nuclear magnetic resonance
PEG	Polyethylene glycol
PES	Polysulphonate
PVAc	Polyvinyl Acetate
RC	Regenerated cellulose
RH	Relative humidity
SEM	Scanning electron microscope
SWCC	Soil-water characteristic curve
XPS	X-ray photoelectron spectroscopy
XRD	X-ray diffraction

LIST OF SYMBOLS

CHAPTER 2 – LITERATURE REVIEW

d_{PEG}	Hydrodynamic diameter in nm
MW	Molecular weight
u_a	Air pressure
u_w	Water pressure
π_{solute}	Osmotic suction due to solution of a known solute
π_{PEG}	Osmotic suction due to concentration of PEG solution
π_{salt}^{1}	Osmotic suction due to expelled cation concentrations
π_{salt}^{2}	Osmotic suction due to retained cation concentrations
S_r	Degree of saturation (%)

CHAPTER 3 – PROPERTIES OF CLAYS

G_s	Specific gravity of soil solid
w_L	Liquid limit (%)
w_P	Plastic limit (%)
w_S	Shrinkage limit (%)
S	Specific surface area (m^2/g)
B	Cation exchange capacity (meq/100g)
SL	Shrinkage limit (%)
V	Volume of wet specimen (cm^3)
V_d	Volume of dry soil
ρ_w	Density of water

[XVII]

m_s Mass of dry soil

CHAPTER 4 – EXPERIMENTAL METHODS

ψ Suction of soil

r_1 Radial distance to the mid-point of the soil specimen

r_2 Radial distance to the free water surface

ω Angular velocity

ρ_w Density of water

S Applied suction

c Concentration of PEG solution (g PEG/g of water)

RH Relative humidity

u_v Partial pressure of water vapour

u_{v0} Saturation pressure of pure water vapour

v_{w0} Specific volume of water (m^3/kg)

ω_r Molecular mass of water vapour (18.016 kg/kmol)

R Universal gas constant (8.31432 J mol^{-1} K^{-1})

T Absolute temperature in Kelvin

M_{clod} Total mass of Clod

M_{soil} Total mass of soil specimen

M_{glue} Mass of glue

V_{clod} Total volume of the Clod

V_{glue} Volume of glue

V_{soil} Volume of soil specimen

M_{air} Mass of the Clod in air

M_{water} Mass of the Clod in water

M_{glue}	Mass of glue
g_f	Mass fraction of glue
ρ_{glue}	Density of glue
w_{soil}	Water content of the soil specimen (%)
M_d	Dry mass of the soil specimen
ρ_{dsoil}	Dry density of soil specimen
e_{soil}	Void ratio of soil specimen

CHAPTER 6 – OSMOTIC SUCTION EQUILIBRIUM IN OSMOTIC TESTS

π	Osmotic suction (kPa)
R	Universal gas constant ($8.32 \ l \cdot kPa \cdot mol^{-1} \cdot K^{-1}$)
T	Absolute temperature (K)
m	Molarity of the pore solution (mol/l)
i	van't Hoff factor

CHAPTER 7 – AIR-ENTRY VALUES FROM DRYING SWCCs AND SHRINKAGE CURVES

w	Gravimetric water content (%)
e	Void ratio
e_{AEV}	Void ratio at air-entry (desaturation point)
e_p	Void ratio at plastic limit
e_s	Void ratio at shrinkage limit
e_0	Void ratio at no shrinkage
β	Slope parameter
φ	Slope of the saturation line

a Model parameter

ξ Model parameter

ζ Model parameter

CHAPTER 9 – SUCTION-WATER CONTENT SWCCs FROM THEORETICAL CONSIDERATIONS

D Diffusivity (m^2/s)

Θ_w Water content (%)

Θ_{wi} Initial water content (%)

x Distance of flow (m)

Θ_s Equilibrium water content (%)

Θ_{w+1}, Θ_{w+2} Consequent water content changes at time, t_1 and t_2

p Swelling pressure (N/m^2)

n_0 Ionic concentration of bulk fluid (ions/m^3)

u Dimensionless midplane potential

T Absolute temperature (K)

k Boltzmann's constant ($=1.38 \times 10^{-23}$ J/K)

ξ Distance function

y Nondimensional potential function at the clay surface

x Distance from the clay surface

z Nondimensional potential function at the surface ($x = 0$)

B Cation exchange capacity (meq/100g)

S Total specific surface area in (m^2/g)

ε_0 Permittivity of vacuum ($= 8.8542 \times 10^{-12}$ C^{2}J^{-1}m^{-1})

D Dielectric constant of bulk fluid ($= 80.4$ for water)

K Diffuse double layer parameter (1/m)

e'	Elementary electrical charge ($= 1.602 \times 10^{-19}$ C)
v	Weighted average valency
e	Void ratio
d	Half distance between two parallel clay platelets
ρ_w	Density of the bulk fluid
F_A	Attractive pressure (N/m^2)
δ	Thickness of the clay platelet
A	Hamaker constant (6×10^{-20} J for water as the bulk fluid)
ψ_m	Matric suction of soil (kPa)
π	Ratio of the circumference divided by diameter ($=3.142$)
t	Thickness of the clay platelet

CHAPTER 1

INTRODUCTION

1.1 Background

In recent decades, rapid industrial development and an increasing number of chemical industries have lead to the generation of substantial amount of hazardous and municipal wastes. In the past, hazardous and municipal wastes were commonly disposed without the consideration of potential impacts on public health and the environment. Improper disposal practices and management as well as accidental spills have created various contaminated sites throughout the world (Rowe et al., 1997; Sharma and Reddy, 2004). In some cases, the contamination was severe and all residents of that vicinity had to be evacuated and the affected area was finally isolated (Beck, 1979). The onset of such problems raised environmental concern and initiated the involvement of geotechnical engineers in environmental matters.

Geoenvironmental engineering covers the aspect of contaminated site remediation (i.e. closure and post treatment of existing sites) and the prevention of future contaminated sites. The design and construction of safer disposal facilities in engineered waste containment facilities, surface impoundments, lagoons, ponds and sanitary landfills help in minimizing environmental impact. For this purpose, highly plastic clays in various forms, such as loose powder, compacted at low dry densities and initially slurried clays have been used for the

1

construction of liners (viz. low-permeability natural clay liners and geosynthetic clay liners), caps, isolation walls and backfill material used at landfills and other types of waste disposal sites (Bouazza and Bowders, 2010). Construction of such engineered systems are essential in minimizing the migration of contaminants of chemical species from both industrial and municipal waste disposal facilities to the general groundwater reservoirs, removing heavy metals to improve the bioavailability of contaminated soils and ponds, controlling moisture and percolation, promoting surface runoff, minimizing erosion, controlling gas emissions and odours (Peavy et al., 1987; Rowe et al., 1997; Oweis and Khera, 1998; Sharma and Reddy, 2004; Benson, 2005; Cruz-Guzman et al. 2006). Bentonites are the generally preferred material for constructing engineered barriers. In some cases, naturally occurring fine grained soils containing kaolinite serve as the undisturbed clayey barriers (Yang and Barbour, 1992). Additionally, in an attempt to develop low cost technologies, locally available kaolinite-rich soils are preferred as the mineral liners.

Another concern that emerged in recent years was the ultimate disposal of high-level nuclear and radioactive wastes, which can remain active after thousands of years (Daniel, 1993). Without appropriate management and disposal practices, these radioactive wastes can adversely impact human health and the environment. The proposed backfill materials may be subjected to high temperature and pressure conditions and are expected to undergo various mechanical, chemical and biological response and interactions (Sharma and Reddy, 2004; Pusch and Yong, 2005; Pusch 2008).

Deep geological disposal is, at present, one of the preferred alternatives for the safe disposal of high level nuclear waste (HLW) (Cutoiu 2003; Villar and Lloret, 2004; Pusch and Yong, 2005; Quirk 2006). Highly compacted bentonite and bentonite-sand mixtures with dry

densities greater than 1.2 Mg/m^3 have been proposed as buffers or sealing elements surrounding copper canisters containing HLW. Bentonites have been considered due to their low permeability, high sorption capacity, self sealing characteristics, and durability in a natural environment (Pusch, 1982; Muller-Vonmoos et al., 1994; Romero, 1999; Pusch and Yong, 2005; Plötze et al. 2007). Once in operation, the host rock is expected to serve as the source of hydration for the compacted bentonites and also acts as confinement against volume change due to the hydration process. The stress convergence of the host rock is important as well as the pressure-void ratio relationship of the compacted saturated bentonite (Tripathy and Schanz, 2004). On the other hand, a bentonite buffer in close proximity to the canister will initially dry and shrink due to receiving heat induced by the canister. Due to the complexity of the repository, interests on the long term behaviour of the bentonite buffers have increasingly gained recognition (Thomas et al., 2003; Villar and Lloret, 2004; Pusch and Yong, 2005).

The change in the water content due to a change in temperature and suction are crucial issues in geoenvironmetal engineering (Villar and Lloret, 2004; Delage and Romero, 2008; Peron et al., 2009). Most problems associated with the behaviour of clay liners and backfill materials are related to the volume change (i.e. the shrinkage and swelling processes) due to changes in the water content (Delage and Romero, 2008; Abuel-Naga and Bouazza, 2010). Drying of soils and the formation of desiccation cracks strongly affect the permeability and may compromise the integrity of clay buffers (Peron et al., 2009). The drying and wetting behaviour (i.e. soil–water characteristic curves, SWCCs) of clays have been extensively studied in the past (Croney and Coleman, 1954; Fleureau et al., 1993; Barbour, 1998; Delage et al., 1998; Marcial et al., 2002). These studies have provided useful information for engineering analyses (Barbour, 1998).

The shrinkage behaviour of highly plastic clays have shown to provide useful information for quantitative assessment of the hydraulic conductivity and shear strength of unsaturated soils (Fleureau et al., 1993; Tripathy et al., 2002; Krosley et al., 2003; Peron et al., 2007). The volume change behaviour of soils due to an increase in suction and net normal stress are usually similar until the air-entry value (AEV) (Fredlund and Rahardjo, 1993). Most commonly, the AEVs of highly plastic clays are less distinct in the drying suction-water content SWCCs. On the other hand, establishing the suction-degree of saturation SWCCs and determination of AEVs require determination of both the water content and the void ratio of soils at each applied suctions. This process is cumbersome and time consuming. Possible errors owing to testing multiple specimens can be eliminated by using a single specimen in Clod test to trace the entire water content-void ratio shrinkage paths of soils (Krosley et al., 2003). Furthermore, Kim et al. (2002) and Cornelis et al. (2006) have shown that the shrinkage paths of soils can be represented by smooth curves using several parametric models. The shrinkage paths in conjunction with the drying suction-water content SWCCs can be used for establishing the suction-degree of saturation SWCCs and further the AEVs of soils can be determined.

There are several methods available currently to apply matric suction in soils. Pressure plate tests and osmotic tests are commonly used. Aitchison (1965) stated that the ionic concentrations of the reference fluid and that of the pore-water of soils must be equal for applying and measuring matric suction. It is generally assumed that the osmotic suctions of the reference fluid and that of the soil tested in pressure plate and osmotic tests are equal. However, this aspect has not been investigated in the past.

For applying matric suctions higher than 1.5 MPa in the osmotic tests, problems related to the intrusion of Polyethylene glycol (PEG) into soils specimens have been reported (Williams and Shaykewich, 1969; Delage and Cui, 2008b). It has been hypothesized that the intrusion of PEG into soil specimens occurs primarily due to failure of semipermeable membranes in restricting the passage of PEG molecules and degradation of PEG with elapsed time (Han, et al., 1995; Tarantino and Mongiovi, 2000; Delage and Cui, 2008b). However, no investigations have been carried out to support these hypotheses.

Several researchers in the past have demonstrated that soil structure, type of soil, mineralogy, density, initial water content, stress history, method of compaction and confining stress have significant influence on the SWCCs (Tinjum et al. 1997; Vanapalli et al. 1999; Lu and Likos, 2004; Thu et al. 2007). The effect of initial dry density on the wetting SWCC of clays has not been fully explored (Delage et al., 1998; Yahia-Aissa et al., 2000; Ye et al., 2010). Similarly, the effects of different confining conditions on the wetting behaviour of clays have not been fully explored.

The volume change behaviour of fine grained soil during drying and wetting is influenced by the physico-chemicals forces (Bolt 1956, Sidharan & Jayadeva 1982; Mitchell, 1993; Tripathy and Schanz, 2007; Schanz and Tripathy, 2009). These studies have shown that the diffuse double layer plays a significant role in controlling the swelling and compressibility behaviour of expanding clay minerals. On the other hand, the long-range van der Waals attractive pressure was found to be more dominant in the case of nonexpanding clay minerals (Rao and Sridharan, 1985). The applicability of the diffuse double layer theory and the attractive pressure theory in the assessments of wetting and drying suction-water content SWCCs of highly plastic clays have not been explored in detail.

5

Apart from the physico-chemical forces, the microstructural arrangement of the clay particles and frictional forces are also important in controlling the behaviour of soils (Griffiths & Joshi 1989, Mitchell, 1993; Saiyouri, et al., 2000; Delage et al., 2006; Pusch and Yong, 2005). The microstructures of soils are usually studied by Scanning Electron Microscopy (SEM) and Xray diffraction (XRD) technique. Microstructural changes during the drying and wetting processes are usually studied using Environmental Scanning Electron Microscope (ESEM) qualitatively, whereas quantitative variations in the c-axis spacing are studied using the XRD technique. The use of XRD technique enabled exploring the crystalline swelling of highly plastic clays (Grim, 1968; Saiyouri et al., 2000; Delage et al., 2006).

The focus of this study was to develop an experimental understanding of the water absorption, desorption and the shrinkage behaviour of highly plastic clays. In addition, the applicability of various available theories on the absorption and desorption behaviour is explored. The soil-water characteristic curves of clays with different mineralogical background (viz. kaolinite and montmorillonite) and for various testing conditions are presented. The understanding of the behaviour of unsaturated highly plastic clays is crucial for assessing their long-term performance as liners and backfill materials (Delage and Romero, 2008). Desiccation cracks and thermal effects are crucial for assessing the water content changes and volume change behaviour of these materials; however, these aspects are beyond the scope of the current study.

A detailed experimental programme was planned and extensive laboratory scale tests were carried out. The study includes wetting and drying SWCC tests using various available laboratory methods, volume measurements, swelling pressure development tests, microstructural investigation and applicability of currently available physico-chemical

theories for assessing the suction-water content SWCCs of highly plastic clays. Three clays of different properties and mineralogical background were chosen in this study, a sodium-rich MX80 bentonite, a divalent-rich Yellow bentonite and Speswhite kaolin. The three clays were selected in this study due to the fact that the clays were commonly used as reference materials in waste disposal facilities as well as for controlling and measuring suction in laboratory (Thomas et al., 2003; Villar and Lloret, 2004; Pusch and Yong, 2005; Koch, 2007; Tarantino et al., 2011). The different properties and mineralogical background of these clays will hope to provide a broad understanding of the absorption, desorption and shrinkage behaviour of highly plastic clays.

1.2 Research objectives

The primary objectives of this research were as follows: (*i*) to determine the drying suction-water content SWCCs of clays from initially saturated slurry conditions at zero external stress, (*ii*) to establish the suction-void ratio SWCCs and the degree of saturation SWCCs of the clays and further determine the air-entry values, (*iii*) to develop a new suction controlled oedometer (*iv*) to determine the wetting suction-water content SWCCs of compacted clays under various confining conditions at zero external stress and (*v*) to explore the applicability of various physico-chemical theories for establishing the suction-water content SWCCs of highly plastic clays. For the latter, the Gouy-Chapman diffuse double layer theory and the van der Waals attractive pressure theory will be used.

1.3 Thesis overview

The thesis is divided into ten consecutive chapters.

CHAPTER 2 presents a detailed review of literature pertaining to the studies undertaken. The chapter covers a brief review on the applications of clays, mineralogy and structural unit of clays, microstructure of clays, clay-water interaction and osmotic efficiency. The concept of soil suction is presented later, followed by suction measurements and control techniques. A review of suction equilibrium in the osmotic tests, the mechanisms controlling suction in osmotic tests, the drying and wetting soil-water characteristic curves, volume measurements and the determination of the air-entry values are also presented. The chapter also presents a review of swelling pressure measurements of compacted clays.

CHAPTER 3 presents and discusses the physical and chemical properties of the clays used in this study and the methods adopted for determining the properties of the clays. The physical properties determined include specific gravity, particle size distribution, minerals composition using X-ray diffraction (XRD) technique, hygroscopic water content, Atterberg limits, and determination of both external and total specific surface areas. The chapter also presents the chemical properties of the clays. The cation exchange capacities, (CEC) of the clays were determined using standard laboratory procedure.

CHAPTER 4 outlines the experimental methodologies adopted and the devices used in this study. This chapter covers the procedure adopted for preparing saturated slurried specimens and compacted specimens of the clays. Various methods used for measuring and applying suction, such as chilled-mirror dew-point, centrifuge, axis-translation, vapour equilibrium, and osmotic techniques are presented briefly. Volume measurements methods, such as Clod and wax tests are also explained. This chapter presents the description of a newly developed suction (vapour) controlled oedometer for multistep wetting and swelling pressure tests under confined condition. Brief descriptions of several devices used in this study, such as

8

Environmental Scanning Electron Microscope (ESEM), Xray Diffraction (XRD), Inductively

Couple Plasma Optical Emission Spectrometry (ICP-OES), Atomic Force Microscope (AFM)

and Fourier Transform Infrared (FTIR) are also presented.

CHAPTER 5 presents the drying suction-water content SWCCs of the three clays at zero

external stress. The drying tests were carried out from initially saturated condition using

centrifuge, axis-translation, vapour equilibrium and osmotic techniques to establish the

suction-water content SWCCs covering suction range of 0.007 to 300 MPa. The water

content versus suction relationships obtained from chilled-mirror dew-point technique are

also presented and compared with the drying suction-water content SWCCs.

CHAPTER 6 presents the osmotic suction equilibration on either side of the semipermeable

membranes in the osmotic tests. The influences of cations expulsion on the drying suction-

water SWCCs were determined by measuring chemical compositions of the expelled pore

fluid in PEG solutions using ICP-OES. The osmotic suctions corresponding to the expelled

cations were then calculated using van't Hoff's equation. The effects of these osmotic

suctions on the applied suctions were evaluated. The AEVs of the clays were determined on

the basis of total suction equilibrium on either side of the semipermeable membrane.

Additionally, the chapter presents investigation conducted on the factors influencing the

intrusion of PEG molecules into clay specimens during osmotic tests. Atomic force

microscopy (AFM) was used to investigate the pore-size of molecular weight cut-off

(MWCO) 14000 and MWCO 3500 semipermeable membranes before and after the osmotic

tests. Fourier transformation infrared (FTIR) spectroscopy was used to explore any changes

in the molecular structure of PEG 20000 and PEG 6000 molecules.

CHAPTER 7 presents the shrinkage behaviour of the clays from saturated slurried condition. The volumes of clay specimens during drying were measured using Clod method with commercially available water base Polyvinyl Acetate (PVAc) glue as an encasement material. The volumes of clay specimens equilibrated in the pressure plate and desiccators were determined using wax method to complement the Clod test results. Two parametric models were used to best-fit the experimental water content-void ratio shrinkage paths of the clays. The drying suction-water content SWCCs were used in conjunction with the water content-void ratio data, to establish the suction-void ratio SWCCs and the suction-degree of saturation SWCCs. The AEVs of the clays were determined using three different approaches, (*i*) based on the suction-water content SWCCs from pressure plate and desiccator test results, (*ii*) based on the conventional method of extending the constant slope portions of the suction– degree of saturation SWCCs to intersect the suction axis at 100% degree of saturation and (*iii*) based on the osmotic test results. Comparisons of the AEVs from the three approaches are presented.

CHAPTER 8 presents the wetting suction-water content SWCCs of the clays studied. The effects of compaction dry density and confining conditions (i.e. unconfined, laterally confined and isochoric conditions) on the wetting suction-water content SWCCs are presented. The applied suction was varied between 300 to 0.05 MPa. Various methods were adopted for controlling suction of the clay specimens, such as axis-translation, vapour equilibrium and osmotic techniques. The bentonites specimens were tested from loose powder and compacted at targeted dry densities of 1.2, 1.3, 1.4, 1.5, 1.6 and 1.7 Mg/m^3. Speswhite kaolin specimens were compacted at targeted dry densities of 1.2, 1.3, 1.4 Mg/m^3 and then tested. The water content versus suction relationships obtained from the

chilled-mirror dew-point tests are also presented and compared with the wetting suction-water content SWCCs of powder specimens of the clays.

This chapter also presents the swelling pressure measurements of both bentonites under isochoric condition. Single step swelling pressure measurements were carried out using deionised water, whereas multistep swelling pressure tests were carried out using vapour equilibrium technique. Bentonites specimens were statically compacted at various dry densities of 1.3, 1.4, 1.5, 1.6 and 1.7 Mg/m^3 at hygroscopic water contents for the single step swelling pressure tests. The swelling pressures of bentonite specimens equilibrated at applied suctions of 38, 21.8, 7.5 and 3.3 MPa were measured. Vapours of saturated salt solutions were circulated at the top and bottom of the specimens. In the multistep swelling pressure tests, only one dry density was considered (i.e. $1.7 Mg/m^3$).

Observations made on the microstructural and fabrics changes during the wetting process for initially compacted specimens equilibrated at various relative humidity environments are presented. Environmental Scanning Electron Microscope (ESEM) was used for this purpose. In addition, the changes in the c-axis spacing of clay specimens equilibrated at different applied suctions in the desiccator tests were measured using low angle XRD. These results are presented towards the end of this chapter.

CHAPTER 9 presents the assessments of water uptake capacities of the clays during drying and wetting from theoretical considerations. Richard's equation was used to evaluate the diffusivity of the clays studied. Furthermore, the elapsed time and water content changes during wetting process were evaluated. The Gouy-Chapman diffuse double layer theory and the van der Waals attractive pressure theory were used to establish the suction-water content

11

changes SWCCs. The calculated suction-water content SWCCs were compared with experimental drying and wetting suction-water content SWCCs of the clays. The changes in the c-axis spacing of powder clay specimens at various applied suction were calculated using parallel plate consideration and compared with the experimental results.

CHAPTER 10 presents the main conclusions drawn based on the findings of this study.

CHAPTER 2

LITERATURE REVIEW

2.1 Introduction

This chapter presents comprehensive reviews on the application of clays, clay mineralogy and structural units, clay microstructures, clay-water interaction, evaluation of c-axis spacing and osmotic efficiency of soils. Additionally, a brief review of concept of soil suction, suction measurement techniques and suction control techniques are presented. Various laboratory methods used for establishing the drying and wetting SWCCs and the factors influencing the SWCCs are presented. Significance of the suction-void ratio SWCCs, various volume measurement techniques, modelling of the shrinkage paths and determination of the air-entry value (AEV) are presented. The final section of this chapter deals with a review of literature on the swelling pressures of compacted bentonites.

2.2 Application of clays

Currently, clays are extensively used in many countries as industrial and construction materials for various important engineering applications. The most important applications have been in the development of engineered waste facilities (Rowe et al., 1997; Sharma and Reddy, 2004; Pusch and Yong, 2005). For instance, highly plastic clays in powder and

compacted at low dry densities are used as liners, barriers and cap systems to provide attenuative measures by minimizing the migration of contaminants of various chemical species from industrial and municipal waste disposal facilities (Peavy et al., 1987; Rowe et al., 1997; Oweis and Khera, 1998; Alther, 2004; Sharma and Ready, 2004; Bouazza and Bowders, 2010). In addition, clays in slurry form are also used as isolation walls for storage or treatment of liquid wastes in ponds, wetlands and impoundments (Rowe et al., 1997; Reeves et al., 2007).

Clays and natural soils containing kaolinite minerals provides low cost materials and are being used as sludge thickener, liner in constructed wetlands, and undisturbed clayey barriers (Yang and Barbour, 1992; Metcalf and Eddy, 2002; Reeves et al., 2007). On the other hand, clays containing montmorillonite minerals are used extensively for water impedance because of the high swelling and sealing capacity (Pusch, 1982; Alther, 2004, Pusch and Yong, 2005). The unique properties allow bentonites to provide confinement for hazardous wastes and to prevent the contamination of the surrounding environment. Furthermore, the chemical exchange characteristic of clays allows the removal of heavy metals and other organic contaminants in wastewater treatment processes (Metcalf and Eddy, 2002). For example, calcium bentonites are used as purification filters in the treatment of wastewater from palm oils and petrochemical industries (Murray, 2007), whereas sodium bentonites are proposed as buffer material in nuclear waste repositories (Pusch and Yong, 2005).

In recent years, major countries including the UK, have opted for the use of highly compacted bentonite as a suitable buffer and backfill material for deep underground nuclear waste repositories (Daniel, 1993; ENRESA, 2000; Pusch and Yong, 2005; Pusch, 2008). Due to the complexity of the repository, intensive research have been rigorously conducted in

studying the thermal, hydraulic, chemical and mechanical behaviour of bentonites (ENRESA, 2000; Pusch and Yong, 2005; Pusch, 2008).

2.3 Mineralogy and structural unit of clays

Clays are naturally occurring materials which are primarily composed of various minerals. Clay minerals are formed with combinations of silica tetrahedral and octahedral sheets (Grim, 1968). The minerals most commonly encountered are kaolinite, illite and montmorillonite (Grim, 1968; van Olphen, 1977; Mitchell, 1993). The unit layers in 1:1 sheet mineral such as kaolinite, are formed from one layer of silica tetrahedral sheet and one alumina octahedral sheet. On the other hand, montmorillonite minerals are 2:1 sheet mineral that are built up by an octahedral sheet that a sandwiched between two tetrahedral sheets. The unit layers of kaolinite and montmorillonite are presented in Figure 2.1.
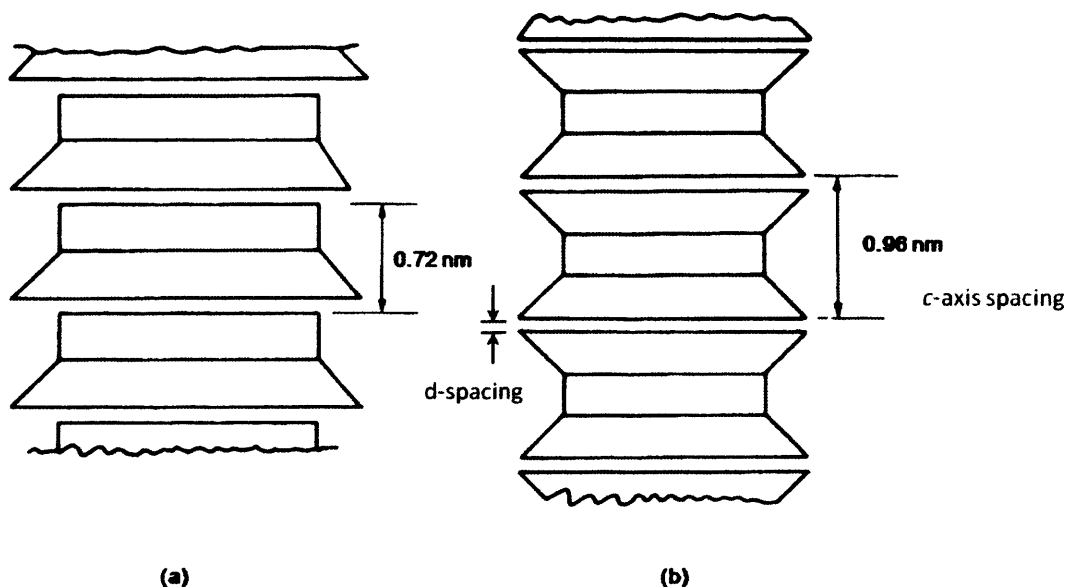
Fig. 2.1: *Unit layer of clays, (a) kaolinite mineral, (b) montmorillonite mineral*

(modified from Mitchell, 1993)

The thickness of nonhydrated unit layers is about 0.72 nm for kaolinite and about 0.96 nm for montmorillonite (Grim, 1968; Mitchell, 1993). The c-axis spacing is referred to as the sum of the thickness of nonhydrated unit layer and the separation distance between clay platelets (i.e. $t + 2d$). Due to the charge deficiency of the clay surface, positively charged exchangeable cations (i.e. Na^+, Ca^{2+}, Mg^{2+}, K^+) are attracted to the surface of the clays (Mitchell, 1993). The amount of available exchangeable cations, B, depends on the available specific surface area, S, of the clays. Commonly, bentonites contain mixture of several types of exchangeable cation (Tripathy and Schanz, 2009). In most cases, sodium and calcium bentonites are most commonly available (Grim, 1968; Mitchell, 1993; Quirk, 1994). The specific surface area and the amount of exchangeable cations in kaolinite are significantly lesser than that of montmorillonite (Grim, 1968; Lambe and Whitman, 1969, Pusch and Yong, 2005).

Kaolinite is usually very stable and has very little tendency for volume change when in contact with water (Rao and Sridharan, 1985; Sharma and Reddy, 2004). The unit layers are stacked and held together by hydrogen bonding from the alumina sheet on one face and oxygens from the silica sheet on the opposite face of the layer (Yong and Warkentin, 1966). This type of bonding is fairly strong. Thus, thicker stacks of clay particles are formed (Sharma and Reddy, 2004). The strong bond also prevents swelling between unit layers in kaolinite. In the case of montmorillonite, bonding of structural unit is via exchangeable ions and water in the interlayer space. Unlike kaolinite particles, due to a larger specific surface area and a greater amount of exchangeable cations, more water is adsorbed that causes high swelling behaviour of montmorillonite (Mitchell, 1993; Delage et al., 2006).

2.4 Microstructure of clays

Clay minerals consist of several unit layers stacked on top of one another to form a particle. A number of particles in a group form clay aggregates (Mitchell, 1993; Tessier et al., 1998). The number of individual unit layer in a particle depends on the water content and initial dry density (Saiyouri et al., 2000; Delage, 2006). A montmorillonite particle is usually made of several unit layers (Saiyouri et al., 2004). Tessier et al. (1998) and Saiyouri et al. (2000) noted that the microstructure of Fourges clay, a mixed valence montmorillonite, consists of aggregates of particles with an average of 10 unit layers, particularly at very high water content. On the other hand, the amount of unit layers increased up to 100 to 350 layers per particle at dry conditions, depending upon the type of exchangeable cations present (Saiyouri et al., 2000; Delage et al., 2006).

The variety of possible soil fabrics and interparticle forces lead to the variety of pore structures (Mitchell, 1993). The unit layers, particles, and aggregates form various types of pores in clays. In compacted soils, clay particles are aggregated together, giving rise to an aggregate microstructure (Delage et al., 2006). For example, Fig 2.2 shows the type of pores in a granular MX80 bentonite.

Interparticle pore (macro-pores)

Interlayer pore (micro-pores)
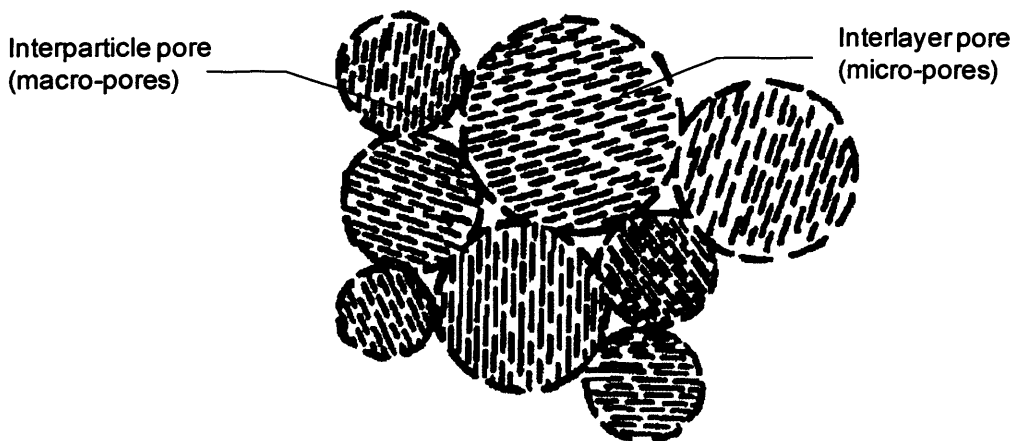
Fig. 2.2: *Type of pores in MX80 bentonite (after Pusch, 1982)*

17

In general, three types of pores can be seen in compacted bentonites (Pusch, 1982; Saiyouri et al., 2000; Salles et al., 2008). The micro-pores are the pores between unit layers inside the clay particles. The pores that exist between the particles inside the aggregates are known as the interparticle pores (Delage et al., 2006). The macropores are the inter-aggregate pores between the aggregates made up of clay particles.

The pore-size distribution is influenced by the initial dry density, water content and aging effects (Delage, 2006). The structure and fabric of clays influence the initial void ratio of a given soil (Mitchell, 1993). The interparticle pores and interconnecting pores reduce with an increase in the dry density (Tinjum et al. 1997; Kozaki et al., 1998; Bourg et al., 2006). Gens and Alonso (1992) stated that larger pores tend to disappear only at very high dry densities (i.e. > 1.84 Mg/m^3).

2.5 Clay-water interaction

The distribution of ions in the pore-water adjacent to a soil particle depends upon the electrical charge at the mineral surfaces, the type and amount of exchangeable cations, the chemical properties of the pore-fluid, the temperature, hygroscopic water content and the applied stress (Verwey and Overbeek, 1948; van Olphen, 1977). Silts and sands are primarily composed of non-clay minerals. The surface texture of grains influences the stress-deformation behaviour of these soils (Mitchell, 1993). On the other hand, due to the presence of the electrical double layer around clay particles, the volume change behaviour of clays is primarily governed by physico-chemical forces (Bolt, 1956).

Due to the differences in ionic concentration in solution near the surfaces and away from the surfaces of the clay particles, the cations near the surfaces of the particles try to diffuse away to equalize the concentration throughout, but is opposed by the negative electric field originating on the particle surfaces. The tendency of the ions to diffuse away and the opposing electrostatic attraction lead to ion distribution adjacent to a clay particle in suspension (Mitchell, 1993). Figure 2.3 shows the distribution of ions adjacent to the clay surface. In a clay–water electrolyte system, the osmotic pressure due to concentration of ions decreases with an increasing distance from the surfaces of the clay particles and attains a minimum value at the central plane between two interacting clay particles.
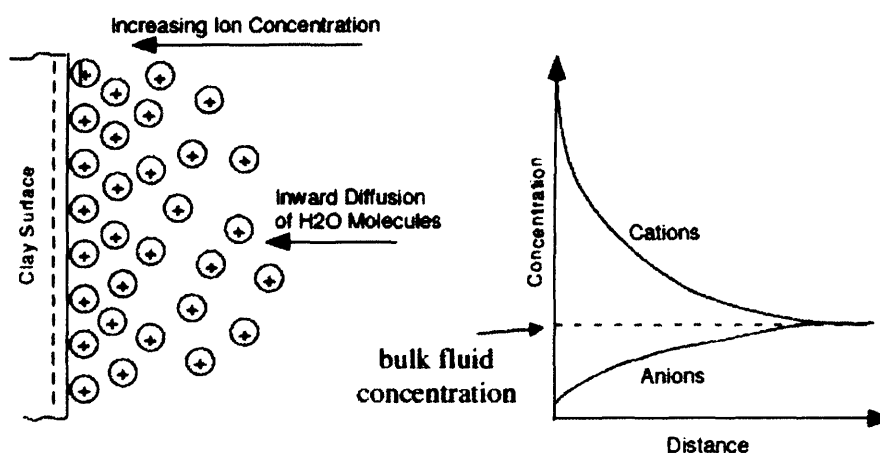
Fig 2.3: *Distribution of ions adjacent to the clay surface (modified from Mitchell, 1993)*

Clays exhibit volume change when in contact with water in the form of vapour or liquid due to insertion of water molecules and the separation between clay platelets in the interlayer pores. The insertion of water molecules in the interlayer occurs in an organised fashion, forming one, two, three and sometimes up to four layers of water (Grim, 1968; Saiyouri et al., 2000; Likos, 2004). Sposito and Prost (1982) have shown that in swelling clays, the wetting/drying mechanisms are controlled by adsorptive forces. The first layer of water adsorbed close to the clay surface is due to hydration of cations (Verwey and Overbeek,

1948). This process is referred to as type I swelling or crystalline swelling (van Olphen, 1977). During the hydration of cations, the negative charge dipole of water molecules are directed towards the cations and weakens the electrostatic interaction between negatively charges layers and interlayers. Water molecules surround the cations and the hydration energy is increased. In addition, the order of water molecules also increased (Alther, 2004). Beyond the crystalline swelling, electrical double layer is formed and influence the swelling behaviour of clays. This is known as type II swelling (Bolt, 1956; van Olphen, 1977; Mitchell, 1993).

2.6 Changes in the c-axis spacing during wetting

The c-axis spacing (Fig.2.2) changes with varying water content. The changes in the c-axis spacing can be measured using low angle XRD technique (Grim, 1968). Studies in the past have shown that insertion of water molecules during the wetting process initiated in the interlayer pores (Grim, 1968; Saiyouri et al., 2000; Likos, 2004, Warr and Berger, 2007). Table 2.1 shows the c-axis spacing and the corresponding number of water layer adsorbed for a homoionised montmorillonite. Due to the stable nature of kaolinite particles, the c-axis spacing usually remains fixed at 0.72 nm (Grim, 1968; Mitchell, 1993).

Table 2.1: *The c-axis spacing and number of water layer for montmorillonite (after Grim, 1968)*

c-axis spacing (nm)	Number of water layer adsorbed
0.96	0
1.26	1
1.56	2
1.86	3

Table 2.1 shows that the c-axis spacing increases from 0.96 nm to about 1.86 nm with an increase in the water content. Furthermore, it was noted that the maximum number of layers adsorbed is about three layers of water (Saiyouri et al., 2000; Likos, 2004, Warr and Berger, 2007). Theoretically, the separation distance between two interacting clay platelets can be calculated from parallel plate consideration using the relationship between the micro and the macro void ratio proposed by Bolt (1956). van Olphen (1963) stated that for calcium montmorillonite, the pressure associated with removing the water from the third, second, and first adsorbed layer were 125, 250, and 600 MPa, respectively. Saiyouri et al. (2000) stated that for a divalent-rich FoCa clay, the suction associated with the third, second, and first adsorbed layer were 7, 50 and 100 MPa. The thickness of diffuse double layer for sodium montmorillonite can extend up to about 12 nm (Grim, 1968; van Olphen, 1977). However the XRD analysis was found to be limited to only 1.86 nm (Saiyoiri et al., 2000; Likos, 2004; Delage et al., 2006; Warr and Berger, 2007).

2.7 Osmotic efficiency

The ability of soils to act as semipermeable membrane in restricting passage of ions at the same time allowing the passage of water is known as osmotic efficiency of soils (Barbour and Fredlund, 1989; Iwata et al., 1988; Mitchell, 1993). The role of osmotic efficiency in highly swelling clays has been studied by several researchers (Kemper and Rollins, 1966; Kemper and Quirk, 1972; Barbour et al., 1991; Malusis et al., 2003). The osmotic efficiency of soils depends on several factors, such as the mineralogical properties, the chemical properties, the pore-fluid chemical composition, the effective pore-size and the water content (Mitchell, 1993). The osmotic efficiency is measured in the scale between 0 to 1. A soil is referred to as an ideal membrane (i.e. osmotic efficiency = 1) when it restricts the passing of ions

completely. On the contrary, a soil is referred to as non ideal membrane (i.e. osmotic efficiency <1) when ions are not fully restricted (Barbour and Fredlund, 1989; Mitchell, 1993). In general, soils with higher liquid limit possess greater osmotic efficiency (Mitchell, 1993). Olsen (1969) showed that compaction increases the membrane efficiency of kaolinite.

2.8 Soil suction

Soil suction was first defined by Schofield (1935) as pressure deficiency in the pore liquid within a soil which drives water to enter during wetting or to flow out of soils during the drying process. The relationships between soil suction and water content changes are useful in describing the volume change behaviour and shear strength behaviour of soils (Barbour, 1998). The total suction is referred to as the free energy state of water and is equal to the sum of matric and osmotic suction (Krahn and Fredlund, 1972; Fredlund and Rahadrjo, 1993).

2.8.1 Matric suction

The matric suction is commonly associated with the capillary phenomenon arising from surface tension of water. The pressure difference between air pressure, u_a, and the water pressure, u_w, (u_a - u_w), is referred to as the matric suction. Matric suction arises from the combined effects of capillary and short-range adsorption (due to surface charge, van der Waals attraction and exchangeable cation hydration) in soils (Lu and Likos, 2004). A soil possesses matric suction due to the retreat of the air-water interface inwards from the surface of the soil and starts to become unsaturated (Fredlund and Rahardjo, 1993). Concurrent with the retreat of air-water interface, the degree of saturation drops below 100% (Fredlund and Rahardjo, 1993; Vanapalli et al., 1998).

2.8.2 Osmotic suction

The osmotic suction is commonly associated with the chemical composition of pore-fluid of soils (Krahn and Fredlund, 1972; Fredlund and Rahardjo, 1993). It is equivalent to the suction derived from measurement of the partial pressure of the water vapour in equilibrium with a solution identical in composition with the soil water, relative to the partial pressure of water vapour in equilibrium with free water (Fredlund and Rahardjo, 1993).

2.9 Suction measurement

Soil suction can be directly or indirectly measured by measuring the negative pore-water pressure of the soil. Various techniques have been adopted in measuring suction of unsaturated soils, such as filter paper method, null-type axis translation, high suction tensiometer, chilled-mirror dew-point technique and suction probe (Ridley and Burland, 1993; Guan and Fredlund, 1997; ASTM D 6836-02, 2003; Lu and Likos, 2004; Agus and Schanz, 2005; Rahardjo and Leong, 2006; Delage et al., 2008; Lourenco et al., 2011). The methods currently available for measuring suction are presented in Fig 2.4.

The most common method of suction measurement is the filter paper method (Gardner, 1937; Fredlund and Rahardjo, 1993; Houston et al., 1994; Bulut et al., 2001; Likos and Lu, 2002; Leong et al., 2003; Agus, 2005; Marinho and Oliviera, 2006; Bulut and Leong, 2008; ASTM D 5298-94, 2010). Among all the known suction measurement methods, the filter paper method is the only method from which both total and matric suction can be measured (Bulut and Leong, 2008).
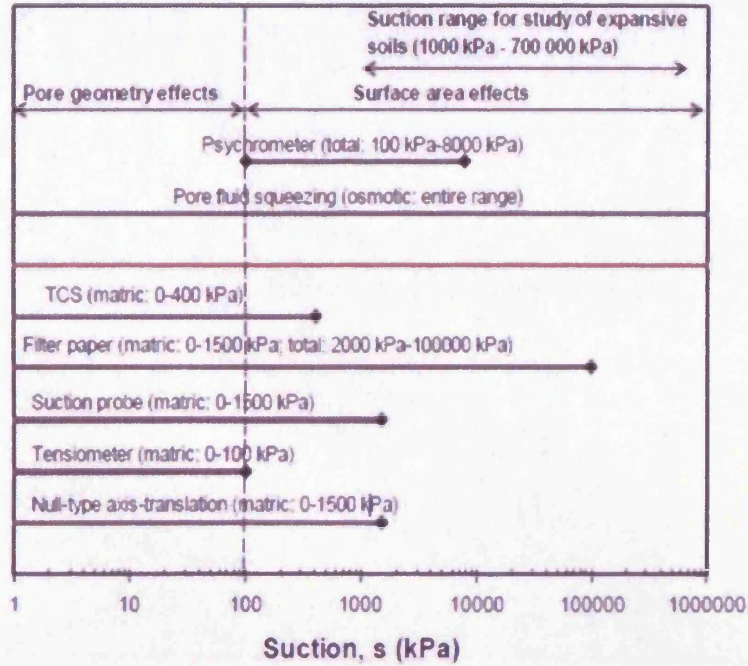
Fig. 2.4: *Suction measurement range for various methods (after Lu and Likos, 2004)*

The chilled-mirror dew-point technique measures the water activity or relative humidity of soil specimens similar to thermocouple psychrometry (Leong et al., 2003; Levitt and Young, 2003; Delage et al., 2008). The suction-water content relationship of clay-water mixture can be established rapidly using this method for RH of 10% to 100%, which corresponds to total suction range of about 0.05 to 100 MPa (Gee et al., 1992; Levitt and Young, 2003; Delage et al., 2008; ASTM D 5298-94, 2010). Agus and Schanz (2004) showed that the chilled-mirror provides the most accurate and rapid determination of suction-water content relationship of clay-water mixture.

Matric suction measurement usually requires a separation between water and air phase, normally by means of a ceramic disc (Fredlund and Rahardjo, 1993). However, cavitation poses restriction to the technique when used for measuring high matric suction (Lu and Likos, 2004). On the other hand, osmotic suction, can be measured by measuring the dissolved salt concentration by squeezing technique (Krahn and Fredlund, 1972; Fredlund and Rahardjo, 1993). The osmotic

pressures of the dissolved salt are generally calculated from van't Hoff equation (Krahn and

Fredlund, 1972; Nelson and Miller, 1992, Rao and Sivanandha, 2005).

2.10 Suction control technique

Several methods are currently available for controlling matric or total suction of soil

specimens. Table 2.2 presents summary of common laboratory methods used for controlling

suction in soils.

Table 2.2 indicates that suction can be applied to soil specimens in the laboratory from 0 to

300 MPa using various methods. The following subchapters describe the review of the main

methods used in this study.

Table 2.2: *Common laboratory methods for controlling suction (after Croney and*

Coleman, 1954)

Technique	Suction component	Measure suction from	Suction range (MPa)	Available suction path
Axis-translation	Matric	Air pressure	0.01 to 1.5	Drying/wetting
Soil column	Matric/total	Negative water head	0 to 0.1	Drying
Centrifuge	Matric	Centrifugal force	0.01 to 1.5	Drying
Osmotic	Matric	Osmotic pressure	0 to 1.5	Drying/wetting
Vapour equilibrium	Total	Salt solution	3 to 300	Drying/wetting

2.10.1 Axis-translation technique

The axis-translation technique is the most commonly used technique for controlling matric suction (e.g. pressure plate extractor) (Croney and Coleman, 1954; Klute, 1986; Fredlund and Rahardjo, 1993, Tarantino et al., 2011). In the pressure plate test, soil specimens exchange water with a high air-entry ceramic disc. Air pressure is applied on the soil specimens, whereas the water pressure below the ceramic disc is maintained close to zero (Fredlund and Rahardjo, 1993). Pressure plate extractors can be used to induce matric suction up to 1.5 MPa. On the other hand, the volumetric pressure plate can be used for applying suction up to 0.2 MPa. Both wetting and drying tests can be carried out using volumetric pressure plate extractors (Fredlund and Rahardjo, 1993).

Although the axis-translation technique provides reasonable results (Delage et al., 2008), the method has been criticised due to some inherent limitations. These aspects include: (*i*) the technique is not representative of field conditions where air pressure is under atmospheric conditions; (*ii*) there are some concern with regard to how the air pressurisation process affects the water pressure when the pore water is held by adsorption mechanism; (*iii*) the application of the technique at nearly saturated state in the absence of a continuous gaseous phase is not straightforward and (*iv*) non equilibrium of clayey soil specimens at suction higher than 0.5 MPa (Tinjum et al., 1997; Vanapalli et al. 1999; Gee et al., 2002; Oliveira and Fernando, 2006; Cresswell et al., 2008; Delage et al., 2008).

2.10.2 Centrifuge technique

The centrifuge technique has been used for applying suction up to 3 MPa (Bouyoucos, 1935; Gardner 1937; Croney and Coleman, 1954). Briggs and McLane (1907) were the first investigators to use the centrifuge technique to relate the soil suction and the water retained by a soil (Khanzode et al., 2002). Different applied suctions were rapidly achieved by varying the distance of the soil specimen from the centre of rotation of the centrifuge and the speed of rotation of the centrifuge. The centrifuge method can be used for rapid determination of suction-water content relationship of soils from 0.003 up to 0.7 MPa (Khanzode et al., 2002). For higher applied suctions, modification of the specimen holder will be required (Khanzode et al., 2002).

2.10.3 Osmotic technique

In the laboratory, suction of soils can be controlled by the osmotic technique. A soil specimen is brought in contact with a solution of Polyethylene glycol (PEG) of predetermined molecular weight separated by a semipermeable membrane. By varying the concentration of PEG solution, various osmotic gradients can be created. In the event of equalisation of the osmotic suction on either side of the semipermeable membrane, the method controls matric suction of soils (Zur, 1966). In the past, several researchers have used the osmotic technique to study the water retention behaviour of soils (Zur, 1966; Williams and Shaykewich, 1969; Fleureau et al. 1993; Marcial et al., 2002). Similarly, the technique has been used to study the volume change behaviour of soils as affected by changes in the soil suction (Kassiff & Ben Shalom, 1971; Dineen & Burland, 1995; Delage et al., 1998; Cuisinier & Masrouri, 2005; Monroy et al., 2007; Delage & Cui, 2008a, Tarantino et al., 2011).

The applied suction in the osmotic technique is related to the concentration of the PEG solution used. Lower molecular weights (*MW*) of PEG are generally used for applying suction higher than 1.5 MPa (Williams and Shaykewich, 1969; Delage et al., 1998). On the other hand, PEG solution with a much larger MW is generally used to generate suction of less than 1.5 MPa. PEG 20000 and PEG 6000 are the most commonly used in geotechnical engineering studies (Delage et al., 1998). Initially, the calibration curves established from total suction measurement as a function of the solution concentration of various PEGs were investigated by measuring the relative humidity above solutions of PEG by using psychrometer (William and Shaykewich, 1969). Dineen and Burland (1995) used tensiometer for determining the suction and PEG concentration relationship. The calibration procedures were later adopted by Tarantino and Mongiovi (2000) and Monroy et al. (2007) using different types of semipermeable membranes. Delage et al. (1998) established a calibration curve based on equilibrium PEG solutions in controlled relative humidity tests. Figure 2.5 shows the PEG solution calibration curve established from different methods.
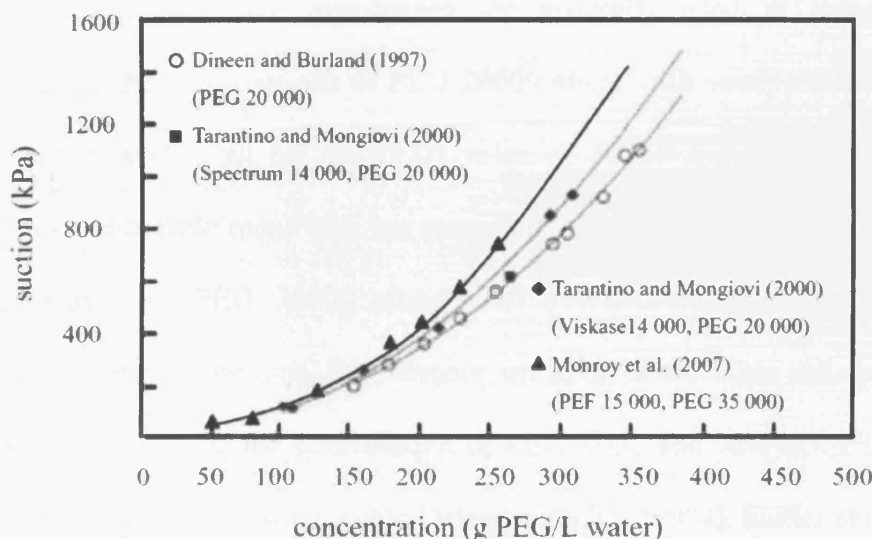
Fig. 2.5: *Dependency of the calibration curve of the osmotic technique with respect to the membrane and PEG used (after Delage and Cui 2008a).*

Comparison of the calibration curves (Fig. 2.5) shows that there are differences in the calibration curves at higher suctions. The differences in the applied suction at the same PEG concentration can be attributed to the methods adopted in establishing the calibration curves and type of membrane used (Money, 1989).

A review of literature suggested that the osmotic technique has been extensively used for applying suctions less than 1.5 MPa. Studies on the applications of the osmotic technique for higher suctions are limited (Delage & Cui, 2008a). The main limitation of the osmotic technique are associated with (*i*) intrusion of PEG into soil specimens during testing (Williams and Shaykewich, 1969; Tarantino & Mongiovi 2000; Delage and Cui 2008b) and (*ii*) the nonlinearity of the calibration curves (Michel and Kaufman, 1973; Money, 1989; Delage et al., 2008). These problems are more relevant at higher applied suctions.

2.10.3.1 Semipermeable membranes used in osmotic tests

Cellulose acetate semipermeable membranes are generally used in osmotic tests. In geotechnical testing, the combinations of PEG 20000 along with semipermeable membrane having a molecular weight cut off (MWCO) value of 14000 and PEG 6000 along with MWCO 3500 semipermeable membrane are commonly used. Delage and Cui (2008b) stated that the combination of PEG 20000 along with MWCO 14000 is preferred as this combination reduces the testing time. Furthermore, intrusion of PEG into soil specimens were observed during testing when the combination of PEG 6000 and MWCO 3500 membrane were used (Williams and Shaykewich, 1969; Delage and Cui, 2008a). Slatter et al. (2000) and Monroy et al. (2007) stated that the membranes are susceptible to bacteria attacks in a longer testing period. The problem however can be minimized by adding penicillin to improve the

bacteria resistance of the membranes (Kassiff & Ben Shalom, 1971). Similarly, due to the amorphous gel-like nature of regenerated cellulose, the membranes are known to be vulnerable against mechanical strain (Spectrum® Laboratories, 2007). Due to these factors, Monroy et al. (2007) suggested the use of a more resilient polysulphonate (PES) membrane in osmotic tests.

The pore-size of semipermeable membranes is usually designated by their MWCO value. Kim et al. (1994) stated that the MWCO alone would not be sufficient for membrane characterization as the actual pore-size of a membrane may differ quite significantly than that specified by the manufacturer. There are several methods available currently to study the pore structures of a semipermeable membrane, such as the use of AFM, Scanning Electron Microscopy (SEM), thermoporometry, and biliquid permporometry (Kim et al., 1994; Elimelech et al., 1997). The AFM studies do not require specimens to be treated with conductive material which could possibly alter the properties of the membrane.

2.10.3.2 PEG molecule size

PEG is a hydrophilic polymer made up of molecular chains having chemical formula: HO-[CH_2-CH_2-O]n-H (Squire, 1985). The chain length *(n)* of the polymer influences the molecular weight (Harris, 1992). In general, larger PEG molecules have greater molecular weights. The size of PEG molecules is usually much larger in a solution than any other molecules of comparable molecular weight (Squire, 1985; Harris, 1992). Thus, the specified molecular weight do not represent the actual molecular size of PEG as there is no direct correlation between a 3-dimensional molecular weight and a 2-dimensional metric length (Spectrum® Laboratories, 2010). For hydrated molecules in solutions, the hydrodynamic

radius, R_h, is generally used to describe the molecular size (Himmel & Squire, 1988; Harris, 1992).

Lentsch et al. (1993) proposed an empirical relationship (Eq. 2.1) between the molecular weight and the hydrodynamic diameter of PEG molecules for the case of constant density of molecules. Using Eq. 2.1, for a known molecular weight (MW) of PEG, the hydrodynamic diameter of PEG molecules (d_{PEG} in nm) can be calculated. For example, the size of molecules for PEG 6000 can be found to be about 4.0 nm, whereas it is about 7.0 nm for PEG 20000.

$$d_{PEG} = 0.09(MW)^{0.44}$$
Eq. (2.1)

Equation (2.1) is also used for estimating the pore-sizes of the semipermeable membranes (Lentsch et al., 1993). The calculated pore-size of the semipermeable membranes with MWCO of 3500 and 14000 can be found to be about 3.3 and 6.0 nm, respectively.

According to Michel & Kaufman (1973) and Minagawa et al. (1994), for PEG solutions of low concentration, longer PEG chains are usually formed due to a lesser interaction between the PEG molecules. On the other hand, the interaction between PEG chains increases with an increase in the concentration of solution that is manifested in the formation of smaller coiled or folded structures (Cosgrove, 2005) of the PEG molecules. Figure 2.6 shows the schematic representation of possible reduction in the hydrodynamic diameter due to an interaction of PEG chains with an increase in the concentration of PEG solution.
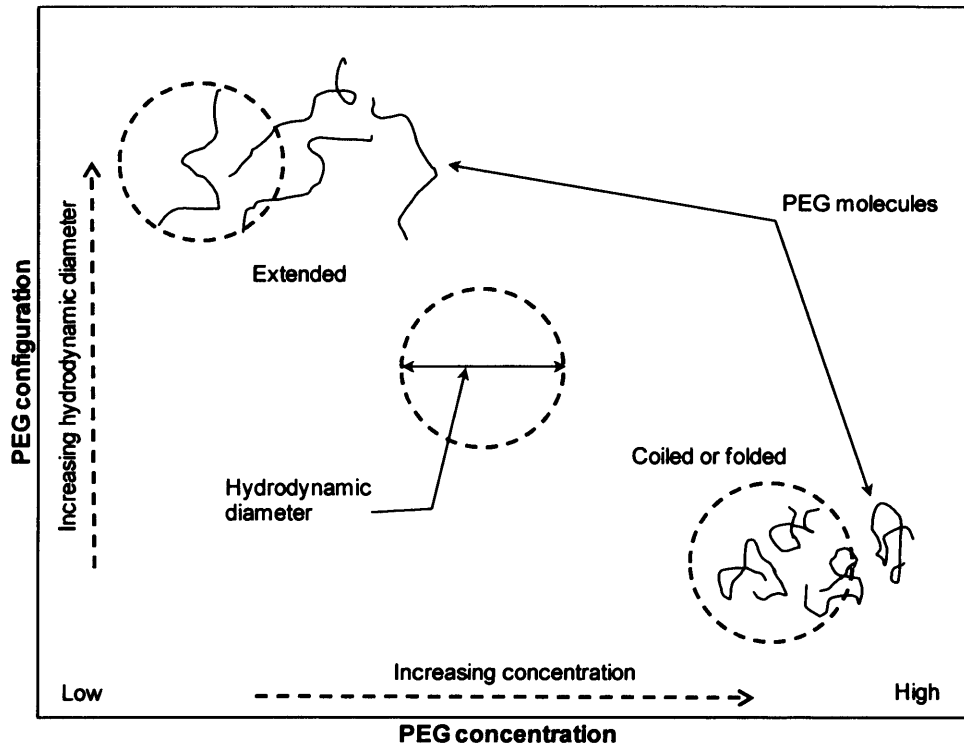
Fig. 2.6: *Schematic representation of PEG molecular chain configuration as a function of*

PEG concentration

Han et al. (1995) stated that PEGs are susceptible to oxidative degradation in the presence of air that may lead to lowering of the molecular weight. Other possible causes of degradation of PEGs are associated with interactions of molecules of PEG with the semipermeable membrane used and that with the expelled ions from the pore-fluid of soil-water systems. Studies concerning the degradation of hydrated PEGs with elapsed time are crucial in order to better the understanding of the osmotic system in controlling matric suction of soils.

Degradation of PEG can be studied using various techniques, such as using X-ray diffraction (XRD) technique, X-ray Photoelectron Spectroscopy (XPS), and Fourier Transform Infrared (FTIR) spectroscopy (Han et al., 1995; Celina et al., 1997; Beamson et al., 2000). The FTIR

spectroscopy is a rapid and non-destructive technique for identifying molecular structures and degradation of organic based polymers (Roberts & Caserio, 1965; Han et al., 1995).

It is to be noted that in the case of an unaltered pore-size of semipermeable membrane during a test, a reduction in the size of PEG molecules (i.e., a degradation) alone may enable passing of PEG into the soil-water system and subsequently reduce the efficiency of the osmotic system (Kemper & Evans, 1963; Iwata et al., 1988).

2.10.3.3 Suction equilibrium in osmotic tests

According to Aitchison (1965), the ionic concentrations of the reference fluid and the soil pore-water must be the same for measuring and applying matric suctions in soils. Multiple soils specimens are usually tested in the pressure plate tests. Therefore, measurements of chemical compositions of the expelled pore-fluid are usually not carried out.

According to Ng and Menzies (2007), at equilibrium, total suction of the PEG solution comprises of osmotic suction due to the PEG solution ($\pi_{solute}= \pi_{PEG}$), osmotic suction due to the salt solution (π_{salt}^1), and matric suction of the solution which is equal to zero. In the soil-water system, osmotic suction of the available salts (π_{salt}^2) and matric suction constitute the total suction. The schematic diagram showing total suction equilibrium on either side of semipermeable membrane in osmotic tests is presented in Fig. 2.7.
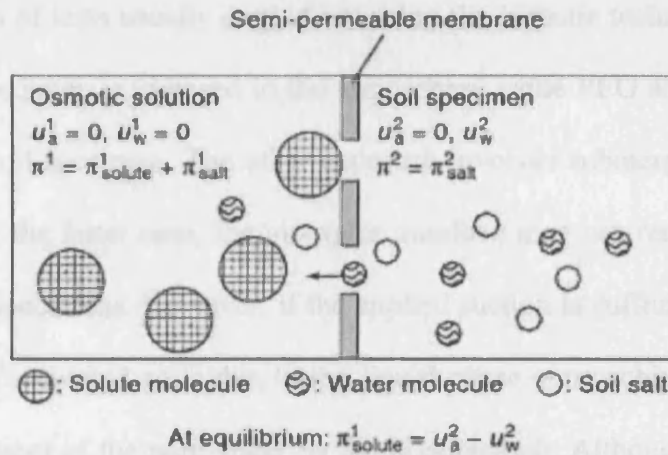
Fig. 2.7: *Schematic diagram of suction equilibrium in osmotic technique (after Ng and Menzies, 2007)*

The influence of matric suction on the PEG solution is not very well known. Since the osmotic suction on both side of the membrane are assumed to be equal (i.e. $\pi_{salt}^1 = \pi_{salt}^2$), total suction in the PEG solution is equal to osmotic suction of the PEG solution (π_{PEG}) and that on the soil side, it is equal to matric suction of the soil. In other words, π_{PEG} is equal to the applied matric suction.

In case of highly plastic clays, a lack of equalization of the osmotic suction between soil pore-fluid and the reference fluid may be anticipated (see Section 2.7). Suction equilibrium in Fig. 2.7 suggests that if the osmotic suction equalization is only partial (i.e. $\pi_{salt}^1 \neq \pi_{salt}^2$) the applied suction then becomes equal to the total suction instead of matric suction with an error due to π_{salt}^1. The diffusive flow in clays is driven by chemical concentration gradient and can be verified by measuring the chemical composition of the expelled pore fluid (Mitchell, 1993). Studies on the efficiency of the osmotic system in terms of equalization of osmotic suction on either side of the membrane have not been carried out in the past.

There are two types of tests usually carried out using the osmotic technique. In one case, the surface of a soil specimen is exposed to the atmosphere while PEG solution is circulated at the bottom of the soil specimen. The other approach involves submerging soil specimens in PEG solutions. For the latter case, the air-water interface may not retreat inwards from the surface of the soil specimens. However, if the applied suction is sufficiently large, cavitation within the pores of saturated soils due to the liquid phase approaching its vapour pressure may cause replacement of the pore-water by the dissolved air. Although free water cavitates below a pressure of -100 kPa; however, in case of soils under the influence of short-range physicochemical interaction effects, cavitation may not occur at the same pressure as that for free water (Lu and Likos, 2004).

2.10.3.4 Mechanisms controlling suction in osmotic tests

Based on physico-chemical considerations laid out in the literature (Verwey and Overbeek, 1948; Bolt, 1956; van Olphen, 1977; Iwata et al., 1988; Mitchell, 1993) (see Section 2.7) and considering that matric suction in osmotic tests is applied only when ($\pi_{PEG} + \pi_{salt}^1$) exceeds that of π_{salt}^2 (see Section 2.10.3.3), two mechanisms may be considered responsible for the water content change in osmotic tests, such as mechanism 1: if ($\pi_{PEG} + \pi_{salt}^1 < \pi_{salt}^2$), the osmotic suction of the soil becomes irrelevant since the ions in the soil-water system would take part in the formation of the electrical double layer around the soil particles; in this case, a decrease in the water content is accompanied by an increase in the osmotic pressure at the central plane between soil particles that in turn will be in equilibrium with ($\pi_{PEG} + \pi_{salt}^1$). In mechanism 2: if ($\pi_{PEG} + \pi_{salt}^1 > \pi_{salt}^2$), the osmotic pressure at the central plane between soil particle becomes irrelevant since the interacting electrical double layer is no longer operative;

in this case, π_{salt}^2 along with matric suction (i.e. matric suction = $(\pi_{PEG} + \pi_{salt}^1 - \pi_{salt}^2)$

contribute the total suction on the soil-water side.

The water content attained by a soil at equilibrium in mechanism 1 will corresponds to full

saturation state (i.e. hydrostatic pressure = 0), whereas in mechanism 2, a reduction in the

water content due to an increase in matric suction will cause a decrease in the degree of

saturation of the soil.

2.10.4 Vapour equilibrium technique

Vapour equilibrium technique involves controlling total suction of saturated salt solutions

and acids dissolutions in a closed system (e.g. vacuum desiccators) (Croney and Coleman,

1954; Fleareau et al., 1993; Delage et al., 1998; Al-Mukhtar et al., 1999; Villar, 1999,

Cuisinier and Masrouri, 2004; Tang and Cui, 2005; Blatz et al., 2008). Water exchange

between the soil pore-water and the vapour space includes the effect of capillary, salt solute

(osmotic suction), and sorptive forces. By varying sulphuric acids concentration, the method

has the ability to induce total suction up to 1000 MPa (Tang and Cui, 2005). However, it is

recommended to limit the use of acid dissolutions to a suction of 400 MPa (Pintado et al.,

2009). Saturated salt solutions are generally used over acid dissolution due to various factors

including (*i*) safety concern and (*ii*) alteration of soil mineralogical composition and damage

of testing equipment due to volatilization of acid solutions (Tang and Cui, 2005; Delage et

al., 2008; Pintado et al., 2009).

The applied suction in vapour equilibrium technique is related to the relative humidities

generated by different salt solutions. A range of salt solutions and the relative humidity levels

that can be generated are available in many published works and chemistry handbook (Blatz, et al., 2008). For instance, O'Brien (1947) presented relative humidity of 88 saturated salt solutions at various temperatures up to 100 °C. The sensitivity of the applied suction in vapour equilibrium technique is related to temperature changes (Delage et al., 1998). Many applications where the vapour equilibrium method is used for controlling suction use a separate independent sensor device such as relative humidity sensors, tensiometer and psychrometer to verify that the target suctions are achieved (Agus and Schanz, 2004; Blatz et al., 2008).

The limitation of vapour equilibrium technique is that the time to reach moisture equalisation is extremely long due to the fact that vapour transfer depends on the diffusion rate (Delage et al. 2008). Testing time can take up to several weeks to several months depending on soil type and testing conditions. The method was later improved by forcing the vapour to flow through the soil specimens by means of a vacuum pump (Delage et al., 1998; Oldecop and Alonso, 2004; Agus, 2005; Pintado et al., 2009; Dueck, 2008; Blatz et al., 2008). The testing time was significantly reduced from few weeks to only a few days.

2.11 Soil-water characteristic curve (SWCC)

The soil-water characteristic curve (SWCC) provides the relationship between suction and water content of soil (Fredlund and Rahadrjo, 1993; Ng and Menzies, 2007). The SWCC physically expresses the amount of equilibrium water a soil can retain at a given suction (Fredlund, 2002). The SWCC can be established by equilibrating a soil specimen to a series of different applied suctions or by using multiple specimens equilibrated at different applied suctions (Fredlund et al., 2001). The SWCC is commonly plotted over mixed of components

of suction (i.e. matric suction and total suction). In other words, matric suction and total suction at higher suction region are routinely plotted together (Ng and Menzies, 2007).

2.11.1 Drying suction-water content SWCCs

The drying suction-water content SWCCs are commonly determined in the laboratory by subjecting saturated soil specimens to an increasing suction at zero external stress (Fredlund and Rahardjo, 1993). Laboratory tests based on axis-translation technique (i.e. pressure plate and pressure membrane tests), vapour equilibrium technique (i.e. desiccator tests), centrifuge technique, and the osmotic technique using PEG solutions are commonly used to establish the suction-water content SWCCs of soils (Schofield, 1935; Croney and Coleman, 1954; Fleureau et al., 1993, Fredlund and Rahardjo, 1993; Delage et al., 1998, Khanzode et al., 2002; ASTM D- 6836-02, 2003; Blatz et al., 2008; Delage et al., 2008). Lourenco et al. (2011) have shown that the suction-water content SWCCs can be determined by continuous drying of soil specimen using high-suction tensiometers.

The drying suction-water content SWCCs are usually established following the first wetting process in the laboratory (Klute, 1986). Additionally, the drying suction-water content SWCCs starting from an initial water content at or slightly greater than liquid limit and up to the shrinkage limit of soils have been shown to provide useful information for engineering analyses (Fredlund and Rahadjo, 1993; Fleureau et al., 1993; Al-Mukhtar et al., 1999; Marciel et al., 2002) and development of theoretical soil mechanics (Croney and Coleman, 1954). Determination of the reduction in the water content, the void ratio, and the degree of saturation associated with an increase in soil suction are imperative for quantitative assessments of the hydraulic conductivity, ion retention capacity, and the shear strength of

unsaturated soils (Barbour, 1998; Fredlund, 2006). Establishing the suction-degree of saturation SWCCs requires the determinations of both the water content and the void ratio of soil specimens at each applied suctions.

2.11.2 Wetting suction-water content SWCCs

The wetting SWCCs are commonly established in the laboratory by decreasing the applied suction (Fredlund and Rahardjo, 1993). Ng and Pang (2000) showed that during a prolonged rainfall, the analysis using wetting suction-water content SWCCs predicted adverse pore-water pressure distributions with depth than those from an analysis using drying suction-water content SWCCs. It was noted that the wetting suction-water content SWCC is influenced by the soil structure, type of soil, mineralogy, density, initial water content, stress history, method of compaction and confining stress (Tinjum et al. 1997; Vanapalli et al. 1999; Lu and Likos, 2004; Thu et al. 2007).

A hysteresis phenomenon is usually observed, especially at lower suction ranges (Tinjum et al. 1997). The hysteresis exist due to differences in the pores and the interconnecting pore throats (e.g. ink bottle effect), changes in the contact angle during drying and wetting phase, and the availability of entrapped air (Fredlund and Rahadjo, 1993; Tinjum et al., 1997; Lu and Likos, 2004; Delage et al., 2006).

2.11.2.1 Influence of confining conditions on wetting suction-water content SWCCs

Tinjum et al. (1997) and Vanapalli et al. (1999) noted that initial water content influences the initial portion of drying SWCCs (i.e at lower suction region). Comparison made on the

SWCC of FoCa clay under free swelling and prevented swelling conditions showed that confining condition plays significant role in the water retention behaviour at lower suction region (Delage, 2006). The water contents of soil specimens tested under prevented swelling condition (i.e. isochoric condition) were found to be significantly reduced. Similarly, Ye et al. (2010) observed differences in the water retention behaviour of compacted GMZ bentonite subjected to wetting under free swelling and prevented swelling conditions. At suction less than 4 MPa, specimens wetted under prevented swelling condition were found to have lower water contents. In the case of free swelling condition, the influence of initial dry density on the water uptake capacity of soil specimens was found to be negligible (Delage et al., 1998; Saiyouri et al., 2000; Delage, 2006; Ye et al. 2009)

2.12 Transient flow in unsaturated soils

Fluid flow and water content in unsaturated soils may vary both spatially and temporally as a result of two basic mechanisms: (*i*) time-dependent changes in environmental conditions (i.e. relative humidity and temperature) and (*ii*) the storage capacity of soil (Lu and Likos, 2004). The flow of fluid in unsaturated soils is governed by conservation of mass and Darcy's law for fluid flow behaviour. Saiyouri et al. (2000) showed that the changes in the water content with elapsed time of soil specimens during the wetting process can be predicted using one-dimensional Richard's diffusivity model. Diffusivity is an important parameter in determining the time required for a soil specimen to reach a steady state condition.

The diffusivity or diffusion coefficient of soils is related to the flow of water in response to a concentration gradient (Fredlund and Rahardjo, 1993). Several researchers in the past have shown that the diffusivity of soils varies between 10^{-9} to 10^{-13} m^2/s. The diffusivity of soils

have been experimentally determined using Nuclear Magnetic Resonance (NMR), neutron

scattering and diffusion cells (Cebula et al., 1981; Kozaki et al., 1998; Saiyouri et al., 2000;

Nakashima, 2004; Sanchez, 2007). It is reported that the diffusivity is influenced by soil type

and compositions, initial dry density, initial water content, viscosity of the fluid, type of

chemical solutes and the boundary condition (Kemper et al., 1964; Cebula et al. 1981;

Idemitsu et al., 1989; Fredlund and Rahardjo, 1993; Kozaki et al., 1998; Saiyouri et al., 2001;

Ochs et al., 2001; Muhammad, 2004; Bourg et al., 2006). Ochs et al. (2001) and Bourg et al.

(2006) showed that the diffusivity of soils reduces with an increase in the dry density.

Similarly, depending upon the degree of saturation of the specimens, test results from Cebula

et al. (1981) showed that the diffusivity reduces with decreasing initial water content. In the

case of restricted swelling, tests results reported by Saiyouri et al. (2000) indicated that the

diffusivity of FoCa clays was slightly lower for specimens underwent free swelling condition.

2.13 Volume change behaviour

Highly plastic clays usually exhibit significant volume change when in contact with water

(Verwey and Overbeek, 1948; Grim, 1968; van Olphen, 1977; Mitchell, 1993; Tripathy and

Schanz, 2004, Tripathy and Schanz, 2009). Volume-change measurements and vertical

deformation measurements are common in geotechnical engineering practices (Tripathy et al.

2002). The volume change of soils can be represented by a typical S shape curve, as shown in

Fig. 2.8. The void ratio is plotted against the water content or the moisture ratio, or even

against suction to designate the volumetric shrinkage path (Tripathy et al., 2002; Cornelis et

al., 2006; Mbonimpa et al., 2006). Two different shrinkage paths of soils are shown in Fig.

2.8, such as that for saturated slurried soils and compacted soils that have undergone

numerous drying and wetting cycles (Haines, 1923; Tripathy et al., 2002).

41
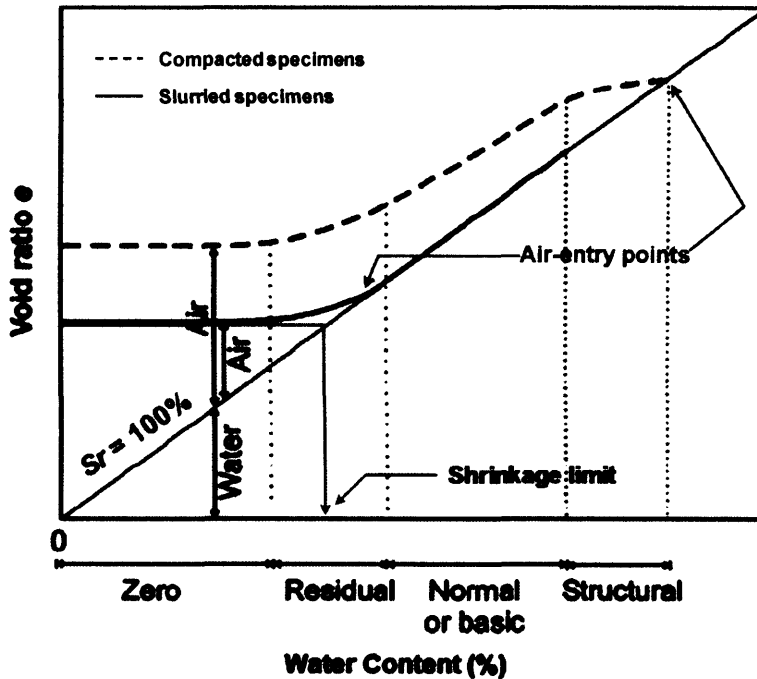
Fig. 2.8: *Typical shrinkage curve (based on Haines, 1923)*

According to Haines (1923), when a soil dries out, four shrinkage stages can be distinguished. The shrinkage phases are: (*i*) structural shrinkage, (*ii*) normal shrinkage, (*iii*) residual shrinkage and (*iv*) zero shrinkage (see Fig.2.8). In the first phase, the large inter-aggregate pores are emptied without considerable change in the bulk volume. In the second phase, the decrease in water volume results in an equal decrease in the bulk soil volume, with the intra-aggregate pores still fully saturated. The normal shrinkage line is often parallel to the theoretical degree of saturation line (i.e. $S_r = 100\%$) (Tripathy et al., 2002). The transition between the normal and residual shrinkage is where the shrinkage curve gets detached from the $S_r = 100\%$ line for soils that follow the 100% saturation line. This point occurs at the water content corresponding to the air entry value (AEV) (i.e. desaturation point where air enters the voids) (Fredlund and Rahardjo, 1993; Cornelis et al., 2006). From this point onwards, the soil becomes unsaturated. Beyond the air-entry points, the volume change

continues to take place until no further volume change is observed with a reduction in the water content. The shrinkage limit water content can be determined by extending the zero shrinkage line to the theoretical degree of saturation line (S_r = 100%) (Ke'zdi, 1980).

2.13.1 Suction-void ratio SWCCs

Determination of reductions in the water content, the void ratio, and the degree of saturation associated with an increase in soil suction are imperative for quantitative assessments of the hydraulic conductivity, ion retention capacity, swelling and shrinkage behaviour and the shear strength of unsaturated soils (Barbour, 1998; Fredlund, 2006). A decrease in suction will cause highly plastic clays to swell. On the other hand, an increase in suction will induce shrinkage and desaturation due to reduction in the water content (Hanafy, 1991). The suction-void ratio SWCCs are usually established by equilibrating multiple soil specimens at various applied suctions. Once equilibrated with the applied suction, specimens are removed for volume measurement (Fredlund and Rahardjo, 1993).

2.13.2 Volume measurement techniques

Several laboratory methods are available to measure the volume of soil specimens, such as dimension measurements using callipers or laser retractometer, fluid displacement method using kerdane oil, rubber balloon method, core method and encasement methods using water repellent solutions (viz. Molten wax, Dow Saran resin dissolved in Methyl Ethyl Ketone (MEK saran), waterproof Polyvinyl Acetate (PVAc) based adhesives) (Brasher, 1966; McKeen, 1985; Nelson and Miller, 1992; Bradeau et al., 1999; Albrecht and Benson, 2001;

Perko et al., 2000; Fleureau et al., 2002; Krosley et al., 2003; Peron et al., 2007; Rossi et al.,

2008).

Encasement method using molten wax requires duplicate soil specimens to be tested to

establish the entire shrinkage path (Lauritzen, 1948; Ward et al., 1965; ASTM D4943-08).

On the other hand, Clod test using Methyl ethyl ketone (MEK) saran or PVAc as encasement

eliminates the need of multiple specimens and only a single specimen is required to establish

the entire shrinkage path (Brasher, 1966; McKeen, 1985; Nelson and Miller, 1992; Clarke

and Nevels, 1996; Perko et al., 2000; Krosley et al., 2003).

In the Clod tests, encased soils are allowed to dry under a free unconfined condition. The

volume is measured by utilising Archimedes' principle (by weighing the soil specimen first

in air and under liquid of known density) (Nelson and Miller, 1992). Krosley et al. (2003)

proposed the use of alternative encasement material, a water based glue (PVAc), which

improved the testing time as compared to MEK saran due to improved vapour permeability of

the glue. The glue is easily available and is non-hazardous.

2.13.3 Modelling of the shrinkage curves

Modelling of soil shrinkage curves has gained significant recognition (Tuller and Or, 2003;

Boivin et al., 2004; Cornelis et al., 2006; Mbonimpa et al., 2006). Mbonimpa et al. (2006)

stated that the suction-degree of saturation SWCCs of clays can be established based on the

basic properties of clays and the suction-void ratio SWCCs that were best fitted with

parametric model. Alternatively, a Virgin Drying Line (VDL) conceptual model can be used

to study the volume change behaviour of soils (Toll, 1995). Shrinkage paths can be replicated

using several currently available empirical models (Kim et al., 2002; Cornelis et al., 2006). Although most of the models are empirically developed, some of these models utilize the basic properties of soils to replicate the shrinkage paths.

Kim et al. (1992) combined an exponential and linear function to best fit shrinkage data points. The model (KEA model) consists of three parameters. The model is currently used in the soil–water and solute transport computer simulation model SWAP (Cornelis et al., 2006). The model is restricted to the representation of the normal shrinkage by a linear function and by expressing the zero and residual shrinkage by an inverse exponential function which gradually approaches to a certain denominator value as the moisture ratio decreases (Kim et al., 1992).

A four parameters shrinkage model (ModGG model) has been proposed by Cornelis et al. (2006). The ModGG model is generally used to describe the moisture ratio as a function of the void ratio under different load pressures. Unlike the three parameters KEA model, the ModGG model covers all the four phase of the shrinkage characteristic curves. These two models will be further discussed in Chapter 7.

2.13.4 Determination of air-entry value (AEV)

During the drying process, the transition from saturated to unsaturated state of soils is indicated by the air-entry value, AEV (Fredlund and Rahardjo, 1993). The AEV is the suction at which the degree of saturation drops below 100%. Highly plastic soils generally possess very high AEVs. The AEVs for soils that undergo insignificant volume change due to an increase in suction are usually identifiable on the suction-water content SWCCs that show a

distinct break accompanied by a rapid decrease in the water content for an increase in suction. On the other hand, the AEVs are usually less distinct on the SWCCs for clayey soils. In this case, the suction-degree of saturation SWCC alone or the suction-water content SWCC in conjunction with the shrinkage curve are usually referred to for determining the AEV (Croney and Coleman, 1954; Fredlund and Rahardjo, 1993; Vanapalli et al., 1999). Conventional determination of AEV requires extending the constant slope portions of the suction – degree of saturation SWCC to intersect the suction axis at degree of saturation, S_r = 100% (Vanapalli et al., 1998).

Fredlund (1964) and Fleureau et al. (1993) noted that an increase in the vertical pressure and suctions has similar influence on the volume change behaviour of highly plastic clays for a large range of applied suctions. Marcial et al. (2002) stated that due to isotropic condition; the void ratio decrease due to a suction increase was greater than that of obtained due to vertical pressure increase. These studies have opined that Terzaghi's effective stress concept remains valid for saturated clays undergoing suction changes up to the air entry value. These studies also indicated that a matric suction change within the AEV must be balanced by the forces within the water-electrolyte system that are purely physico-chemical in nature, while the hydrostatic pressure at equilibrium under a given applied suction is zero (Schanz and Tripathy, 2005).

2.14 Swelling pressure measurement

Insertion of water molecules within the interlayer and interparticle pores causes montmorillonite clay to swell (van Olphen, 1962). However, if volume change is not allowed, the specimen will exert swelling pressure equivalent to the net repulsive force exerted

between the clay platelets (Bolt, 1956; Tripathy et al., 2004; Schanz and Tripathy 2009). Swelling of montmorillonitic clays exposed to water or electrolytes is primarily due to two mechanisms: (i) the crystalline swelling and (ii) the diffuse double-layer swelling (van Olphen, 1977). The magnitude of swelling pressure depends on the specific surface area, available exchangeable cations, temperature, initial dry density, and initial water content (Villar, 1999; Villar, and Lloret, 2004; Tripathy et al., 2004; Tripathy and Schanz; 2007; Tripathy and Schanz, 2009).

Measurements of swelling pressure of expansive soils during the hydration process have been conducted in the laboratory by using various methods (Kassif and Ben Shalom, 1971; Villar 1999; Romero, 1999). The swelling pressure measurement methods are broadly classified into three main categories, namely constant volume (i.e. isochoric condition), swell-under-load, and swell-load methods (Sridharan, et al., 1986).

In the isochoric method, swelling pressure of an expansive soil can be determined by saturating the specimen with distilled water or with other solutions in one step (Sridharan, et al., 1986). On the other hand, swelling pressure measurement conducted on specimen equilibrated at various applied suction is known as multistep swelling pressure test (Ariffin and Schanz, 2007). Multistep swelling pressure tests are generally conducted using suction controlled oedometer (Dineen and Burland, 1995; Romero, 1999; Villar, 1999; Villar and Lloret, 2004; Cuisinier and Masrouri, 2004; Dueck, 2008; Blatz et al., 2008).

2.15 Concluding remarks

In this chapter, a brief review on the absorption and desorption characteristics as well as the volume change behaviour of highly plastic clays were presented. General information on the behaviour of highly plastic clays was discussed. The laboratory methods used for establishing the drying suction-water content SWCCs, the wetting suction-water content SWCCs, the suction-void ratio SWCCs, the suction-degree of saturation SWCCs, and swelling pressure measurements were covered. A review of literature indicated that some specific aspects related to SWCCs and shrinkage behaviour of highly plastic clays are not fully understood. These aspects include: (*i*) total suction equilibrium on either side of the semipermeable membrane during osmotic tests, (*ii*) factors affecting the intrusion of PEG during osmotic tests, (*iii*) determination of AEVs of highly plastic clays based on the suction-water content SWCCs and shrinkage paths, (*iv*) influence of confining conditions on the wetting characteristics of compacted clays and (*v*) applicability of physico-chemical theories in assessing the suction-water content SWCCs of highly plastic clays.

CHAPTER 3

PROPERTIES OF CLAYS

3.1 Introduction

The engineering properties of soils (viz. volume change, shear strength, permeability) depend upon the physical properties of the soil solids and chemical properties of the pore fluid (Mitchell, 1993). This chapter describes the physical and chemical properties of the clays used and the commonly adopted laboratory methods for the determination of soil properties. The studies of properties are divided into two parts; physical properties (specific gravity, determination of particle size distribution, hygroscopic water content, Atterberg limits, mineral compositions, specific surface area) and chemical properties, such as the cation exchange capacity of the clays. The properties of the clays determined were compared with the properties of similar clays reported in the literature.

3.2 Materials used

In total three clays were used in this study. Two of the clays were highly swelling bentonites, namely MX80 and IBECO® DEPONIT CA-N bentonite (called Yellow bentonite from here onwards), whereas the other being Speswhite kaolin. Granular MX80 bentonite is greyish bentonite mined in Benton formation of Wyoming, USA. It is currently being extensively investigated and nominated as one of the appropriate buffer material in many countries for

49

the disposal of nuclear waste. Yellow bentonite is commonly available from S&B Industrial

Minerals GmbH, Germany. The bentonite originates from the deposits of Eastern isle of

Milos in Greece. It is considered as a reference material and as European alternatives to

MX80 bentonite in nuclear waste repository (Koch, 2007). The yellowish and fine powder

appearance is distinct to that of MX80 bentonite. Speswhite kaolin is a highly refined

kaolinite of ultrafine particles. This white kaolin is mined in south west of England from

Cornish deposits and supplied by IMERYS Mineral Ltd. In the laboratory, the clays were

kept in sealed bags and placed in steel drums at ambient temperature to avoid contamination.

In a more recent study, both the MX80 bentonite and the Speswhite kaolin have been used for

establishing a benchmark of experimental techniques for measuring and controlling suction

(Tarantino et al., 2011). All three clays are commonly being used as reference material for

waste barriers and backfilling materials (Pusch, 1982; Muller-Vonmoos et al., 1994; Thomas

et al., 2003; Villar and Lloret, 2004; Carlson, 2004; Pusch and Yong, 2005; Plötze et al.

2007).

3.3 Physical properties

3.3.1 Specific gravity of soil solids

The most common geotechnical approach of determining specific gravity is by pycnometer

method (Ke'zdi, 1980; BS 1377-2, 1990). In addition, the specific gravity can also be

calculated based on the clay crystallographic structure (Grim, 1968; Lambe and Whitman,

1969; van Olphen, 1977). The dehydrated specific gravity can be calculated based on the

crystal structure without taking into consideration the structure of adsorbed water (Grim,

1968). These values can be far lower (e.g. 2.2 to 2.5 for Na bentonite) than the hydrated

condition (e.g. 2.7 to 2.8 for Na bentonite) (Deeds and van Olphen, 1963; Grim, 1968). Perkins et al. (1937) proposed the use of carbon tetrachloride-bromoform solution for the determination of specific gravity.

The pycnometer method can be difficult to conduct especially on highly swelling clays with high montmorillonite content. Bentonite when mixed with water will tend to flocculate (Verwey and Overbeek, 1948). The incomplete penetration of water on the particles and possibility of chemical or physical change can affect the accuracy of measurements (Grim, 1968). For this reason, the specific gravity measurements for bentonites are conducted by using non polar liquid or gas (Allen, 1974) as substitute to water. van Olphen (1977) stated that non polar liquid such as alcohol or other organic solvent may be adsorbed on the clay surface in competition of water thus affecting the surface charge and the Stern potential.

In this study, kerosene was used as a substitute for water for determining the of specific gravity of the bentonites, whereas deionised water was used for the non swelling Speswhite kaolin following BS 1377-2 (1990). The specific gravity values after correction were found to be 2.8 and 2.84 for MX80 bentonite, Yellow bentonite, and 2.61 for Speswhite Kaolin. The specific gravity of MX80 bentonite was reported to vary between 2.76 to 2.82 (Bradbury and Baeyens 2002; Tripathy et al. 2004; Villar and Gomez-Espina, 2008). The specific gravity of Speswhite kaolin measured in this study is similar to that reported by Grim (1968) and Folly (2001).

3.3.2 Particle size analysis

Particle size of fine grained soils and clay–size fraction (i.e. < 2.0 μm in diameter) are usually determined on the basis of the settling rate of the particles in a liquid following Stoke's law (Lambe and Whitman, 1969; Ke'zdi, 1980; Terzaghi et al., 1996). The most commonly used technique in geotechnical testing is the hydrometer method, plummet balance (Slager and Koenigs, 1964; Walker and Hutka, 1971; Najaraj and Sivapullaiah, 1984) and the pipette method (Stein, 1985; Singer et al., 1988). While all these methods have been proved to be relatively accurate and inexpensive, they still suffer from limitations that can render erroneous and inconsistency results in determining clay fractions in soils (Vitton et al., 1997). Determination of particle size also consumes a lot of time with minimum of 24 hours testing period (Vitton et al., 1999).

Over the last decades, numerous automated systems have been developed for faster and more precise analysis of particles size determination for soils. These devices utilise different principles in particle size measurements with the most common being laser diffraction and light scattering (Schiebe et al., 1983; Singer et al., 1988; Vitton and Sadler, 1997; Vitton et al., 1999; Sperazza et al., 2004), x-ray absorption (Stein, 1985; Singer et al, 1988, Vitton and Sadler, 1997; Vitton et al., 1999) and resistivity zone sensing (Walker and Hutka, 1971; Walker et al., 1974; Schiebe et al., 1983; Singer et al., 1988; Vitton et al., 1999). Although the principles behind the determination are completely different, the preparation of sample in general remained unchanged–clay particles must be completely dispersed in fluid for accurate measurement of particle size distribution.

Clay particles are lyophilic in nature due to electrical charge of the surface and are difficult to disperse completely in water (Verwey and Overbeek, 1948). Tchillingarian (1952) studied various dispersing agents and noted that sodium hexametaphosphate solution yield maximum defloculation capability. The concentration of fine grained soil in suspension must be very low (25 to 50 g per litre of solution) in order to avoid errors in measurements (Ke´zdi 1980; Schiebe, et al., 1983; Stein et al. 1985; BS 1377-2, 1990; ASTM D442-63, 2002). Besides the use of dispersing agents, the use of ultrasonic treatment has also been widely used to assists colloid stability (Walker and Hutka, 1971; Allen, 1974).

In the present study, three methods were used for determining the particle size of the clays. A Malvern MasterSizer X laser diffractometer (Fig. 3.1), a Beckman Coulter Multisizer 3 (Fig. 3.2) and a Micromeritics Sedigraph 5100 (Fig. 3.3) were used.

Fig. 3.1: *Malvern MasterSizer X*

Fig. 3.2: *Beckman Coulter Multisizer 3*

Fig. 3.3: *Micromeritics Sedigraph 5100*

Sodium hexametaphosphate solutions were prepared by mixing 33 g of sodium hexametaphosphate and 7 g of sodium carbonate with deionized water to make 1.0 litre of solution. A gram of air dry clay powder was used and dispersed in 50 ml of sodium hexametaphosphate solution and treated with ultrasonic bath for 15 minutes (Stein, 1985) prior to all tests conducted. The test results are presented in Figs 3.4, 3.5 and 3.6. Using Mastersizer X, the particle size of less than 2 µm was found to be 96.4% for MX80 bentonite,

97.18 % for Yellow bentonite and 97.92% for Speswhite kaolin. Similarly, using Coulter Multisizer 3, the particle size of less than 2 μm was found to be 99.63% for MX80 bentonite, 99.92% for Yellow bentonite and 99.97% for Speswhite kaolin. On the other hand, the Sedigraph showed that all the clays tested had particles of less than 2 μm throughout the entire testing period. In this case, the percent finer was found to be nearly 100%. The Sedigraph test results indicate that the particle remained in suspension throughout the testing period. Vitton et al. (1999) reported that Sedigraph provides excellent results in comparison to the hydrometer results for silty soils but the deviation increases with increase in soil plasticity for clayey soils.
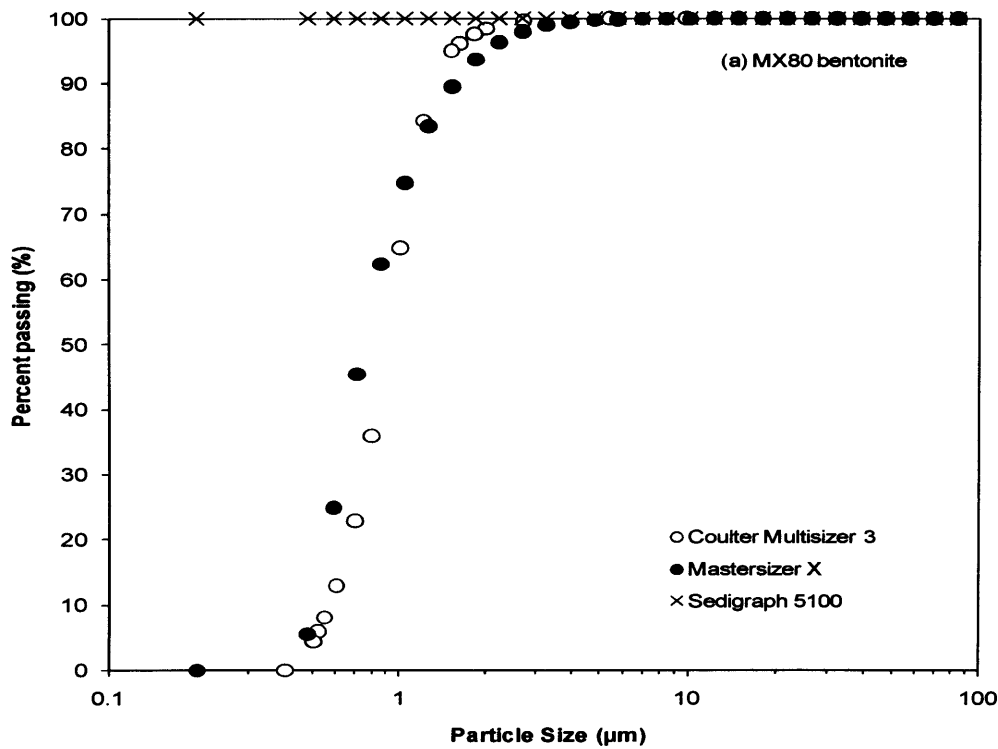
Fig. 3.4: *Comparison of particle size obtained from various methods for MX80 bentonite*
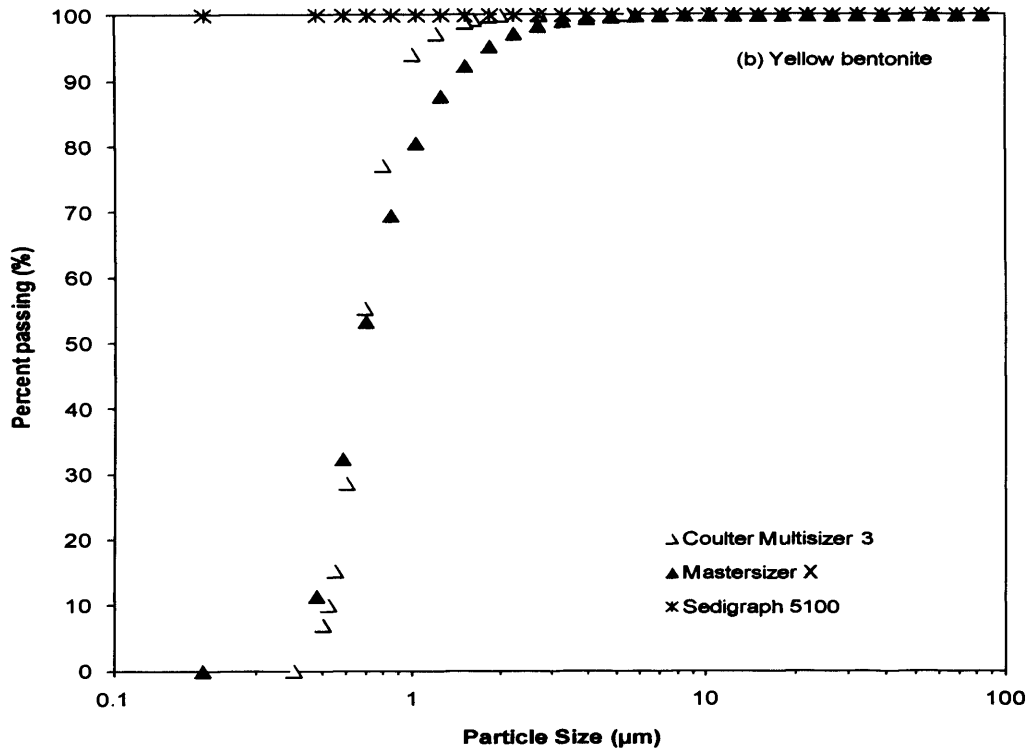
Fig. 3.5: *Comparison of particle size obtained from various methods for Yellow bentonite*
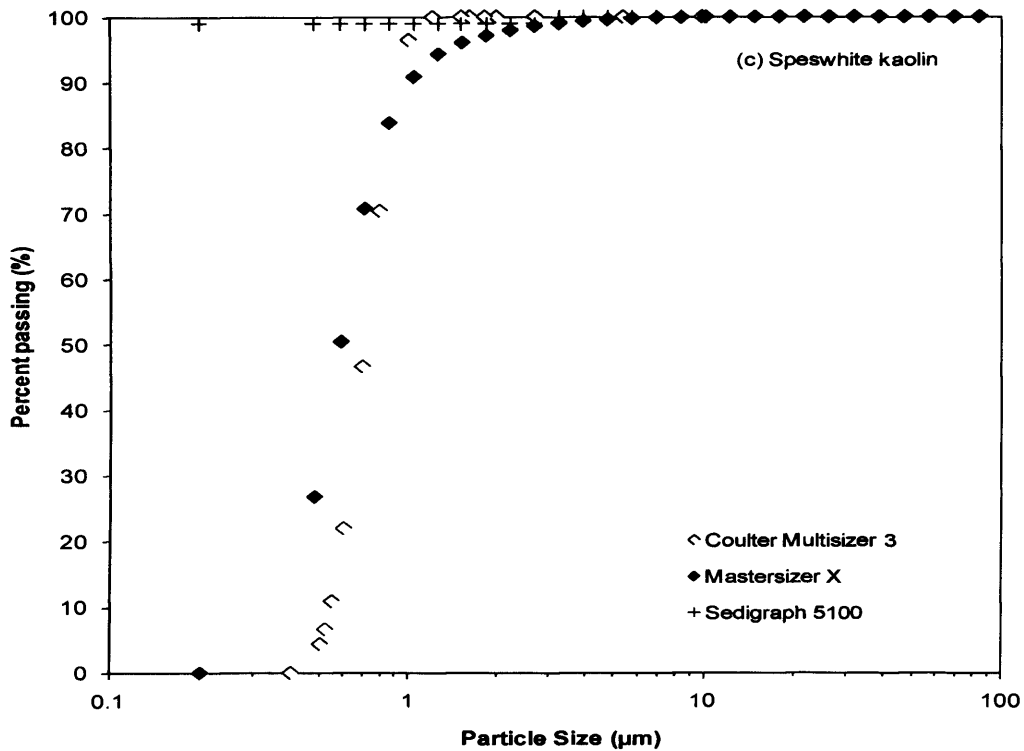
Fig. 3.6: *Comparison of particle size obtained from various methods for Speswhite kaolin*

Stein (1985) stated that for soil specimens having high clay content of about 50% or more are subjected to inaccuracy in measurements using the Sedigraph. Unlike silt and sand particles, once dispersed by dispersing agent and ultrasonic treatment, the clay fractions remain constantly in suspension. The suspended clay fractions are influenced by Brownian motion, thus affecting the accuracy of measurement (Schiebe et al., 1983). Stein (1985) also suggested that the use of sodium hexametaphosphate solution as a dispersing agent is not advisable in Sedigraph and will hinder the settling effects of clay fractions. Longer period of time is anticipated in order to determine the particle size of the clays using Sedigraph. A minimum period of 24 hours was suggested by Vitton et al., (1999). The tests results showed that automated systems can provide rapid and good producible data as compared to conventional and standardised methods of particle size analysis.

3.3.3 Hygroscopic water content

The hygroscopic water content is defined as film of water that adheres to the soil particle when in equilibrium with an atmosphere with a relative humidity of 50% at 20°C (Bear, 1972) and does not evaporate with ambient temperature (Levitt and Young, 2003). It should be identified in order to accurately prepare slurry or compacted specimens at a targeted dry densities. According to Hillel (1982), an air-dry soil will generally contain several percentage of water higher than oven-dried soil. The amount of water adsorbed depends upon the type of cations present and the specific surface area (Mitchell, 1993). The clays were oven-dried at 105 °C according to BS 1377-2 (1990) for 24 hours. The hygroscopic water contents were found to be 9.6%, 17.6% and 0.66% for MX80 bentonite, Yellow bentonite and Speswhite kaolin, respectively.

The water content for MX80 bentonite at laboratory condition was reported to be 8 to 11% (Villar and Gomez-Espina 2008). Similarly, Gattermann et al. (2001) reported that water content for divalent-rich bentonite is usually about 17% which is consistent with the water content determined for Yellow bentonite. The initial water content for Speswhite kaolin was found to be 0.6% less than reported by the manufacturer (about 1.2%).

3.3.4 Atterberg limits

The Atterberg limits (i.e. liquid limit, plastic limit and shrinkage limit) were determined following methods described in BS 1377-2 (1990) and ASTM D 4943-08 (2010). The liquid limit of MX80 bentonite, Yellow bentonite and Speswhite kaolin were found to be 437%, 135% and 51.4%, respectively as determined by cone penetrometer test at 20 mm penetration. The plastic limits of the clays were determined by the standard thread rolling method. The plastic limits of the clays were found to be 63%, 58% and 32% for MX80 bentonite, Yellow bentonite and Speswhite kaolin, respectively.

The shrinkage limits of the clays were determined following method described in ASTM D4943-08 (2010). Clay specimens were prepared at 1.2 times their respective liquid limit values and placed within a greased shrinkage dish. Mass measurements were conducted frequently until no further reductions were noted. The specimens were then removed for water content determination and volume measurement using wax method. The shrinkage limits of the clays were then calculated using Eq. 3.1.

$$SL(\%) = \frac{[(V - V_d)\rho_w]}{m_s} \times 100 \qquad\qquad \text{Eq. (3.1)}$$

58

The SL is the shrinkage limit, V is the volume of wet specimen (i.e. volume of the shrinkage dish in cm^3), V_d is the volume of dry soil, ρ_w is the density of water and m_s is the mass of dry soil. The shrinkage limit for MX80 bentonite was found to be 12.2%, whereas the shrinkage limits of 13.6% and 26.5% were determined for Yellow bentonite and Speswhite kaolin, respectively.

Typical value of liquid limit for montmorillonite is within the range of 100 to 900%, whereas the liquid limit for kaolinite is around 30 to 60% (Lambe and Whitman, 1969). Similarly, montmorillonite possesses significantly higher plastic limit value as compared to kaolinite (Mitchell, 1993). The shrinkage limit for kaolinite is greater than that of montmorillonite with a typical value ranging from 25 to 29% for kaolinite and 8.5 to 15% for montmorillonite (Lambe and Whitman, 1969; Mitchell, 1993). The liquid limit value was reported to be 512% for MX80 bentonite (Villar and Gomez-Espina, 2008), and 150 to 157% for Yellow bentonite (Johannesson and Nilsson, 2006) and 32% for Speswhite kaolin (Folly, 2001), similar to the values obtained in this study.

3.3.5 Mineral compositions

Mineral compositions of clays are commonly investigated using X-ray diffraction (XRD) method (Grim, 1968; Mitchell, 1993). According to Bragg's law, the XRD identifies minerals by relating the angle of incidence of the X-rays, θ, to the c-axis spacing, d. A complete XRD pattern consists of a series of reflections of different intensities and values of θ (Mitchell, 1993).

In the present study, a Philips PW1710 automated diffractometer along with PW3060 goniometer was used. Clay powders with hygroscopic water contents were tested (see Section 3.3.3). The diffractometer is equipped with a copper tube which generates X-rays by CuKα radiation at 35 kV and 40 mA. In order to investigate the mineral content of the clays, both bentonites were scanned from 2θ of 0° to 70°, whereas 2θ of 0° to 80° was used for Speswhite kaolin. Clay specimens are normally pretreated with ethylene glycol prior to XRD test (Likos and Lu, 2006). The glycolation process was adopted to discriminate between swelling and non swelling clays (Kunze, 1955; Brindley, 1966; Inoue et al., 1989; Sato et al., 1992; Mosser-Ruck et al., 2005).

The XRD charts are presented in Fig. 3.7. Semi-quantitative analyses were conducted to determine the percentage of minerals. The XRD test results indicated that the predominant mineral of MX80 bentonite used was montmorillonite (75%). The bentonite also contains other traces of minerals, such as cristobalite (15%) and quartz (10%). Similarly, Yellow bentonite was predominantly consists of montmorillonite (81%), whereas traces of graphite (19%) was also found. On the other hand, Speswhite kaolin consists of mainly kaolinite (95%) and traces of illite (5%).

Villar and Gomez-Espina (2008) reported that MX80 bentonite consists mainly of montmorillonite (65 to 82 %). Similarly, the montmorillonite content of high-grade Yellow bentonites is in the range of 75 to 80 % as reported by Carlson (2004). Similar amounts of other minerals, such as quartz and graphite found in the bentonites are consistent with the studies of Carlson (2004) and Villar and Gomez-Espina (2008).
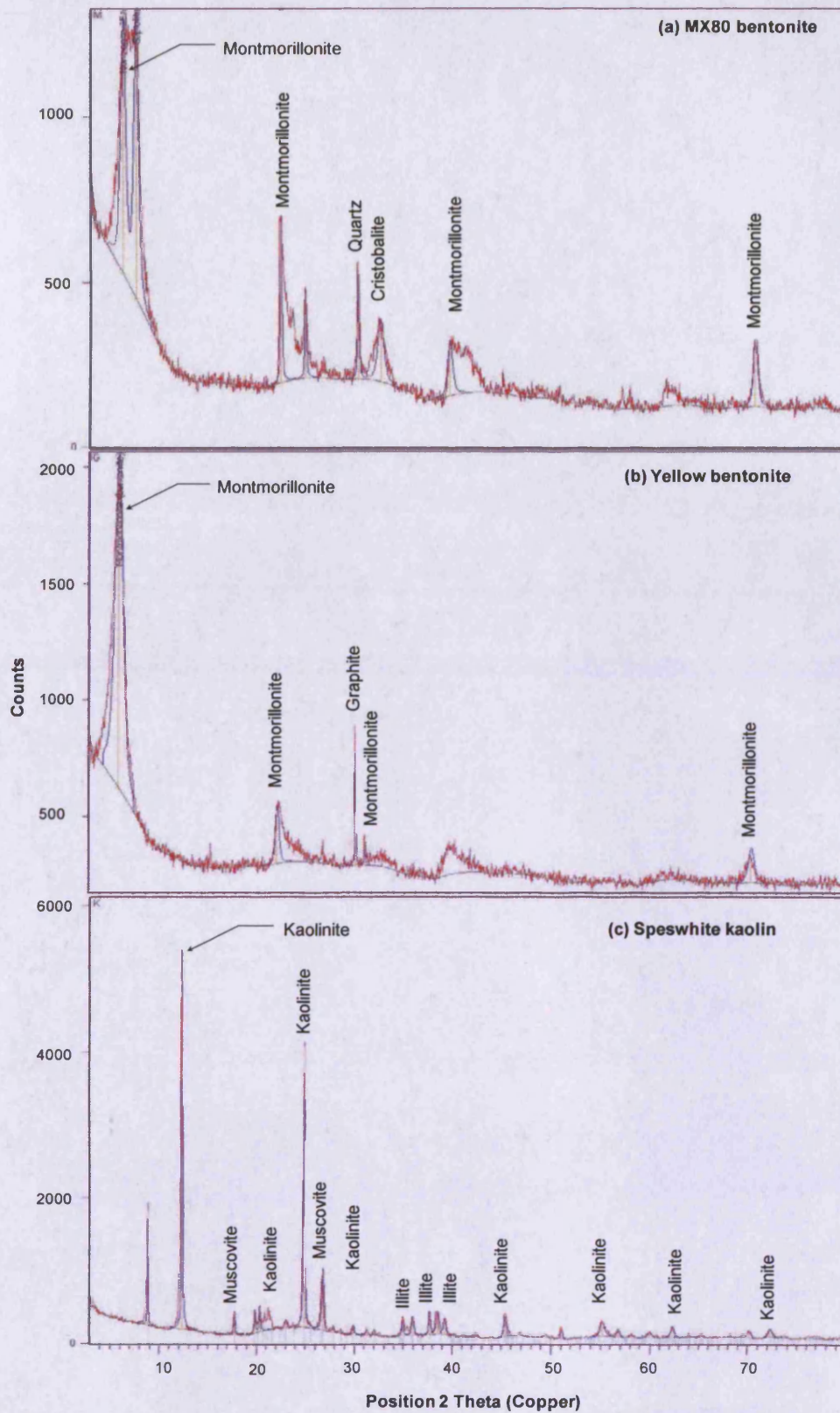
Fig. 3.7: *X-ray diffraction chart for (a) MX80 bentonite, (b) Yellow bentonite and (c)*

Speswhite kaolin

3.3.6 Specific surface area

There are various methods available to measure specific surface area of clays, either in dry or wet conditions. In both dry and wet methods, the measurements are conducted by forming a monolayer of adsorbate on the clay surface. Determination of surface area in dry condition involves gas adsorption using Brunauer-Emmett-Teller (BET) isotherm method (Grim, 1968; Allen, 1974). Nitrogen gas is usually used for this purpose. The BET method only measures the external surface area of swelling clays, as only limited amount of gas can be adsorbed into the interlayer space (Alymore et al., 1969; Santamarina et al., 2002), whereas in wet condition, adsorption and cation exchange take place thus both the internal and external surface areas are measured.

Various wet techniques for determining total surface area have been suggested. For instance, water sorption (Newman 1983), Methylene Blue Adsorption (Hang and Brindley 1969; Chen et al., 1991; Cokca, 2001; Santamarina et al., 2002) and Ethylene Glycol Monoethyl Ether (EGME) method (Eltantawy and Arnold, 1973; Churchman et al., 1991; Mitchell, 1993; Cerato and Lutenegger, 2002) are commonly used. Water molecules and ions which are held in clays with expanding minerals are located in the external and internal surfaces (Santamarina et al., 2002). Therefore, swelling clays usually possess higher values of specific surface area ranging from 800 to 1000 m^2/g (Lambe and Whitman, 1969; Mitchell, 1993; Saiyouri et al, 2000; Cerato and Lutenegger, 2002; Santamarina et al., 2002). Nonexpanding clay such as kaolinite typically has low specific surface area, ranging from 10 to 40 m^2/g (Grim, 1968; Mitchell 1993; Cerato and Lutenegger, 2002). In a recent study, Arnepalli et al. (2008) compared several methods for determining specific surface area of clays and noted

that EGME method yields the most reliable results. In this study, both external and total specific surface area of the clays were measured using BET and EGME methods.

3.3.6.1 External specific surface area - (BET) method

The external specific surface areas of the clays were measured using the Brunauer-Emmett-Teller Adsorption (BET) method using nitrogen gas as the adsorbate. A Flowsorb II 2300 specific surface area analyzer from Micromeritics was used in this study. The external specific surface area of MX80 bentonite, Yellow bentonite and Speswhite kaolin were found to be 19.77, 128.68 and 7.3 m^2/g, respectively. The external specific surface area for montmorillonite was reported to be in the range of 39.8 to 120 m^2/g (Alymore et al., 1969), whereas the external specific surface area of kaolinite was reported to be about 16 m^2/g (Grim, 1968).

3.3.6.2 Total specific surface area - (EGME) method

The total specific surface area of the clays were determined using EGME method. As EGME is a hazardous substance, the tests were conducted in a fume cupboard. The total specific surface area of MX80 bentonite and Yellow bentonite were found to be 676 and 797 m^2/g. These values are higher than that determined by BET method. The total specific surface area of Speswhite kaolin total specific surface area was found to be 7.8 m^2/g, similar to that determined by BET.

The total specific surface areas for both bentonites were lower than 800 m^2/g as reported in the literature (Lambe and Whitman, 1969; Mitchell 1993; Saiyouri et al, 2000; Cerato and

Lutenegger, 2002; Santamarina et al., 2002). The lower values of total specific surface area for both bentonites obtained are attributed to several factors. MX80 bentonite contains traces of other minerals such as quartz and cristobalite that contribute in reducing the specific surface area as compared to very pure montmorillonite (Saiyouri et al., 2000).

3.4 Chemical properties

3.4.1 Cation exchange capacity

The cation exchange capacity (CEC) or base exchange capacity is the ability of soil to retain certain amount of positively charged ions in exchangeable fashion on the negatively charge surface (Bache, 1976). The exchange capacity represents the amount of readily available exchangeable cations that can be replaced by leaching with a solution containing greater reactivity dissolved cations than the adsorbed cations (Grim, 1968; Mitchell, 1993). For any given soil, due to the environment and mineralogy conditions the CEC is neither a fixed nor a single value. The CEC is usually expressed in unit of positive charge (miliequivalent) per weight of dry soil or frequently in 100 g of dry soil (van Olphen, 1977). Typical value of CEC for montmorillonite is 80-150 meq/100g while less than 15 meq/100g was observed for kaolinitic clays (Grim, 1968; Mitchell, 1993).

Ross (1995) stated that laboratory measurements of CEC is not a direct measure but rather an estimated values based on the fractional and summed up of the total cations extracted. The general methods of measuring CEC are by ammonium acetate method (Chapman, 1965; Lavkulich, 1981) and the barium chloride compulsive exchange method (Hendershot and Duquette, 1986; Hendershot et al., 2007) by saturating the soil with NH_4^+ and Ba^{2+} at pH 7

(Grim, 1968). Significant portion of CEC is occupied by H^+ ions thus initial adjustments are required and that the use of extractant buffered at high pH (i.e. pH = 7) is necessary (Ross, 1995). This step is essential to neutralize the H^+ ions. Hence, the pH level must be kept consistent throughout the test. Mechlich (1938) suggested a pH of 8.2 to be used in CEC determination using barium chloride method. Burrafato and Miano (1993) noted that CEC of various montmorillonite, illite and kaolinite suspension can also be determined by surface tension measurement using hexadecylpyridinium chloride. This method although is simple and can provide satisfactory reproducible data, it is not widely used in the geotechnical engineering.

In this study, the CEC values for the clays were determined by ammonium acetate method at pH 7 following a simplified method suggested by Lavkulich (1981). 5 g of each clay were mixed with ammonium acetate solution in a 50 ml Whatman Vectaspin 20 centrifuge tube and ammonium hydroxide solution was used to increase the pH value to 7. A Jenway 3450 pH and conductivity meter was used as an indicator that the pH is at a constant level of 7. The samples were then placed into a centrifuge and subjected to a rotation of 115 rpm for 15 minutes. After agitation in the centrifuge, the mixtures were left to stand overnight. The clay solid fractions were then filtered using Whatman 42 filter paper with the assist of a vacuum pump to accelerate the extraction process. 30 ml of 1 M ammonium acetate solution were poured four times, by letting each portion filtered completely before pouring the next to rinse the clay samples. Sufficient care was taken not to allow samples to become dry or crack during this extraction process (Hendershot et al, 2007; Carter and Gregorich, 2007). The liquid extracted from each test was collected and then analyzed using Inductively Coupled Plasma Optical Emission Spectrometry (ICP-OES) manufactured by Perkin Elmer for various

fractional of cations (Na, K, Ca^{2+}, Mg^{2+} and Al^{3+}) and the total of the cation complexes were determined.

The fractions of ions obtained from ICP-OES are in mg/L. The results were then converted to meq/100g. Note that the conversion is sensitive to the solid to liquid ratio used in the test. Errors in solid to liquid ratio will overestimate or underestimate the CEC value converted from mg/L unit. The CEC value for MX80 bentonite was found to be 90.31 meq/100g. The CEC values of Yellow bentonite and Speswhite kaolin were found be 84.91 and 3.17 meq/100g, respectively. Carlson (2004) reported that CEC value for MX80 bentonite varied between 80 to 110 meq/100g. The CEC for Yellow bentonite reported by Carlson (2004) based on $BaCl_2$ method was 74.5 meq/100g, which is lower than the value determined in this study. The fractions of cations present within each clay also indicated that MX80 bentonite is predominantly consists of sodium ions (51.24 meq/100g), whereas Yellow bentonite is mainly calcium based (63.424 meq/100g).

The weighted average valencies of the clays were calculated. The weighted average valency of exchangeable cations is described by Tripathy and Schanz (2007) as the ratio of sum of the product of individual cation exchange complex and the valency of exchangeable cations to the total cation exchange capacity. These values can be used to assess the thickness of diffuse double layer for interacting clay platelets. An increase in weighted average valency will result in suppression of the midplane concentration and potential between interacting clay platelets, thus leading to a decrease in interplate repulsion (Mitchell, 1993). The weighted average valencies were 1.42, 1.90 and 1.55 for MX80 bentonite, Yellow bentonite and Speswhite kaolin, respectively.

3.5 Concluding remarks

The properties of the clays are summarised in Table 3.1. The physical and chemical properties determined in this chapter will be used for further analyses in the following chapters.

i.   The particle size using Mastersizer X and Coulter Mastersizer 3 showed nearly similar results. On the other hand, Sedigraph test results indicated that settling of clay particles was hindered and a longer period of time are required.

ii. Both bentonites are highly plastic since the bentonites contain high amount of montmorillonite. Thus, the swelling and volume change behaviour are expected to be significant as compared to that of Speswhite kaolin.

iii. Both bentonites have very high specific surface area, and very high CEC values. Thus, the water uptake capacity may be expected to be very high for the bentonites.

Table 3.1: *Summary of properties of clays in this study*

Properties	MX80 bentonite	Yellow bentonite	Speswhite kaolin
Specific gravity of soil, G_s	2.8	2.84	2.61
Liquid limit, w_L (%)	437	135	51.4
Plastic limit, w_P (%)	63	58	32
Shrinkage limit, w_S (%)	12.2	13.6	26.5
Specific surface area, S (m²/g)	676	797	7.8
Cation exchange capacity, B (meq/100g)			
Na^+	51.24	7.66	1.06
Ca^{2+}	28.24	63.42	1.09
Mg^{2+}	9.43	12.97	0.66
K^+	1.40	0.86	0.37
Al^{3+}	0	0	0
Weighted average valence of exchangeable cations*	1.42	1.90	1.55
Grain size distribution			
< 75 μm (%)	100	100	100
< 2 μm (%)	96.4	97.18	97.92
Mineral compositions			
Montmorillonite (%)	75	81	-
Kaolinite (%)	-	-	95
Illite (%)	-	-	5
Quartz (%)	10	-	-
Graphite (%)	-	19	-
Cristobalite (%)	15	-	-

Note: * *ratio of the sum of the product of individual cation exchange complex and valence of exchangeable cations to the total cation exchange capacity*

CHAPTER 4

EXPERIMENTAL METHODS

4.1 Introduction

This chapter presents the experimental methods adopted and several devices that were used in this study. A detailed experimental programme was planned and several laboratory tests were carried out. Various techniques were used to establish the drying suction-water content SWCCs, such as centrifuge technique, axis-translation technique (pressure plate tests), osmotic technique (osmotic tests) and vapour equilibrium technique (desiccator tests). After the osmotic tests, chemical analyses of the PEG solutions were carried out using Inductively Coupled Plasma Optical Emission Spectrometry (ICP-OES) to verify osmotic suction equilibrium on either side of the semipermeable membrane. Additionally, in order to explore an intrusion of PEG molecules during osmotic tests, Fourier transform infrared spectroscopy (FTIR) was used to study any degradation of PEG molecules with elapsed time. Atomic force microscopy (AFM) was used to examine the pore structure changes of the semipermeable membrane used.

The void ratios of clay specimens during the drying process were measured using wax method in order to establish the suction-void ratio SWCCs. Clay specimens tested in pressure plate and desiccator tests were considered for this purpose. The water content-void ratio shrinkage paths were established using Clod test. The Clod test results along with suction-

water content SWCCs enabled establishing the suction-degree of saturation SWCCs of the clays.

The wetting suction-water content SWCCs under various confining conditions (unconfined, laterally confined and isochoric) were determined using volumetric pressure plate extractor, osmotic technique (osmotic tests) and vapour equilibrium technique (desiccator tests). The water content versus suction relationships of the clays were established using chilled-mirror dew-point technique. The swelling pressures of compacted bentonites were determined under isochoric condition. A modified oedometer was used for this purpose. Additionally, a newly developed suction controlled oedometer was used to study the influence of suction on the swelling pressure and the water content of the bentonites. Microstructural studies (ESEM and XRD) were also undertaken to explore the micstructural and c-axis spacing changes during the wetting process.

The chapter is presented in the following order. The first part of the chapter presents the specimen preparation methods, the methods used for determination of the suction-water content SWCCs during drying and wetting processes, the chemical analyses of PEG solutions in the osmotic tests, followed by the methods adopted for FTIR and the AFM analyses. The chilled-mirror device used for establishing the water content versus suction relationships is presented. Volume measurement using Clod and wax methods and the measurement of swelling pressures of the bentonites are then presented. Subsequently, the ESEM and XRD devices used in the determination of microstructure of the clays are presented. The concluding remarks are presented towards the end of the chapter.

4.2 Specimen preparation

Clay specimens were prepared in various forms, such as loose powders, compacted and saturated slurry conditions. Powder and compacted specimens were used in the wetting tests to establish the wetting suction-water content SWCCs, whereas the saturated slurried specimens were prepared for establishing the drying suction-water content SWCCs and drying suction-void ratio SWCCs. The Clod tests were carried out on initially saturated specimens. The slurried specimens were first subjected to a suction of 0.05 MPa in the pressure plate prior to the Clod tests. The detailed procedure are later described in Section 4.5.1.

4.2.1 Saturated slurried specimens

Clay specimens were prepared by mixing air dried clay powders thoroughly with deionised water at targeted water content equals to 1.2 times the respective liquid limits of the clays. The purified water used in this study was high quality laboratory standard 18-megohm deionised water. The clay-water mixtures were then stored in sealed plastic bags and kept in air tight containers to allow for water equilibration to take place for about seven days prior to being tested.

4.2.2 Compacted specimens

In this study, small cylindrical compacted specimens were considered. The clay specimens were prepared by statically compacting clay powders to various targeted dry densities at hygroscopic water contents of the clays (see Section 3.3.3). A special compaction mould was

designed and fabricated to facilitate the compaction of clay specimens. Figure 4.1 shows the compaction mould used in this study.
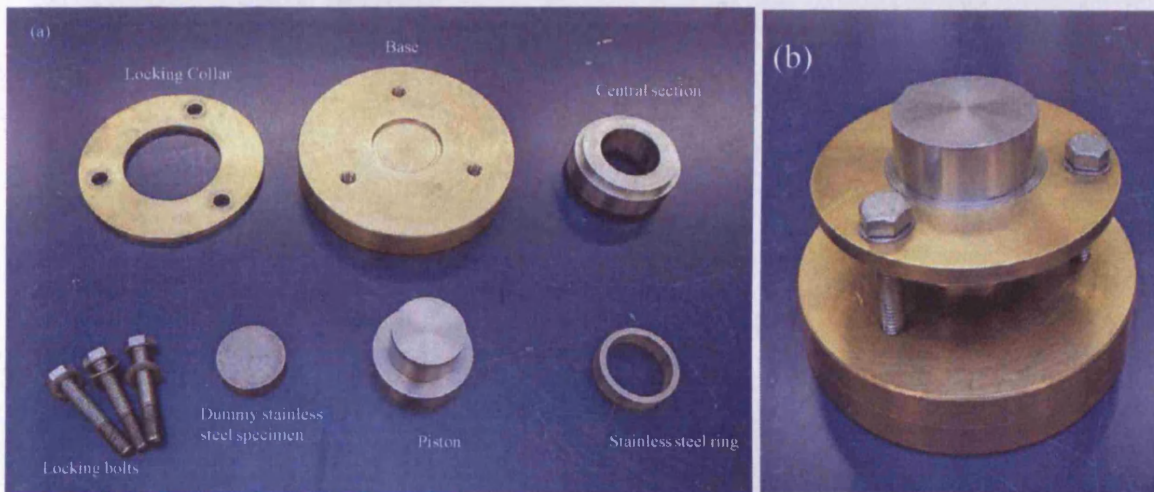
Fig 4.1: *Static compaction mould, (a) components of compaction mould and (b) assembled compaction mould*

The compaction mould consists of a brass base, a stainless steel central section, stainless steel specimen ring, a locking collar, a piston and three locking bolts. The central section holds a specimen ring into position and at the same time accommodates clay powder during the compaction process. The central section also guides the piston in the vertical direction during compaction. Two specimen rings were used in this study; a 45 mm in diameter x 12 mm height and a 42 mm diameter x 12 mm height. The specimen rings were lubricated with silicon grease to prevent cracking of the specimens. The compaction of clay specimens were conducted using a stress controlled compression testing machine. The clay specimens were prepared at targeted dry densities of 1.2, 1.3, 1.4, 1.5, 1.6 and 1.7 Mg/m^3.

Typical pressures required to statically compact MX80 bentonite specimens in a 42 mm x 12 mm specimen ring to targeted dry densities are presented in Table 4.1. Table 4.1 indicated that the applied pressure increased with an increase in the dry density of the clay specimens.

A vertical pressure of 54.2 MPa was required to prepare compacted specimen at targeted dry density of 1.7 Mg/m^3, whereas a vertical pressure of 4.3 MPa was required to prepare specimen to a dry density of 1.2 Mg/m^3. Similar vertical pressures were applied to prepare specimens of Yellow bentonite and Speswhite kaolin.

Table 4.1: *Applied pressure during specimen preparation*

Targeted dry density (Mg/m^3)	Compaction Load (kN)	Cross sectional area of specimens (m^2)	Applied pressure MPa
1.2	6		4.3
1.3	9		6.5
1.4	15		10.8
1.5	21	1.38×10^{-3}	15.2
1.6	50		36.1
1.7	90		54.2

4.2.2.1 Confining conditions during the wetting tests

4.2.2.1.1 Compacted specimens tested under unconfined condition

Directly after compaction at desired dry densities, the compacted specimens were extruded from the specimen rings. The extruded compacted specimens were then equilibrated at various applied suctions. In this case, it was found that specimen compacted at targeted dry density of 1.2 Mg/m^3 crumbled upon extrusion. Thus, under unconfined condition, bentonite specimens were compacted at targeted dry densities of 1.3, 1.4, 1.5, 1.6 and 1.7 Mg/m^3, whereas specimens of Speswhite kaolin were compacted to targeted dry densities of 1.3 and 1.4 Mg/m^3.

4.2.2.1.2 Compacted specimens tested under laterally confined condition

Bentonite specimens were compacted at targeted dry density of 1.2, 1.3, 1.4, 1.5, 1.6 and 1.7 Mg/m^3, whereas specimen of Speswhite kaolin were compacted to targeted dry density of 1.2, 1.3 and 1.4 Mg/m^3. The compacted specimens were directly tested at various applied suctions after compaction. The stainless steel specimen rings served as lateral confinement to the compacted specimens during the wetting tests.

4.2.2.1.3 Compacted specimens tested under isochoric condition

Under isochoric condition, compacted specimens were tested using a modified oedometer and a newly developed suction controlled oedometer. Compacted specimens were prepared similar to that of unconfined specimens. Only the bentonites were considered in this case. Bentonite specimens compacted at targeted dry densities of 1.2, 1.3, 1.4, 1.5, 1.6 and 1.7 Mg/m^3 were prepared for the swelling pressure tests in the modified oedometer. However, only one dry density was considered for swelling pressure tests under suction controlled conditions. In this case, bentonite specimens were compacted at targeted dry density of 1.7 Mg/m^3.

Directly after compaction, the compacted specimens were extruded from the stainless steel rings. Once extruded, the specimens expanded. Therefore, it was not possible to directly reinsert the bentonite specimens into the rings. Reinserting the specimens into the rings required resizing of the specimens. Resizing was done by using fine sand paper. Finally, the specimens were reinserted into the stainless steel specimen rings before being placed inside the oedometer cells. The extrusion and reinsertion of the bentonite specimens were carried

out for two specific reasons, (*i*) to imitate the actual field condition (i.e. bentonite blocks are usually compacted in factories, and transported to sites) and (*ii*) to eliminate the post-compaction residual stress effects.

4.3 Suction-water content SWCCs

The drying suction-water content SWCCs were established using centrifuge technique, axis-translation technique, osmotic technique and vapour equilibrium technique, whereas the wetting suction-water content SWCCs were determined using volumetric pressure plate extractor, osmotic technique and vapour equilibrium technique. Additionally, chilled-mirror dew-point technique was considered for establishing water content versus suction relationships of the clays. The methods used are described in the following sections.

4.3.1 Centrifuge technique

Centrifuge technique was used to determine the water contents of the initially saturated slurried clay specimens at an applied suction of 0.007 MPa. Gardner's (1937) equation (Eq. 4.1) was used to relate suction imposed with the rotational speed and the height of specimen.

$$\psi = \frac{\rho_w \omega^2}{2g}(r_1^2 - r_2^2)$$

Eq. (4.1)

The suction of soil specimen in kPa, ψ, is related to the radial distance to the mid-point of the soil specimen, r_1, and the radial distance to the free water surface, r_2. By increasing the

angular velocity, ω, the gravitational force, g, applied on the clay specimens increased. In Eq. 4.1, ρ_w is the density of water.

A Sigma 6K15 refrigerated centrifuge was used. The centrifuge used in this study is shown in Fig. 4.2. The centrifuge consists of 4 swinging buckets connected to the rotor and temperature control panel. The temperature of the testing chamber was set to at 25 °C. Saturated slurried clay specimens were placed in the centrifuge insert tube filters of Whatman Vectaspin 20 micro centrifuge tubes (Fig.4.3a). The 20 ml insert tube filter has a 0.45 μm polysulfone membrane at the bottom of the tube and able to retain the soil sample in place throughout the test (see Fig. 4.3a). The slurried specimen along with the tube filter was then inserted into the centrifuge tube. The top part of the centrifuge tube was then fastened with the top cap.

Fig. 4.2: *Sigma 6K15 refrigerated centrifuge*

A special holder (Fig. 4.3b) was place inside the bucket to firmly hold the specimen in place when the test was commenced. Each specimen holder has the capacity of holding three centrifuge tubes, and twelve specimens can be placed simultaneously.
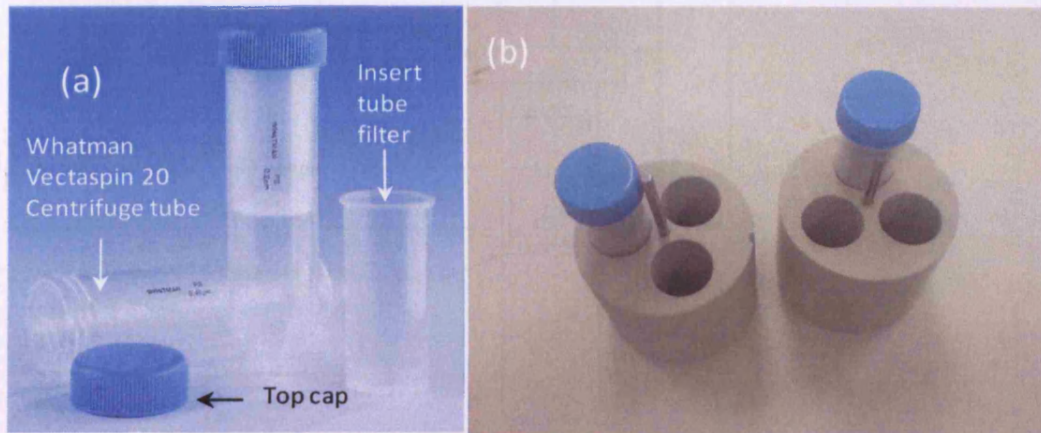
Fig 4.3: (a) *Whatman Vectaspin 20 micro centrifuge tube and insert filter, (b) Centrifuge tube holder*

Figure 4.4a shows the schematic diagram of the tube. During testing, the position of the tube changes from vertical position to horizontal position (Fig. 4.4b). Unlike specimens holder proposed by Khanzode et al. (2002), the limitation of using centrifuge tubes is that the height of specimens will remain fixed at all times. It was noted that the tubes are fragile and prone to breakage at high gravitational force. Single rotation speed of 2500 rpm was used in this study. Thus, only one suction was achievable using centrifuge technique.
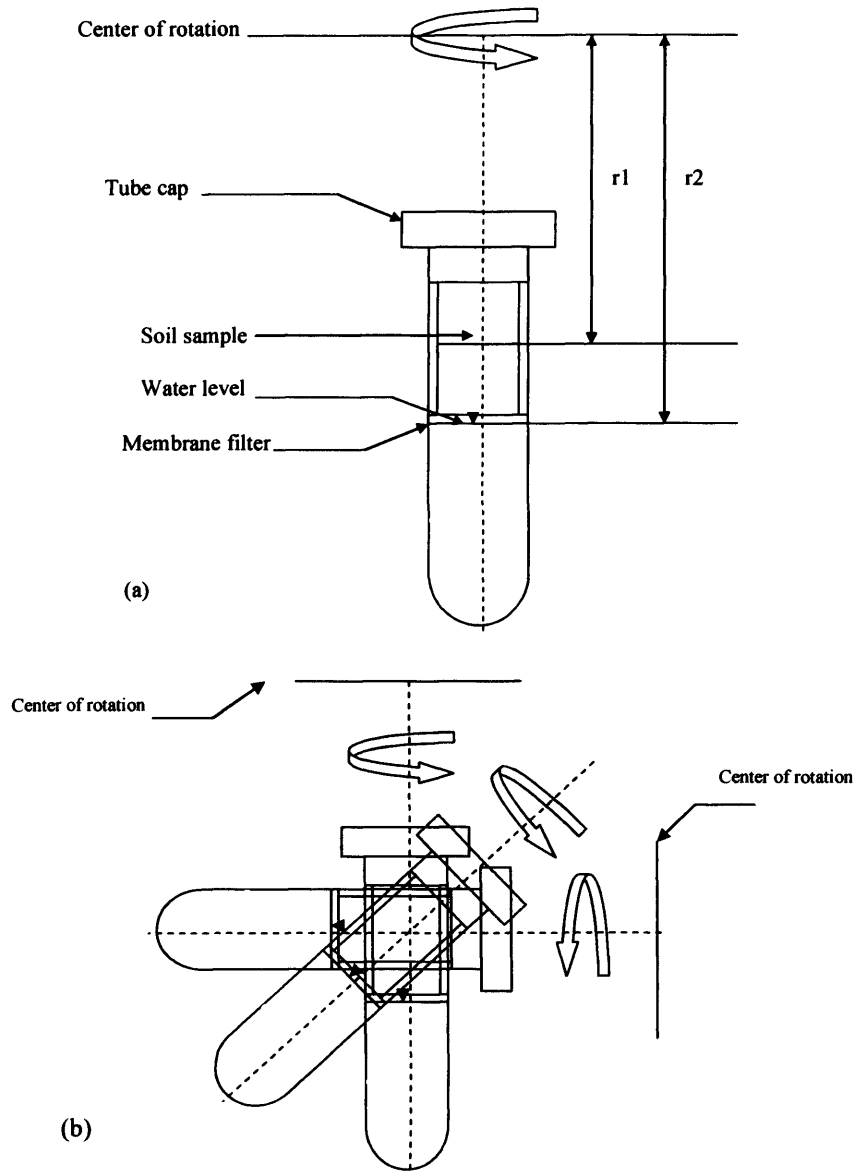
Fig. 4.4: *(a) Schematic diagram of centrifuge tubes, (b) schematic demonstrates the tubes*

assume horizontal position during centrifugation

4.3.2 Axis-translation technique

4.3.2.1 Pressure plate extractor

Pressure plate tests were carried out to apply matric suctions of 0.05, 0.1, 0.2 and 0.4 MPa using a 5-bar pressure plate extractor from Soilmoisture Equipment Corporation. Figure 4.5 shows the pressure plate used in this study.

Fig. 4.5: *5-bar pressure plate extractor*

The main components of the pressure plate apparatus are a high-air entry ceramic disc, a pressure chamber, a water compartment and an air supply system. The water outlet in the pressure plate apparatus was connected to a burette for flushing purpose and for collecting water that expelled out of the specimens. Before commencement of the tests, it is crucial to saturate the ceramic disc with deionised water to remove any entrapped air (Soilmoisture, 2008a). During the flushing process, the water compartment located between the ceramic disc and the neoprene membrane was filled with approximately 500 ml of deionised water. Deionised water was subsequently poured on the ceramic disc surface. Flushing of the

ceramic was done by applying an air pressure of 0.05 MPa until all air bubbles were completely removed.

In order to establish the drying suction-water content SWCC and the drying suction-void ratio SWCCs, saturated slurried specimens were prepared in stainless steel specimen rings and transferred onto the ceramic discs. The stainless steel rings were lubricated with silicon grease to avoid development of desiccation cracks during drying (Peron et al., 2007). Pre-wetted Whatman 3 filter paper was used as a separation material to avoid loosing of clay particles and blocking the pores of the ceramic disc. A thin layer of water was left on the ceramic disc prior to the specimens being placed on the ceramic disc in order to provide good contact between clay specimens and the ceramic disc (Cresswell et al., 2008).

For each clay, a total number of nine specimens were considered. At an applied suction of 0.05 MPa, three duplicate clay specimens were tested. One specimen was prepared for the Clod test, whereas the other two specimens of each clays were used for water content determination and for volume measurement using wax method. On the other hand, at applied suctions of 0.1, 0.2 and 0.4 MPa, only two specimens were used, one each for water content determination and volume measurement using wax method. The clod test and wax method are described later in Section 4.5. For reproducibility of the test results, the tests were repeated three times. A total number of 27 specimens were tested for each clay.

Resaturation of the ceramic disc and flushing process were repeated after 3-4 days and the change in mass of individual specimens were measured at the same time. The mass of the clay specimens were monitored periodically to infer the suction equilibration. Specimens

equilibrated at applied suctions were then removed for water content determination by oven-drying method and void ratio measurement using wax method.

4.3.2.2 Volumetric pressure plate extractor

The suction-water content relationship during wetting and drying process can be established using a volumetric pressure plate apparatus (Soilmoisture, 2008b). The device has the ability to apply suctions between 0.05 and 0.2 MPa (Fredlund and Rahardjo, 1993). A 2-bar volumetric pressure plate extractor from Soilmoisture Equipment Corporation (Fig. 4.6) was used in this study.

Fig. 4.6: *2-bar volumetric pressure plate*

The ceramic disc of the volumetric pressure plate extractor was initially removed and immersed in deionised water. Low vacuum was applied to remove entrapped air bubbles and to fully saturate it. After the saturation process was completed, a thin layer of water was left on the surface of the ceramic disc.

In this study, only wetting tests were carried out using the volumetric pressure plate extractor. The wetting suction-water content SWCCs were established for applied suctions of 0.05, 0.1

and 0.2 MPa. Hysteresis attachment was not used in this study; instead both inlet and outlet of the volumetric pressure plate were connected to burettes. The burettes were used as reservoir that supplied water to the clay specimens during the wetting tests.

Clay powders and compacted specimens were placed on top of the ceramic disc separated by a filter paper. Bentonite powders compacted at targeted dry densities of 1.2, 1.3, 1.4, 1.5, 1.6 and 1.7 Mg/m^3 were considered, whereas Speswhite kaolin specimens were compacted to dry densitie of 1.2, 1.3 and 1.4 Mg/m^3. For the wetting tests, two confining conditions were considered, namely unconfined and laterally confined conditions.

4.3.3 Osmotic Technique

Osmotic technique (Zur 1966; Kassif and Ben Shalom 1971; Delage et al. 1998; Delage and Cui 2008b; Delage et. al 1998; Monroy et al, 2007; Cui et al. 2006; Blatz et al., 2008) was used for establishing both drying and wetting suction-water content SWCCs. Drying of slurried clay specimens were carried out at applied suctions of 0.5, 0.11, 0.44, 0.99, 1.76, 2.75, 3.96, 5.39, 7.04, and 8.91 MPa. On the other hand, the technique was used up to an applied suction of 3.96 MPa for the wetting tests. Only dry clay powders were considered for the wetting tests.

Polyethylene glycol (PEG) 20000 along with Spectra/Por cellulose acetate semipermeable with molecular weight cut-off value (MWCO) of 14000 were used for applying applied suctions up to 3.96 MPa, whereas PEG 6000 and MWCO 3500 semipermeable membrane were used for applying suctions greater than 4.0 MPa. Deionized water was used for

preparing the clay-water mixtures as well as for preparing the PEG solutions. The solutions were prepared according to the calibration curve reported by Delage et al. (1998).

As the concentration of the PEG is directly linked to the osmotic potential, any changes in the concentration will affect the suction applied to the clay specimen. Delage et al. (1998) suggested an empirical relationship (Eq. 4.2) to relate the concentration of PEG with the applied suctions.

$$s = 11 \ c^2$$ Eq. (4.2)

The applied suction, s, is related to the square of the PEG solution concentration in g of PEG/g of water, c.

During the tests, the concentration of PEG was frequently monitored using a commercially available optical handheld refractometer to ensure that the applied suctions remained constant throughout the testing period. Refractometers are usually used for measuring the concentration of sugar. PEG chains consist of organic compounds, similar to compounds found in sugar. The refractometer used was capable of measuring the Brix Index of the solutions from 0-50%. The Brix value corresponds to refractive value of anhydrous saccharose (0% being pure water and 100% being pure anhydrous saccharose) (Delage et al., 1998). A similar device has been used by Delage and Cui (2008a).

Figure 4.7 shows the measured Brix index versus concentration of PEG plot reported by Delage et al. (1998). The PEG concentration and the corresponding Brix index measured in this study are plotted in Fig.4.7. The Brix index increases with an increase in the

concentration of PEG solutions. Figure 4.7 indicated that the Brix index values measured were similar to the values reported by Delage et al. (1998).
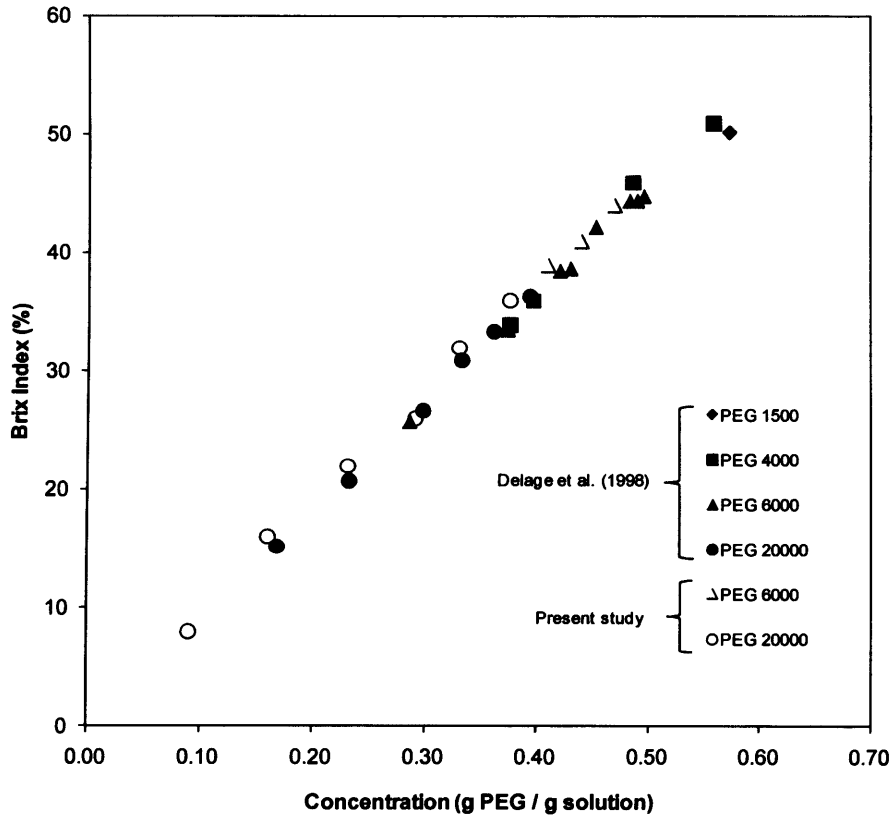
Fig. 4.7: *Measured Brix index versus PEG concentration plot*

The semipermeable membranes used in this study were first immersed in deionized water for approximately 30 minutes to remove the glycerine preservatives coating prior to the tests (Delage and Cui 2008a). For the drying tests, saturated slurried clay specimens were carefully inserted in to the cylindrical shaped membranes. For the wetting tests, air dried clay powders were carefully inserted into the membranes. Both ends of the semipermeable membrane were then fastened using special polypropylene dialysis clips prior to immersing them in the PEG solutions stored in a hollow cylindrical flask. The test setup is shown in Fig. 4.8. The top of the flask was covered with a plastic cover to avoid evaporation to occur during the tests. Magnetic stirrers were used to homogenize the PEG solutions during the tests. For some

applied suctions, the mass of the clay specimens were monitored periodically to infer the

suction equilibration. The tests were usually carried out for a period of 7 to 15 days.
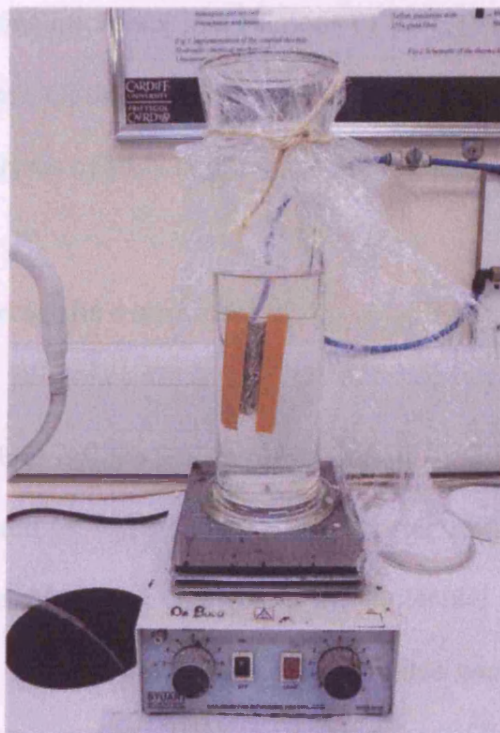
Fig. 4.8: *The test setup for osmotic tests*

The concentration of PEG solution is sensitive to temperature changes (Marcial et al., 2002). The heat produced from electrical magnetic stirrer may change the concentration of PEG and hence the suction imposed. It was suggested that the test may be carried out in a temperature controlled water bath (Delage et al., 1998; Marcial et al., 2002; Cuisinier and Masrouri, 2004). In this study, the tests were conducted in a temperature controlled room at near constant temperature of 25 °C.

4.3.3.1 Chemical analysis of PEG solution in osmotic tests

Measurements of cation concentration in the PEG solutions before and after completion of the osmotic tests were carried out at applied suctions of 0.11, 0.44, 3.96, 5.39 and 8.91 MPa. Inductively Coupled Plasma Optical Emission Spectrometry (ICP-OES) was used for this purpose. The chemical analyses of PEG solutions are presented in Chapter 6.

4.3.3.2 PEG intrusion during the osmotic tests

In order to explore the factors influencing the intrusion of PEG intrusion during the osmotic tests, two very specific studies were undertaken. Fourier transformation infrared (FTIR) spectroscopy was used to explore any changes in the molecular structure of PEG molecules with elapsed time. Atomic force microscopy (AFM) studies were carried out to explore the pore structure of the MWCO 14000 and MWCO 3500 semipermeable membranes before and after the osmotic tests.

Drying tests were conducted on initially saturated slurried MX80 bentonite specimens using osmotic technique. Applied suctions of 0.44 and 7.04 MPa were considered. PEG 20000 was used along with Spectra/Por® MWCO 14000 membrane for applying a suction of 0.44 MPa, whereas PEG 6000 was used along with Spectra/Por® MWCO 3500 membrane for applying a suction of 7.04 MPa.

4.3.3.2.1 FTIR spectroscopy (degradation of PEG molecules)

PEG degradation can be studied using various techniques, such as using X-ray diffraction (XRD) technique, X-ray Photoelectron Spectroscopy (XPS), and Fourier Transform Infrared (FTIR) spectroscopy (Han et al., 1995; Celina et al., 1997; Beamson et al., 2000). The FTIR is a rapid and non-destructive technique for identifying molecular structures and degradation of organic based polymers (Roberts & Caserio, 1965; Han et al., 1995).

FTIR spectroscopy was conducted to explore any changes in the molecular structure of PEG molecules with elapsed time. PEG 20000 and PEG 6000 solutions were prepared at applied suction of 0.44 and 7.04 MPa. Freshly prepared PEG solutions and solutions aged 15 for days were tested.

4.3.3.2.2 AFM study of semipermeable membranes

Atomic Force Microscopy (AFM) is a form of scanning probe microscopy (SPM) that performs high resolution imaging function by measuring property of a surface, such as the height, optical absorption, or magnetic properties (Cosgrove, 2010). The AFM employs a small piezo element mounted under a cantilever to make it oscillate at its resonance frequency. The changes in the oscillation usually involve a decrease in resonant frequency, a decrease in amplitude, and a phase shift. Changes in oscillation characteristics can be used to generate a map that characterizes the surface of the sample and information on the topography. The advantages of AFM over electron microscopy are: (*i*) it generates true, 3-dimensional surface images; (*ii*) it does not require special sample treatments; and (*iii*) it does not require a vacuum environment in order to operate. On the other hand, The AFM is slow at

constructing images as compared to almost real-time observation using a scanning electron microscope.

An Atomic Force Microscope (AFM), Multimode III Scanning Probe Microscope from Veeco (Digital Instruments), was used to scan the topography of the membranes prior and after the completion of the osmotic tests. After the completion of the osmotic tests, the membranes were carefully removed and rinsed before being transferred to the device.

4.3.4. Vapour equilibrium technique

Vapour equilibrium technique was implemented by controlling the relative humidity in an air space above saturated salt solutions in a closed system. This method controls total suction (Fredlund and Rahardjo, 1993; Delage et al., 1998; Tang and Cui, 2005; Blatz et al., 2008). The tests were carried out in closed-lid desiccators for inducing suctions of 3.3, 7.5, 21.9, 38.2, 114.1 and 296.7 MPa using saturated salt solutions of K_2SO_4, KNO_3, KCl, NaCl, K_2CO_3, and LiCl, respectively. Figure 4.9 shows the test desiccators used in the study. All tests were carried out at near constant temperature of 25 °C.

Fig. 4.9: *Desiccator test setup*

Total suction can be described in terms of the free energy state of soil pore water, which can be measured in terms of relative humidity (Fredlund and Rahardjo, 1993; Likos and Lu, 2002; Leong et al., 2003). The relationship between total suction, ψ, and relative humidity, RH, can be described by Eq. 4.3 (Fredlund and Rahardjo, 1993).

$$\psi = -\frac{RT}{v_{w0}\omega_r}\ln\left(\frac{u_v}{u_{v0}}\right) = -\frac{RT}{v_{w0}\omega_r}\ln(\frac{RH}{100})$$

Eq. (4.3)

where u_v and u_{v0} is the partial pressure of water vapour and the saturation pressure of pure water vapour, v_{w0} is the specific volume of water (m^3/kg), ω_r is the molecular mass of water vapour (18.016 kg/kmol), R is the universal gas constant (8.31432 J mol^{-1} K^{-1}), T is the absolute temperature in Kelvin and RH is the relative humidity.

For the drying tests, initially saturated slurried clay specimens were first subjected to a matric suction of 0.4 MPa in pressure plates before being transferred to the test desiccators. The initial drying was found to be appropriate to speed up the drying process as drying in desiccators alone generally requires a longer testing period. The mass changes of the specimens were monitored and the water contents of the specimens were determined using oven drying method. The suction-water content SWCCs were then established for all three clays studied.

For establishing the wetting suction-water SWCCs for the clays, multiple powder and compacted specimens were considered. For the compacted specimens, two confining conditions were considered, namely unconfined and laterally confined conditions. Figure 4.10 shows the compacted specimens placed within the desiccators.
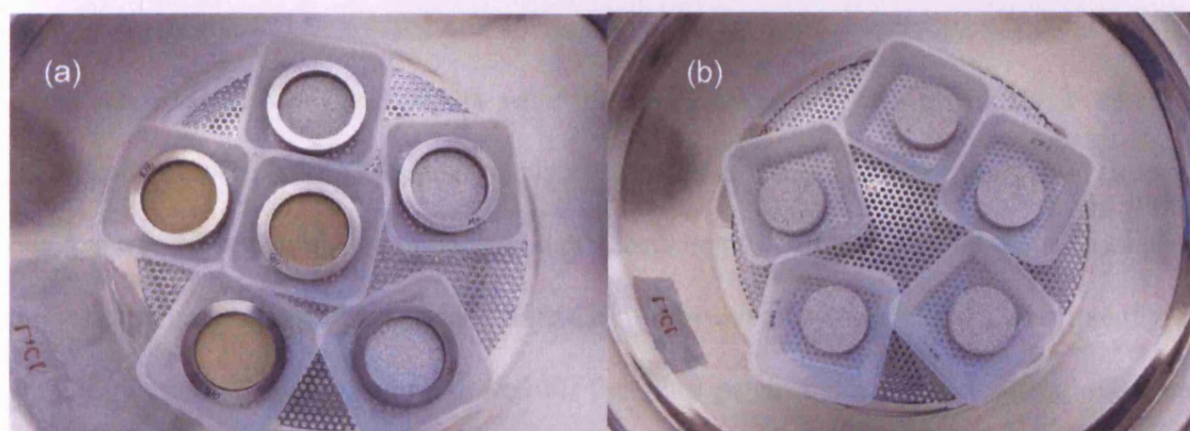
Fig. 4.10: *Compacted specimens within the tests desiccators, (a) laterally confined*

specimens and (b) unconfined specimens

Figures 4.10a and b show laterally confined specimens and unconfined specimens, respectively. The specimens were placed inside plastic containers before being transferred into the test desiccators. A stainless steel mesh was used to separate the salt solutions from being in contact with the clay specimens. The mass of the clay specimens were monitored periodically to infer the suction equilibration. Once the specimens were equilibrated at each applied suction, the specimens were removed for water content determination by oven drying method.

4.3.4.1 Verification of total suction applied in desiccator tests

Verification of the applied total suction in the desiccator tests were carried out using the filter paper method and relative humidity sensors.

4.3.4.1.1 Filter paper method

The filter paper method was only used in the desiccator tests to verify the applied suctions. In the present study, the non contact filter paper method was adopted. Whatman No. 42 was

used to verify the RH generated and suction imposed by several aqueous salt solutions. The initial mass of the test filter papers were measured using a 0.0001 g balance. Further, the filter papers were placed inside a plastic container before being transferred into the desiccators. After equilibrium was established between the filter paper and the salt solutions, the water content of the filter paper was measured by oven drying method. Subsequently, the applied suction were determined based on the filter paper water contents using calibration curve following ASTM D5298-03 (2010).

4.3.4.1.2 Relative humidity sensors

Verifications of the applied suctions in the desiccator tests were also carried out by using a handheld Rotronic Hydrolog relative humidity and temperature sensor. Figure 4.11 shows the humidity probe used in this study.
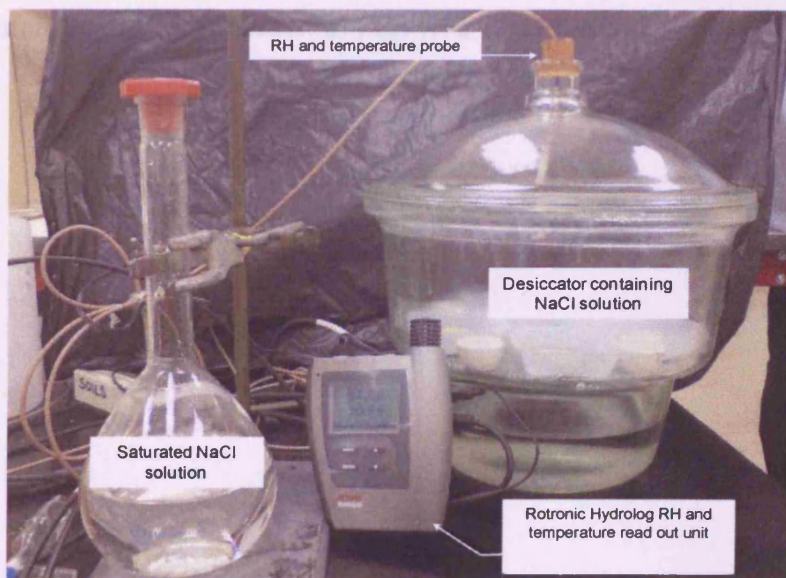
Fig. 4.11: *Rotronic Hydrolog relative humidity probe*

The RH sensor is coupled with a temperature sensor. The probe utilizes the step phase system where the readings were taken at constant time intervals. The probe was initially calibrated using two point calibration method with known RH generated by two salt solutions. Saturated NaCl and KCl saturated solutions were used in this study for calibrating the sensors. During the calibration process, the sensor was placed above the salt solution in an air tight closed volumetric flask. The time versus RH readings were monitored until no significant changes in the RH reading were detected. The final readings of the probe were compared with the known RH value for each salt solution at the specified temperature. The accuracy of the probe was found to be with a precision of $\pm 2\%$.

After the completion of the calibration process, measurements of the RHs in the vapour space of the test desiccators were made. The sensors were pushed into a rubber stopper and placed on the lid of the desiccators (see Fig.4.11). To prevent any air gap between the rubber stopper and the desiccator lid, silicon grease was applied around the stopper. The response time of the RH probe was monitored and presented in Fig. 4.12.
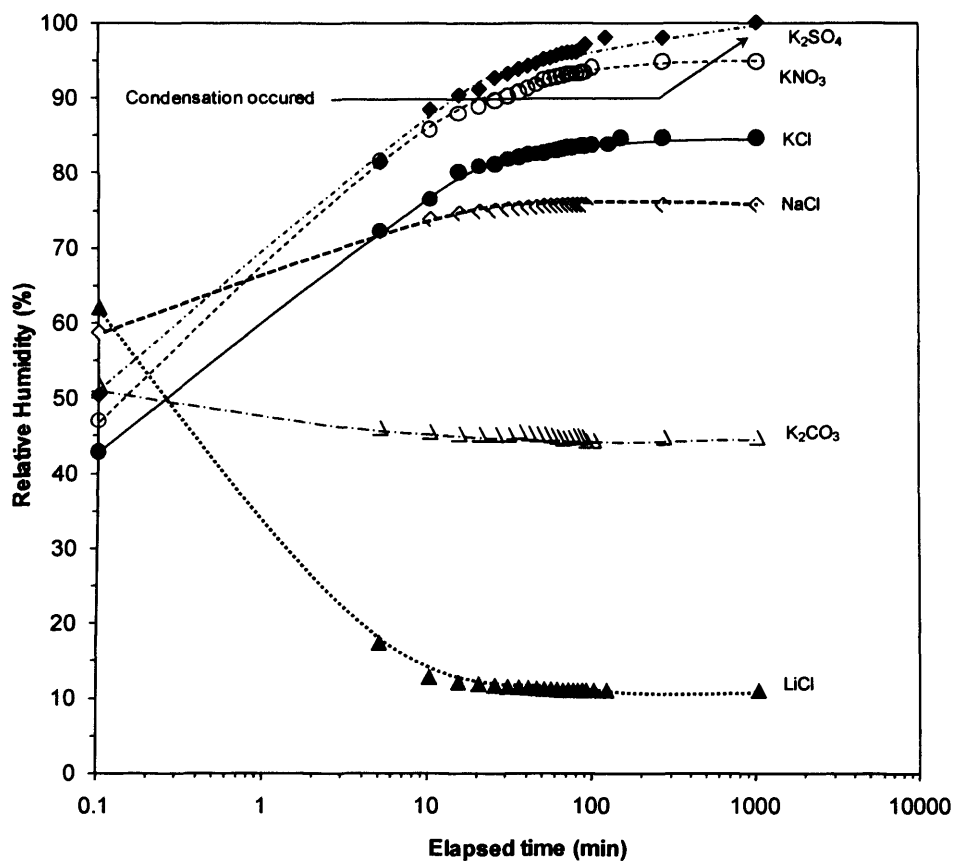
Fig. 4.12: *Response of the RH sensor with RH generated from several salt solutions*

For the salt solutions considered in this study, an equilibration period of approximately 100 to 120 minutes was found to be sufficient for the sensors to record stable RH readings. However, in the case of K_2SO_4 (RH = 97.6%), the probe showed a near 100% RH value. The limitation of the probes to measure very high relative humidity was observed as the probe used was not equipped with a heating function to eliminate condensation. Thus, it was anticipated that condensation occured around the sensor at higher RH conditions.

The suctions generated from the salt solutions using both filter paper and RH sensors were compared. The test results are presented in Table 4.2. Table 4.2 showed that the RH values from the filter paper method and the RH values measured using RH probes were similar.

Overall good agreements were noted between the two independent RH measurement methods. The RHs determined by filter paper method were used as a reference for suction determination in the vapour equilibrium technique.

Table 4.2: *Relative humidity and applied suction verifications at 25 °C*

Saturated salt solution	Targeted RH* (%)	Targeted suction (MPa) (Eq. 4.1)	Measured Filter paper water content (%)	RH from filter paper method+ (%)	RH probe results (%)	Calculated suction based on filter paper method (MPa)	Calculated suction based on RH probe results (MPa)
LiCl	13.0	279.9	1.54	11.50	11.00	296.7	302.8
K$_2$CO$_3$	43.0	115.8	4.29	43.53	44.80	114.1	110.2
NaCl	75.5	38.6	8.28	75.69	75.53	38.2	38.5
KCl	84.5	23.1	9.57	85.24	84.83	21.9	22.6
KNO$_3$	93.0	9.96	14.47	94.68	94.94	7.5	7.1
K$_2$SO$_4$	97.3	3.75	20.68	97.62	98.00	3.3	2.8

* After O'Brien (1948) and ASTM E 104-02 (2007)

$\psi = -137182 \times \ln\left(\dfrac{RH}{100}\right)$ - *suction and relative humidity relationship at reference temperature*

of 25 °C

+ from ASTM D5298-94 (2000)

4.4 Water content versus suction relationships of clay-water mixtures

4.4.1 Chilled-mirror dew-point technique

An Aqualab water activity meter was to measure the total suction of clay-water mixtures. The device used in this study and the schematic of the device are shown in Fig. 4.13.
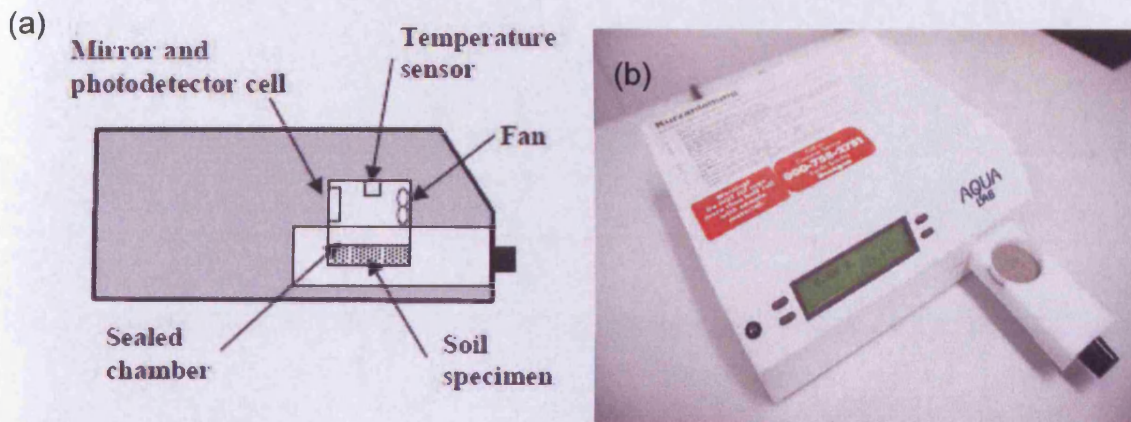
Fig. 4.13: *Chilled-mirror dew-point device (a) schematic (Leong et al., 2003) and (b) photograph of the device*

The device has a special closed chamber of about 12 cm^3 in volume, where a soil specimen can be placed. A cylindrical specimen holder was used to place the clay specimens into the device chamber. The device was first calibrated with a standard solution provided by the manufacturer. The chilled-mirror dew-point technique was found to measure total suction precisely with a response time of about 2 minutes (Leong et al. 2003; Agus and Schanz 2004).

A soil-water mixture equilibrates with the water vapour in the air space above the soil specimen. An internal fan speeds up the measurement process by circulating air within the

95

specimen chamber. A mirror with an accurate temperature sensors are controlled by thermoelectric cooler. The mirror detects the first point in which condensation occurred using a beam of light. The light is then detected by a photodetector cell. The change in the reflectance at an exact temperature at which the point of condensation occurred is then recorded by thermocouple attached to the mirror (Leong et al. 2003).

Clay-water mixtures were prepared by mixing clay powders with deionised water at targeted water contents with increments of 3%. The clay-water mixtures were then allowed to equilibrate for 7 days before being tested. The specimen holder was filled less than half the volume (6 cm^3) to minimize contamination to the testing chamber (Leong et al., 2003; Bulut and Leong, 2008).

4.5 Drying suction-void ratio SWCCs and shrinkage paths

For establishing the shrinkage paths and suction-void ratio SWCCs of the clays, duplicate slurried clay specimens were considered. Volumes of clay specimens equilibrated at several applied suctions were determined. The procedure adopted for the Clod tests are presented first, followed by the procedure adopted for the wax test.

4.5.1 Clod test

The specimens for the Clod tests were first subjected to a suction of 0.05 MPa in a 5 bar pressure plate before being coated with the PVAc glue. The procedure adopted was due to two specific reasons; (*i*) to bring the clays to compositions similar to that of specimens in the

drying SWCC tests and (*ii*) for ease of handling and coating the Clod specimens with the encasement glue.

The clay specimens in this study were coated with commercially available Unibond Waterproof PVAc glue. Krosley et al. (2003) tested different types of coating materials and has recommended the use Elmer's glue as an alternative encasement material for the Clod test. The PVAc glue was found to be a substitute for its US counterparts, Elmer's glue. The PVAc glue had higher water repellent properties than the MEK resin and is non hazardous (Krosley et al., 2003). To improve the workability of the glue, the PVAc glue was first diluted with deionised water. A ratio of 10 part of glue to 1 part of deionised water was considered.

Figure 4.14 shows the clay specimens in the Clod tests. The Clod specimens were hung by threads and allowed to dry out at an ambient laboratory temperature. Determination of the initial volume in Clod tests proved quite difficult. This is due to the fact that immediately after coating, the glue required some time to solidify. Whilst the glue was still wet (see Fig.4.14a), the volume of clay clods could not be correctly determined as it requires the coated specimens to be immersed in water during mass measurements. Measurement of the mass of the clay specimens were only undertaken once the surface of the glue hardened in about an hour after the coating process (see Fig. 4.14b). The mass of the Clod in air and in water were measured to determine the volume of the clay specimens and the respective water contents. The glue allows water vapour to escape from the Clod during the drying process, but prevents liquid water from flowing into the Clod during mass measurement in water (Krosley et al., 2003). After each successful mass measurement made in water, the Clods were carefully wiped with dry paper towel to remove excess water on the surfaces. The void

ratios of the clay specimens were calculated using volume-mass relationship. Frequent volume measurements were carried out until no further reduction in the mass of the Clod was observed.
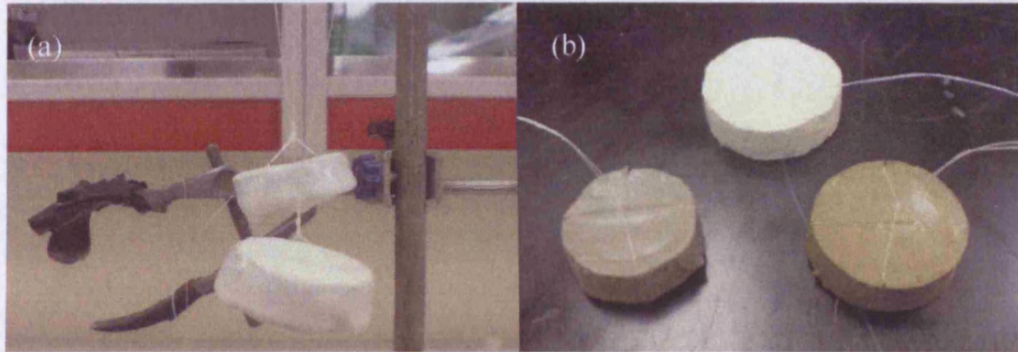
Fig. 4.14: *Clay specimen in Clod tests, (a) directly after coating and (b) after the glue dried*

out

The Clod tests provided information on the volume change of the clay specimens with a decrease in the water content during the shrinkage process. The initial total mass of the Clod, $M_{clod(i)}$, comprises of the initial total mass of the soil, $M_{soil(i)}$, and the initial mass of glue, $M_{glue(i)}$ (Eq. 4.4), where i stands for the initial condition. Similarly, at any given time t, the total volume of the Clod, $V_{clod(t)}$, comprises of the volume of specimen, $V_{soil(t)}$, and the volume of glue, $V_{glue(t)}$. The total volume of the Clod, $V_{clod(t)}$, can be determined by measuring the mass of the Clod in air, $M_{air(t)}$, and the mass of Clod in water $M_{water(t)}$ (Eq. 4.5). By knowing $M_{glue(i)}$, the mass fraction of the glue at any given time during drying process ($g_{f(t)}$) from Fig. 4.3, the density of the glue (ρ_{glue}), and by applying volume-mass relationships, the volume of the glue, $V_{glue(t)}$, can be calculated from Eq. 4.6. The water content of the soil specimen, $w_{soil(t)}(\%)$, can be calculated by knowing the initial water content of the soil specimen, $w_{soil(i)}(\%)$, and the dry mass of the soil specimen, M_d, from Eq. 4.7. The dry density of the soil, $\rho_{dsoil(t)}$, and the void ratio, $e_{soil(t)}$, can be calculated from Eqs. 4.8 and 4.9.

$$M_{clod(i)} = M_{soil(i)} + M_{glue(i)}$$

Eq. (4.4)

$$V_{clod(t)} = M_{air(t)} + M_{water(t)}$$

Eq. (4.5)

$$V_{soil(t)} = V_{clod(t)} - V_{glue(t)} = V_{clod(t)} - \left[\frac{(M_{glue(i)} \times g_{f(t)})}{\rho_{glue}}\right] = V_{clod(t)} - \left[\frac{M_{glue(t)}}{\rho_{glue}}\right]$$

Eq. (4.6)

$$w_{soil(t)}(\%) = \left[w_{soil(i)} - \left[\frac{\{(M_{soil(i)} - (M_{air(t)} - M_{glue(t)}))\}}{M_d}\right]\right] X\,100$$

Eq. (4.7)

$$\rho_{dsoil(t)} = \left[\left(\frac{(M_{air(t)} - M_{glue(t)})}{V_{soil(t)}}\right) \div (1 + \frac{w_{soil(t)}}{100})\right]$$

Eq. (4.8)

$$e_{soil(t)} = \left(\frac{G_s}{\rho_{dsoil(t)}} - 1\right)$$

Eq. (4.9)

4.5.1.1 Calibration of glue mass

The PVAc glue is a water based material that tends to loose water during solidification. The amount of water lost from the glue during the drying process was determined from independent tests by smearing a known mass of diluted glue onto a light plastic sheet. A sensitive four decimal point balance was used for measuring the changes in the mass of the glue with elapsed time. The change in the mass fraction of the diluted glue with elapsed time for two similar tests is shown in Fig. 4.15.

The loss of water from the diluted glue was found to be significant within about first eight hours. Figure 4.15 showed that the volume measurement for clay specimens within about first twenty four hours should be corrected with the variable glue mass fractions, whereas a single

value of glue mass fraction correction of 0.41 was found to be adequate for mass measurements carried out after twenty hours period.
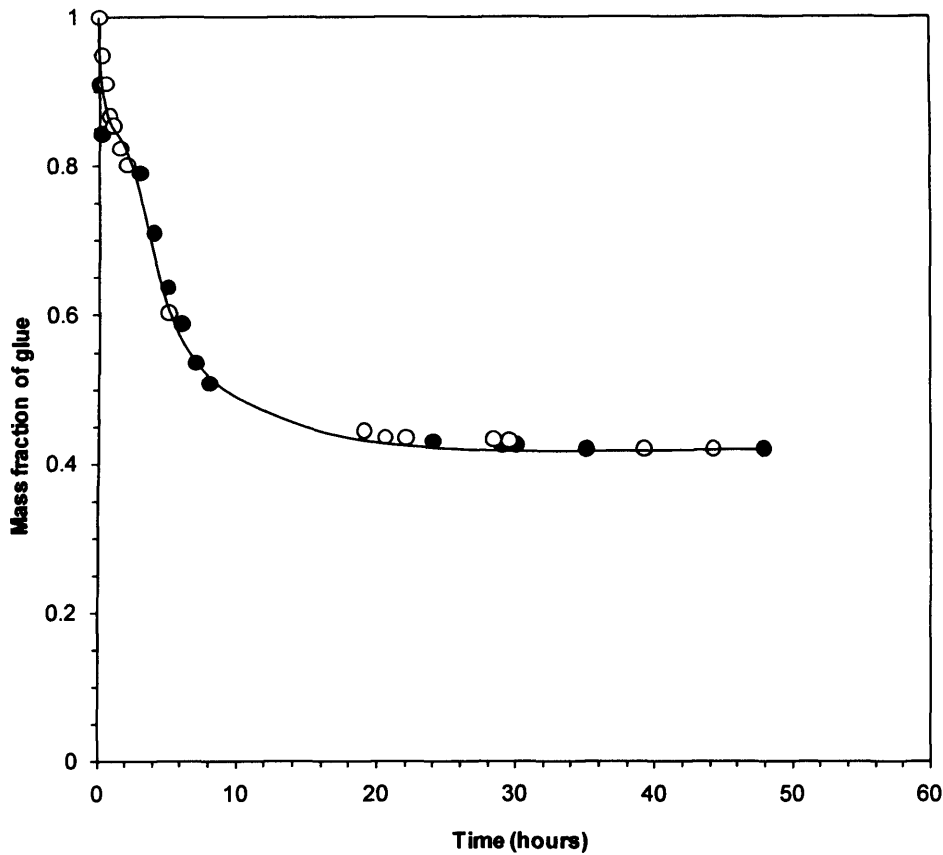
Fig. 4.15: *Glue mass fraction calibration curve*

It was also noted that the density of glue would change due to reduction in water content of the glue. The variation of glue density was found to be insignificant and a single density of 1.05 Mg/m^3 was considered for the calculations.

4.5.2 Wax method

The void ratios of clay specimens tested for drying suction-water content SWCCs were determined using wax method (ASTM D4943-94, 2000). The wax method is generally used for the determination of shrinkage limit of soil specimens. The method was also used for volume measurement of multiple duplicated soil specimens (Lauritzen, 1948; Ward et al.,

100

1965). The applied suctions considered were 0.05, 0.1, 0.2 and 0.4 MPa using pressure plate tests and 3.3, 7.5, 21.9, 38.2, 114.1 and 296.7 MPa using desiccator tests. Paraffin wax with a density of 0.77 Mg/m^3 and a melting point of 55 °C was used in this study. The wax was melted in a melting pot. Figure 4.16 shows the melting pot used in this study. The melting pot consists of a heating element. A thermometer was used to monitor the temperature of the molten wax. Coating of clay specimens were conducted by initially tying the specimens with threads and instantaneously dipping them into the molten wax.

Fig. 4.16: *Wax melting pot*

Temperature measurement is not usually carried out during wax tests. In this study, differences were noted on the void ratios measured when clay specimens were coated with molten wax at 60 °C and 80 °C. It was noted that test results from specimens coated with molten wax at 80 °C were randomly scattered with an increase and decrease of the degree of saturation. Furthermore, the molten wax was found to intrude the clay specimens tested. Temperatures higher than 70 °C lead to evaporation of volatile hydrocarbons which inevitably reduce the sealing efficiency of the wax (Heymann and Clayton, 1999). Thus, the wax tests were carried out at a constant temperature of 60 °C. A thermometer dipped into the molten wax ensured that the molten wax temperature did not exceed 60 °C during the tests.

The mass of the coated specimens were measured in air and in water similar to that determined in the Clod tests.

4.6 Swelling pressures of compacted bentonites

Swelling pressures of compacted bentonites tested under isochoric conditions were measured during the wetting process. Multistep swelling pressure and single step swelling pressures tests were conducted using suction controlled oedometer. The main use of the suction controlled oedometer in this study the suction-swelling pressure and suction-water content relationships under confined conditions. The salient features of the device used are presented in the subsequent sections.

4.6.1 Multistep swelling pressure tests

Swelling pressures of compacted specimens can be measured by equilibrating the specimens to known suction values. Such tests are usually known as multistep swelling pressure tests (Ariffin and Schanz, 2007). Multistep swelling pressure tests were carried out using a newly fabricated suction controlled oedometer. The components of the suction controlled oedometer are shown in Fig. 4.17. Figure 4.18 shows the schematic of the cell used in this study.

Most parts of the cell were fabricated using 316 grade stainless steel. The 316 grade stainless steel contains molybdenum that provides improved corrosion resistance. The corrosion resistance offered by the 316 grade was the crucial factor considered for designing the cell as vapour generated by the salt solutions was circulated during the multistep swelling pressure tests. The specimen ring, the piston, the central section, the base and the locking collar were

102

all fabricated using this material. The pedestal of the cell was fabricated using phosphors bronze.
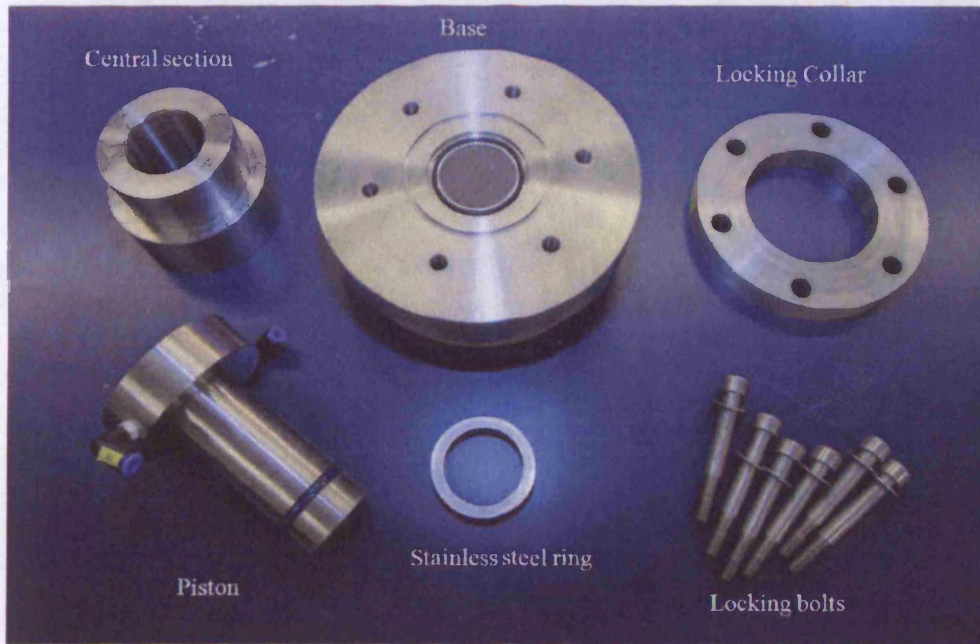
Fig. 4.17: *Components of the suction controlled oedometer*
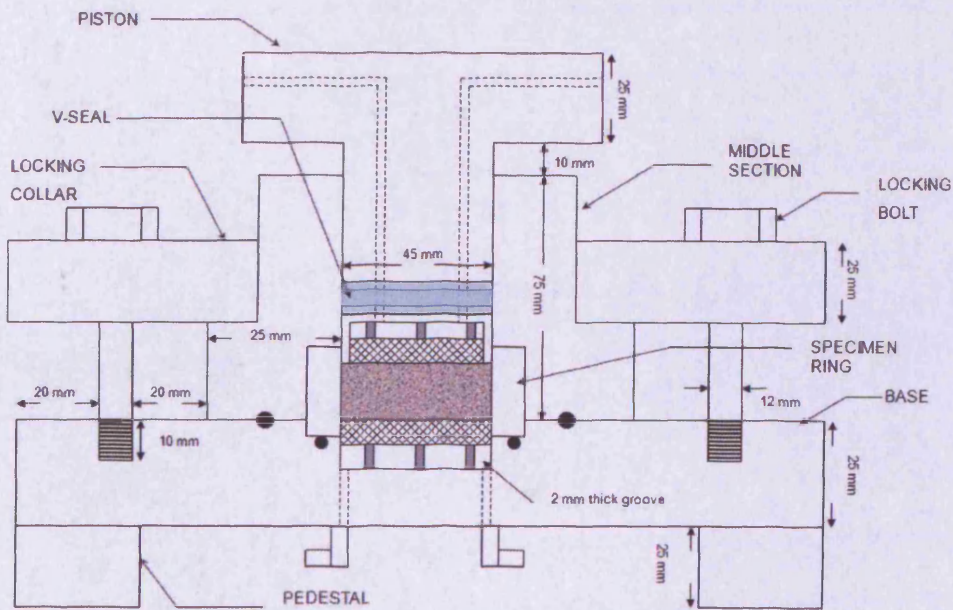
Fig. 4.18: *Schematic of the suction controlled oedometer*

The tests setup is shown in Fig. 4.19. The test setup consists of the vapour (suction) controlled oedometer, a triaxial frame, a display meter, a vacuum pump, a vapour chamber and an external load cell. A triaxial frame was used to provide restraint on both top and bottom of the cell. The cell was connected to a vacuum pump which circulated the vapour generated by salt solutions in the vapour chamber.
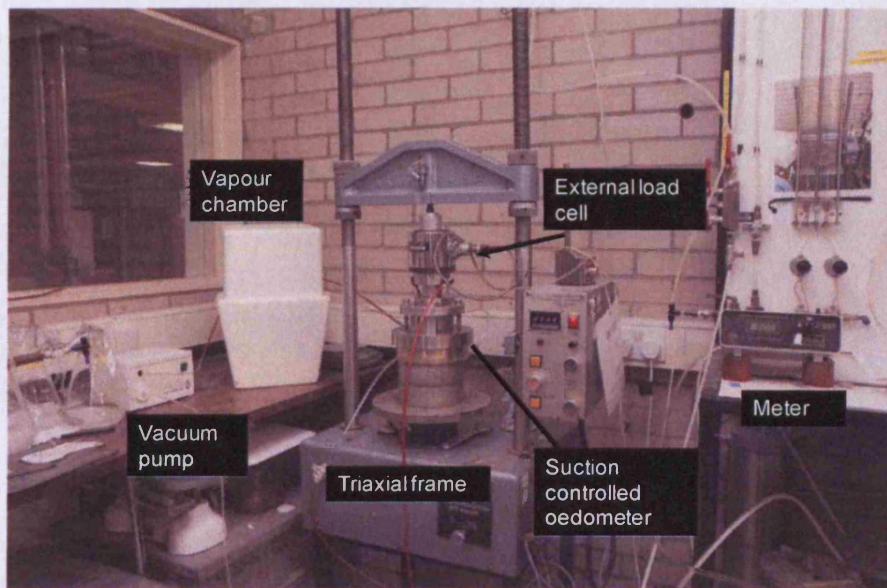
Fig. 4.19: *Multistep swelling pressure test setup*

Specimens of both bentonites were tested. The dry density of the specimen was 1.7 Mg/m^3. Several salt solutions were prepared for applying suctions of 38 MPa, 21.8 MPa, 7.5 MPa and 3.3 MPa using saturated solutions of NaCl, KCl, KNO$_3$ and K$_2$SO$_4$, respectively. The tests were carried out by changing the salt solutions from a higher to a lower suction. A salt solution was kept in a sealed flask within an air tight container (vapour chamber) to maintain a constant temperature. Figure 4.20 shows the flask inside the vapour chamber.
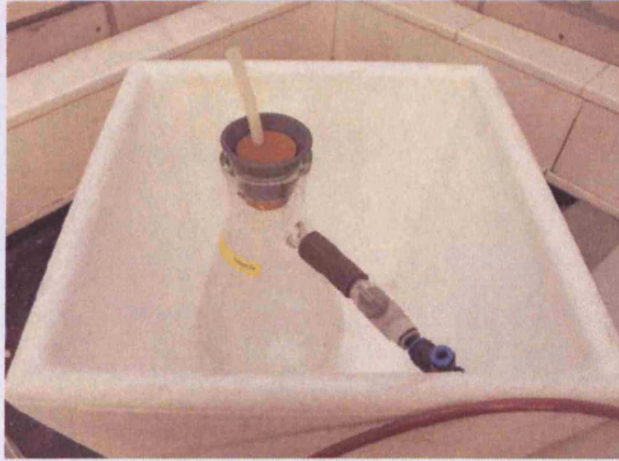
Fig. 4.20: *Salt solution in flask within the vapour chamber*

The heat produced from the vacuum pump when used continuously may change the suction imposed (Delage et al., 1998; Marciel et al., 2002; Cuisinier and Masrouri, 2004). The temperature within the container was monitored by a thermometer. Thus, the applied suctions could be monitored throughout the testing period. The temperature of the vapour chamber was found to be about 25 °C and was not affected by the heat generated by the pump.

Four specimens of each bentonite were used to establish the swelling pressure development with elapsed time. During the wetting process, the external load cell connected to the display meter provided the vertical load exerted by clay specimens. An equilibrium was reached under each applied suction once the vertical load exerted by the specimens remained constant. After the equilibrium was reached, the specimens were removed for determination of the water content by oven-drying method. Thus, at all applied suctions, the swelling pressures and the water contents of the specimens were determined.

4.6.2 Single step swelling pressure tests

Single step swelling pressure tests were carried out using a modified oedometer by supplying deionised water to compacted bentonite specimens. The oedometer was initially used to study the volume change behaviour of soils (Folly, 2001). Figure 4.21 showed the digital photograph of the components of the cell. Most parts of the cell were fabricated using stainless steel.

The device consists of a main cell, a top cap with built-in vertical piston, and a specimen holder. A stainless steel ring containing bentonite specimen was placed inside the specimen holder. The specimen holder consists of a specimen ring, a porous plate at the top, a porous plate at the bottom and a top cap with two locking screws. The specimen ring was fastened using the specimen holder cap by 2 locking screws. The specimen holder was then placed in the cell. The top cap was then placed and the vertical piston was lowered until it was in contact with the top porous plate. Once the top cap was fastened and the vertical piston was in place, the cell was later transferred to a triaxial frame to be tested.
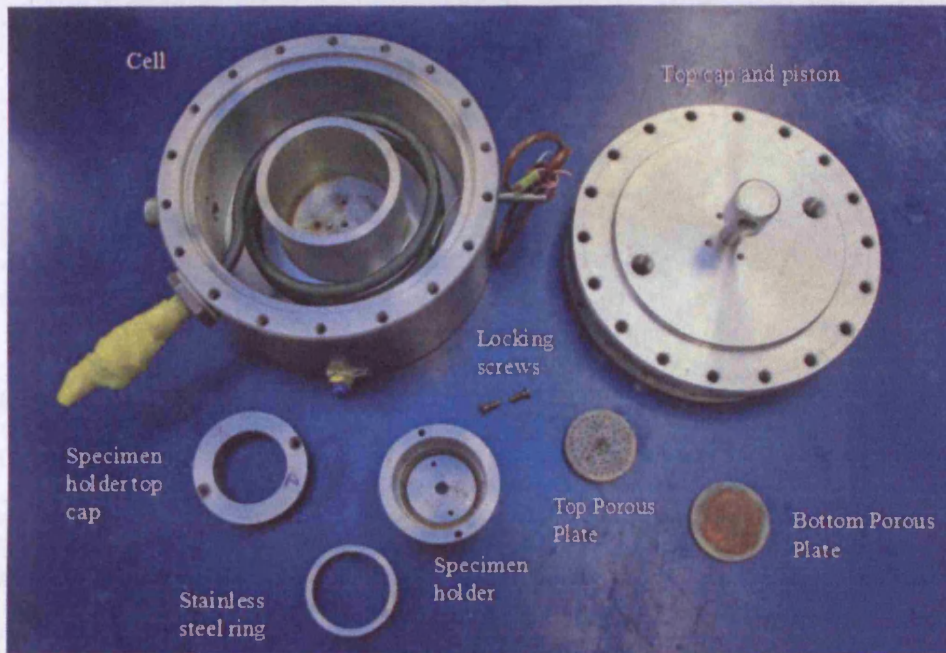
Fig. 4.21: *Components of modified oedometer*

The test setup is shown in Fig. 4.22. The test setup consists of the modified oedometer cell, a triaxial frame, a display meter, a water reservoir and an external load cell. The triaxial frame was used to provide restraint on both top and bottom of the cell. Deionized water was supplied to hydrate specimens from both top and bottom. During the wetting process, the external load cell connected to a display meter provided the vertical load exerted by clay specimens.

Bentonite specimens were tested at dry densities of 1.2, 1.3, 1.4, 1.5, 1.6 and 1.7 Mg/m^3. The tests were carried out for several days until no further changes in swelling pressures were recorded. Once equilibrium was reached, the specimens were dismantled and the water contents of the specimens were determined by oven-drying method.
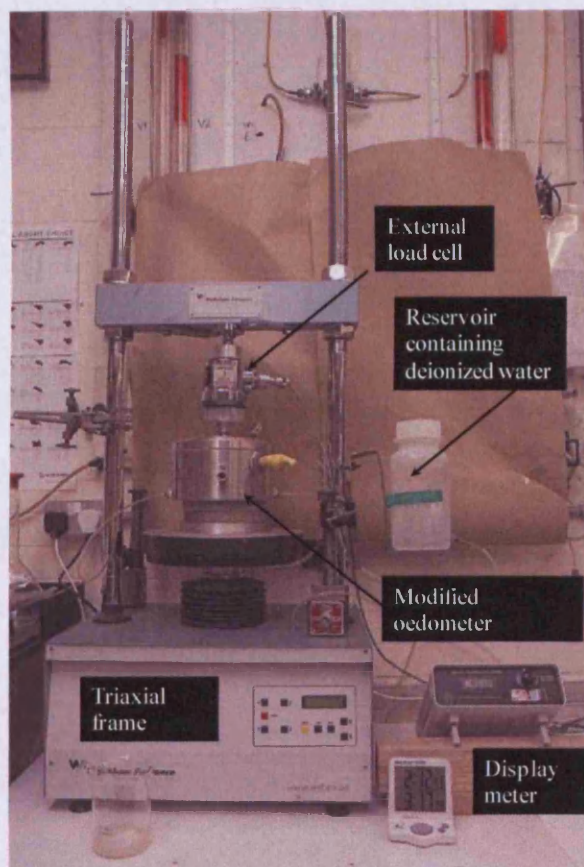
Fig. 4.22: *Single step swelling pressure test setup*

4.6.3 Calibration of the cell

The modified oedometer cell was calibrated by using a dummy stainless steel specimen and subjected to loading and unloading in a compression testing machine. The cell expansions were recorded at different loads and correction factors were applied to the dry densities of the clay specimens. The calibration curve used is presented in Fig. 4.23.
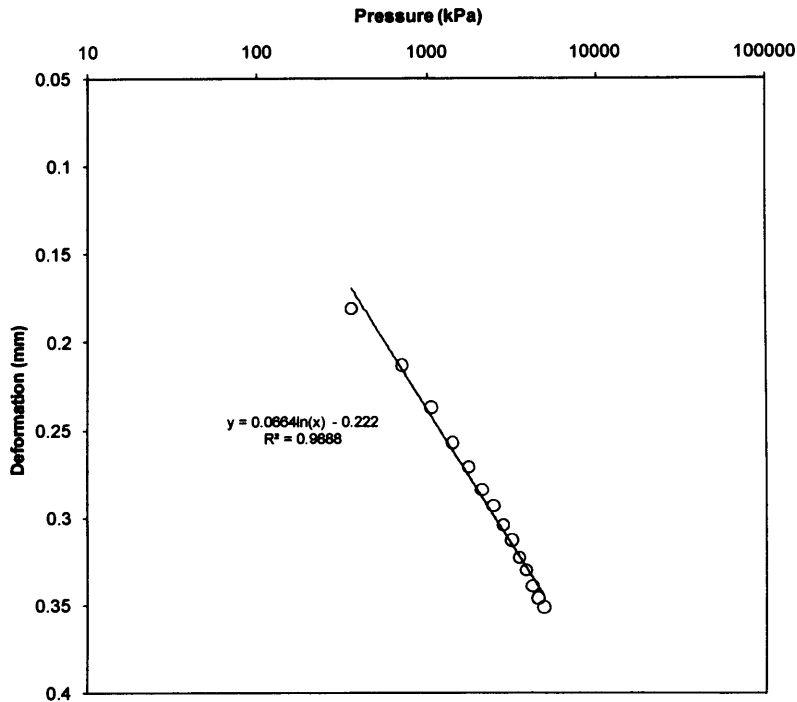
Fig 4.23: *Cell expansion calibration curve*

Figure 4.23 indicated that the deformation of the cell increased with an increase in the vertical pressure. The pressure deformation relationship was found to be almost linear. During the swelling pressure tests, the bentonite specimens exerted pessures that caused the cell to expand. Thus, the overall volume of the specimen increased proportionate to the expansion of the cell.

4.7 Microstructure studies

Understanding structure and fabric of clays is important for understanding their engineering behaviour (Gens and Alonso, 1992). Pusch and Yong (2005) and Delage et al. (2006) have shown that the behaviour of clays at microscopic level plays a significant role on the volume change behaviour at macro level. The structure and fabric changes and the changes in the *c*-

axis spacing during wetting at microscopic level was studied using environmental scanning electron microscope (ESEM) and XRD technique.

4.7.1 Environmental Scanning Electron Microscope (ESEM)

The microstructure of compacted bentonites at different relative humidity conditions were studied using ESEM. For ESEM studies, specimens are not required to be initially coated with gold or freeze-dried (Delage and Lefebvre, 1984; Ye et al., 2010). Therefore, the microstructural changes of specimen can be observed at different relative humidity conditions (Ye et al., 2010). The device used was a Veeco FEI (Philips) XL30 ESEM Field Emission Gun (FEG). The device was fitted with a secondary electron detector (SE), a back scatter electron detector (BSE) and a gaseous secondary electron detector (GSE).

Compacted bentonite specimens were statically compacted following procedure described in section 4.2.1. MX80 bentonite and Yellow bentonite specimens were prepared at a dry density of 1.6 and 1.4 Mg/m^3, respectively. The specimens were prepared at hygroscopic water contents. The specimens were then carefully cut into small sections approximately 3 mm in length and placed inside a 5 mm metallic holder within the ESEM chamber. Subsequently, the chamber was closed and water vapour was allowed to enter the testing chamber at a desired chamber pressure. Each bentonite specimen was subjected to only wetting tests. The limitation of the ESEM is that the chamber temperature must be adjusted simultaneously along with the relative humidity. In order to achieve higher relative humidity, the chamber temperature was reduced. The temperature of the chamber was adjusted to increase the chamber pressure and relative humidity. Table 4.3 presents the RH and corresponding adjusted chamber temperatures.

110

Table 4.3: *Relative humidity and corresponding ESEM chamber temperature*

Relative Humidity (%)	Temperature (°C)
10 – 53	20
54 -81	10
82-100	5

All the wetting tests using volumetric pressure plates, osmotic technique and desiccator tests in this study were conducted at a constant temperature of about 25 °C. However, in the ESEM, temperatures of 5 to 20 °C were considered to obtain an entire range of RH. Hence, the ESEM observation did not simulate the laboratory testing conditions.

A range of magnification between 150x to 15000x were used in this study. The contrast and brightness were adjusted to improve the clarity of the micrographs at higher RHs. The specimens were allowed to equilibrate as each relative humidity for 20 minutes before further increasing the relative humidity as suggested by Montes-H et al. (2005).

4.7.2 X-Ray Diffraction (XRD)

XRD technique is commonly used to identify and quantify minerals in crystalline compounds within a mixture or a pure phase (Mitchell, 1993). The XRD identifies minerals by relating the angle of incidence of the X-rays to the distance between atomic planes of the unit layers according to Bragg's law (Mitchell, 1993). This distance is called the 001-basal (d_{001}) or c-spacing (van Olphen, 1977). XRD technique has been used to study the changes in the c-axis spacing during the hydration process (Grim, 1968; Saiyouri et al., 2000; Lu and Likos, 2006, Warr and Berger, 2007).

For the XRD tests, all three clays were tested. Clay powders equilibrated at applied suctions of 3.3, 7.5, 21.8, 38, 114 and 296.7 MPa in the desiccator tests during the wetting process were considered. The clay powders were tested in the XRD device for determination of the change in the c-axis spacing. In order to achieve enhanced mineralogical peaks and c-axis spacing precisely, the clay powders were slowly scanned at low angles from 2θ of $3°$ to $30°$ with a step time of 0.02 and a step scan time of 0.5 seconds (Saiyouri et al., 2000).

CHAPTER 5

DRYING SOIL-WATER CHARACTERISTIC CURVES

5.1 Introduction

The drying suction-water content SWCCs starting from an initial water content at or slightly greater than the liquid limits and up to the shrinkage limits of soils at zero external stress have been shown to provide useful information for engineering analyses (Fredlund and Rahadjo, 1993; Fleureau et al., 1993; Al-Mukhtar et al., 1999; Marciel et al., 2002). In this chapter, the drying suction-water content SWCCs of MX80 bentonite, Yellow bentonite and Speswhite kaolin are presented. The drying suction-water content SWCCs were further used in conjunction with the suction-void ratio SWCCs and Clod test results for establishing the suction-degree of saturation SWCCs. The suction-void ratio SWCCs and the suction-degree of saturation SWCCs are presented in Chapter 7.

The objectives of this chapter were (*i*) to determine the drying suction-water content SWCCs of clays from initially saturated slurried conditions at zero external stress using various available laboratory methods and (*ii*) to compare the drying suction-water content SWCCs with the water content versus suction relationships from chilled-mirror dew-point tests.

This chapter comprises of several sections which includes the experimental programme, the time equilibration plots, the drying suction-water content SWCCs and comparison of the

suction-water content SWCCs with water content versus suction relationships from chilled-mirror dew-point tests. The concluding remarks are presented towards the end of the chapter.

5.2 Experimental programme

5.2.1 Drying suction–water content SWCCs

The drying suction-water content SWCCs of the three clays from saturated slurry conditions at zero applied stress were experimentally determined using centrifuge, axis-translation, vapour equilibrium and osmotic techniques. A wide range of suction from 0.007 to 300 MPa were considered. Clay specimens were prepared by mixing clay powder with deionised water to targeted water content of equal to 1.2 times the liquid limit values. Centrifuge tests were carried out at a single applied suction of 0.007 MPa. Pressure plate tests were carried out for applied suctions of 0.05, 0.1, 0.2 and 0.4 MPa using a 5-bar pressure plate extractor. The applied suctions in the desiccator tests were 7.5, 21.9, 38.2, 114.1 and 296.7 MPa corresponding to the relative humidities of aqueous solutions of KNO_3, KCl, $NaCl$, K_2CO_3 and $LiCl$, respectively. Several osmotic tests were carried out for applying suctions of 0.5, 0.11, 0.44, 0.99, 1.76, 2.75, 3.96, 5.39, 7.04 and 8.91 MPa. The clay specimens tested in the desiccators were initially subjected to a matric suction of 0.4 MPa in the pressure plate before being transferred to the test desiccators. Therefore, the experimental results from centrifuge, pressure plate and desiccator tests can be considered as the SWCC test results. The equilibrated water contents of the specimens were determined by oven-drying method.

5.2.2 Water content versus suction relationship of clay-water mixture (chilled-mirror dew-point tests)

Several clay-water mixtures were prepared by thoroughly mixing clay powders with deionized water. The water contents of the clay specimens were increased by increments of 3%. The clay–water mixtures were then left in sealed plastic bags for seven days for equilibration. The suction-water content relationship of the clay-water mixtures were established using the chilled-mirror dew-point technique.

5.3 Test results and discussion

5.3.1 Suction equilibration in centrifuge tests

Elapsed time versus water content decrease for an applied suction of 0.007 MPa in the centrifuge tests for the clays are shown in Fig. 5.1. Rapid reduction in the water contents were noted within the first 5 minutes. In the case of Yellow bentonite and Speswhite kaolin, the reductions in the water content were found to be lesser as compared to MX80 bentonite. Concurrent with the liquid limits of the clays, the final water content of MX80 bentonite was found to be far greater than that of Yellow bentonite and Speswhite kaolin. In all cases, the equilibration time of 10 hours was found to be adequate.
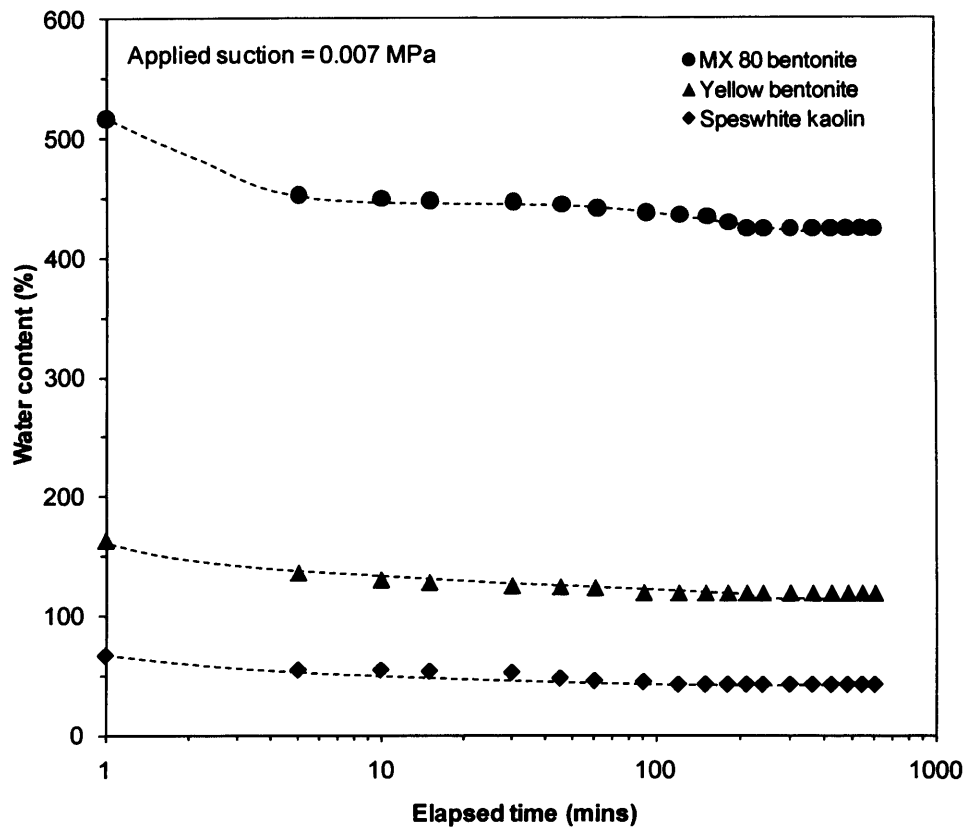
Fig. 5.1: *Equilibrium time in centrifuge at applied suction of 0.007 MPa*

5.3.2 Suction equilibration in pressure plate and osmotic tests

Typical elapsed time versus water content decrease for the clays studied at an applied suction of 0.05 MPa in the pressure plate and osmotic tests are shown in Fig. 5.2. Figure 5.2 indicated that the changes in the water content of the clay specimens were significant during the first 5 days of testing. Similar to the centrifuge method, the ordering of the final water contents of clay specimens were found to be concurrent with the liquid limits of the clays. The water content of MX80 bentonite at equilibrium remained greater than that of Yellow bentonite and Speswhite kaolin. The agreements between the tests results from the pressure plate tests and the osmotic tests were found to be very good.
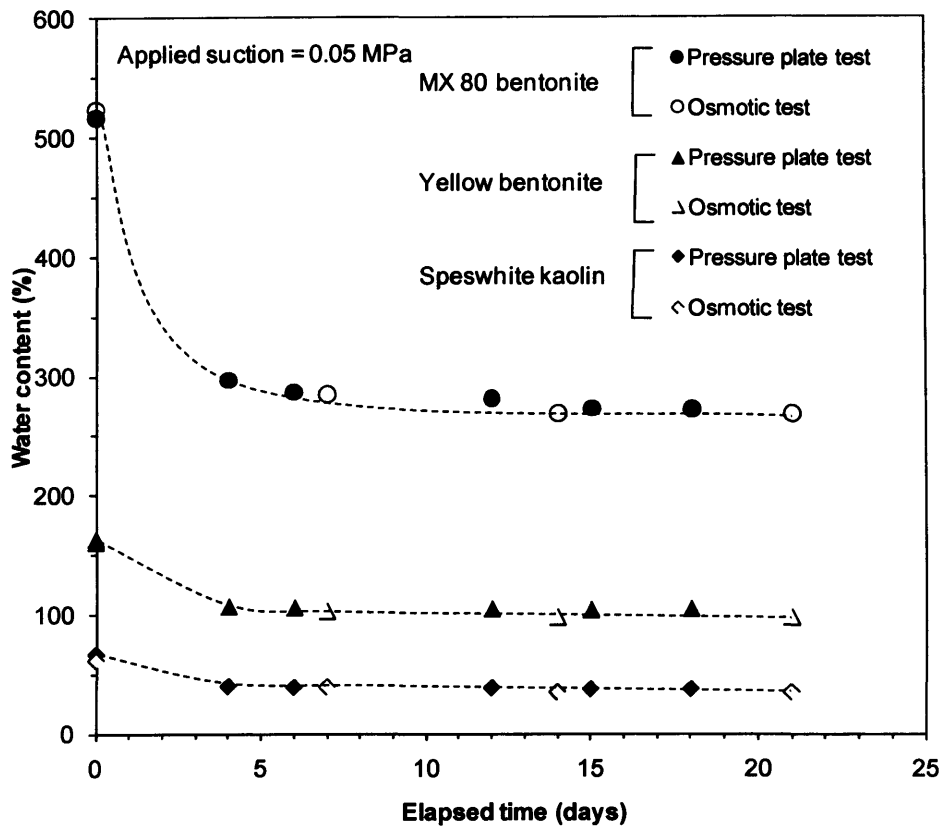
Fig. 5.2: *Equilibrium time in osmotic and pressure plate tests at applied suction of 0.05*

MPa

5.3.3 Suction equilibration in osmotic test at higher suctions

Dismantling the bentonite specimens that were subjected to suctions greater than 1.5 MPa in the osmotic tests revealed that the surfaces of the specimens were glazed in places. These glazed surfaces became more apparent and turned into white patches after oven-drying. Figure 5.3 shows the white patches on an oven-dried MX80 bentonite specimen. The white patches are believed to be the intruded PEG.

In order to explore the influence of the intruded PEG on the equilibrium water contents of the clay specimens in the osmotic tests, additional tests were carried out at an applied suction of

117

7.04 MPa. For these tests, a known amount of dry mass of the clays (approximately 5 g) was used in the tests. PEG 6000 was used for applying the predetermined suction. The changes in mass of the specimens were monitored at predetrmined time intervals. The tests were terminated after 9 days. The dry mass of the specimens were again measured and compared with the actual dry mass.
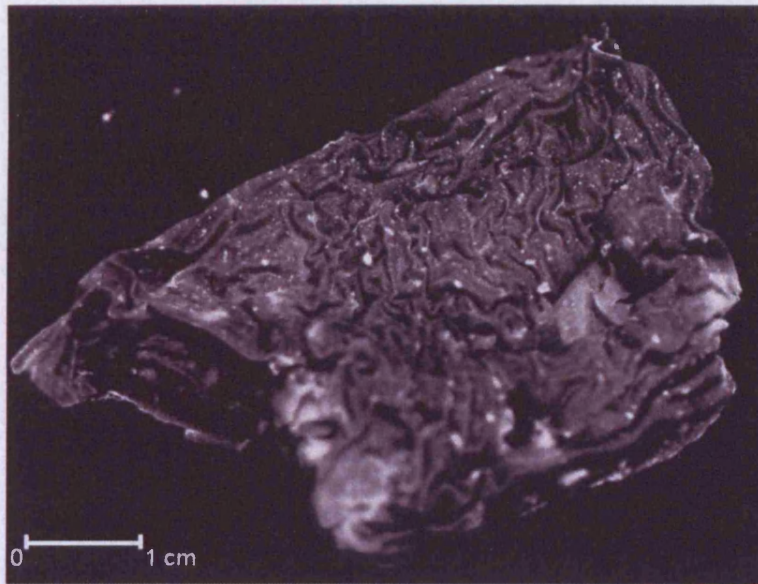
Fig. 5.3: Intrusion of PEG solution in MX80 bentonite

Figure 5.4 shows the suction equilibrium plot in the osmotic tests for the clays at an applied suction of 7.04 MPa. Some variation was observed in the time versus water content plots which were not as smooth as that occurred for specimens at an applied suction of 0.05 MPa (see Fig. 5.2), particularly for the bentonite specimens. The mass of bentonite specimens initially decreased and further increased after 6 days of the tests. A slight increase in the final dry mass was detected (0.224 g for MX80 bentonite and 0.3 g for Yellow bentonite) which in turn indicated that PEG had intruded the bentonite specimens, concurrent with the visualization of discoloration of the specimens and white patches (Fig. 5.3). No change in the mass occurred for the specimen of Speswhite kaolin.

118
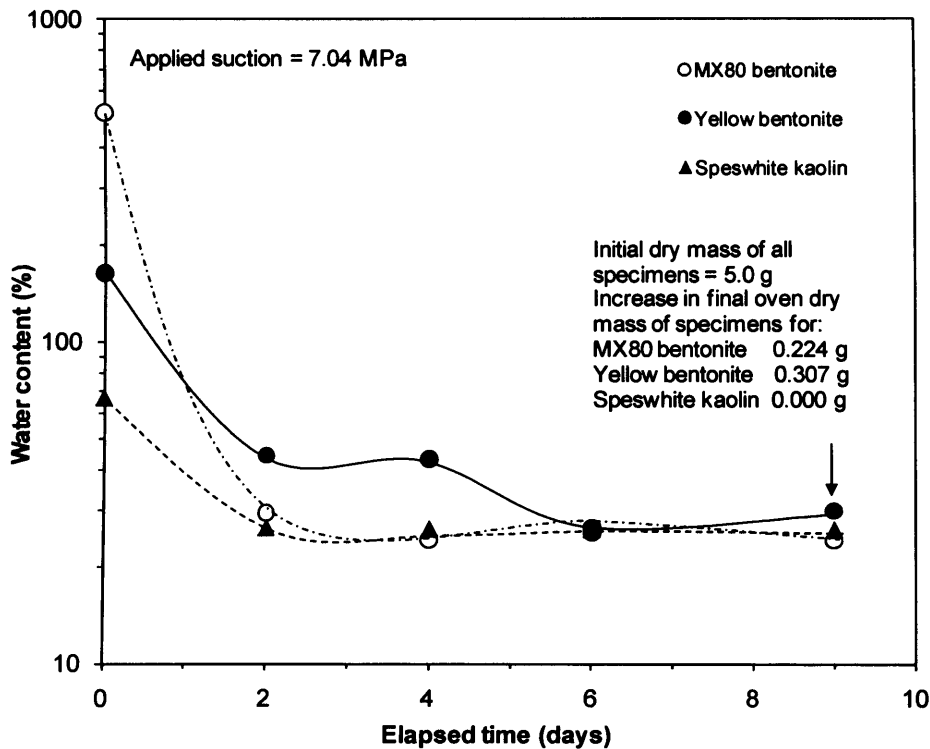
Fig. 5.4: *Equilibration time in osmotic tests at applied suction of 7.04 MPa*

The amounts of intruded PEG were considered for calculating the corrected water contents of the bentonites. The water contents of the bentonites increased by about 1.5%. Although PEG intrusion effect was found to be insignificant, the main reason behind the intrusion of PEG is not very well understood. The intrusion of PEG during the osmotic tests will be further discussed in Chapter 6.

5.3.4 Suction equilibration in desiccator tests

After the clay specimens were equilibrated in the pressure plate at an applied suction of 0.4 MPa, they were transferred to the test desiccators. Figure 5.5 presents typical suction equilibrium plot for the clays in the desiccator tests at an applied suction of 300 MPa.

119
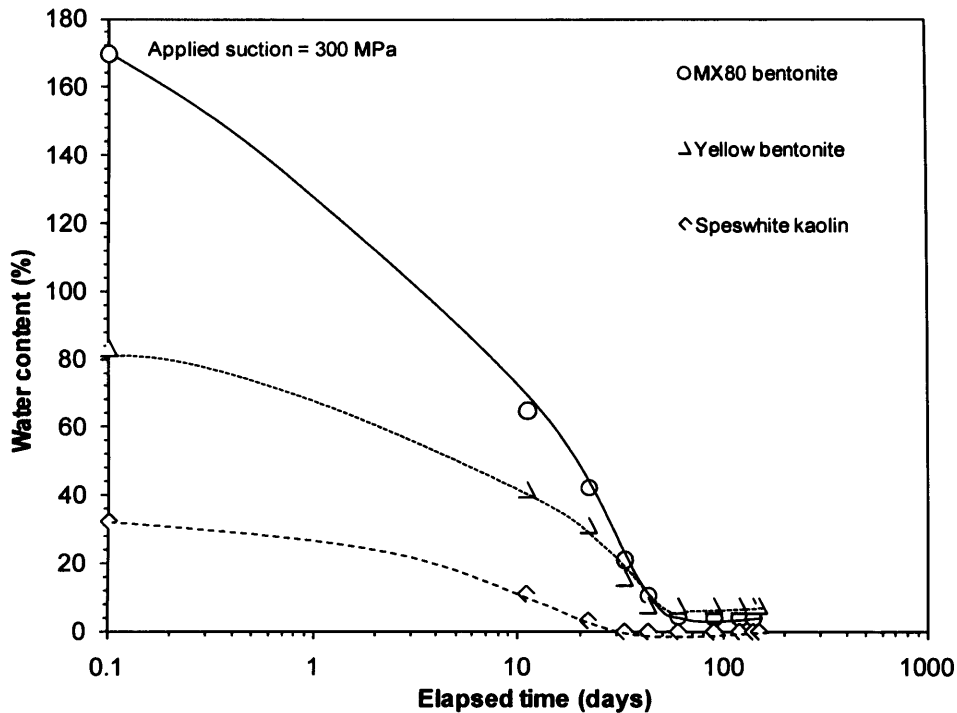
Fig. 5.5: *Equilibration time in desiccator tests at applied suction of 300 MPa*

The ordering of the water content of the clay specimens during the initial stage of drying process was found to be similar to that other test methods discussed earlier. Additionally, the ordering of the water contents of clay specimens was found to follow the specific surface area of the clays after about 15 days (i.e. higher the specific surface area, greater is the equilibrium water content). The equilibrium water content of Yellow bentonite was greater than the water content of MX80 bentonite and Speswhite kaolin. The equilibration time in the desiccator tests was found to vary between 15 days to 20 weeks depending upon the clay type and the magnitude of applied suction.

5.3.5 Drying suction-water content SWCCs

The equilibrium water contents of the clays at various applied suctions in centrifuge, pressure plate, desiccator and osmotic tests are presented in Fig. 5.6. The experimental data of the

120

clays from centrifuge, pressure plate and desiccator tests were joined with the help of smooth

curves to represent the suction-water content SWCCs. The shrinkage limit water contents of

the clays are also marked in Fig. 5.6.
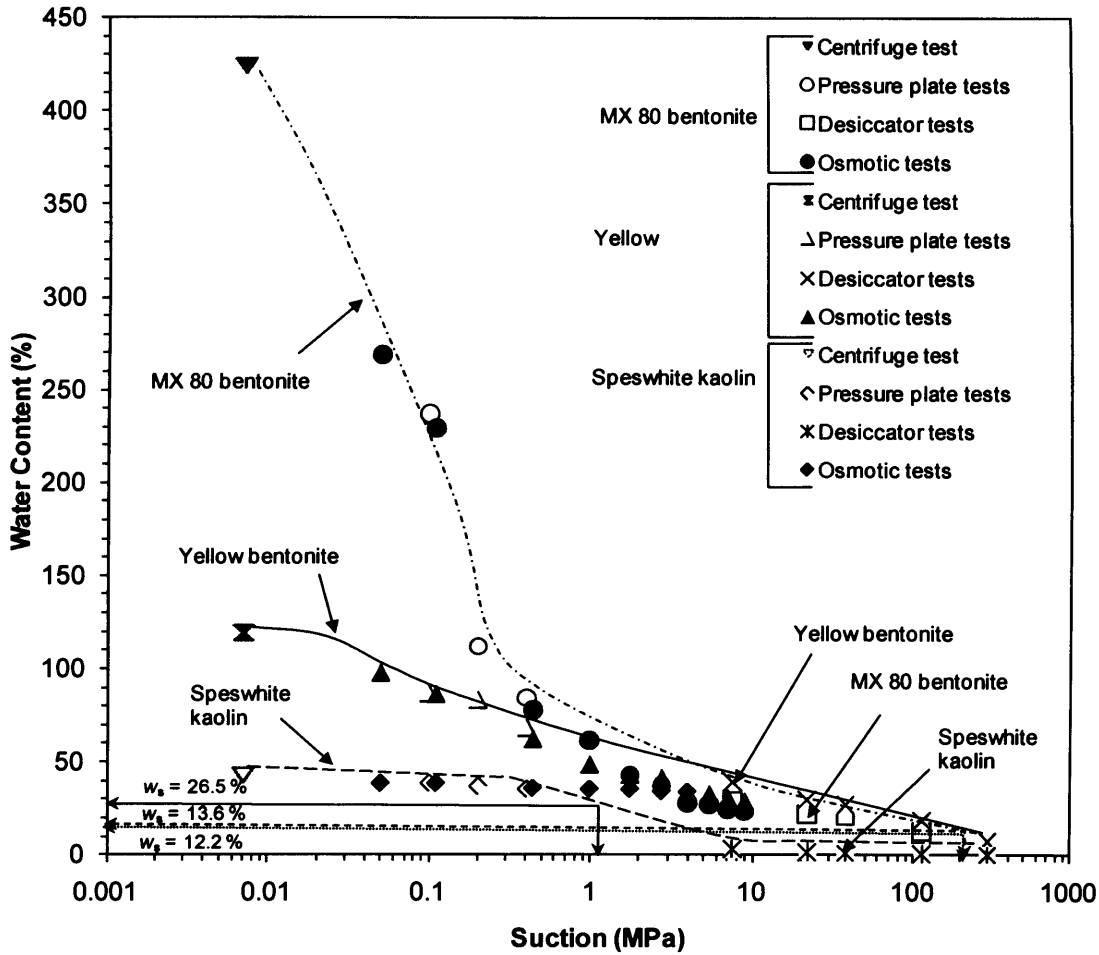
Fig. 5.6: *Suction-water content SWCCs of the clays studied*

The water contents of the clays at an applied suction of 0.007 MPa in the centrifuge tests

were found to be 424%, 119% and 43% for MX80 bentonite, Yellow bentonite and

Speswhite kaolin, respectively. Several researchers in the past have shown that highly plastic

soils tend to equilibrate from initially saturated slurry conditions (about 1.5 times the liquid

limit values) to the respective liquid limit water contents at an applied suction of about 6 kPa

to 10 kPa (Russell and Mickle, 1970; Wroth and Wood, 1978; Fam and Dusseault, 1999;

121

Nagaraj and Miura, 2001). However, in this study, the slurried specimens were prepared at much lower targeted water contents (see Section 4.2.1). Thus, the water contents of the clays equilibrated at an applied suction of 7 kPa were found to be slightly lower than the liquid limits (approximately 15% lower for both bentonites and 8.5% lower for Spewhite kaolin) as compared to the corresponding liquid limit values of the clays.

Referring to Fig. 5.6, the suction-water content SWCC of Speswhite kaolin remained distinctly below that of bentonites due to a smaller specific surface area and cation exchange capacity (Lambe and Whitman, 1969; Mitchell, 1993). The experimental results of the clays from the pressure plate and osmotic tests for applied suctions less than 0.44 MPa were found to be similar indicating that axis-translation technique and osmotic technique brought soil specimens of the same clay to similar water contents when the applied suctions were similar in both the techniques (Zur, 1966).

For applied suctions greater than 1.0 MPa, the water contents of the bentonites in the osmotic tests were found to be somewhat lower as compared to the smooth SWCCs. On the other hand, the water contents of Speswhite kaolin from the osmotic tests remained distinctly above that of the drying SWCC. Figure 5.7 shows the differences in the water content at overlapping suction region.
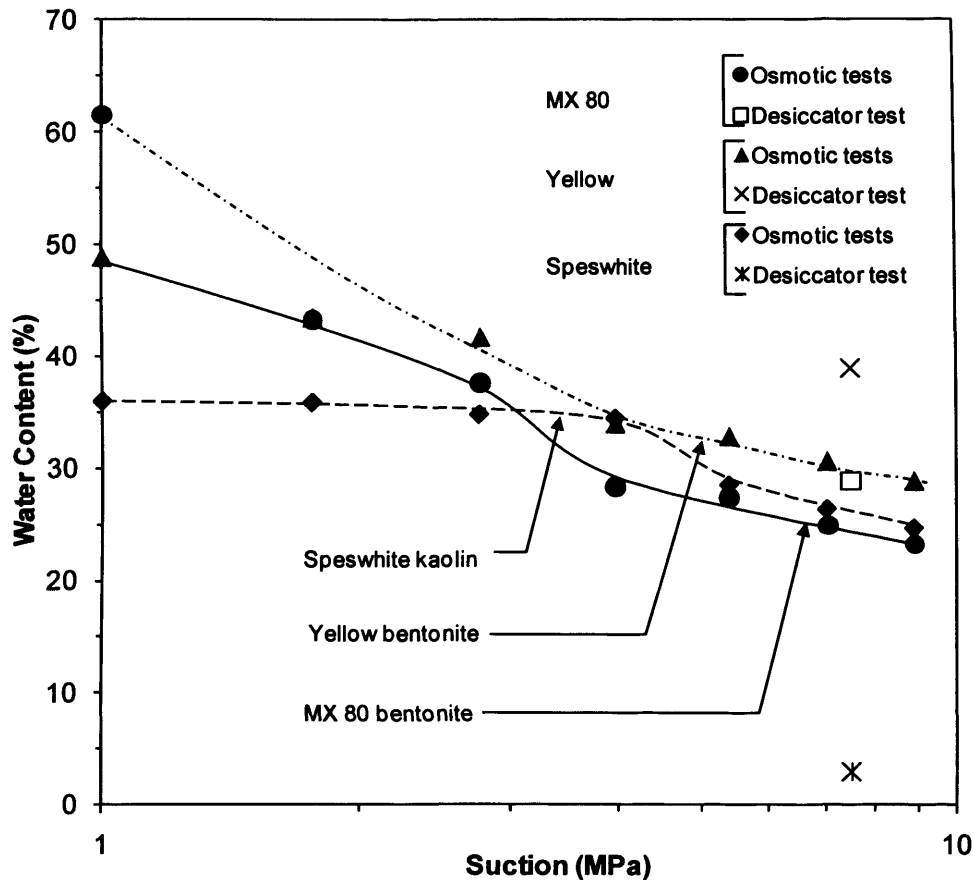
Fig. 5.7: Differences in the water content in osmotic and desicator tests at overlapping suction region

Differences in the water contents between the osmotic test and desiccator test results in the overlapping suction range (i.e. between suctions 7 and 10 MPa) were also noted. In the overlapping suction region of 7 to 10 MPa, the water contents of the bentonites obtained from the desiccator tests were distinctly greater than that obtained from the osmotic tests, whereas the reverse was true for Speswhite kaolin. The differences between the water contents from the osmotic and the desiccator tests at a suction of 7.5 MPa (see Fig. 5.7) were found to be about 21.0%, - 8.0%, and - 4.0% for Speswhite kaolin, Yellow bentonite, and MX80 bentonite, respectively. Additionally, the reductions in the water content for Speswhite kaolin for an increase in suction from 0.4 to 4 MPa in the osmotic tests were found to be negligible. On the other hand, it can be seen in Fig. 5.6 that a reduction in the water content for

Speswhite kaolin due to an increase in the applied suction from 0.4 MPa in the pressure plate test to 7.5 MPa in the desiccator test was significant. It will be shown later in Chapter 7 that the degree of saturation of Speswhite kaolin between applied suctions of 0.4 and 4 MPa remained at 99.5%, whereas it decreased further sharply beyond for applied suctions greater than 4 MPa. The test results clearly showed that vapour equilibrium technique was more effective in reducing water contents of Speswhite kaolin than that occurred due to applied suctions in the osmotic tests. An insignificant decrease in the water content between applied suctions of 0.4 to 4 MPa for Speswhite kaolin indicated that prior to cavitation in the pore-water the tensile strength of the pore-water resisted the applied suction. The bentonites did not exhibit such behaviour.

Up to an applied suction of less than 3.0 MPa, the ordering of the SWCCs was found to be concurrent with the liquid limit of the clays, whereas at higher suctions, the SWCC of Yellow bentonite crossed the SWCC of MX80 bentonite and remained above. The crossing of SWCCs with an increasing suction is attributed to the commencement of the interference of compact ion layers (i.e. Stern layers) that in turn depends upon the hydrated ionic ion size of the exchangeable cations (Verwey and Overbeek, 1948). The suction corresponding to the shrinkage limits of the bentonites were found to be about 200 MPa and about 1.0 MPa for Speswhite kaolin (see Fig. 5.6 and Table 3.1).

Chemical analyses of the PEG solutions in the osmotic tests were carried out to explore the osmotic suction equilibrium on either side of the semipermeable membrane. The test results are presented in Chapter 6.

5.3.6 Comparison of SWCCs and water content versus suction relationships from chilled-mirror dew point technique

The suction-water content SWCCs and water content versus suction test results from chilled–mirror dew-point technique are shown in Fig. 5.8. The chilled–mirror test results were obtained between suctions of 1.0 MPa to 120 MPa. Tests results from pressure plate and centrifuge were removed from the plot for clarity. Very good agreements were noted between the test results from chilled-mirror and desiccator tests. The chilled-mirror test results were found to remain slightly higher in the case of the bentonites as compared to the results from the osmotic tests, whereas in the case of Speswhite kaolin, up to a suction of about 2.0 MPa, the chilled-mirror test results remained lower as compared to osmotic test results.
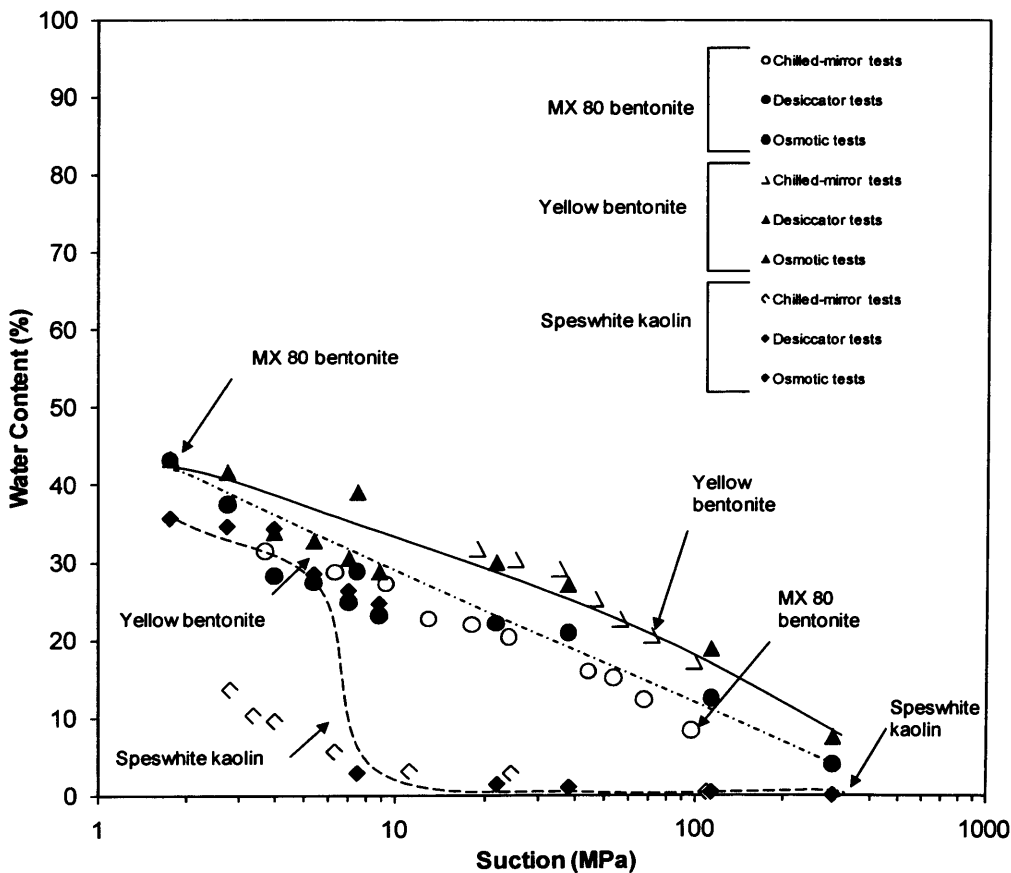
Fig. 5.8: *Comparison between SWCCs and suction-water content from chilled-mirror dew point technique*

5.4 Concluding remarks

The main findings from this chapter can be summarised as follows:

i. The suction-water content data from the centrifuge used in this study was found to be limited to an applied suction of 0.007 MPa.

ii. Very good agreements were noted between the pressure plate and osmotic test results for applied suctions less than 0.4 MPa. Differences were noted between the water contents obtained from the osmotic tests and the desiccator tests in the overlapping suction region. The osmotic test results were lower than that of desiccator test results for the case of bentonites, whereas much higher water contents were attained by Speswhite kaolin in the osmotic tests as compared to that in the desiccator tests.

iii. The liquid limits of the clays were found to influence the water content at suctions less than about 3 MPa in that higher the liquid limit, greater is the equilibrium water content. On the other hand, for suctions greater than 3 MPa the water contents of divalent-rich Yellow bentonite were greater than that of monovalent-rich MX80 bentonite due to higher specific surface area.

iv. In the osmotic tests, a decrease in the water content for Speswhite kaolin between applied suctions of 0.4 to 4 MPa was found to be insignificant, whereas vapour equilibrium technique was found to be more effective in reducing the water content of Speswhite kaolin at higher suctions. Further increase in suction beyond 4 MPa in the osmotic tests caused a decrease in the water content of Speswhite kaolin. This

indicated that prior to cavitation in the pore-water the tensile strength of pore-water resisted the applied suctions thereby delaying the desaturation for Speswhite kaolin. The cavitation phenomenon was not observed in the case of the bentonites.

v. Intrusion of PEG occurred at higher applied suctions in the osmotic tests. The effects of PEG intrusion on the water content of the bentonites were found to be marginal (about 1.5%).

vi. Good agreements were noted between the water content-suction relationships obtained from the chilled-mirror dew-point tests and the desiccator tests at higher suctions. Differences were noted between the osmotic test results and the chilled–mirror test results.

CHAPTER 6

OSMOTIC SUCTION EQUILIBRIUM IN OSMOTIC TESTS

6.1 Introduction

A soil possesses matric suction (i.e. negative porewater pressure) due to the retreat of air-water interface from the surface of the soil (Fredlund and Rahardjo, 1993). The ionic concentrations of the reference fluid and the soil pore-water must be equal for applying and measuring matric suction of soils (Aitchison, 1965). In an osmotic test, the total suction of the PEG solution comprises of osmotic suction due to the PEG solution (π_{PEG}), osmotic suction due to the salt that have expelled from the soil (π_{salt}^1), and matric suction of the solution which is equal to zero. In the soil-water system, osmotic suction of the available salts (π_{salt}^2) and matric suction constitute the total suction. If π_{salt}^1 is considered equal to π_{salt}^2, the total suction of the PEG solution is equal to the osmotic suction of the PEG solution (π_{PEG}) and that on the soil side, it is equal to matric suction of the soil (Zur, 1966; Ng and Menzies, 2007). However, in the case of highly plastic clays, it is anticipated that an imbalance may exist between the osmotic suctions due to the expelled and the retained salts on either side of the semipermeable membranes. The imbalance of the osmotic suction may occur primarily due to the osmotic efficiency of the clays (Barbour and Fredlund, 1989; Mitchell, 1993).

Determinations of the osmotic suctions (π_{salt}^1 and π_{salt}^2) will be required to ensure that predetermined matric suctions are applied to the soil. Alternatively, the total osmotic suction can be calculated from CEC data, whereas π_{salt}^1 can be determined based on the chemical analysis of PEG solution. Therefore, π_{salt}^2 can be calculated. From physico-chemical

considerations, a condition of $\pi_{salt}^{1} = \pi_{salt}^{2}$ can only be achieved when the electrical double layer effect is completely eliminated. Elimination of the electrical double layer effects within soil-water systems causes the adsorbed water layers on the surfaces of the soil particles to overlap (Verwey and Overbeek 1948). An increase in suction beyond this stage would initiate dehydration of the hydrated ions and further enable desaturation of the soil. In other words, in an osmotic test, $(\pi_{PEG} + \pi_{salt}^{1})$ should be greater than π_{salt}^{2} to apply a matric suction and cause desaturation of soils (i.e. Sr < 100%).

The main limitation of the osmotic technique is associated with the intrusion of PEG into soil specimens (Williams and Shaykewich, 1969; Tarantino & Mongiovi 2000; Delage and Cui 2008a). It has been hypothesized in the past that the intrusion of PEG occurs either due to failure of the semipermeable membrane in restricting passage of PEG molecules or a degradation of PEG molecule into smaller sizes.

The objectives of this study were (*i*) to measure the cation concentrations in the PEG solutions after the osmotic tests, (*ii*) to determine the osmotic suctions corresponding to the ions that remained in the clay-water systems and that expelled from the clays during osmotic tests (π_{salt}^{1} and π_{salt}^{2}) and (*iii*) to explore the factors influencing intrusion of PEG during osmotic tests.

This chapter is presented in several sections. The experimental programme is presented first. Under results and discussion, the chemical analyses of PEG solutions in the osmotic tests are presented. This section covers several aspects, such as the measured cation concentrations in the PEG solutions after the osmotic tests, the modified CEC versus applied suctions and the osmotic pressures (i.e. osmotic suctions) calculated from measured cation concentrations.

Determinations of the AEVs based on the chemical analyses of PEG solution and total suction equilibrium on either side of the semipermeable membranes are also presented in this section. The investigations carried out concerning the intrusion of PEG during osmotic tests are presented. This covers membrane pore size studies and whether there are any changes to the molecular structure of PEG (i.e. degradation) with elapsed time. The concluding remarks are presented towards the end of the chapter.

6.2 Experimental programme

6.2.1 Measurement of cation concentrations in the osmotic tests

Measurements of Na^+, Ca^{2+}, Mg^{2+} and K^+ concentrations in the PEG solutions after the completion of the osmotic tests were carried out using Inductively Coupled Plasma Emission Spectrometry (ICP-OES). All three clays were considered. Clay specimens were prepared at 1.2 times the corresponding liquid limit values. The water content results are presented in Section 6.3.3. Applied suctions of 0.11, 3.96, 5.39 and 8.91 MPa were considered. The osmotic pressures based on the expelled cation concentrations were calculated using van't Hoff's equation (see Section 6.2.2).

6.2.2 Calculated osmotic pressures (osmotic suctions)

The osmotic suction of a soil is related to the osmotic pressure due to the salts that are freely available in the pore water and is devoid of the electrical double layer effect. In case of non plastic soils (e.g. sand), the electrical double layer effect is insignificant. On the other hand, in case of highly plastic soils, the electrical double layer effect dominates the hydraulic and

mechanical behaviour (Bolt, 1956; Lambe and Whitman, 1969; Mitchell, 1993). A majority of ions usually resides within the diffuse double layer (Mitchell, 1993). The ionic concentration of the soil pore fluid decreases from the surface of the clay particles. The osmotic pressure at the central plane between soil particles is called the interparticle repulsive pressure (van Olphen, 1977, Sridharan and Jayadeva, 1982). For a known chemical composition of the soil, the total osmotic suction can be calculated. The osmotic pressure at the central plane between two soil particles then becomes a fraction of the osmotic suction of the soil.

The osmotic suction due to the salts present in a soil can be calculated based on thermodynamic principles. van't Hoff equation (Eq. 6.1) has been used to calculate osmotic pressures of salt solutions and osmotic suctions of clays by several researchers (Lang, 1967; Warkentin and Schofield, 1962; Barbour et al, 1991; Rao and Shivananda, 2005).

$$\pi = -imRT \hspace{8cm} \text{Eq. (6.1)}$$

where π is the osmotic suctions (kPa) of the salt solution, R is the universal gas constant (8.32 $1 \cdot kPa \cdot mol^{-1} \cdot K^{-1}$), T is the absolute temperature (K), m is the molarity of the pore solution (mol/l), and i is the van't Hoff factor.

Arnikar et al. (1992) stated that the factor i is close to the number of ions that would be formed, if the solute molecules are disassociated following Arrhenius theory. Thus,

$i = 2$ for 1-1 electrolytes such as NaCl or KCl

$i = 3$ for 2-1 electrolytes such as K_2SO_4 or K_2CO_3

Equation 6.1 has been successfully used for calculating osmotic pressures of solutions with low concentrations (Lang, 1967; Kutchai, 1980; Barbour et al, 1991; Garcia, 1999; Rao and Shivananda, 2005).

For analyzing the osmotic suctions due to the expelled cations from the clays, the following assumptions were made, such as (*i*) the cations are present in combined state and associate with anions to form salt molecules; that is, expulsion of anions from clay-water systems would take place proportionately along with the clay fluid for attaining the electroneutrality conditions (i.e. cation-anion pairs diffuse together) (Mitchell, 1993) and (*ii*) the concentration of anions will associate with the same concentration of cations (i.e. dissolution of 0.1 moles of NaCl yields 0.1 moles of Na^+ and 0.1 moles of Cl^-) (Lang, 1967; Arnikar et al., 1992).

Solid to liquid ratio plays a significant role in determining the osmotic suctions of expelled cations (ENRESA, 2000). For the same amount of salt expelled but different liquid ratio considered, the calculated osmotic suction will vary significantly. In other words, if the expelled salt concentration remained constant and the liquid ratio is less, the calculated osmotic suctions will be higher than the actual values. Therefore, calculations of the osmotic suctions were carried out very carefully.

6.2.3 Intrusion of PEG during osmotic tests

6.2.3.1 Degradation of PEG

Fourier transformation infrared (FTIR) spectroscopy was used to explore any changes in the molecular structure of PEG molecules with elapsed time. PEG 20000 and PEG 6000

solutions were prepared corresponding to suctions of 0.44 and 7.04 MPa. Freshly prepared PEG solutions and solutions aged for 15 days were tested. The FTIR spectrums obtained from both tests were then compared.

6.2.3.2 Membrane pore-size

Investigations were carried out to explore the pore-size of the semipermeable membranes before and after the osmotic tests using Environmental Scanning Electron Microscope (ESEM) and Atomic Force Microscope (AFM). Both the MWCO 14000 and MWCO 3500 were considered in this study.

6.3 Test results and discussion

6.3.1 Chemical analysis of PEG solutions in osmotic tests

Tables 6.1 to 6.3 present the measured concentrations of Na^+, Ca^{2+}, Mg^{2+} and K^+ in the PEG solutions at five different suction levels for the clays studied. The results from the chemical analysis were expressed in mg/l. Anion concentrations were not measured.

Tables 6.1, 6.2 and 6.3 show that irrespective of the applied suctions, a specific amount of cations were expelled during the osmotic tests. The concentrations of the expelled Na^+ ions were the greatest in the all the clays studied. Based on the retained cations in the clays, the modified CECs were calculated. The procedure adopted for calculating the modified CECs are explained in the next section.

Table 6.1. Measurements for cation concentrations in PEG solutions in osmotic tests for

MX80 bentonite

Clay	MX80 bentonite				
Suction (MPa)	0.11	0.44	3.96	5.39	8.91
Cation type	Concentration (mg/l of PEG solution)				
Na^+	37.860	35.200	21.975	46.005	47.602
Ca^{2+}	0.985	0.875	6.440	1.050	0.890
Mg^{2+}	0.124	0.390	0.736	0.140	0.165
K^+	1.823	1.595	0.966	0.739	6.247
Calculated modified CEC (meq/100 g)	82.79	82.99	84.18	80.95	80.02
Percent reduction in CEC	8.32	8.84	6.78	10.36	11.39
Weighted average valence of exchangeable cations	1.45	1.45	1.43	1.46	1.47

Table 6.2. Measurements for cation concentrations in PEG solutions in osmotic tests for

Yellow bentonite

Clay	Yellow bentonite				
Suction (MPa)	0.11	0.44	3.96	5.39	8.91
Cation type	Concentration (mg/l of PEG solution)				
Na^+	34.820	30.870	23.095	20.148	15.307
Ca^{2+}	1.024	8.170	6.742	14.469	8.973
Mg^{2+}	0.276	2.750	0.940	1.866	1.030
K^+	1.896	1.390	1.036	0.648	6.454
Calculated modified CEC (meq/100 g)	78.24	76.64	78.94	77.59	79.27
Percent reduction in CEC	7.86	9.74	7.04	8.63	6.65
Weighted average valence of exchangeable cations	1.97	1.96	1.94	1.94	1.94

Table 6.3. M*easurements for cation concentrations in PEG solutions in osmotic tests for*

Speswhite kaolin

Clay	Speswhite kaolin				
Suction (MPa)	0.11	0.44	3.96	5.39	8.91
Cation type	Concentration (mg/l of PEG solution)				
Na^+	4.605	5.083	4.912	4.065	4.370
Ca^{2+}	0.235	0.645	0.210	1.210	0.770
Mg^{2+}	0.008	0.110	0.040	0.230	0.190
K^+	1.655	2.125	1.398	0.945	1.065
Calculated modified CEC (meq/100 g)	2.13	1.74	2.12	2.06	2.09
Percent reduction in CEC	33.12	39.98	33.35	35.32	34.50
Weighted average valence of exchangeable cations	1.78	1.83	1.80	1.70	1.73

6.3.2 Modified cation exchange complex versus applied suctions

For calculating the modified CECs of the clays in Tables 6.1 to 6.3, the following procedure

was adopted. For a known mass of specimens (5 g of clay were used in each test), the total

mass of each of the exchangeable cation type was calculated based on the total exchangeable

cations (Table 3.1). For the measured concentrations of various exchangeable cations and by

considering the sum of the volume of PEG solution prepared plus the volume of water

expelled from the clay specimens, the mass of the exchangeable cations in the PEG solutions

were calculated. At any applied suction, the difference between total mass of each

exchangeable cation type based on the CECs and the mass of the cations expelled gave the

mass of the retained cations. The mass of exchangeable cation was then converted to the CEC

unit based on the amount of clays considered for the tests. For example, for calculating the

modified CEC of Na^+ in the case of MX80 bentonite, the measured total CEC of Na^+ (see

Table 3.1) was first converted to mg/kg; 51.24 meq/100g × 10 × 23 = 11785.2 mg/kg. For 5 g

of the clay considered, the amount of Na^+ available was $(11785.2 \times 5)/1000 = 58.926$ mg; Volume of water taken for preparing the PEG solution = 200 ml and volume of water expelled at 0.11 MPa during the drying process = 14.53 ml. Thus, the total volume of water = 214.53 ml; Na^+ expelled from MX80 at suction of 0.11 MPa, $x/(214.53/1000) = 37.86$ mg/l (see Table 6.1), $x = 8.122$ mg. The retained Na^+ in MX80 specimen = $58.926 - 8.122 = 50.803$ mg in 5 g; conversion to meq per 100g, $(50.803/5) \times 1000 = 10160.6$mg/kg, $10160.6/(10 \times 23) = 44.177$ meq/100g. Similarly, for Ca^{2+}, Mg^{2+} and K^+ the remaining cation exchange complex in the specimen at applied suction of 0.11 MPa can be calculated as 28.03, 9.386 and 1.199 meq/100g. Thus, the percentage reduction = $100 \times (90.31 - 82.79)/90.31 = 8.32\%$ (see Tables 3.1 and 6.1). At higher PEG concentrations, it was noted that the viscosity of the PEG solutions were far greater to be tested in the ICP-OES. Hence, the solutions were diluted and the volume of water used to dilute the PEG solutions were carefully monitored and considered to calculate the modified CECs.

The osmotic tests were conducted on specimens that were not subjected to monotonic increase in suction (i.e. independent specimens were tested at each suction level). The modified cation exchange complexes versus applied suctions for the clays are presented in Fig. 6.1. Figure 6.1 shows that except for the fraction of Na^+ for Yellow bentonite that increased slightly with an increase in suction (i.e. expulsion of Na^+ reduced with an increase in suction) and the fraction of K^+ that decreased at suction of 8.91 MPa for the bentonites, for all other cases, specific amounts of exchangeable cations expelled from the clays during the osmotic tests. Thus, at all suction levels considered the CECs of the clays reduced as compared to the initial CECs of the clays; however, remained nearly unchanged.
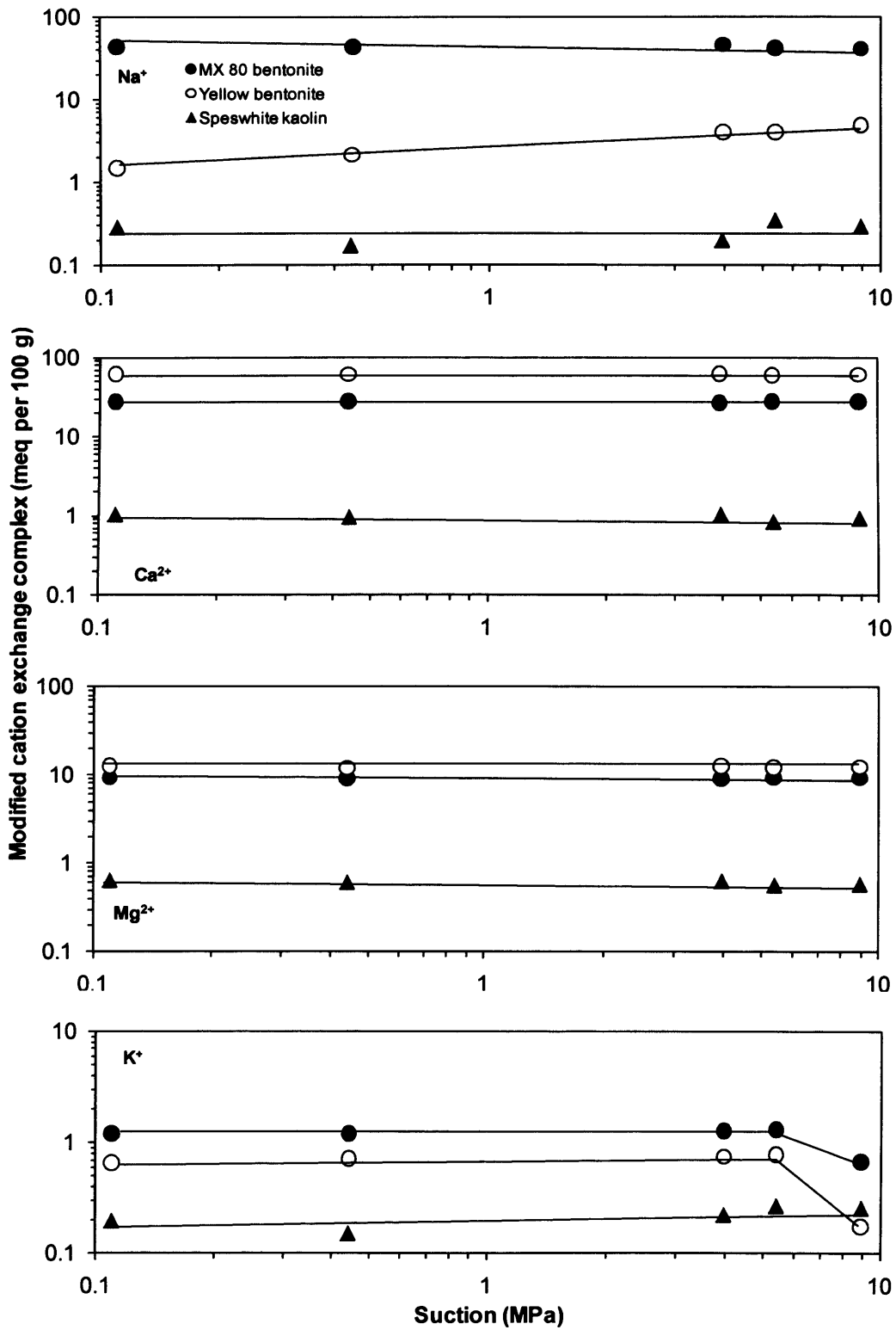
Fig. 6.1: Applied suction versus modified CECs

Percentage reduction in the CECs remained between 6.78 to 11.39% for MX80 bentonite, 6.65 to 8.63% for Yellow bentonite, and 32.18 to 35.32% for Speswhite kaolin (see Tables 6.1 to 6.3). The weighted average valence of the exchangeable cations was found to increase slightly for the bentonites, whereas a greater percentage of expelled Na^+ significantly increased the weighted average valence of Speswhite kaolin (see Fig. 6.1 and Tables 3.1, 6.1, 6.2 and 6.3). Considering that similar percentages of the exchangeable cations in the clays took part in the osmotic equilibrium process (based on π_{salt}^1 and π_{salt}^2 criteria), the percentage of the exchangeable cations that remained inert in the clay systems were found to be 76 to 88% for MX80 bentonite, 80 to 88% for Yellow bentonite, and 20 to 36% for Speswhite kaolin for all applied suctions considered. Therefore, clearly for all cases, the osmotic suction equilibrium was only partially achieved during the osmotic tests. The results showed that the osmotic efficiencies of the bentonites are far greater than that of Speswhite kaolin. In general, clays having higher liquid limits possess greater osmotic efficiency. The weighted average valence of the exchangeable cations (see Tables 6.1 to 6.3) were found to increase slightly for the bentonites (approximately 4% for both bentonites), whereas the greater percentage of Na^+ expelled increased the weighted average valency of Speswhite kaolin, 18% higher than the initial value (see Tables 3.1 and 6.3).

6.3.3 Calculated osmotic suctions (π_{salt}^1 and π_{salt}^2)

Tables 6.4, 6.5 and 6.6 present the calculated osmotic suctions, π_{salt}^1 and π_{salt}^2, for the clays. In each table, the initial water contents, w_i, applied suctions, equilibrium water contents, w_f, w_i-w_f, the expelled and retained volumes of water and the osmotic suctions due to the expelled cations and due to the retained cations are presented. The procedure adopted for calculating the osmotic suctions are explained in Section 6.2.2

Table 6.4: *Calculated osmotic suctions for MX80 bentonite*

	MX80 bentonite				
Initial water content, w_i (%)	520.00				
Suction (MPa)	0.11	0.44	3.96	5.39	8.91
Final water content, w_f (%)	229.50	77.91	28.00	25.94	25.20
w_i - w_f (%)	290.50	442.09	492.00	494.06	494.80
expelled water (ml)	14.53	22.10	24.60	24.70	24.74
remaining water (ml)	11.48	3.90	1.40	1.30	1.26
Expelled cation type	π_{salt}^{1} (kPa)				
Na^+	8.16	7.59	4.74	9.92	10.26
K^+	0.23	0.20	0.12	0.09	0.79
Ca^{2+}	0.37	0.33	2.40	0.39	0.33
Mg^{2+}	0.08	0.24	0.46	0.09	0.10
Total	8.84	8.36	7.71	10.49	11.49
Retained cation type	π_{salt}^{2} (kPa)				
Na^+	954.56	2825.42	8314.70	8077.06	8252.54
K^+	25.86	77.28	227.76	250.84	133.29
Ca^{2+}	908.41	2674.43	7117.60	8029.93	8276.33
Mg^{2+}	304.17	885.41	2431.67	2688.75	2764.94
Total	2193.00	6462.56	18091.73	19046.58	19427.10

Table 6.5: *Calculated osmotic suctions for Yellow bentonite*

	Yellow bentonite				
Initial water content, w_i (%)	165.00				
Suction (MPa)	0.11	0.44	3.96	5.39	8.91
Final water content, w_f (%)	86.70	62.72	35.00	32.00	31.30
w_i - w_f (%)	78.30	102.28	130.00	133.00	133.70
expelled water (ml)	3.92	5.11	6.50	6.65	6.69
remaining water (ml)	4.34	3.14	1.75	1.60	1.57
Expelled cation type	π_{salt}^{1} (kPa)				
Na^+	7.51	6.66	4.98	4.34	3.30
K^+	0.24	0.18	0.13	0.08	0.82
Ca^{2+}	0.38	3.04	2.51	5.38	3.34
Mg^{2+}	0.17	1.70	0.58	1.16	0.64
Total	8.30	11.58	8.20	10.96	8.10
Retained cation type	π_{salt}^{2} (kPa)				
Na^+	84.85	169.91	497.39	625.61	777.34
K^+	38.03	56.61	106.75	123.12	28.37
Ca^{2+}	5423.29	7313.51	13182.78	14047.27	14631.25
Mg^{2+}	1104.26	1424.28	2686.60	2864.28	2996.74
Total	6650.44	8964.31	16473.51	17660.28	18433.71

Table 6.6: *Calculated osmotic suctions for Speswhite kaolin*

	Speswhite kaolin				
Initial water content, w_i (%)	59.00				
Suction (MPa)	0.11	0.44	3.96	5.39	8.91
Final water content, w_f (%)	38.94	36.31	34.42	28.50	24.67
w_i - w_f (%)	20.06	22.69	24.58	30.50	34.33
expelled water (ml)	1.00	1.13	1.23	1.53	1.72
remaining water (ml)	1.95	1.82	1.72	1.43	1.23
Expelled cation type	$\pi_{salt}{}^1$ (kPa)				
Na^+	0.99	1.10	1.06	0.88	0.94
K^+	0.21	0.27	0.18	0.12	0.14
Ca^{2+}	0.09	0.24	0.08	0.45	0.29
Mg^{2+}	0.00	0.07	0.02	0.14	0.12
Total	1.29	1.67	1.34	1.59	1.48
Retained cation type	$\pi_{salt}{}^2$ (kPa)				
Na^+	32.66	23.49	29.09	60.74	59.28
K^+	25.73	20.91	32.91	47.85	52.76
Ca^{2+}	199.56	196.63	226.85	221.36	282.41
Mg^{2+}	125.61	127.39	139.78	152.16	179.81
Total	383.57	368.42	428.62	482.10	574.26

For both bentonites, $\pi_{salt}{}^1$ (sum of Na^+, Ca^{2+}, Mg^{2+} and K^+) remained between 7.71 to 11.58 kPa (Tables 6.4 and 6.5). The calculated $\pi_{salt}{}^1$ for Speswhite kaolin remained less than 2 kPa for all suctions considered (Table 6.6). Imbalance was noted between the cation concentrations on the either side of the semipermeable membrane. The calculated total $\pi_{salt}{}^2$ for all clays were found to be far greater than the calculated $\pi_{salt}{}^1$.

The calculated $\pi_{salt}{}^2$ (sum of Na^+, Ca^{2+}, Mg^{2+} and K^+) varied between 2.19 to 19.4 MPa for MX80 bentonite, 6.65 to 18.43 MPa for Yellow bentonite and 0.38 to 0.57 MPa for Speswhite kaolin. The test results indicated that the applied suctions had very little influence on the calculated $\pi_{salt}{}^1$ values. On the other hand, the calculated $\pi_{salt}{}^2$ were found to increase with an increase in the applied suction for all the clays. The increase in $\pi_{salt}{}^2$ was primarily due to a decrease in the water content of the clay specimens.

6.3.4 Determination of air-entry values from chemical analysis of PEG solution and total suction equilibrium

Based on the calculated osmotic suctions due to the expelled and the retained salts, the commencement of desaturation (i.e. AEV) in the osmotic tests can be determined. Two distinct mechanisms were identified to explain the water content decrease in the osmotic tests based on physico-chemical considerations and total suction equilibration on either side of the permeable membrane (see Section 2.10.3.4). Recalling the two mechanisms, a soil remains fully saturated if $(\pi_{PEG} + \pi_{salt}^{1}) < \pi_{salt}^{2}$ (Mechanism 1), whereas the degree of saturation falls below 100% if $(\pi_{PEG} + \pi_{salt}^{1}) > \pi_{salt}^{2}$ (Mechanism 2). Thus, the difference between $(\pi_{PEG} + \pi_{salt}^{1})$ and π_{salt}^{2} would enable determination of applied matric suctions. The threshold criteria $(\pi_{PEG} + \pi_{salt}^{1}) = \pi_{salt}^{2}$ is the condition for matric suction = 0, which may be considered as the lower bound of the AEV.

Figure 6.2 presents the influence of π_{PEG} on total suction of PEG solution, $(\pi_{PEG} + \pi_{salt}^{1})$, and osmotic suction due to the retained salts within the clays, π_{salt}^{2}. Figure 6.2 shows the influence of an increase in π_{PEG} on $(\pi_{PEG} + \pi_{salt}^{1})$ and π_{salt}^{2} for all three clays studied. A near-linear relationship (approximately 45°) was obtained between π_{PEG} and $(\pi_{PEG} + \pi_{salt}^{1})$.
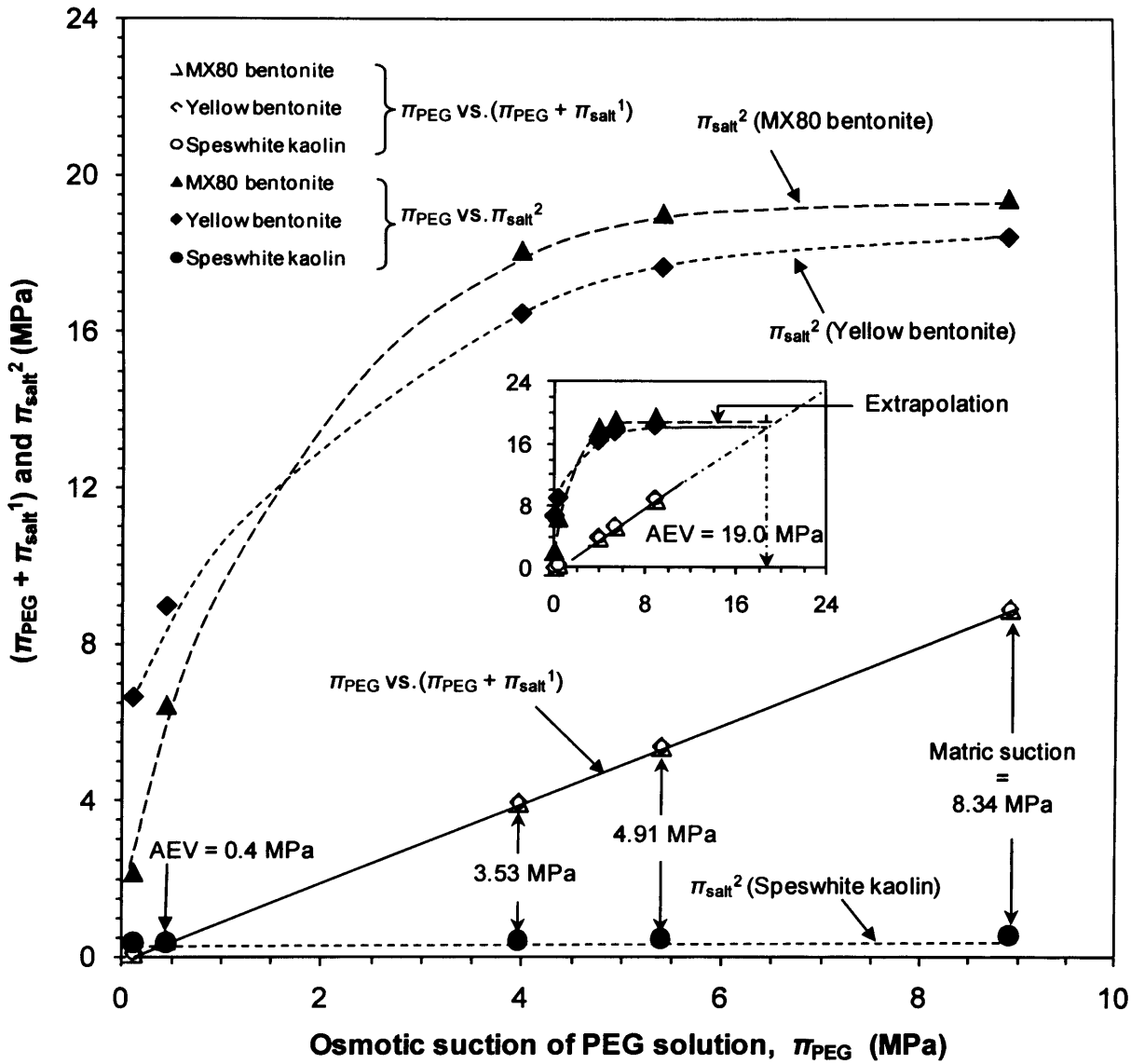
Fig. 6.2 Influence π_{PEG} on total suction of PEG solution, ($\pi_{PEG} + \pi_{salt}{}^{1}$), and osmotic suction, $\pi_{salt}{}^{2}$

For Speswhite kaolin, $\pi_{salt}{}^{2}$ increased from 0.38 MPa to 0.57 MPa with an increase in applied π_{PEG} from 0.11 to 8.91 MPa. At an applied π_{PEG} of 0.11 MPa, $\pi_{salt}{}^{2}$ was found to be greater than ($\pi_{PEG} + \pi_{salt}{}^{1}$), whereas the reverse trend was observed for applied π_{PEG} values greater than about 0.4 MPa.

142

For the bentonites, a reduction in the water content due to an increase in π_{PEG} caused an increase in π_{salt}^2 and the values of (π_{PEG} + π_{salt}^1) remained smaller than π_{salt}^2 for all π_{PEG} considered. π_{salt}^2 increased from 2.19 MPa to 19.43 MPa of MX80 bentonite and from 6.65 to 18.43 MPa for Yellow bentonite for the range of applied suction considered. Higher applied π_{PEG} had less influence on the water content for the bentonites. Therefore, an increase in π_{salt}^2 was far lesser than that occurred at lesser applied suctions.

The test results clearly indicated that the combined influence of π_{PEG} and π_{salt}^1 induced matric suction and enabled reductions in the water content of Speswhite kaolin at π_{PEG} greater than 0.4 MPa (see Fig. 6.2 for applied suction suctions of 3.53, 4.91 and 8.34 MPa). In other words, Mechanism 2 prevailed for applied π_{PEG} values greater than 0.4 MPa for Speswhite kaolin. On the other hand, up to an applied π_{PEG} of 8.91 MPa for bentonites and up to 0.4 MPa for Speswhite kaolin, Mechanism 1 prevailed. Therefore, the clays are expected to remain saturated up to these suctions. The osmotic tests could not be extended beyond 8.91 MPa. Therefore, it is assumed that π_{salt}^2 of the bentonites will be maintained as that occurred at 8.91 MPa and considering (π_{PEG} + π_{salt}^1) is directly proportional to π_{PEG}, extrapolations of the test results (see insert Fig. 6.2) indicated that MX80 bentonite will desaturate at a suction of about 19.0 MPa and will posses matric suction. Similarly, Yellow bentonite will desaturate at about 17.0 MPa and posess matric suction. The AEVs determined in this chapter (i.e. 19 MPa for MX80 bentonite, 17 MPa for Yellow bentonite and 0.4 MPa for Speswhite kaolin) will be compared with the AEVs of the clays determined from the suction-degree of saturation SWCCs in Chapter 7.

6.3.5 Compatibility of various techniques in applying suction

Based on the drying suction-water content SWCCs of the clays (see Fig. 5.6), the test results from pressure plate and osmotic tests were found to be in good agreements up to applied suctions of 0.44 MPa. Therefore, it is reasonable to assume that in terms of composition of the clays, ion expulsion effects were similar in both tests. Similarly, since the clay specimens tested in desiccator tests were initially subjected to a suction of 0.4 MPa in the pressure plate tests, the osmotic test results and the test results from desiccator tests can be compared on the basis of similar chemical composition of the clays.

Chemical analyses of PEG solutions clearly indicated that at any applied suction in the osmotic tests, the water contents attained by the clays were devoid of the influence of osmotic suction corresponding to those fractions of the total available salts in the clays which took part in the osmotic equilibrium process (i.e. $\pi_{salt}^{1} \neq \pi_{salt}^{2}$) and with a reduced salt content due to the fractions of the salts that expelled out of the clays into the PEG solutions (i.e. π_{salt}^{1}). Hence, at any given water content in the overlapping suction range (see Fig. 5.6), the differences between the applied suctions in the osmotic and desiccator tests are primarily due to π_{salt}^{1}. In other words, at any given suction the difference between the water contents in the osmotic and desiccator tests is the water content associated with osmotic suction corresponding to π_{salt}^{1}. However, differences were noted in the overlapping suction region between osmotic and desiccator test results (see Fig. 5.6). In other words, in the overlapping suction range, the differences in suctions were found to be greater than the total calculated π_{salt}^{1} values.

Some difference in the applied suctions may be expected due to the non-linearity of the calibration curve, particularly at higher PEG concentrations, and due to the difference in the experimental methods used for establishing the calibration curve (Michel and Kaufman 1973; Money 1989). However, it appears that neither of the explanation satisfactorily explains the disproportionate effect of greater water contents attained by Speswhite kaolin in the osmotic tests at higher applied suctions (see Fig. 5.6). This indicates that prior to the cavitation in the osmotic tests, the tensile strength of the pore-water resisted the applied suction and caused the water content to remain higher than that obtained from the desiccator tests in the overlapping suction range.

6.3.6 Intrusion of PEG in the osmotic tests

PEG intrusion is generally observed at higher applied suctions (Williams and Shaykewich, 1969). A review of literature suggested that the intrusion of PEG is attributed to the failure of the membrane and the degradation of PEG molecules into smaller size. FTIR analysis of the PEG solutions and AFM studies on the semipermeable membranes are presented in the following sections.

6.3.6.1 FTIR analysis on degradation of PEG

PEG is known to be susceptible to degradation when exposed to air (Hans et al., 1995). Degradation of PEG reduces the molecular weight and the chain length of the molecules. In order to bring out the chemical changes to the PEG molecules, FTIR spectroscopy was employed. Figure 6.3 presents the FTIR spectrums of freshly prepared PEG 20000 and PEG 6000 solutions.
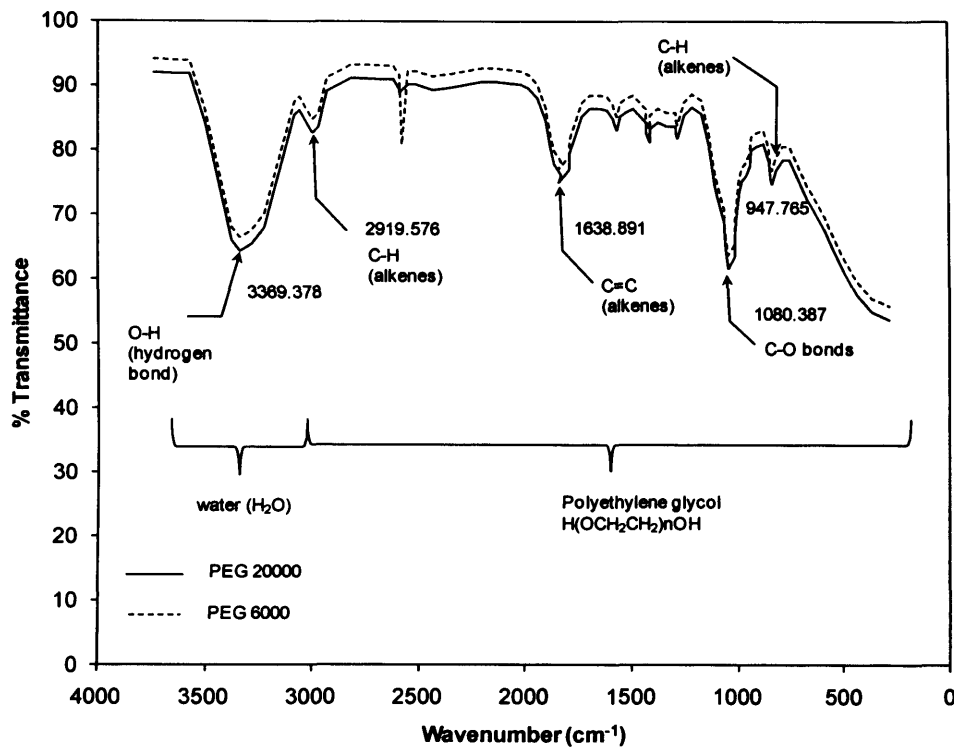
Fig. 6.3: Comparison of FTIR transmittance spectrums for PEG 20000 and PEG 6000

The spectrums are generated based on the amount of infrared transmitted by the solutions corresponding to various values of wavelength or wavenumber. Figure 6.3 clearly showed that molecules of both PEG types consist primarily of carbon, oxygen, and hydrogen covalent bonds (i.e. between wavenumbers 0 to 2920 cm^{-1}). The spectrums corresponding to the wavenumber of approximately 3370 cm^{-1} are for O-H bonds and for the deionized water that was used for preparing the solutions. The FTIR spectrums of the PEG solutions were found to be very nearly similar indicating a similarity in the chemical compositions of both PEGs used. On the other hand, the FTIR spectrum for PEG 6000 remained greater than that occurred for PEG 20000. A greater transmittance for PEG 6000 is primarily due to its shorter chain length that absorbed lesser intensity of the infrared. Delage & Cui (2008a) stated that a longer chain may be expected for PEG 20000 as compared to that of the PEG 6000.

Figures 6.4 and 6.5 compares the FTIR spectrums of PEG solutions tested at zero and 15 days durations. Comparisons of the spectrum of freshly prepared and after 15 days are similar for both PEG 20000 and PEG 6000. No distortion of shifting of the spectrums was detected. Overlapping of the spectrums in Figs. 6.4 and 6.5 clearly indicated that PEG molecules did not degrade at least up to a period of 15 days. The influence of the clay-water systems on the degradation of PEG molecules with elapsed time is beyond the scope of this study.
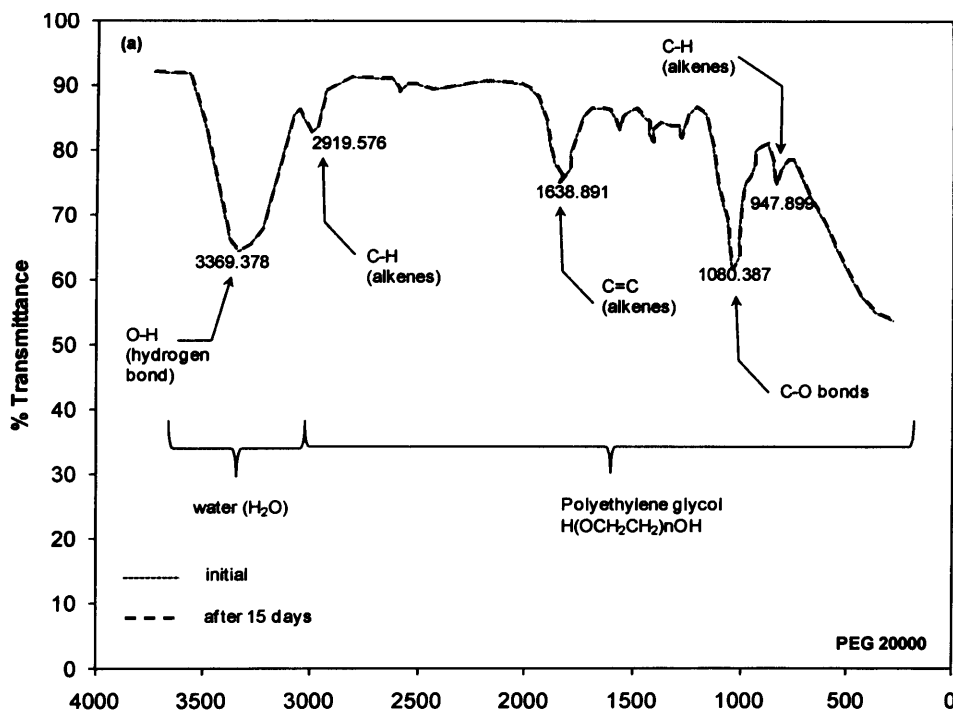
Fig. 6.4: *FTIR transmittance spectrums of PEG 20000*
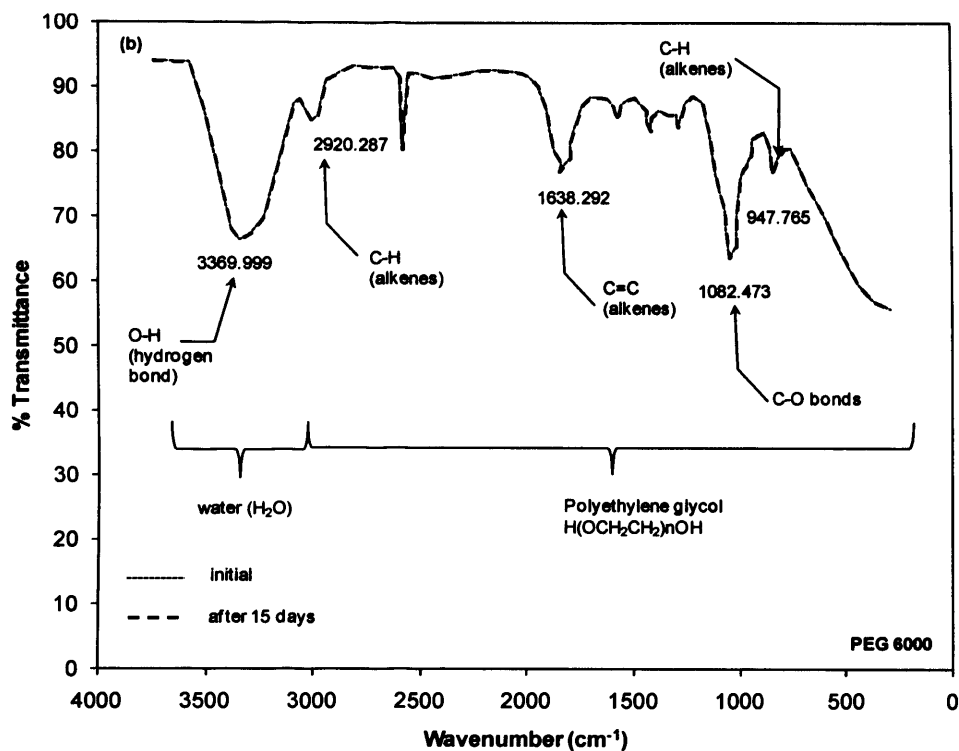
Fig. 6.5: *FTIR transmittance spectrums of PEG 6000*

6.3.6.2 Membrane pore-size analysis

An attempt was made to explore the pore structures of the semipermeable membranes used using Environmental Scanning Electron Microscope (ESEM) as suggested by Kim et al. (1994) and Elimelech et al. (1997). Due to the transparent nature of the semipermeable membrane, it was not possible to explore the pore structure using this method. Thus, the membrane was coated with conductive material (i.e. gold coating). However, conductive coating applied was found to damage the surface of the fragile semipermeable membrane as shown in Fig. 6.6. Therefore, the AFM studies were undertaken. The device and methodology adopted for the AFM studies are presented in Section 4.3.3.2.2.
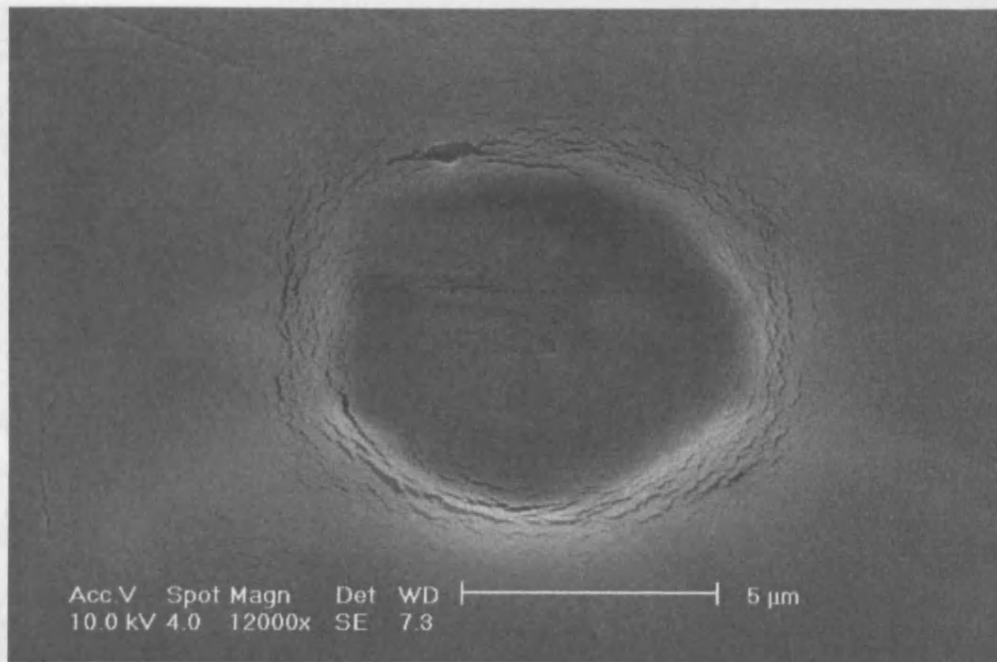
Fig. 6.6: ESEM image of cracking in the surface of MWCO 3500 semipermeable

membrane after coated with conductive material

The AFM phase images of membranes are presented in Fig. 6.7. For each membrane type, the AFM images before and after the osmotic tests are presented. Figures 6.7a and b show the AFM images of MWCO 14000 semipermeable membrane before and after the osmotic tests, respectively. Similarly, the AFM images of MWCO 3500 semipermeable membrane before and after the osmotic tests are shown in Figs. 6.7c and d. Figure 6.7 revealed that the semipermeable membrane composed of well organised regenerated cellulose (RC) strands or chains that interlock onto one another to form a mesh like formation. These cross-link structures acts like pores (Spectrum® Laboratories, 2007) that allow the passage of water and dissolved salts, and at the same time prevent the passage of PEG molecules. The pores of semipermeable membranes in this study were found to vary in size from 1 to 16 nm for MWCO 14000 membrane and 1 to 8 nm for the membrane with MWCO 3500.

Fig. 6.7: *AFM images of MWCO 14000 semipermeable membrane (a) before osmotic test; (b) after osmotic test; and images of MWCO 3500 semipermeable membrane (c) before osmotic test; (d) after osmotic test*

According to Lentsch et al. (1993), the average pore-size of MWCO 14000 and MWCO 3500 is approximately 6 nm and 3.3 nm respectively. The measured pore-sizes in this study were also found to be somewhat larger than the manufacturer's specifications (Spectrum® Laboratories, 2010). An examination of Fig. 6.7d clearly revealed that at an applied suction of 7.04 MPa, the membrane pores were significantly altered and the maximum pore-size increased to about 30 nm. The study showed that irrespective of the magnitudes of applied suction, some alterations of the pore-size occurred during the osmotic test.

FTIR spectrums of PEG solutions did not provide any evidence of a degradation of PEG molecules. However, PEG 6000 with greater MW exhibited higher transmittance due to its shorter chain length. Therefore, at higher applied suction both an increase in the pore-size of the membrane and further a decrease in the size of PEG molecules enabled passing of PEG into the clay specimens. At smaller applied suctions, an insignificant change in the pore-size of the membrane and relatively longer chain length of PEG molecules maintained the osmotic gradient across the membrane.

6.4 Concluding remarks

The test results presented in this chapter can be summarised as follows:

i.   Significant imbalances were noted between the osmotic suctions due to the expelled and the retained salts (i.e. $\pi_{salt}{}^1$ and $\pi_{salt}{}^2$) on either side of the semipermeable membranes in the osmotic tests. The osmotic efficiencies of the highly plastic clays were held responsible for such inequalities in the osmotic suctions. The osmotic suctions due to the expelled cations (i.e. $\pi_{salt}{}^1$) were found to be less than 12 kPa for

the bentonites and less than 2 kPa for Speswhite kaolin. Therefore, the influence of π_{salt}^{1} on the applied suctions was insignificant.

ii. Based on the physico-chemical considerations as applicable to clay-water systems and the total suction equilibrium on either side of semipermeable membranes in the osmotic tests, two distinct mechanisms were found to explain well the water content decrease due to applied suctions for highly plastic clays. In mechanism 1, a change in the water content prior to the air-entry is controlled by the osmotic pressure at interparticle level with the pore-water pressure being zero and in mechanism 2; a decrease in the degree of saturation following the air-entry is primarily on account of the matric suction.

iii. The AEVs of the clays were determined based on the chemical analyses of the PEG solutions in the osmotic tests. The total suction equilibrium on either side of the semipermeable membrane showed that both bentonites desaturated at applied suctions of about 19 (MX80 bentonite) and 17 MPa (Yellow bentonite), whereas Speswhite kaolin was found to desaturate at about 0.4 MPa.

iv. Considering that the water content decrease for Speswhite kaolin between suctions 0.4 and 4.0 MPa in the osmotic tests was negligible (Fig. 5.6), the results concerning the AEV of 0.4 MPa obtained from the total suction equilibrium on either side of the semipermeable membrane (Fig. 6.2) clearly suggested that the delay in desaturation was primarily on account of cavitation in the pore-water of the clays.

v. FTIR spectrums of PEG solutions did not provide any evidence of a degradation of PEG molecules with elapsed time. However, PEG 6000 with greater MW exhibited higher transmittance due to its shorter chain length.

vi. AFM images indicated that PEG intrusion at higher applied suction is attributed to some alteration of the membrane pore-size.

CHAPTER 7

AIR-ENTRY VALUES FROM DRYING SWCCs AND SHRINKAGE CURVES

7.1 Introduction

During the drying process, a transition from saturated to unsaturated state of soils is indicated by the AEV. Highly plastic soils usually possess high AEVs. The AEVs for soils that undergo insignificant volume change due to an increase in the soil suction are usually identifiable on the suction–water content SWCCs that show a distinct break accompanied by a rapid decrease in the water content with an increase in suction. The distinct break is usually less identifiable in case of clayey soils. In this case, the suction–degree of saturation SWCCs alone or the suction–water content SWCCs in conjunction with the shrinkage curves are usually referred to for determining AEVs (Croney and Coleman, 1954; Fredlund and Rahardjo, 1993). For the latter, the suction corresponding to the shrinkage limit has been referred to as the AEV (Fleureau et al. 1993; Fredlund and Rahardjo, 1993). However, soil may well desaturate prior to the shrinkage limit (see Fig. 2.8). Thus, determination of a continuous water content-void ratio path will be necessary for precise determination of the water content and void ratio at the air entry.

For establishing the suction-degree of saturation SWCCs, measurements of both the water content and the void ratio will be required at each applied suctions. The AEV is usually

determined by extending the constant slope portions of the suction–degree of saturation SWCC to intersect the suction axis at degree of saturation of 100% (Vanapalli et al., 1998). In this study, the AEVs of the clays were considered at suctions where the degree of saturation drops below 100%. The objectives of this study were (*i*) to determine the water content-void ratio shrinkage paths of the clays using Clod and wax method, (*ii*) to best-fit the shrinkage paths of the clays from Clod tests using currently available parametric models and (*iii*) to establish the suction-degree of saturation SWCCs based on the suction-water content SWCCs and the shrinkage paths and further determine the AEVs of the clays studied.

The experimental programme is presented first. The test results concerning the volume measurements by wax method and the suction–void ratio SWCCs of the clays are then presented. The volume measurements of the clays by Clod method, the shrinkage paths of the clays, the shrinkage paths of the clays best-fitted with parametric models and the void ratios at air-entry are covered in the following sections. The suction-degree of saturation SWCCs of the clays established based on the suction-water content SWCCs and the shrinkage curves in this chapter are then compared with the AEVs determined from the chemical analyses of PEG solutions and the total suction equilibrium in the osmotic tests presented in Chapter 6. The concluding remarks are presented towards the end of the chapter.

7.2 Experimental programme

Volume measurements of clay specimens during drying from initially slurried conditions were carried out by wax method. Clay specimens in the case were equilibrated at various applied suctions. Additionally, continuous shrinkage paths of the clays were established by Clod method. The procedures adopted for these tests are presented in Chapter 4. However,

for the sake of completeness, the tests carried out are presented briefly in the following sections.

7.2.1 Wax method

Initially slurried clay specimens were equilibrated at several suctions in the pressure plate and desiccator tests. Pressure plate tests were carried out for applying suctions of 0.05, 0.1, 0.2, and 0.4 MPa. The applied suctions in the desiccator tests were 7.5, 21.9, 38.2, 114.1, and 296.7 MPa. Two specimens of each clays were considered at each applied suction, one for water content determination, whereas the other for volume measurement. The suction-water content SWCCs results are presented in Chapter 5. The procedure adopted for measuring volume of clay specimen by wax method is presented in Section 4.5.2.

7.2.2 Clod method

Slurried clay specimens were first equilibrated in the pressure plate at an applied suction of 0.05 MPa. In the Clod tests, the clays specimens were coated with PVAc glue as an encasement material. The Clods were then hung and left to dry in ambient laboratory conditions. The mass and volumes of the specimens were measured frequently in air and in water to determine the volume. The experimental methodology adopted is presented in Section 4.5.1.

7.3 Test results and discussion

7.3.1 Suction-void ratio SWCCs

The measured volumes of the clay specimens equilibrated in the pressure plate and desiccator tests were considered. The void ratios of the clay specimens were determined based on volume-mass relationships that enabled establishing the suction-void ratio SWCCs of the clays. Figure 7.1 presents the suction–void ratio SWCCs of the clays. The suction-void ratio SWCCs of the clays were obtained by joining the pressure plate and desiccator test results with smooth curves. The shapes of the water content and the void ratio SWCCs for the bentonites were found to be similar (see Fig. 5.6 and Fig. 7.1).
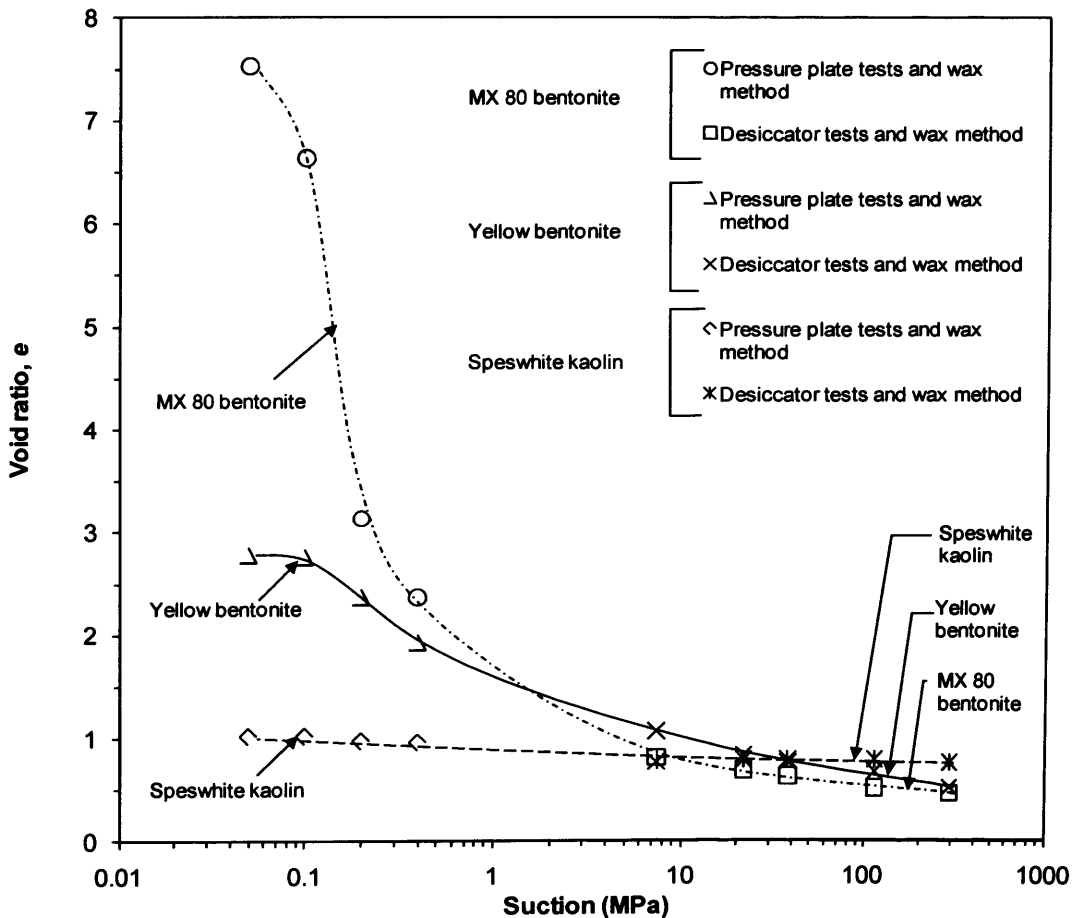
Fig. 7.1: Suction-void ratio SWCCs for the clays studied

157

For Speswhite kaolin, a decrease in the water content and the void ratio were found to be similar up to an applied suction of about 0.4 MPa, whereas an increase in suction had less influence on the void ratio changes at higher suctions giving rise to dissimilar shapes of the water content and void ratio SWCCs. Up to an applied suction of 2.0 MPa, the ordering of the void ratio SWCCs for both bentonites were found to be concurrent with the liquid limits of the clays. At higher suctions, the suction-void ratio SWCC of Yellow bentonite crossed the SWCC of MX80 bentonite and remained above. The suction-void ratio SWCC for Speswhite kaolin crossed the suction-void ratio SWCCs of MX80 bentonite and Yellow bentonite at applied suctions of about 8.0 MPa and 40 MPa, respectively.

In the case of bentonites, the crossing of SWCCs with an increasing suction is attributed to the commencement of the interference of compact ion layers (i.e. Stern layers) that in turn depends upon the hydrated ionic ion size of the exchangeable cations (Verwey and Overbeek, 1948). Similar results have been reported by Marcial et al. (2002) for the bentonites. The test results also suggested that the specific surface area of clays can have significant influence on the pattern of volume change due to an increase in the applied suction.

7.3.2 Volume measurement using Clod method

The volume changes of the Clod specimens against log-elapsed time during the shrinkage process are shown in Fig. 7.2. The test results plotted in normal-scale are shown in the inset of Fig. 7.2. It was noted that the times required for drying of clay specimens to constant volumes were about 30 days for Speswhite kaolin and about 120 days for both the bentonites. At the end of the drying periods, the water contents of the clays were found to be similar to that of the initial water contents of the clay powders stored in similar ambient laboratory

conditions (temperature 25 °C and relative humidity of 60%). The final void ratios of the clod specimens were generally greater than that of the void ratios of the clays at the corresponding shrinkage limits. The water contents of the clay specimens in the Clod tests could not be further reduced. Figure 7.2 shows that the volume change of the clay specimens depend upon the initial water contents of the clays. The magnitude of shrinkage was found to be dependent on the clay type and the liquid limits of the clays.
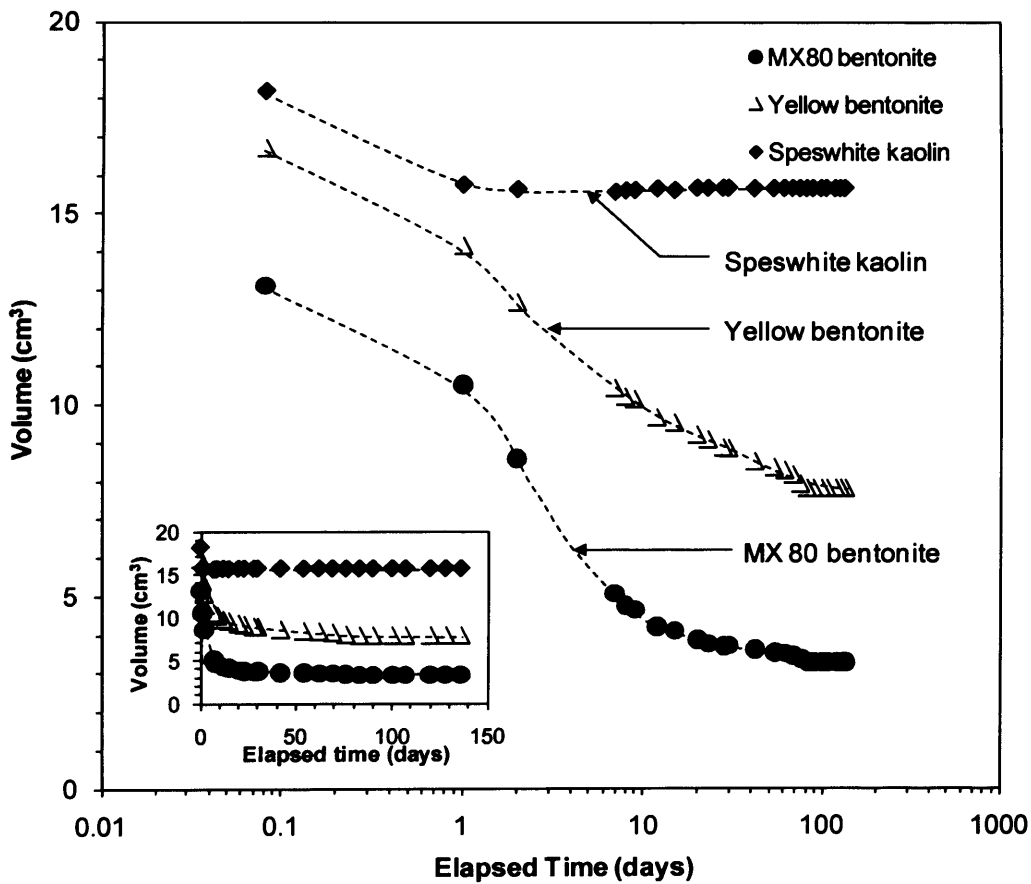
Fig. 7.2: Elapsed time versus volume decrease of the clay specimens in Clod tests

7.3.2.1 Shrinkage paths

Continuous shrinkage paths of the clays were established from the Clod test results. The equations used for determining the void ratios of the clays are presented in Section 4.5.1.

Figures 7.3, 7.4 and 7.5 show the shrinkage paths (i.e. wG_s versus e plots) for the clays

159

studied based on the Clod tests. The test results from wax method are plotted together for comparison.
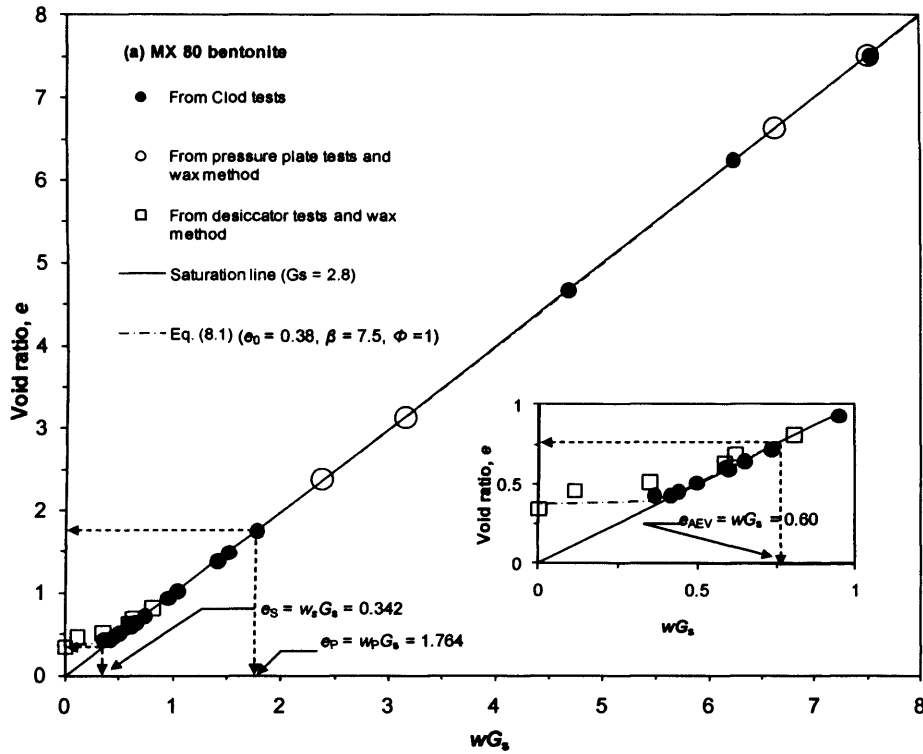
Fig. 7.3: Shrinkage plot for MX80 bentonite
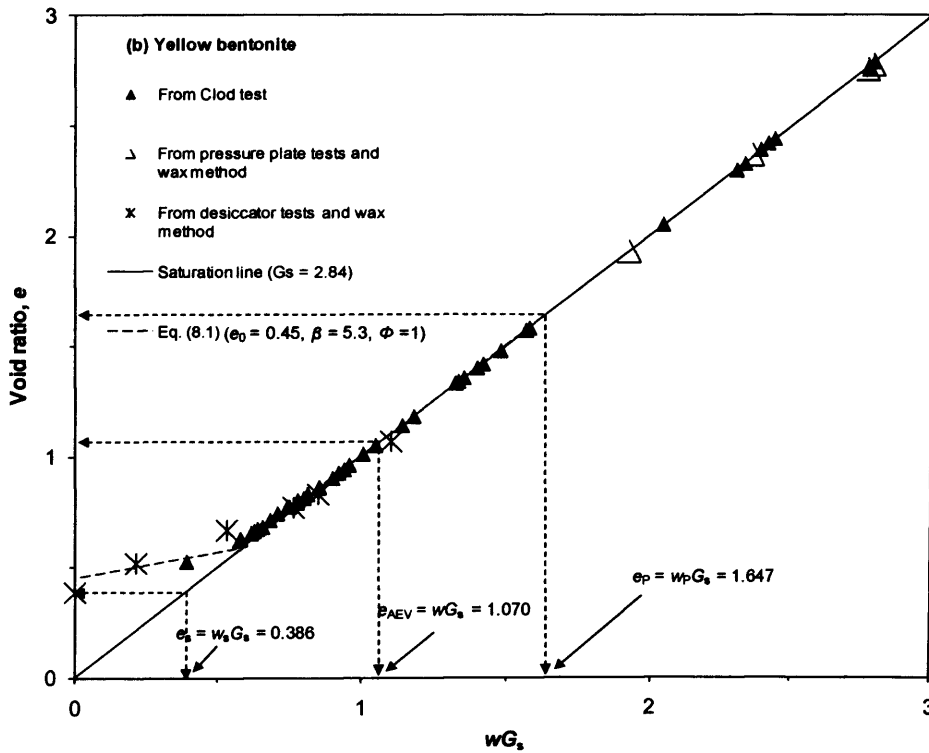
Fig. 7.4: Shrinkage plot for Yellow bentonite
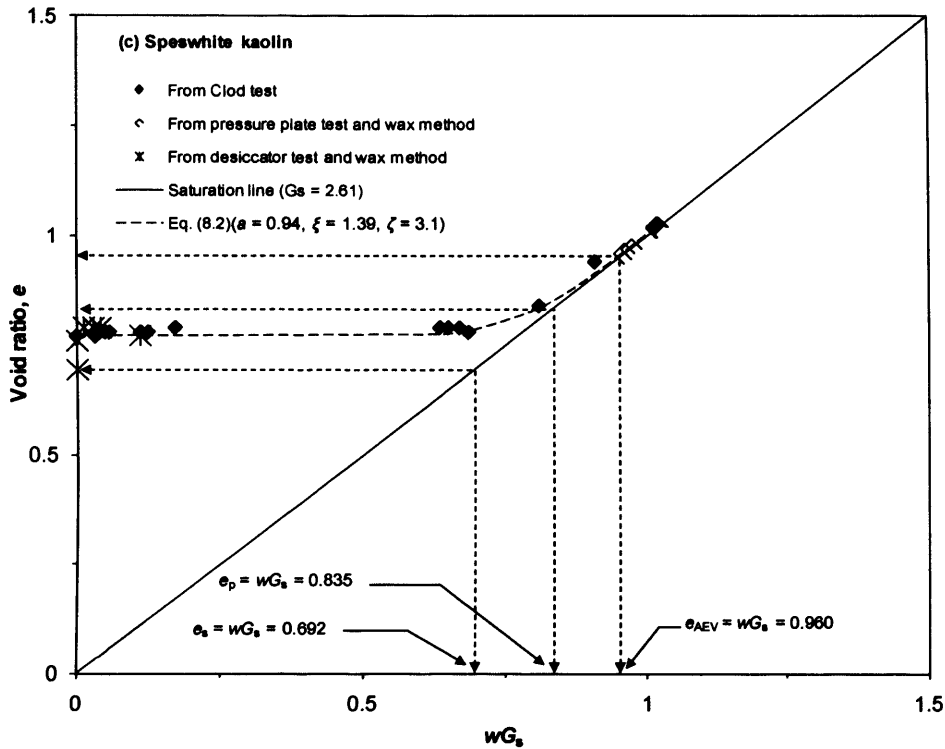
Fig. 7.5: Shrinkage plot for Speswhite kaolin

The wG_S versus e plots enabled precise determination of the desaturation points (i.e. e_{AEV} = $w_{AEV}G_S$, where e_{AEV} and w_{AEV} are the void ratio and water content at air-entry) of the clays. The e_{AEV} for MX80 bentonite, 0.60 (inset Fig. 7.3), was found to be smaller than that of Yellow bentonite, 1.07 (see Fig. 7.4). e_{AEV} for Speswhite kaolin (=0.96) (Fig 7.5) was found to remain in between e_{AEV} of MX80 bentonite and that of Yellow bentonite.

The void ratios of the clays at plastic limits (e_p) and shrinkage limits (e_s) (i.e. $e_p = w_pG_S$ and $e_s = w_sG_S$) are shown in Figs. 7.3, 7.4 and 7.5. The liquid limit (w_l) values were not considered as the initial water contents and void ratios of the clays in the Clod tests were found to be far lesser. Comparison of the void ratios at both e_p and e_s of the bentonites showed that the e_{AEV} remained between e_p and e_s. However, in the case of Speswhite kaolin, the e_{AEV} was found to be slightly greater than e_p. These void ratios are the true representative for the desaturation of the clays (i.e. $S_r < 100\%$). On the other hand, the AEV is usually considered equivalent to the shrinkage limit void ratio (e_s) (Fleureau et al. 1993).

Interestingly, in all cases, e_s for the clays were found to be slightly smaller than the void ratios attained by the specimens at the end of the Clod tests. The differences between the final void ratios in the Clod tets and the shrinkage limit tests are in accordance with the percent reduction in the CECs of the clays (see Tables 6.1 to 6.3). It is hypothesized that during the pressure plate tests expulsion of cations reduced the plasticity characteristics of the clays. A greater percentage of expelled cations affected the Clod test results for Speswhite kaolin. In this case, a significant difference was noted between e_s and the final void ratio at the end of the Clod test.

The tests results indicated that the void ratios determined from wax tests and Clod tests were comparable. Figures 7.3, 7.4 and 7.5 clearly indicated that in all cases, the clay specimens desaturated prior to the shrinkage limits.

7.3.2.2 Best-fit shrinkage paths using parametric models

In order to obtain smooth shrinkage paths for the clays and further determine the suction-degree of saturation SWCCs, the Clod test results were best-fitted using currently available shrinkage models. Several parametric models were considered. However, two models were found to be suitable for the clays studied. A three parameter KEA model proposed by Kim et al. (1992) (Eq.8.1) and a four parameter model (ModGG model) proposed by Cornelis et al. (2006) (Eq. 8.2) were used for best-fitting the shrinkage paths of the clays. Equation 8.1 was found to be suitable for shrinkage paths of the bentonites used in this study, whereas the four parameter model (Eq.8.2) was found to be suitable for Speswhite kaolin.

$$e = e_0 \exp(-\beta w G_s) + \varphi w G_s \qquad\qquad \text{Eq. (8.1)}$$

$$e = e_0\, e + a \left[\exp \frac{-\xi}{(wG_s)^\zeta} \right]$$

Eq. (8.2)

In Eqs. 8.1 and 8.2, e_0 is the void ratio at no shrinkage, β is the slope parameter that depends on the air-entry point, φ and is the slope of the saturation line, w is the water content, a, ξ and ζ are the model parameters.

The void ratios corresponding to the last drying data in the Clod tests were fitting data while accounting for the expelled exchangable cations. Solver functions in Microsoft Excel were used to generate the best-fitted curves for the shrinkage paths for the clays studied. The best-fitted curves were further adjusted manually to force the calculated relationships through the air entry points while maintaining a reasonable best-fit to all Clod test data. The parameters used in best-fitting of the shrinkage curves based on Eq. 8.1 and Eq. 8.2 are presented in Table 7.1.

Table 7.1: *Model parameters determined for the clays studied*

Clay	Kea Model (Eq. 8.1)		ModGG Model (Eq.8.2)		
	β	φ	a	ξ	ζ
MX80 bentonite	5.80	1	567.91	6.89	0.224
Yellow bentonite	3.95	1	53.798	4.6122	0.377
Speswhite kaolin	1.45	0.825	0.94	1.39	3.1

Some difficulties were encountered while best fitting the test results for the bentonites. The main challenge was to force the calculated relationships through the air-entry points while maintaining a reasonable best-fit to all the Clod data.

7.3.2.3 Suction-degree of saturation SWCCs

Based on the suction-water content SWCCs (see Fig. 5.6) and the best-fitted shrinkage paths (see Figs. 7.3, 7.4, and 7.5, Eqs. 8.1 and 8.2, and Table 7.1) the suction-degree of saturation SWCCs for the clays were established. For the water content data in Fig. 5.6 for pressure plate and desiccator tests, the e values were calculated based on the best-fitted shrinkage curves. Similarly, the water contents corresponding to various applied suctions in the osmotic tests (see Fig. 5.6) were considered to calculate the void ratios from the best-fit shrinkage curves. The degree of saturation corresponding to any void ratio was calculated based on volume-mass relationship. Figures 7.6, 7.7 and 7.8 show the suction-degree of saturation SWCCs for the MX80 bentonite, Yellow bentonite and Speswhite kaolin, respectively. The suction-degree of saturation experimental data from the pressure plate tests and desiccator tests for which the void ratio were calculated based on the wax test results are also shown for comparison.
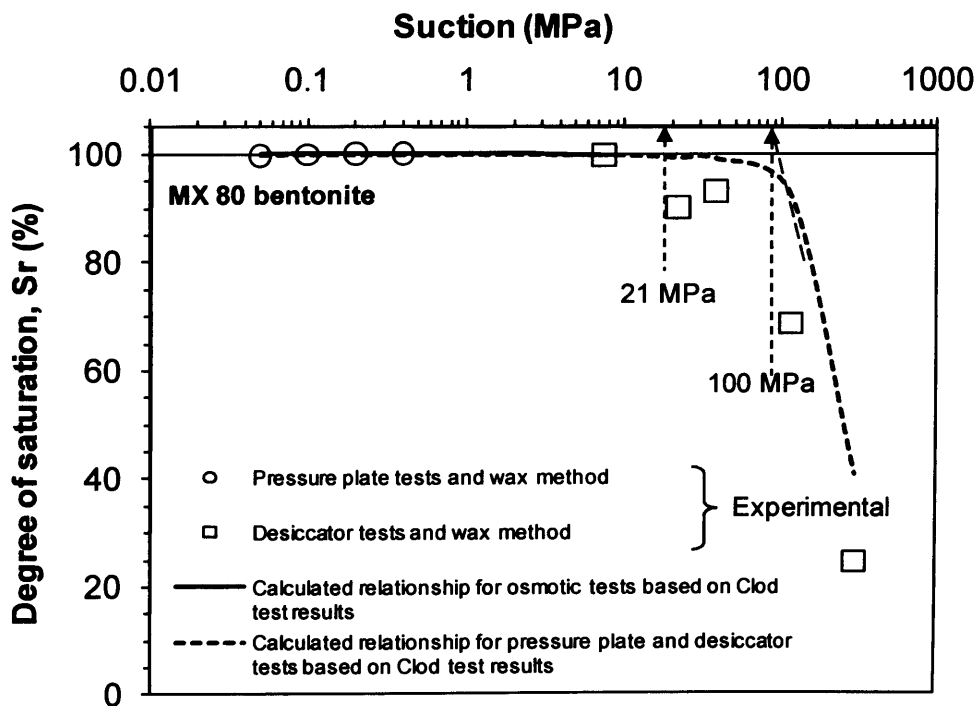
Fig. 7.6: Suction–degree of saturation SWCCs for MX80 bentonite

Suction (MPa)
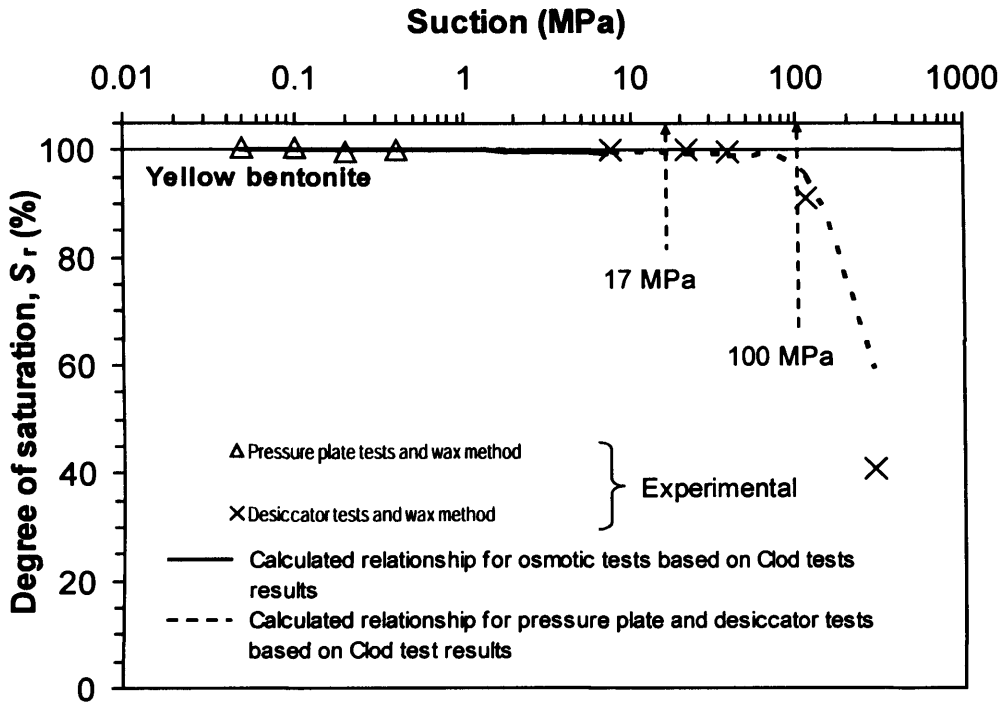
Fig. 7.7: Suction–degree of saturation SWCCs for Yellow bentonite

Suction (MPa)
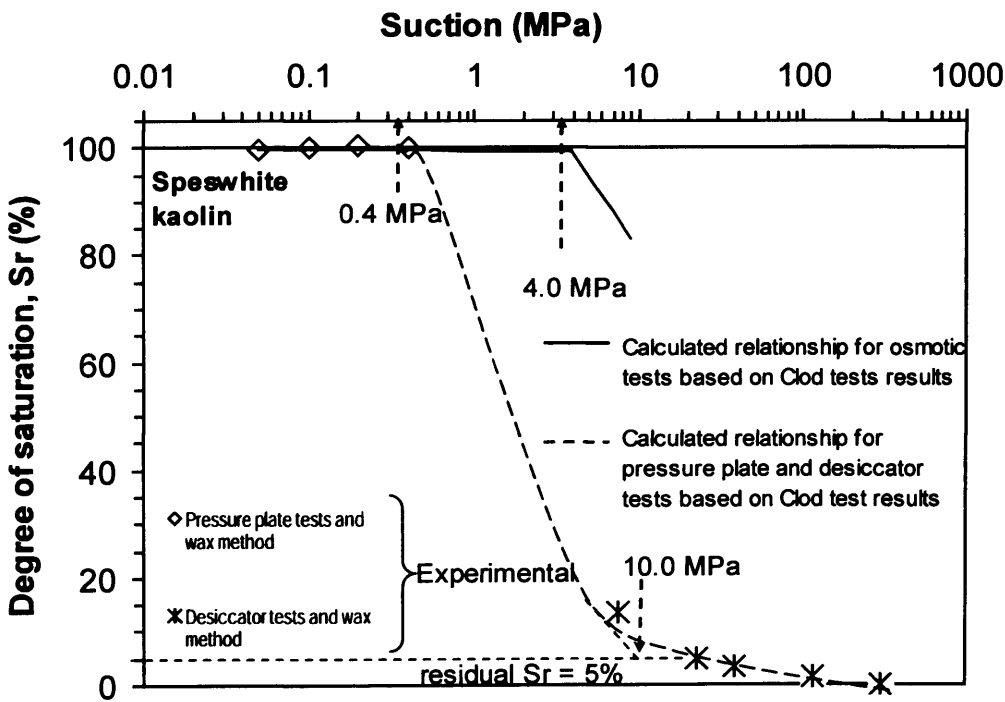
Fig. 7.8: Suction–degree of saturation SWCCs for Speswhite kaolin

165

7.3.2.4 Determination of AEVs

The AEVs of the clays were determined from three different approaches. In approach (*i*), the the suction-degree of saturation SWCCs established based on the suction-water content SWCCs (pressure plate and desiccator test results) in conjunction with the best-fit shrinkage paths were considered. In approach (*ii*), the constant slope portions of the suction-degree of saturation SWCCs in approach (*i*) were extended to intersect the suction axis at $S_r = 100\%$ (Vanapalli et al., 1998). In approach (*iii*), the AEVs of the clays were determined based on the test results from osmotic and Clod tests.

Table 7.2 presents the comparisons of the AEVs determined from different approaches. The AEVs of the clays determined based on chemical analyses of PEG solutions and total suction equilibrium in osmotic tests are also presented for comparison.

Table 7.2: *Comparisons of AEVs of the clays from different approaches*

Clay	AEV based on approach (*i*)* (MPa)	AEV based on approach (*ii*)** (MPa)	AEV based on approach (*iii*)*** (MPa)	AEV from chemical analyses & total suction equilibrium in osmotic tests (MPa)+
MX80 bentonite	21.0	100.0	-	19.0
Yellow bentonite	17	100.0	-	17
Speswhite kaolin	0.4	0.45	0.45	0.4

* Based on the suction-water SWCCs of the clays (pressure plate and desiccator test results in conjunction with the Clod test results)

** Based on extending the constant slope portions of the suction-degree of saturation SWCCs to intersect the suction axis at $S_r = 100\%$

*** Based on the osmotic tests and best-fit Clod tests

+ Refer to Section 6.3.4

Referring to Figs. 7.6, 7.7 and 7.8, and Table 7.1, based on approach (*i*), the AEVs were found to be about 21, 17 and 0.4 MPa for MX80 bentonite, Yellow bentonite and Speswhite kaolin, respectively. On the other hand, based on the approach (*ii*), the AEVs of the bentonites were found to be similar, about 100 MPa, whereas in the case of Speswhite kaolin, the AEV was found to be slightly higher (about 0.45 MPa) than that determined from approach (*i*). The AEVs of the bentonites could not be determined from approach (*iii*) as the S_r remained at 100%, whereas for Speswhite kaolin the AEV was about 4.0 MPa.

Differences were noted in the AEVs of the clays from approach (*i*) and (*ii*) considered. However, similarities were noted between the AEVs determined from the total suction equilibrium in the osmotic tests and those obtained from approach (*i*). The differences between the AEVs from approach (*ii*) and that from the total suction equilibrium in the osmotic tests are primarily due to the different considerations adopted for choosing the air-entry points. In the osmotic tests, the bentonites remained saturated up to a suction of 8.91 MPa (see Figs. 7.6 and 7.7), whereas although the degree of saturation for Speswhite kaolin was found to be about 99.5% (see Fig. 7.8) at an applied suction of 0.44 MPa; the AEV became distinct only at 4.0 MPa. The results confirmed that for Speswhite kaolin prior to the cavitation in the osmotic tests, the tensile strength of the pore-water resisted the applied suction thereby shifting the AEV further than the actual value. The residual degree of saturation for Speswhite kaolin was found to be about 5.0% corresponding to suction of 4.0 MPa (see Fig 7.8) following the procedure suggested by Vanapalli et al. (1998). On the other hand, the residual degree of saturation of the bentonites could not be determined. An applied suction of greater than 300 MPa is required to establish the entire suction-degree of saturation SWCCs for the bentonites.

7.3.5.1 Suction at shrinkage limits

In a water content-void ratio plot, determination of the shrinkage limit water content requires extending the driest void ratio to the theoretical 100% degree of saturation line. The degree of saturation of soils at shrinkage limit is 100%. However, when the shrinkage limit water contents were marked on the suction–water content SWCCs (see Fig 5.6), the corresponding suctions were found to be approximately 200 MPa for the bentonites and about 1.0 MPa for Speswhite kaolin. These suction values may not be acceptable as AEVs of the clays due to the fact that the degree of saturation values of the clays corresponding to these suctions in Figs. 7.6, 7.7 and 7.8 are less than 100%.

7.4 Concluding remarks

The findings from the study can be summarised as follows:

i.   The Clod tests were found to be effective in establishing the entire shrinkage paths for the clays studied. The desaturation points for the clays were determined from the shrinkage paths. The clay specimens were found to be desaturated well prior to the shrinkage limits. Good agreements were noted between the wax and Clod test results.

ii.   The suction-water content SWCCs in conjunction with the Clod test results enabled establishing the suction-degree of saturation SWCCs and the determination of AEVs of the clays.

iii.   The AEVs of the clays can be determined from several approaches. The agreements between the AEVs determined from the chemical analyses of PEG solutions and total suction equilibrium in the osmotic tests and from the suction-degree of saturation SWCCs were found to be very good.

iv.   The degree of saturation of Speswhite kaolin based on the water contents obtained from the osmotic tests and the corresponding void ratios obtained from the Clod tests remained constant at 99.5% between applied suctions of 0.4 and 4 MPa. The degree of saturation further decreased at higher applied suctions. This indicated that the AEV of Speswhite kaolin was delayed in the osmotic tests. Such a phenomenon can be described by cavitation in the pore-water.

v.   The AEVs determined from the shrinkage limits of the clays may not be reasonable as the degree of saturation of the clays were found to be lower than 100%.

CHAPTER 8

EFFECTS OF COMPACTION DENSITY & CONFINING CONDITIONS ON WETTING BEHAVIOUR

8.1 Introduction

The wetting suction-water content SWCCs are commonly established in the laboratory by decreasing the suction of soils (Fredlund and Rahardjo, 1993). The wetting SWCC is influenced by the soil structure, type of soil, mineralogy, density, initial water content, stress history, method of compaction and confining stress (Tinjum et al. 1997; Vanapalli et al. 1999; Thu et al. 2007). From a practical point of view, clays are usually compacted at different dry densities. Low dry densities (1.1 to 1.2 Mg/m^3) are generally used in the construction of clay liners in municipal solid waste disposal and ponds (Rowe et al., 1997), whereas heavily compacted clays (1.6 to 2.0 Mg/m^3) are used for buffer material in nuclear waste repositories (Komine, 2004). A comprehensive study on the effect of compaction density (1.5 to 1.7 Mg/m^3) on the wetting characteristics of FEBEX bentonite has been reported by Villar and Lloret (2004). The test results indicated that the effect of dry density was insignificant under unconfined conditions. Similar results were also reported by several other researchers for different clays (Delage et al., 1998; Saiyouri et al., 2000; Ye et al., 2010). Under isochoric condition, Komine and Ogata (1994) noted that the water uptake capacity of compacted specimens decreases with an increase in the compaction density.

The water uptake capacities of compacted clays under confined and unconfined conditions have been studied in the past (Delage et al., 1998; Yahia-Aissa, 2001; Villar and Lloret, 2004; Ye et al., 2010). The test results indicated that the water contents of clay specimens in the confined tests were lower than that of the specimens tested under unconfined condition, most notably at suctions lower than 5 MPa. In all cases, the effect of confinement was found to reduce the water uptake capacity of clays. Additionally, the effect of confinement on the water uptake capacities of the clays was found to be minor at applied suctions greater than 5 MPa.

From microstructural perspectives, insertion of water molecules during the wetting process occurs in two steps, (*i*) insertion of water in the elementary layers followed by (*ii*) filling of larger interparticle pores (Saiyouri et al., 2000). The insertion of water molecules in the interlayer occurs in an organised fashion, forming one, two, three and sometimes up to four layers of water (Grim, 1968; Saiyouri et al., 2000; Likos, 2004; Delage et al., 2006). The amount of water adsorbed depends on the specific surface area, available exchangeable cations, valency and temperature (Bolt, 1956; Sposito and Prost, 1982; Pusch, 1982; Mitchell, 1993; Schanz and Tripathy, 2009).

The objectives of this study were (*i*) to determine the wetting suction-water SWCCs of the clays, (*ii*) to determine the influence of initial dry density on the wetting suction-water content SWCCs of compacted clay specimens, (*iii*) to determine the influence of confining conditions on the water uptake capacity of compacted clay specimens under unconfined, laterally confined and isochoric conditions (*iv*) to measure the swelling pressures of bentonites under isochoric condition and (*v*) to investigate the microstructural changes of

bentonites during the wetting process using ESEM and low angle XRD analysis. In all cases, only the suction-water content SWCCs were studied.

The experimental programme is presented first, followed by time equilibration plots and the wetting suction-water content SWCCs of powder specimens. The wetting SWCCs under various confining conditions are then presented, such as the wetting SWCCs under unconfined condition, the wetting SWCCs under laterally confined condition, and the wetting SWCCs under isochoric condition. The swelling pressures of compacted bentonite specimens are then presented, followed by the results from investigations of microstructure of the clays. The concluding remarks are presented in the end of the chapter.

8.2 Experimental programme

8.2.1 Wetting suction-water content SWCCs

The wetting suction-water content SWCCs of the three clays were determined for both powder and compacted specimens at hygroscopic water contents. The wetting tests were conducted on specimens having initial water contents of 9.6%, 17.6% and 0.66% for MX80 bentonite, Yellow bentonite and Speswhite kaolin, respectively. Various compaction densities and confining conditions were considered. Bentonite powders were compacted at targeted dry densities of 1.2, 1.3, 1.4, 1.5, 1.6 and 1.7 Mg/m^3, whereas Speswhite kaolin specimens were prepared at dry densities of 1.2, 1.3 and 1.4 Mg/m^3. However, for studying the water uptake under isochoric condition, only the bentonites were considered and prepared at a single targeted dry density of 1.7 Mg/m^3.

Table 8.1 shows the experimental programme adopted in this study. The wetting suction-water content SWCCs were determined by volumetric pressure plate for applied suctions of 0.05, 0.1 and 0.2 MPa. Desiccator method was used to apply suctions of 3.3, 7.5, 21.9, 38, 114.1 and 300 MPa. Several osmotic tests were carried out only on powder specimens at applied suctions of 0.05, 0.11, 0.44, 0.99, 1.76, 2.75 and 3.96 MPa. The osmotic tests were not considered for laterally confined and isochoric conditions.

Table 8.1: *Experimental programme for wetting suction-water content SWCCs for the clays*

Clays	Initial dry density (Mg/m^3)	Confinement conditions	Suction control with	Applied suctions (MPa)
Powder				
MX80 bentonite Yellow bentonite Speswhite kaolin	-	Unconfined	Desiccator tests	300, 114.1, 38, 21.9, 7.5, 3.3
			Osmotic tests	3.96, 2.75, 1.76, 0.99, 0.44, 0.11
			Volumetric pressure plate tests	0.2, 0.1, 0.05
Compacted				
MX80 bentonite Yellow bentonite Speswhite kaolin	1.3, 1.4, 1.5, 1.6, 1.7	Unconfined	Desiccator tests	300, 114.1, 38, 21.9, 7.5, 3.3
			Volumetric pressure plate tests	0.2, 0.1, 0.05
MX80 bentonite Yellow bentonite Speswhite kaolin	1.2, 1.3, 1.4, 1.5, 1.6, 1.7	Laterally confined	Desiccator tests	300, 114.1, 38, 21.9, 7.5, 3.3
			Volumetric pressure plate tests	0.2, 0.1, 0.05
MX80 bentonite Yellow bentonite	1.7	Isochoric	Suction controlled oedometer	38, 21.9, 7.5, 3.3

No attempt was made to measure the volume changes of the specimens during the transient wetting process and after the completion of the tests. Severe peeling of the specimens

surfaces were observed in the desiccators tested under laterally confined conditions. Furthermore, specimens tested in the volumetric pressure plate under unconfined condition were found to be segregated particularly at low applied suctions, causing volume measurement a difficult task. Special care was taken during measurement of the mass changes to avoid loss of materials.

8.2.2 Water content versus suction relationship of clay-water mixtures (chilled-mirror dew-point tests)

Several clay-water mixtures were prepared by thoroughly mixing clay powders with deionized water. The experimental procedure is described in Section 4.4.

8.2.3 Swelling pressures of compacted bentonites

8.2.3.1 Multistep swelling pressure tests

Compacted bentonites exhibit swelling pressure when wetted under isochoric condition. The swelling pressures of the bentonites were measured. Multistep wetting tests were conducted by equilibrating bentonite specimens at applied suctions of 38, 21.9, 7.5 and 3.3 MPa by means of vapour equilibrium technique. Tests were carried out using a newly developed vapour controlled oedometer. Details of the device are described in Section 4.6.1. Once equilibrated at each applied suctions, the water contents of the specimens were measured by oven-drying method.

174

8.2.3.2 Single step swelling pressure tests using deionised water

Single step swelling pressure tests were carried out by hydrating compacted bentonites with deionised water. Tests were carried out using a modified oedometer described in Section 4.6.3. After the swelling pressure tests were completed, the water contents of the specimens were measured by oven-drying method.

8.2.4 Microstructural investigations

8.2.4.1 Environmental Scanning Electron Microscope (ESEM)

In order to explore the changes in the microstructures of compacted bentonites during the wetting process, compacted bentonite specimens were tested in the ESEM. The tests were carried out by increasing the relative humidity of the testing chamber of the ESEM (see Section 4.7.1). MX80 bentonite was compacted at dry density of 1.6 Mg/m^{3}and tested. In addition, Yellow bentonite prepared at a targeted dry density of 1.4 Mg/m^3 was also tested.

8.2.4.2 X-Ray Diffraction (XRD)

XRD at low angle were performed on powder clay specimens equilibrated at various applied suctions in the desiccator tests. Applied suctions of 300, 38, 21.8, 7.5 and 3.3 MPa were considered. Additionally, clay powders equilibrated at laboratory condition and at applied suction of 0.05 MPa in the volumetric pressure plate tests were considered. The changes in the c-axis spacing were measured and the numbers of layers of adsorbed water were determined.

8.3 Test results and discussion

8.3.1 Suction equilibration in osmotic and volumetric pressure plate tests (powder)

Typical elapsed time versus water content of powder specimens studied at an applied suction of 0.11 MPa in the volumetric pressure plate and osmotic tests are shown in Fig. 8.1. Figure 8.1 shows that the water contents of the clays obtained from the osmotic tests and pressure plate tests are very nearly similar. The ordering of the water contents of the specimens were found to be concurrent with the liquid limit values of the clays. A longer equilibration time of about 60 days was required for specimens in the volumetric pressure plate.
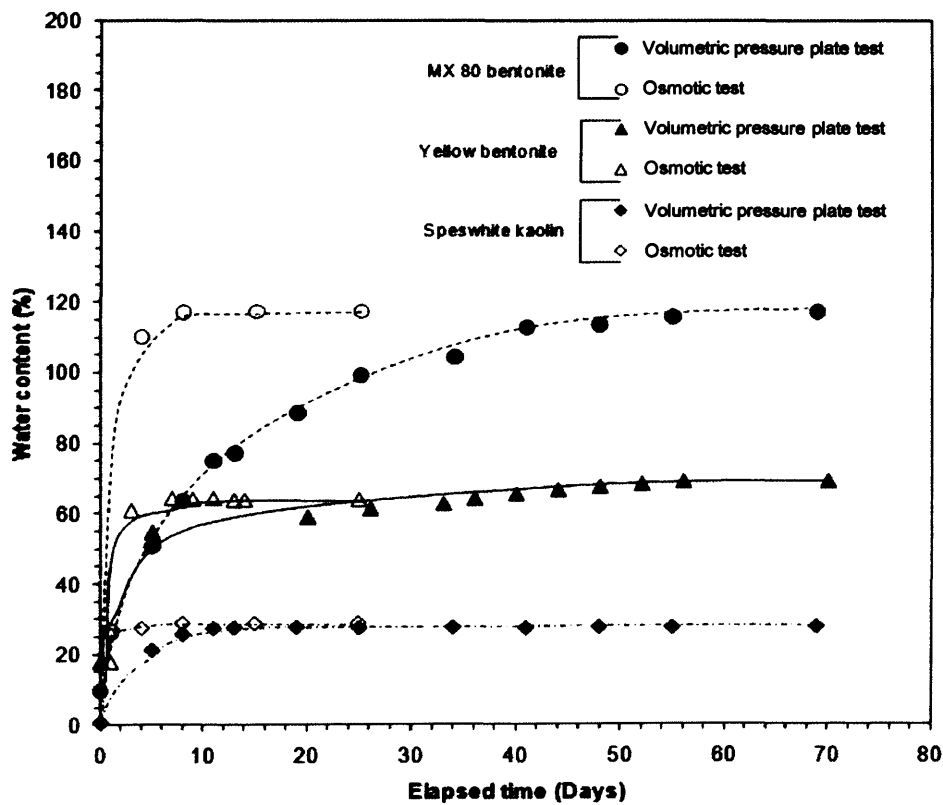
Fig. 8.1: *Comparison of equilibration time in volumetric pressure plate and osmotic tests*

8.3.2 Suction equilibration in desiccator tests

The elapsed time versus the water content increase for the clay powders equilibrated at applied suctions of 3.3 to 300 MPa in the desiccator tests are shown in Figs. 8.2, 8.3 and 8.4. The water contents of the clays at equilibrium increased with a decrease in the applied suction. The water contents of the clays were found to be the highest at an applied suction of 3.3 MPa (equilibrated with K_2SO_4 solution).
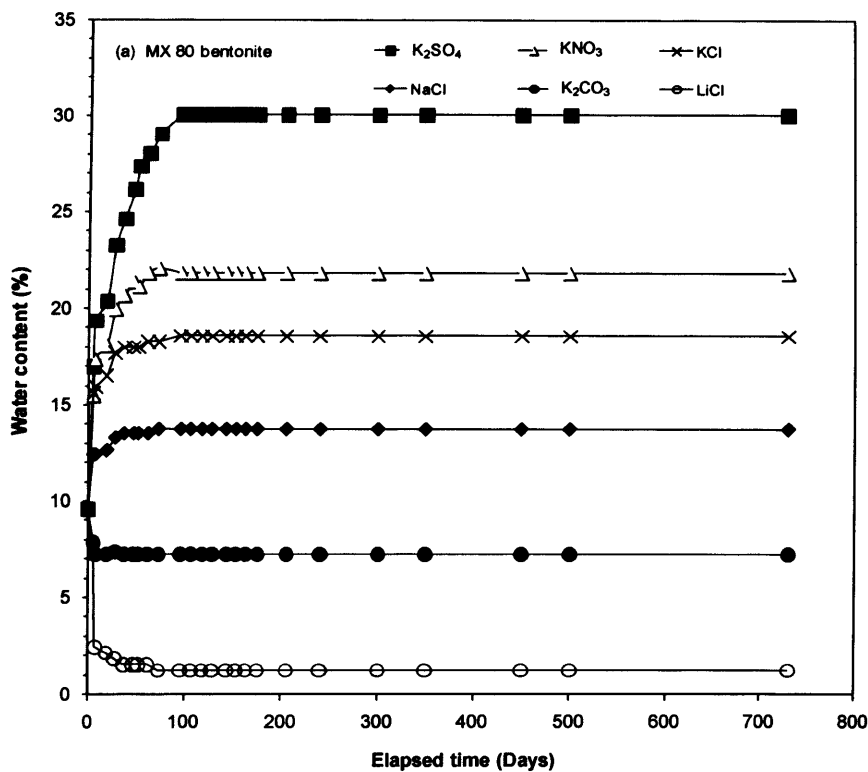
Fig. 8.2: *Equilibration time in desiccator tests for MX80 bentonite*

In all cases, it was observed that at an applied suction of 300 MPa (i.e. LiCl), the water contents of the clays were reduced as compared to other applied suctions (see Figs. 8.2, 8.3 and 8.4). A slight increase in the water content was detected for Speswhite kaolin tested at applied suction of 114.1 MPa (i.e. K_2CO_3). On the other hand, the water contents of both bentonites decreased at an applied suction of 114.1 MPa (i.e. K_2CO_3). An equilibration

period of about 100 days was found to be adequate for both bentonites, whereas an

equilibration time of about 50 days was found to be sufficient in the case of Speswhite kaolin.

Testing times in the desiccator tests were found to be longer than that occurred for osmotic

tests and volumetric pressure plate tests. Delage et al. (1998) stated that that water exchange

that occurred in liquid states is generally faster as compared to vapour exchange. Differences

were noted between the equilibration times in the volumetric pressure plate tests and the

osmotic test results. The differences could be attributed to the methodology adopted. In the

case of volumetric pressure plate tests, clay specimens were wetted only from the bottom,

whereas in the osmotic tests the clay specimens were submerged in the PEG solutions (i.e. 3-

dimensional wetting).
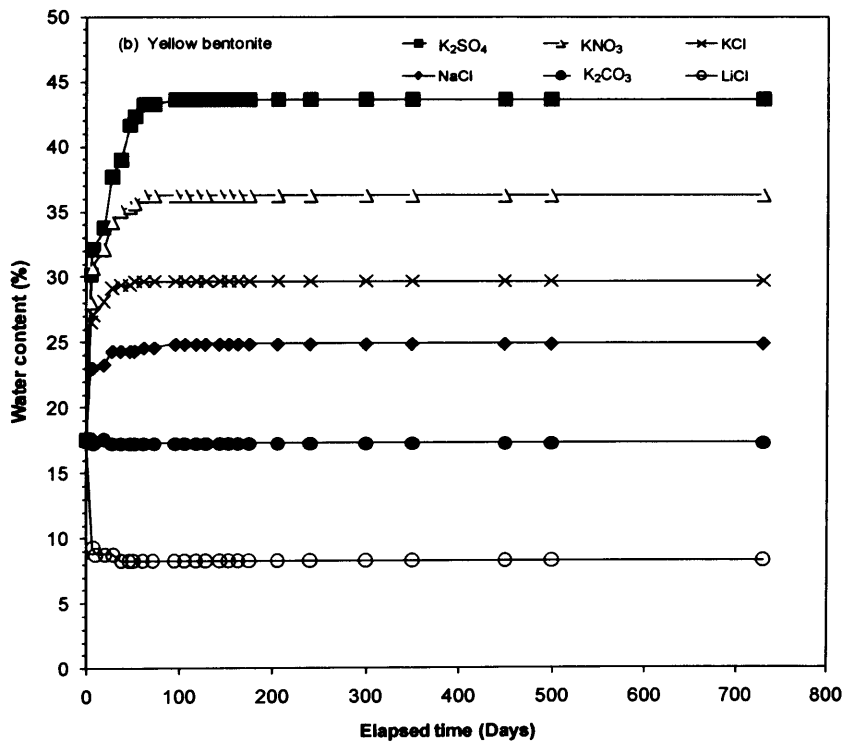
Fig. 8.3: *Equilibration time in desiccator tests for Yellow bentonite*
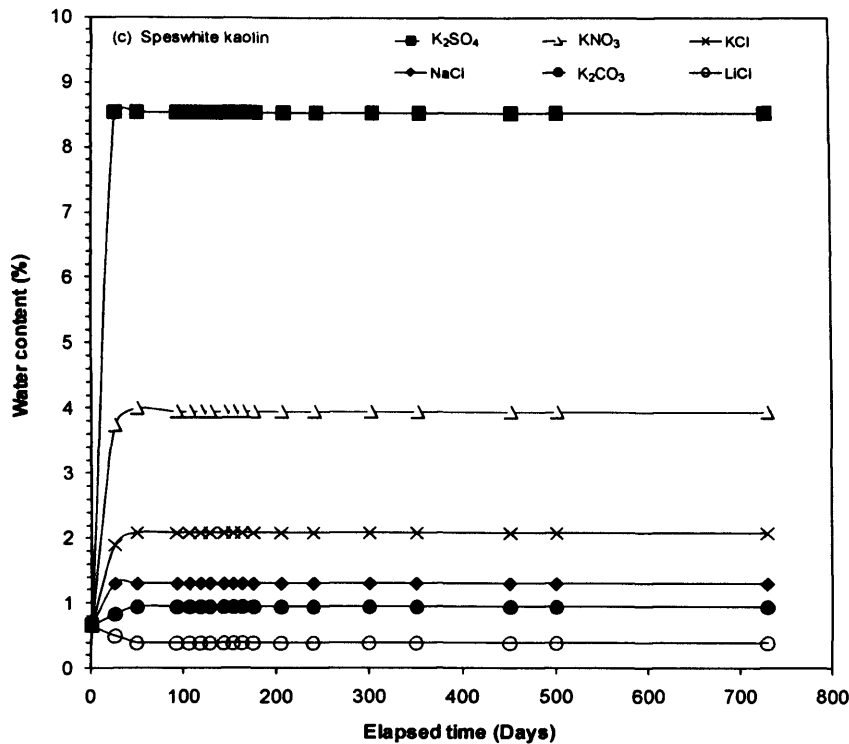
Fig. 8.4: *Equilibration time in desiccator tests for Speswhite kaolin*

8.3.3 Wetting suction-water content SWCCs of powder specimens

The wetting SWCCs of powder specimens established from volumetric pressure plate tests, osmotic tests and desiccator tests are presented in Fig. 8.5. The water content versus suction relationships from chilled-mirror tests are plotted together for comparison.

The experimental data were joined with smooth curves in order to bring out the influence of clay-type on the water absorption behaviour. Between applied suctions of 300 to 0.4 MPa, the ordering of the SWCCs was found to be concurrent with the specific surface area of the clays (Yellow bentonite, MX80 bentonite and Speswhite kaolin), whereas at lower suctions, the SWCC of Yellow bentonite crossed the SWCC of MX80 bentonite and remained below.
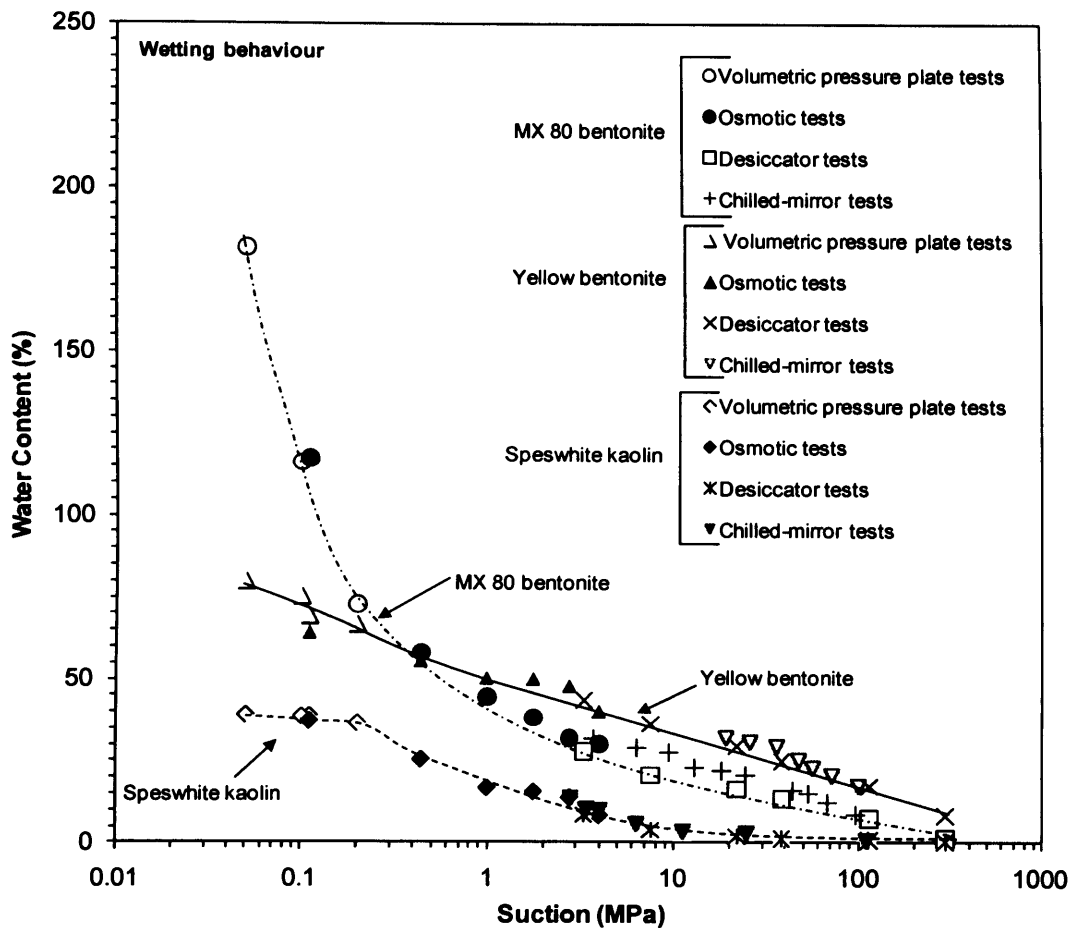
Fig. 8.5: *Wetting suction-water content SWCCs of powder specimens*

It was noted that at applied suctions lower than 0.4 MPa, the ordering of the SWCCs followed the respective liquid limit values of the clays. However, in all cases the water contents attained by the specimens were far lower than the respective liquid limit values. The SWCC of Speswhite kaolin for all suction range considered was found to be far lower than the SWCCs of both bentonites. This is primarily due to low CEC value and low specific surface area of Speswhite kaolin (Mitchell, 1993).

The water content versus suction relationships of clay-water mixtures from chilled-mirror tests were found to be somewhat higher than the SWCCs of the bentonites, whereas good agreements were noted in the case of Speswhite kaolin. This phenomenon can be attributed to

180

the different methodology adopted in preparing the clay-water mixtures tested in the chilled-mirror device. In this case, water is thoroughly mixed with clay powders (see Section 4.4.1). On the other hand, in the wetting tests, clay powders were equilibrated at different suctions from dry condition.

8.3.4 Wetting suction-water content SWCCs under unconfined condition (compacted specimens)

The wetting suction-water content SWCCs of compacted specimens under unconfined condition are presented in Fig. 8.6. In Fig. 8.6, the powder SWCCs from Section 8.3.3 are plotted together with the compacted suction-water content SWCCs to bring out the influence of clay-type and initial dry density on the water uptake capacities of the clays. The wetting suction-water content SWCCs of the clay powders are presented by smooth curves. The shape and the ordering of the SWCCs were found to be similar to that of determined for the powder specimens.

Similar to the powder specimens, the test results indicated that the clay-type plays a significant role in the water uptake capacities of the clays. However, differences were noted at applied suction of less than 0.1 MPa. At this suction region, it was noted that the water contents for MX80 bentonite were slightly lower than that determined for the powder specimens (see Fig. 8.6). The water contents of the clays decreased with an increase in the dry density of the bentonite specimens. In the case of Speswhite kaolin, it was noted that there was no significant density effect on the water uptake capacity under unconfined condition. The differences at lower applied suction are primarily attributed to the changes in the pore structure of the specimens with increasing dry density (Tinjum et al., 1997).

181
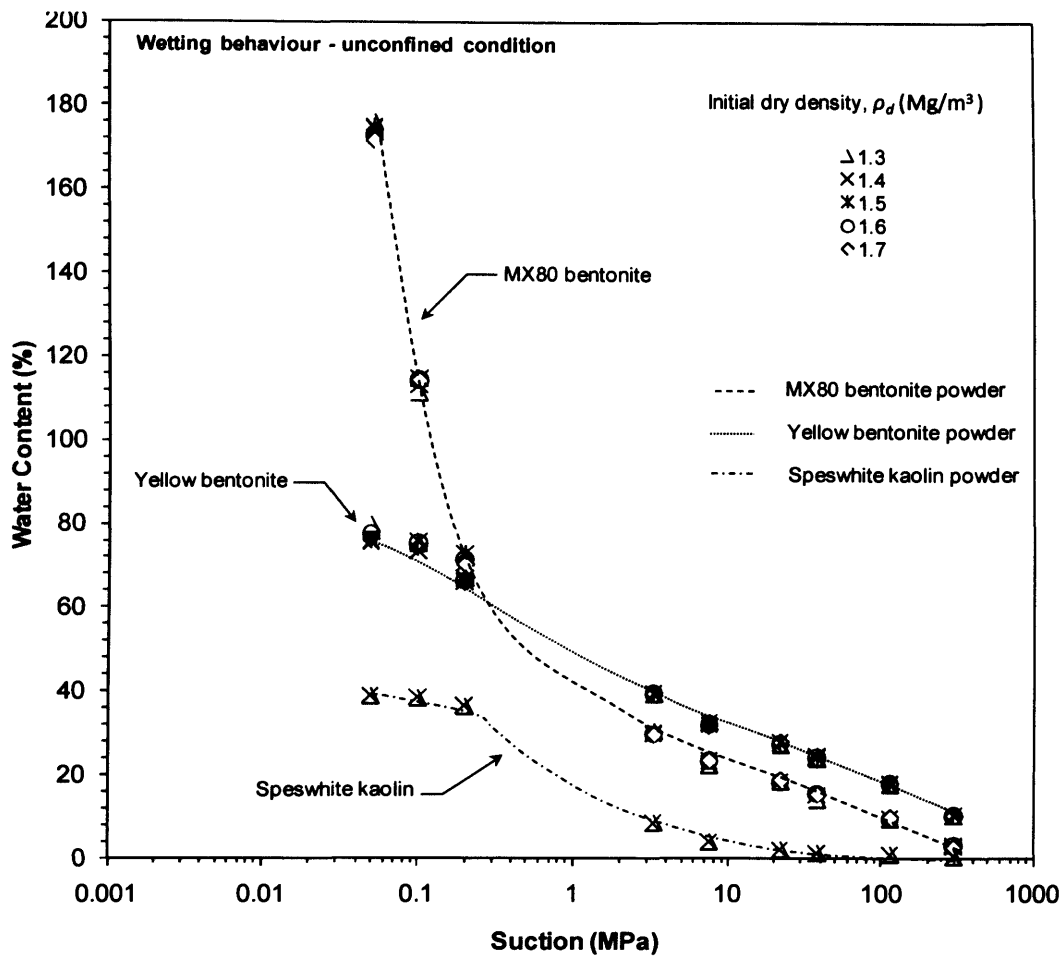
Fig. 8.6: *Wetting SWCCs under unconfined condition*

8.3.5 Wetting SWCCs under laterally confined condition (compacted specimens)

The wetting suction-water content SWCCs of compacted specimens tested under laterally confined condition from volumetric pressure plate tests and desiccators tests are presented in Figs. 8.7, 8.8 and 8.9. The wetting SWCCs of the clays from powder specimens are presented for comparisons (marked as powder SWCCs). Significant differences in the water contents of bentonites were noted, particularly at lower applied suctions. On the contrary, for suctions of 38 to 3.3 MPa, no significant differences were noted between the water contents attained by

182

both bentonites as compared to the water contents of the powder specimens. Similarities in the water contents of Speswhite kaolin is noted for all suctions considered. It is noted that partial confinement provided by the specimen rings reduced the water uptake capacities of the bentonites at low applied suctions.
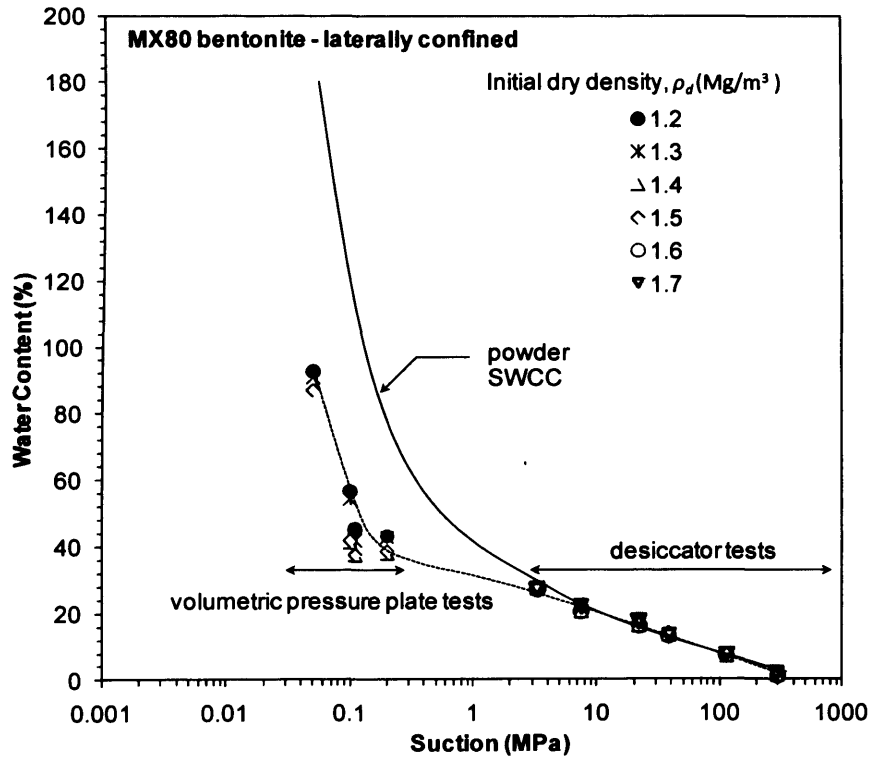
Fig. 8.7: *Suction-water content SWCCs under laterally confined condition*

for MX80 bentonite
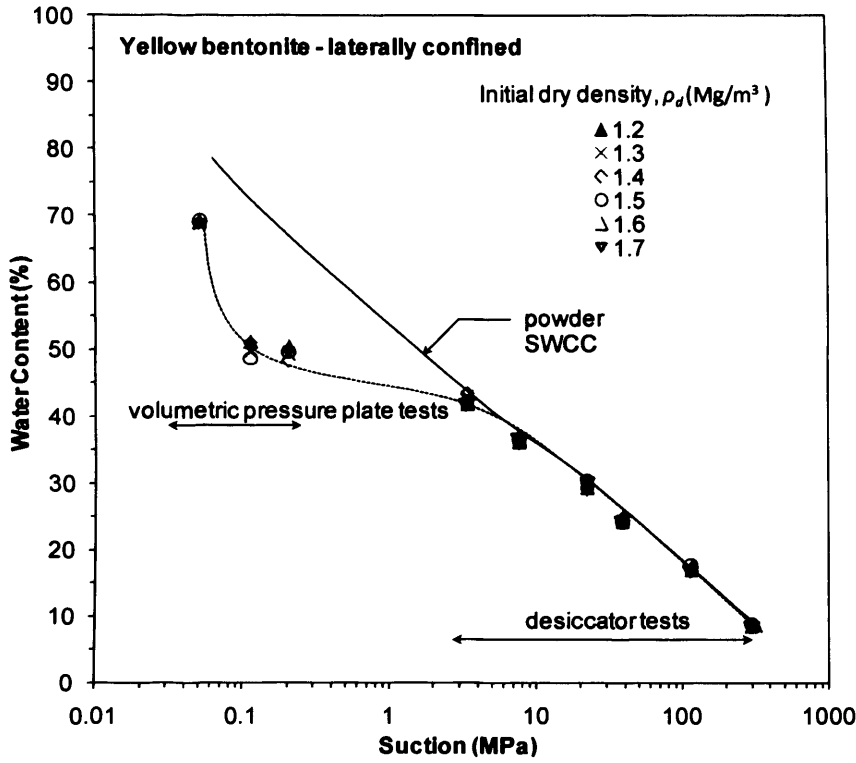
Fig. 8.8: *Suction-water SWCCs under laterally confined condition for Yellow bentonite*
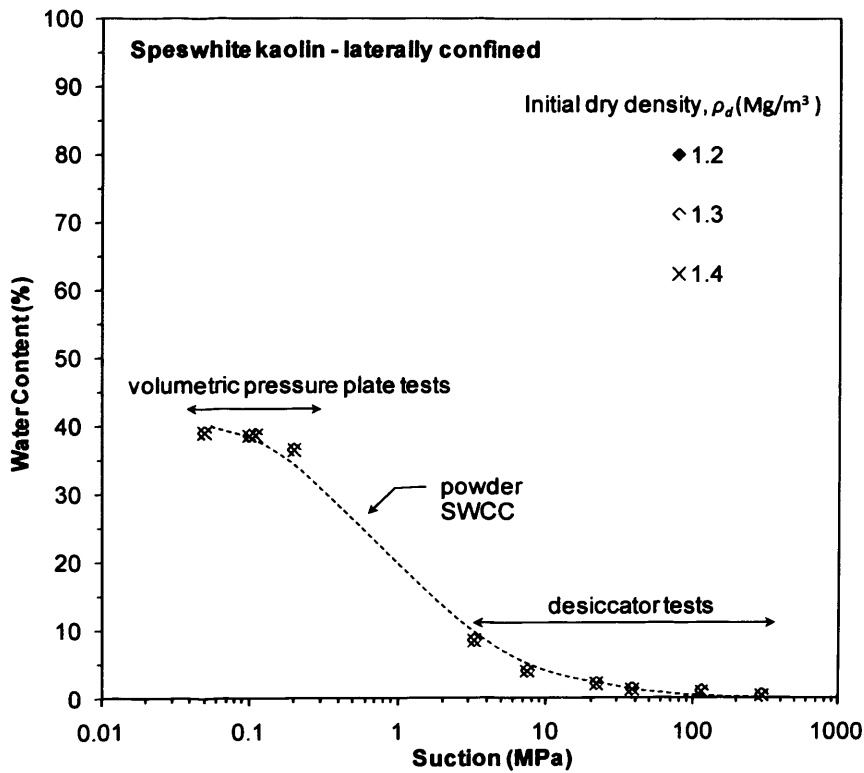
Fig. 8.9: *Suction-water content SWCCs under laterally confined condition for Speswhite kaolin*

8.3.6 Suction-water content relationships under isochoric condition (compacted specimens)

The wetting suction versus water content relationships of compacted bentonite specimens tested under isochoric condition from suction controlled oedometer tests are presented in Fig. 8.10. The wetting SWCCs of the clays from powder specimens are presented together to bring out the influence of clay-type, initial dry density and the confining condition on the water absorption behaviour of bentonites. The suction-water content relationships at applied suctions from 38 up to 3.3 MPa showed similar water contents, irrespective of the confining conditions and the initial dry densities. Figure 8.10 clearly indicated that the water contents of Yellow bentonite remained above that of MX80 bentonite for all applied suctions considered (i.e. 38 to 3.3 MPa). The ordering of the suction-versus water content relationships was found to be concurrent with the specific surface area of the bentonites (i.e. higher the specific surface area, greater is the water content) (see Table 3.1).

It is expected that for all suctions considered, the adsorption of water molecules occurred within the interlayer pores (Grim, 1968; Saiyouri et al., 2000). Overall, excellent agreement was noted between the suction-water contents relationships from vapour controlled oedometer test results and the SWCCs of the bentonites between applied suctions of 38 to 3.3 MPa. The tests results clearly indicated that the effects of both dry density and confining conditions on the water uptake capacities of the clays were negligible at higher suction ranges (Delage et al., 1998; Yahia-Aissa et al., 2001; Ye et al., 2009).
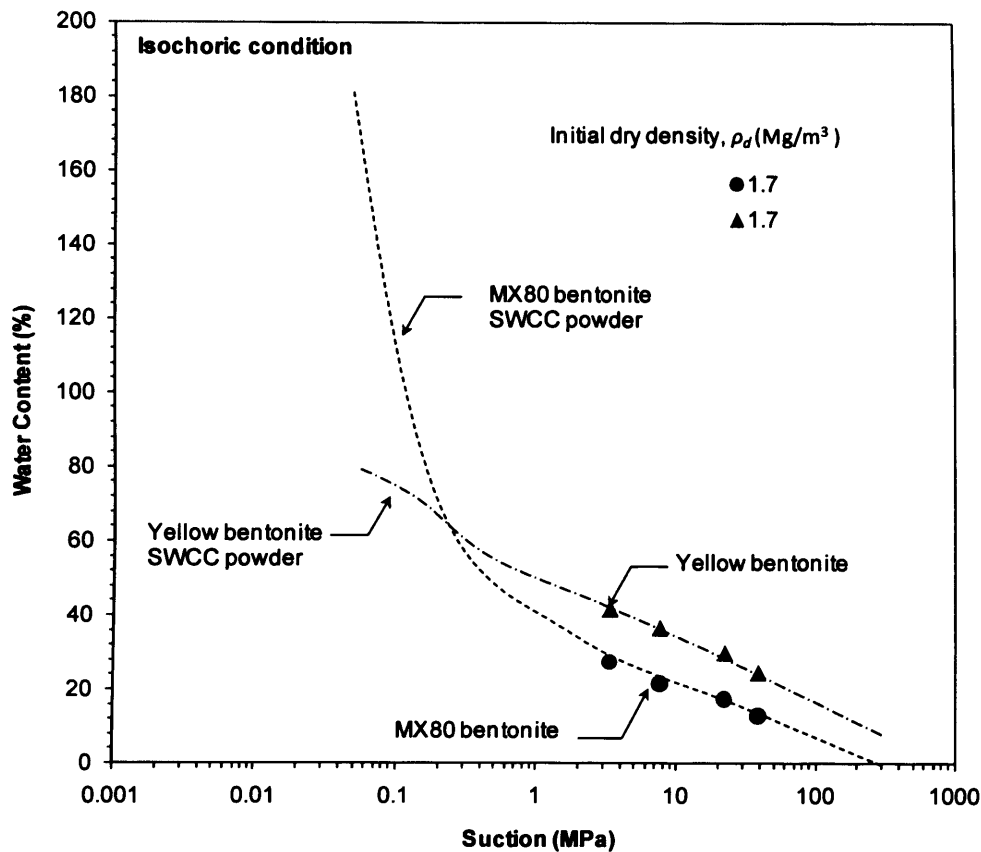
Fig. 8.10: *Suction versus water content relationship under laterally confined condition for MX80 bentonite, and Yellow bentonite*

8.4 Swelling pressures of compacted bentonites

8.4.1 Multistep swelling pressure tests

The swelling pressures of bentonite specimens were measured simultaneously during the wetting tests under isochoric condition. The swelling pressures developed at various applied suctions are presented in Fig. 8.11 and Fig. 8.12 for MX80 bentonite and Yellow bentonite, respectively.

The test results shown in Figs. 8.11 and 8.12 indicated that the swelling pressure of both bentonite increased with the decrease in the applied suctions. Equilibration time of about

20000 minutes was found to be adequate for all suction considered. Figure 8.13 shows the suction versus swelling pressure of both bentonites. For MX80 bentonite, the swelling pressure recorded was about 2.55 MPa at applied suction of 3.3 MPa. The swelling pressure exhibited by Yellow bentonite was found to be greater than that of MX80 bentonite at all applied suctions considered. Divalent-rich Yellow bentonite exhibited greater swelling pressures than that of monovalent-rich MX80 bentonite. The swelling pressures of bentonites were found to be concurrent with the specific surface area and the valency of the dominant exchangeable cations of the bentonites (Schanz and Tripathy, 2009).
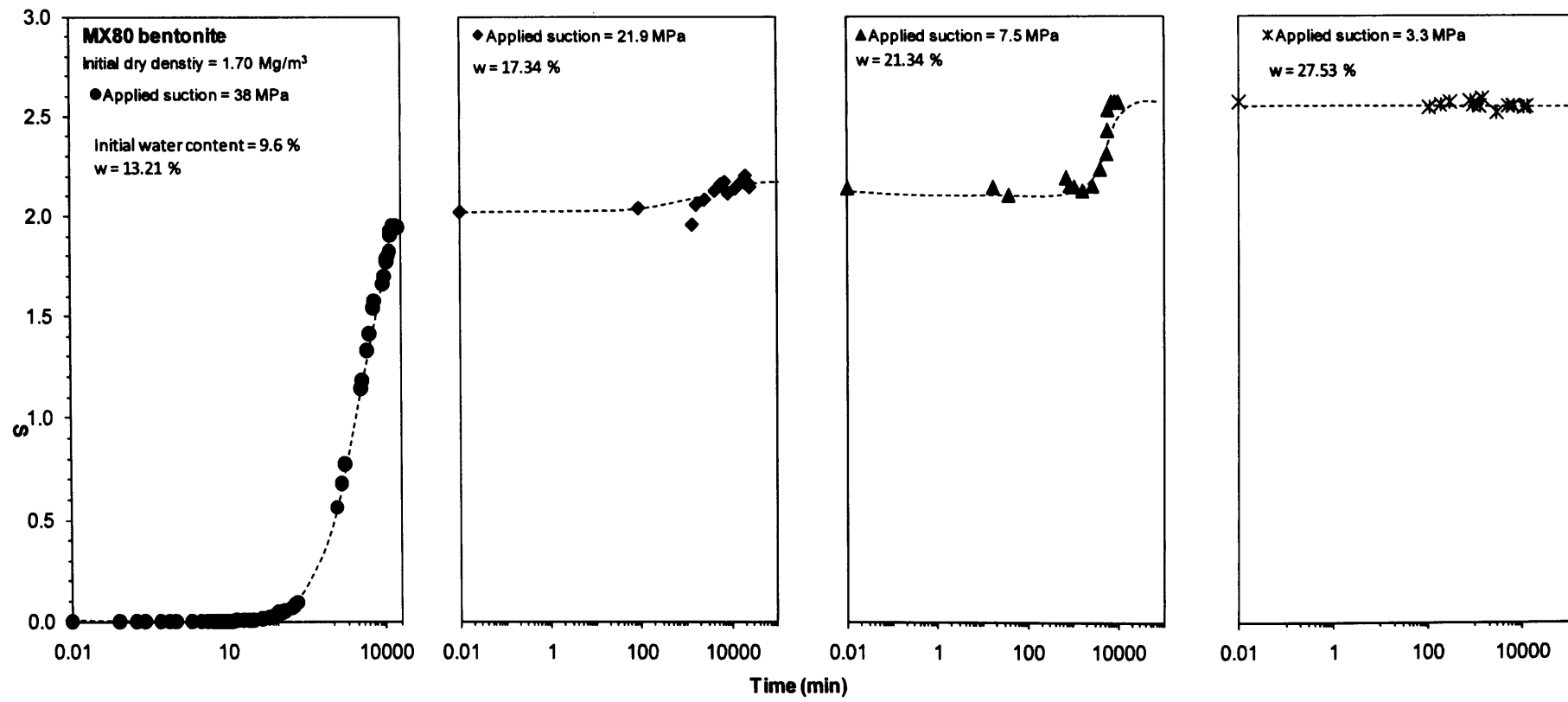
Fig. 8.11: *Development of swelling pressure of MX80 bentonite during wetting under isochoric condition*
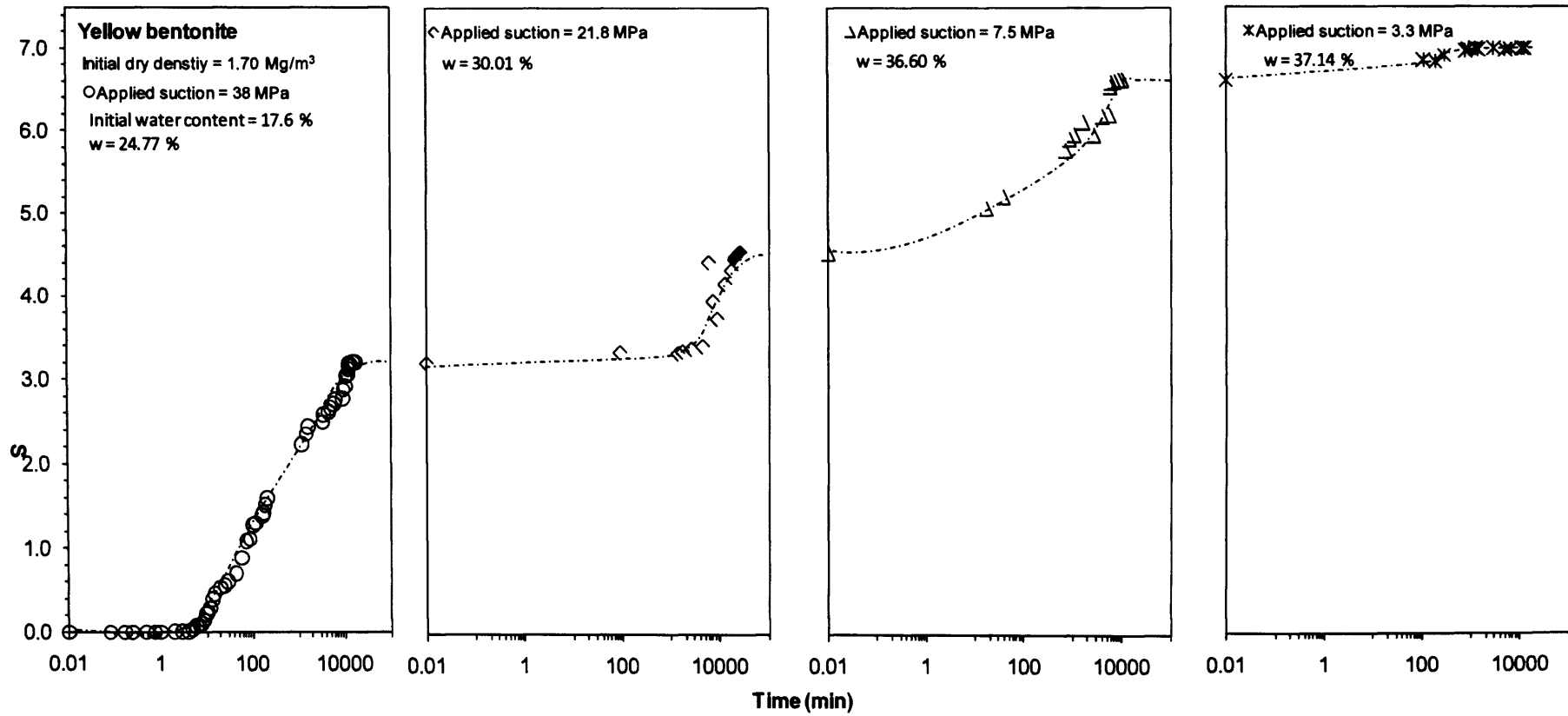
Fig. 8.12: *Development of swelling pressure of Yellow bentonite during wetting under isochoric condition*
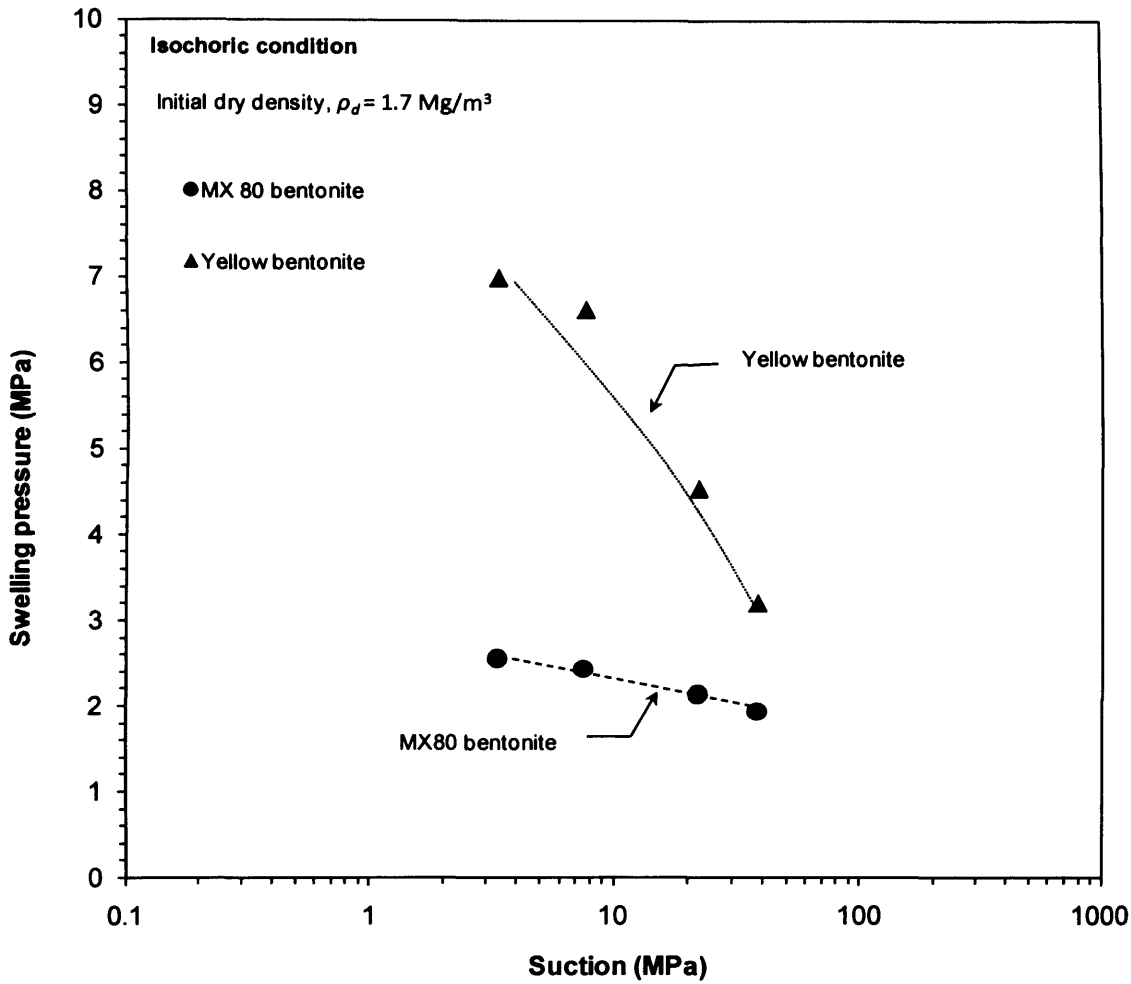
Fig. 8.13: *Suction versus swelling pressure during wetting under isochoric condition*

8.4.2 Single step swelling pressure tests using deionised water

An attempt was made to explore the effect of compaction density on the swelling pressure and water uptake capacities of the bentonites wetted under isochoric condition. Figures 8.14a and b show the typical elapsed time and swelling pressure development for the bentonites hydrated with deionised water. The water contents of the specimens after the completion of the tests were determined and are shown in Figs. 8.14a and b.

190
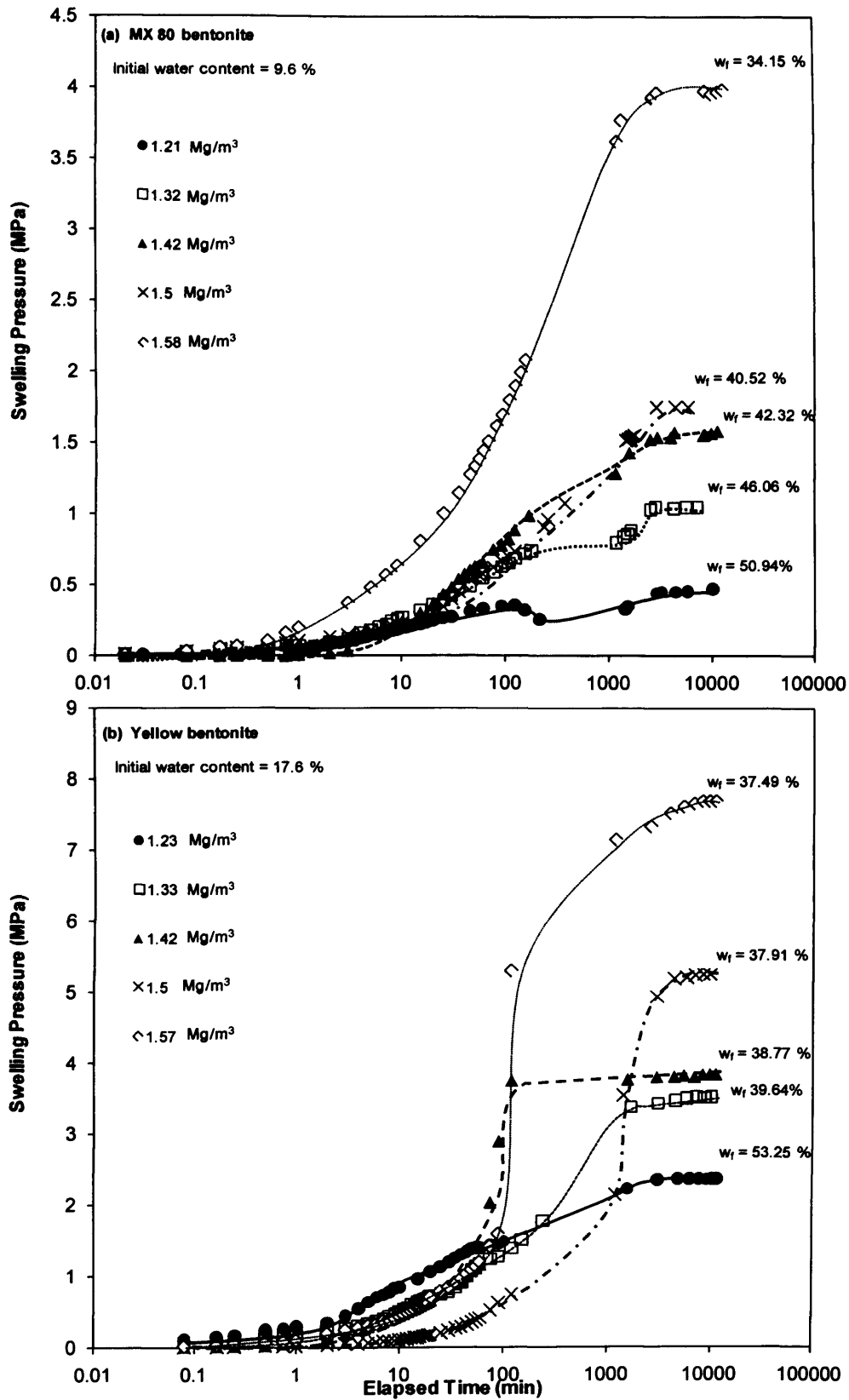
Fig. 8.14: *Swelling pressures and equilibrium water contents under isochoric conditions using deionised water, (a) MX80 bentonite and (b) Yellow bentonite*

The swelling pressure developed with elapsed time was smooth for Yellow bentonite (see Fig. 8.14b). In the case of MX80 bentonite (see Fig. 8.14a) smooth elapsed time versus development of swelling pressure was observed for specimens with dry densities between 1.42 to 1.58 Mg/m^3. Imbert and Villar (2006) reported similar behaviour for the swelling pressure development of FoCa clay compacted at a range of dry densities between 1.3 to 1.6 Mg/m^3. A decrease and further increase and subsequently a decrease in the swelling pressure during the wetting process is attributed to the rearrangement of clay particles and redistribution of water molecules (Schanz and Tripathy, 2009). Equilibration time of about 10000 minutes was found to be adequate for both bentonites used in this study. The equilibration time for swelling pressure tests were reported to be in the range of 10000 to 18000 minutes (Sridharan et al., 1986; Komine and Ogata, 1994; Schanz and Tripathy, 2009).

Figure 8.15 shows the effect of dry density on the water content and swelling pressure of both bentonites. Figure 8.15 indicated that the swelling pressure is influenced by the compaction dry density. In the suction controlled swelling pressure tests, the swelling pressures of bentonite specimens were influenced by the increase in the water content due to suction decrease (see Fig. 8.13). However, a reverse trend was observed in the case of swelling pressure measurements using deionised water under isochoric condition. A much greater swelling pressures were exhibited by both bentonites that had very low equilibrium water contents, particularly at higher dry densities. At low dry densities, although greater water contents were measured, the swelling pressures of compacted bentonites were less. Based on the test results of wetting tests using deionised water, it was noted that the water uptake capacities of the bentonites were reduced with an increase in the dry density. Hence, the tests results suggested that the dry density had a significant role on the swelling pressures and

water absorption behaviour of bentonites under isochoric condition. The test results were concurrent with the findings reported by Villar and Lloret (2004).
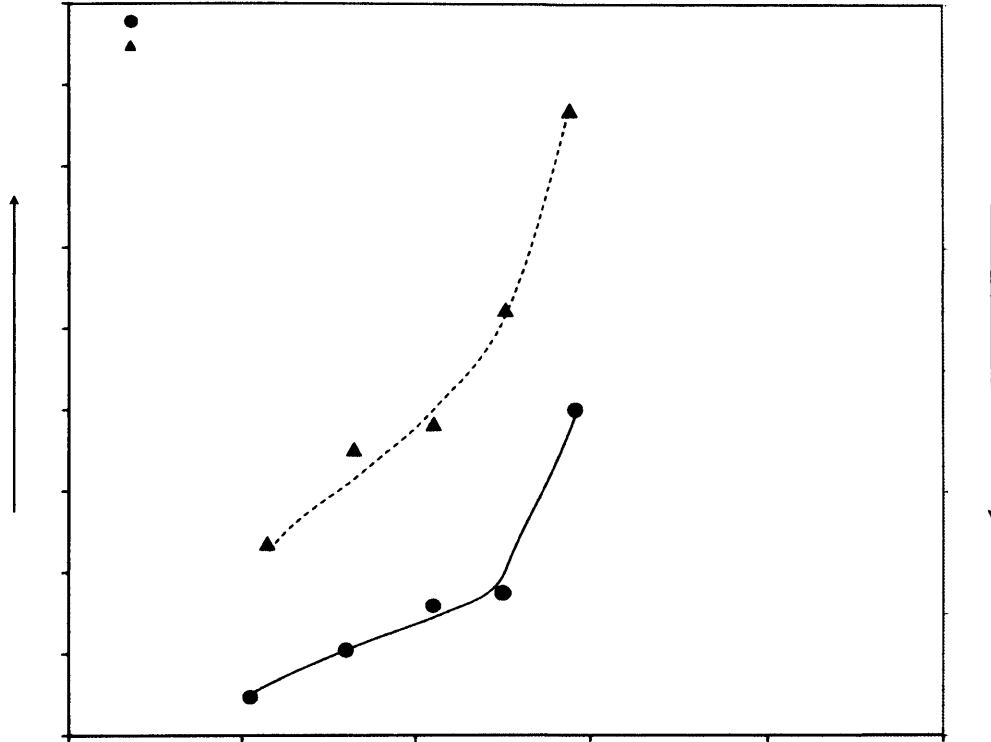
Fig. 8.15: *Influence of dry density on the water content and swelling pressure*

8.5 Microstructural investigations

8.5.1 Environmental Scanning Electron Microscope (ESEM) analysis

Figures 8.16 and 8.17 show the microstructural changes that occurred for MX80 bentonite and Yellow bentonite during the wetting process. The ESEM studies generally simulate the wetting process similar to that of wetting under unconfined conditions (Section 8.3.4). In Figs. 8.16a and 8.17a, prior to the wetting process, it was observed that initially both

bentonites comprised of series of unit layers stacked together (Grim, 1968; van Olphen, 1977; Delage et al., 2006). Most of the clay plates were observed to be parallel to each other and were aggregated together (see Fig. 8.16). It can be observed from Figs. 8.16 and 8.17 that pore spaces existed between these aggregated particles. The pore spaces were used as a reference to monitor the swelling behaviour of compacted bentonites at microscopic level during the wetting process.
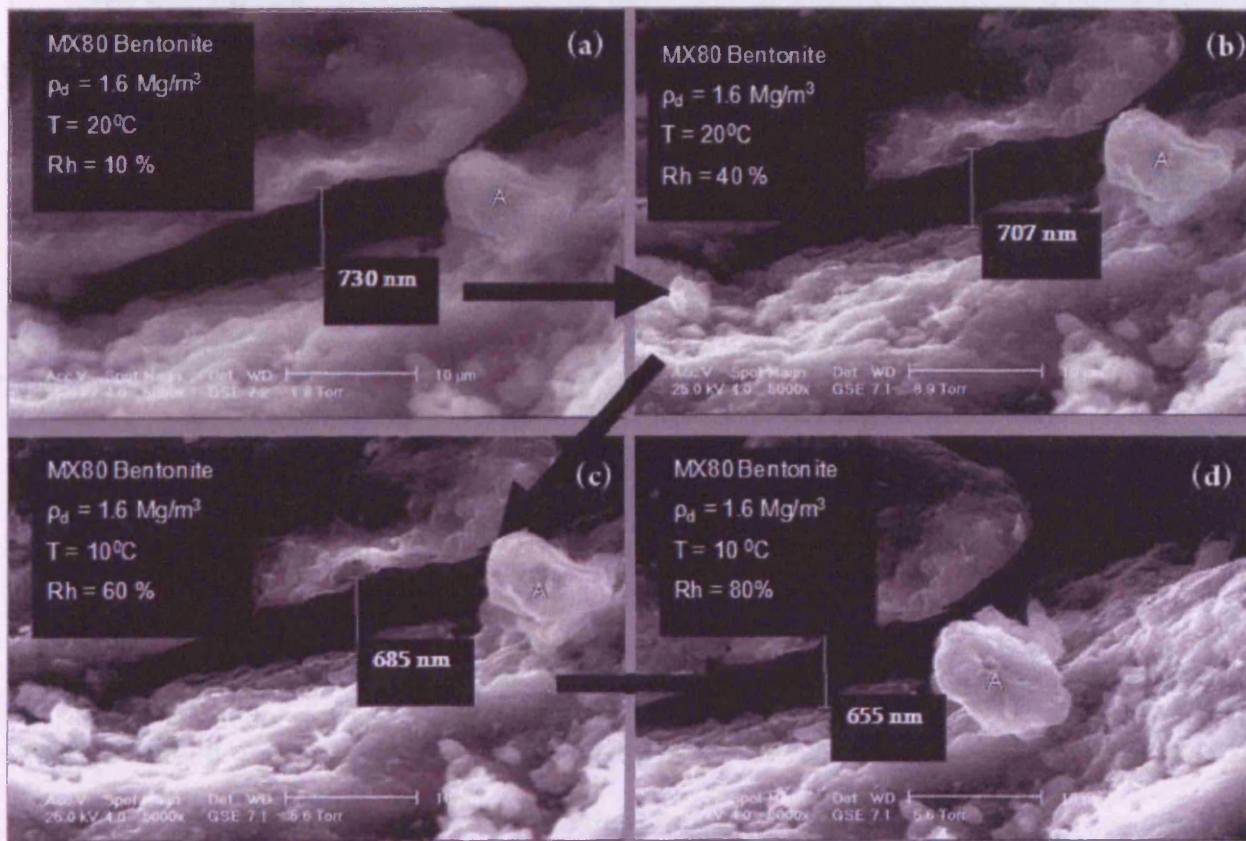
Fig. 8.16: *ESEM micrograph of MX80 bentonite during wetting*

Referring to Figs. 8.16 and 8.17, in both cases, the sizes of the macro pores were reduced with an increasing in the relative humidity. This indicated that swelling of the aggregates occurred during the wetting process. The space between aggregates in MX80 bentonite was initially observed to be about 730 nm and reduced to about 655 nm at RH = 80% (see Figs. 8.16a and d), whereas a reduction in the size of the reference pore in the case of Yellow

8.5.2 Low angle XRD analysis

XRD was employed at low angle in order to evaluate the changes in the interlayer space (c-axis spacing) during the wetting process. Bentonite powder specimens equilibrated in the desiccator tests and volumetric pressure plate tests were considered. In addition, bentonite powders at hygroscopic water contents were also tested. Once equilibrated at each applied suctions, the wetted clay powders were directly transferred to the XRD device. Figures 8.18and 8.19 present the c-axis spacing results for MX80 bentonite and Yellow bentonite, respectively. The horizontal dotted lines in Figs. 8.18 and 8.19 present the variation of the c-axis spacing and the corresponding number of layer water adsorbed for homoionised montmorillonite (Grim, 1968). The test results reported by Likos (2004) for MX80 bentonite are also presented (see Fig. 8.18). Similarly, the test results for Fourges, a Ca-rich bentonite, reported by Saiyouri et al. (2000) was compared with the results obtained for Yellow bentonite in this study (see Fig 8.19).

Figure 8.18 shows that at ambient laboratory conditions, MX80 bentonite specimen had a c-axis spacing of slightly greater than 1.26 nm (at water content of 9.6%). Similarly, at water content of 17.6% (at ambient laboratory conditions), the c-axis spacing for Yellow bentonite was found to be about 1.55 nm. In other words, two layers of water were present in the case of Yellow bentonite at the ambient condition. The test results clearly indicated that the c-axis spacing increased with a decrease in the applied suction. Only one layer of water was present at applied suctions of higher than 20 MPa and 10 MPa for MX80 bentonite and Yellow bentonite, respectively. It is noted that two layers of water were present at applied suctions between 38 MPa to 0.05 MPa for MX80 bentonite, whereas two layers of water were present at applied suctions between 30 MPa to 3.3 MPa for Yellow bentonite. Interestingly, at an applied suction of 0.05 MPa, the c-axis spacing for Yellow bentonite was found to be greater

than that of MX80 bentonite. Note that the water content of MX80 bentonite at 0.05 MPa, was greater than that of Yellow bentonite (see Fig. 8.5). The third layer of water was only observed in the case of Yellow bentonite for applied suction less than 3.3 MPa, corresponding to a c-axis spacing of 1.94 nm. In this case, a further decrease in the applied suction (i.e. increase in the water content) did not affect the expansion of the c-axis spacing (Schanz and Tripathy, 2009). Although a much larger separation distance between interacting clay platelets were anticipated, the XRD test results were limited to crystalline swelling (Grim, 1968). The crystalline swelling is more dominant in case of divalent-rich bentonite, than that occurred for a monovalent-rich bentonite (van Olphen, 1977; Quirk, 1994). In the case of MX80 bentonite, with an increase in the water content, the hydrated cations dissociate from the clay surface and form the electrical diffuse double layer (van Olphen, 1977; Delage et al., 2006; Schanz and Tripathy, 2009).
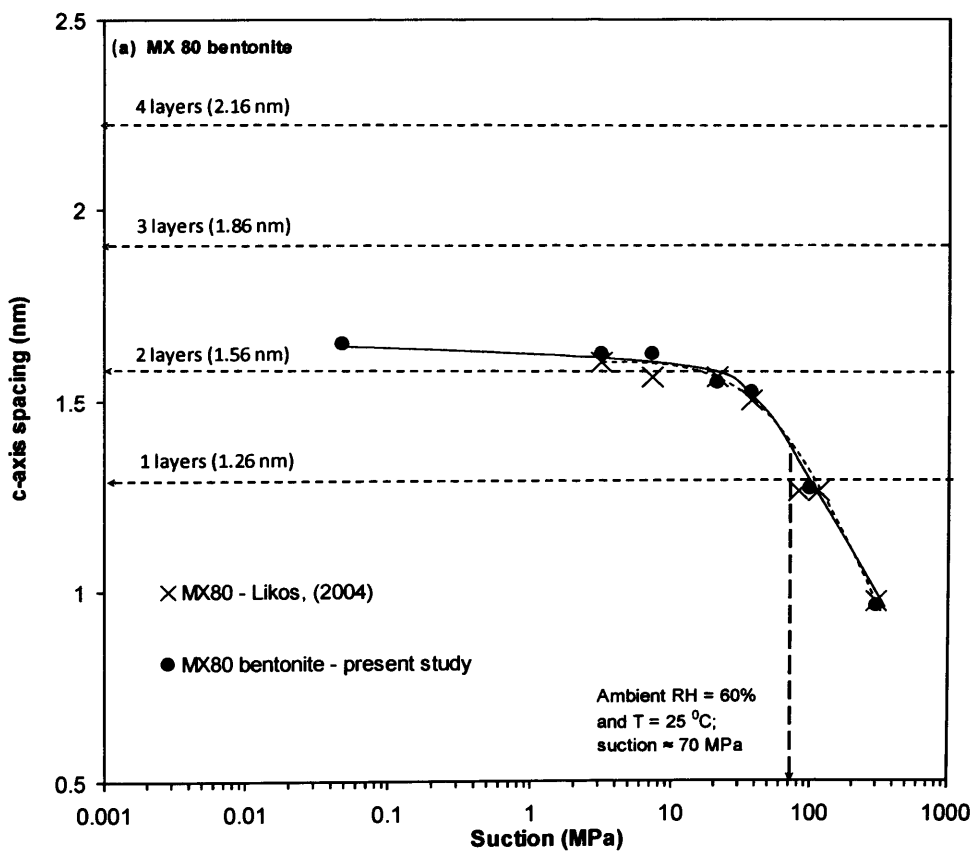
Fig. 8.18: *c-axis spacing versus suction for MX80 bentonite*
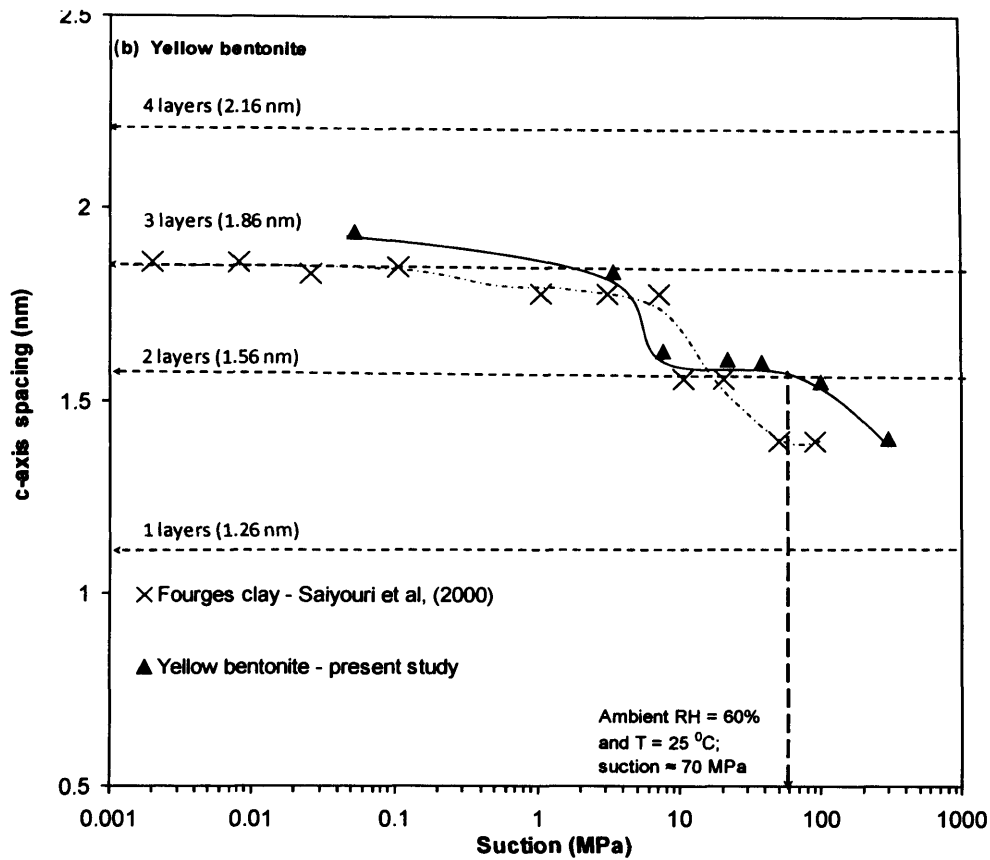
Fig. 8.19: *c-axis spacing versus suction for Yellow bentonite*

8.6. Concluding remarks

The main findings of this study are summarised as follows:

i.   The equilibration time was found to be faster in liquid phase (i.e. volumetric pressure

plate and osmotic tests) as compared to vapour transfer (i.e. desiccator tests).

ii.   The wetting behaviour of highly plastic clays was found to be influenced by the clay-

type and the physical and chemical properties. At higher applied suctions, the SWCCs

were governed by the specific surface area (i.e. higher the specific surface area,

greater is the equilibrium water content). On the other hand, the liquid limits played a

198

significant role at lower applied suctions (i.e. higher the liquid limit, greater is the equilibrium water content).

iii. The effect of dry density on the wetting SWCCs was found to be dependent upon the confining conditions. The effect of compaction density on the wetting SWCCs was found to be negligible under unconfined conditions. However, for laterally confined and isochoric conditions, the water uptake capacities of the bentonites were significantly reduced with an increasing in the dry densities.

iv. Both the confining conditions and dry density effects were found to have less influence on the wetting SWCCs of the bentonites at large suction (>3.3 MPa). These effects however were more dominant in the lower suction regions. On the contrary, the SWCC of Speswhite kaolin was not affected by both compaction densities and confining conditions.

v. Under isochoric condition, the swelling pressures of the bentonites were found to increase with an increase in the dry density.

vi. ESEM observations showed that the pore spaces in the bentonites tested were reduced, indicating that swelling occurred in the interlayer space. Rearrangement of the clay particles occurred during the wetting process.

vii. Low angle XRD analysis indicated that crystalline swelling occurred to a maximum three number of water layers in the case of Yellow bentonite, whereas two number of water layers in the case of MX80 bentonite. Further increase in the water contents was

199

not manifested on the changes in the c-axis spacings primarily due to the fact that the

changes in the c-axis spacing are only limited to crystalline swelling.

CHAPTER 9

SUCTION-WATER CONTENT SWCCs FROM THEORETICAL CONSIDERATIONS

9.1 Introduction

Interparticle repulsive and attractive pressures on account of physico-chemical forces in clay-water systems have been shown to be very useful for assessing the behaviour of clays (i.e. volume change, water content change and swelling pressure) (Verwey and Overbeek, 1948; Bolt, 1956; van Olphen, 1977; Sridharan and Jayadeva, 1982; Tripathy et al., 2004, Schanz and Tripathy, 2009). For instance, the Gouy–Chapman diffuse double layer theory and the van der Waals attractive pressure theory have been shown to be applicable for predicting the swelling and compressibility behaviour of clays (Verwey and Overbeek, 1948; Bolt, 1956; van Olphen, 1977; Mitchell, 1993; Sridharan and Jayadeva, 1982; Rao and Sridharan, 1985; Tripathy et al., 2004, Schanz and Tripathy, 2009, Frydman and Baker, 2009). Both the theories have been used for steady state conditions.

The diffusivity of clays plays a significant role on the water content uptake and transient flow in unsaturated soils (Saiyouri et al., 2000; Lu and Likos, 2004). The diffusivity or the diffusion coefficient of soils is related to the flow of water in response to a concentration gradient (Fredlund and Rahadrjo, 1993). The diffusivity can be determined from permeability measurements (Saiyouri et al., 2000). A review of literature suggested that Richard's

equation can be used for the determination of elapsed time versus water content changes during the wetting process (Saiyouri et al., 2000; Lu and Likos, 2004; Gens et al., 2009). The objectives of this study were (*i*) to compare experimental results concerning the changes in the water content with elapsed time of the clays with that calculated results based on Richard's equation, (*ii*) to compare the experimental drying and wetting SWCCs of the clays studied with those calculated from the Gouy–Chapman diffuse double layer theory and the van der Waals attractive pressure theory and (*iii*) to compare the changes in the measured *c*-axis spacing during the wetting process (for clay powders tested under unconfined condition) with that calculated results based on parallel plate consideration.

The experimental programme is presented first, followed by the theoretical approaches considered. Under test results and discussion, the influence of diffusivity on the water uptake capacity of clays are presented followed by the suction–water content SWCCs based on diffuse double layer theory and the attractive pressure theory. Comparisons of the theoretical and experimental *c*-axis spacing for the clays are then presented. The concluding remarks are presented towards the end of the chapter.

9.2 Experimental programme

9.2.1 Water content change with elapsed time (unconfined condition)

The elapsed time versus water content changes were experimentally determined during the wetting process for powder specimens of the clays. The mass of the clay specimens in the desiccator tests were measured periodically. After equilibration, the water contents of the clay specimens were determined by oven-drying method. The water contents of the clays during

the transient wetting process were back-calculated from the equilibrated water contents. An applied suction of 3.3 MPa (aqueous solution of K_2SO_4) was considered.

9.2.2 Drying suction-water content SWCCs

The drying suction-water content SWCCs of the clays were established using axis-translation, vapour equilibrium and osmotic techniques. A wide range of suctions from 0.05 to 300 MPa were considered. The detailed experimental programme is presented in Section 5.2.1. The drying suction-water content SWCCs of the clays are presented in Fig. 5.6. In this chapter, the test results presented in Fig. 5.6 are compared with the calculated suction-water content SWCCs from the diffuse double layer and the attractive pressure theories.

9.2.3 Wetting suction-water content SWCCs

The wetting suction-water content SWCCs of the clays were established using axis-translation, vapour equilibrium and osmotic techniques. Clay powders with hygroscopic water contents (see Table 3.1) were wetted step-wise from higher to lower suctions. Applied suctions of 300 to 0.05 MPa were considered. The detailed experimental programme is presented in Section 8.2.1. The wetting suction-water content SWCCs of the clays are presented in Fig. 8.6. In this chapter, the test results presented in Fig. 8.6 are compared with the calculated suction-water content SWCCs from the diffuse double layer and the attractive pressure theories.

9.2.4 Changes in the c-axis spacing

The c-axis spacing of powder clay specimens equilibrated in the desiccator tests were determined by using XRD technique (see 8.5.2). Applied suctions of 300, 38, 21.8, 7.5 and 3.3 MPa were considered. In addition, clay powders equilibrated at laboratory condition (i.e. at hygroscopic water contents) and at applied suction of 0.05 MPa in the volumetric pressure plate tests were considered. In this chapter, the test results presented in Figs. 8.19 and 8.20 are compared with the c-axis spacing results from parallel plate consideration.

9.3 Theoretical considerations

9.3.1 Richard's equation – transient wetting

According to Saiyouri et al. (2000), the fluid flow in porous media is governed by conservation of mass and obeys Darcy's law. In one-dimensional case, the flow of water within a soil column during transient conditions can be determined by Richard's equation (Eq. 9.1).

$$\frac{\partial \theta_w}{\partial t} = \frac{\partial}{\partial x}\left(D(\theta_w)\frac{\partial \theta_w}{\partial x}\right)$$

Eq. (9.1)

The change in the diffusivity, D, generally influence the water content, Θ_w, with elapsed time. At time, $t = 0$, Θ_w is assumed to be equal to the initial water content, Θ_{wi}, for all values of x (x is the distance of the flow). For $t > 0$, $\Theta_w = \Theta_s$ at $x = 0$, where Θ_s is the water content at steady state conditions. Due to the nonlinearity of the equation, solving Eq. 9.2 often involves the use of finite difference software such as Hydrus-1D (Gens et al., 2008; Simunek et al., 2008).

In this study, the Richard's equation was solved manually by finite difference method by expanding the Eq. 9.1. Several assumptions were made, such as (i) the fluid flow is one-dimensional and deformations are small (ii) the effects of gravity is negligible and (iii) Darcy's law can be applied to the flow behaviour.

The numerical equations are presented in Eq. 9.2 and Eq. 9.3.

$$\theta_{w+1} = \frac{16\theta_{wi} + D(\theta_w)\theta_{w+2}dt + \theta_{w+2} + \theta_i dt}{16 + dt + D\theta_w dt}$$

Eq. (9.2)

$$\theta_{w+2} = \frac{\theta_{w+1}(16 + dt + D\theta_w dt) - 16\theta_w - \theta_w dt}{D(\theta_w)dt + 1}$$

Eq. (9.3)

where θ_{w+1} and θ_{w+2} are the consequent water content changes at t_1 and t_2. Both sides of the equation must be solved simultaneously. Thus, an iterative approach was adopted.

Diffusivity of different clays have been extensively studied and reported in the literature. Some relevant values of diffusivity of various clays are presented in Table 9.1.

Table 9.1: *Diffusivity of various clays*

Clay	Diffusivity, D (m²/s)	Authors
MX80 bentonite	2.0×10^{-10}	Muurinen et al., 1987
	1.0×10^{-10}	Nakashima, 2004
FoCa clay	1.0×10^{-12}	Saiyouri et al., 2000
Kunigel V1	1.0×10^{-12}	Ochs et al., 2001
Kunipia–F	1.0×10^{-12}	Sato et al., 1992
Deponit CA–N*	2.08×10^{-11}	Archos et al., 2008
Tsukino bentonite	6.0×10^{-13}	Idemitsu et al., 1989
Kuroishi bentonite	3.0×10^{-13}	Idemitsu et al., 1989
Kaolinite	1.33×10^{-10}	Sanchez, 2007

* Deponit CA-N is the commercial name for Yellow bentonite (see Section 3.2)

Table 9.1 shows that the diffusivity of clays can vary between the order of 10^{-10} to 10^{-13} m^2/s. In order to bring out the influence of diffusivity on the water content changes of the clay specimens with elapsed time, the diffusivity values for some selected clays presented in Table 9.1 were used in Eqs. 9.2 and 9.3. The calculated elapsed time versus water content relationships were compared with the experimental results of the clays used in this study. Only powder specimens wetted under unconfined condition at an applied suction of 3.3 MPa were considered. Additionally, Eqs. 9.2 and 9.3 were used to best-fit the experimental data in order to determine the diffusivity of the clays used in this study.

9.3.2 Gouy–Chapman diffuse double layer theory

The osmotic pressure at the mid-plane between interacting parallel clay platelets can be calculated based on the diffuse double layer theory (Verwey and Overbeek, 1948; Bolt, 1956; van Olphen, 1977; Sridharan and Jayadeva, 1982; Tripathy et al., 2004; Schanz and Tripathy, 2009). The following equations can be used for establishing the swelling pressures-void ratio relationship for clays (Sridharan and Jayadeva, 1982):

$$p = 2n_0 kT (\cosh u - 1) \qquad\qquad \text{Eq. (9.4)}$$

$$-\left(\frac{dy}{d\xi}\right)_{x=0} = \sqrt{(2\cosh z - 2\cosh u)} = \left(\frac{B}{S}\right)\sqrt{\left(\frac{1}{2\varepsilon_0 Dn_0 kT}\right)}; at\ x=0, y=z \qquad \text{Eq. (9.5)}$$

$$\int_z^u \frac{1}{\sqrt{(2\cosh y - 2\cosh u)}} dy = \int_0^d d\xi = -Kd \qquad\qquad \text{Eq. (9.6)}$$

$$K = \left(\frac{2n_0 e^{\prime 2} v^2}{\varepsilon_0 DkT}\right)^{\frac{1}{2}} \qquad\qquad \text{Eq. (9.7)}$$

$$e = G_s \rho_w S d \times 10^6$$

<div align="right">Eq. (9.8)</div>

where p is the swelling pressure in N/m^2, n_0 is the ionic concentration of the bulk fluid in ions/m^3, u is the dimensionless midplane potential, T is the absolute temperature in Kelvin, k is the Boltzmann's constant ($=1.38 \times 10^{-23}$ J/K), ξ is the distance function, y is the nondimensional potential function at the clay surface at a distance of x from the clay surface, z is the nondimensional potential function at the surface ($x = 0$), B is the cation exchange capacity (meq/100g), S is the total specific surface area in (m^2/g), ε_0 is the permittivity of vacuum ($= 8.8542 \times 10^{-12}$ C^{2}J^{-1}m^{-1}), D is the dielectric constant of bulk fluid ($= 80.4$ for water), K (1/m) is the diffuse double layer parameter, e' is the elementary electrical charge ($= 1.602 \times 10^{-19}$ C), and v is the weighted average valency of the exchangeable cations present within the clay system.

For a given soil, Eq. 9.8 relates the void ratio, e, to the specific gravity, G_s, the half distance between two parallel clay platelets, d, the specific surface area, S, and the density of the bulk fluid, ρ_w. Equation 9.8 proposed by Bolt (1956) is valid for saturated clays and for all water contents and spacing between the clay platelets (Schanz and Tripathy, 2009).

For given properties of the clay and for known bulk fluid properties, prediction of swelling pressure is done by relating the u values obtained from Eq. 9.4 with the values of the nondimensional distance function, Kd. For a range of assumed swelling pressures, the u values can be calculated from Eq. 9.4. The corresponding values of z can be calculated from Eq. 9.5. Knowing z and u for any given swelling pressure, Eq. 9.6 can be used to calculate Kd. Knowing Kd and K from Eq. 9.7, d is determined, and e from Eq. 9.8 (Sridharan and Jayadeva, 1982; Tripathy et al., 2004; Schanz and Tripathy, 2009).

Although the diffuse double layer theory has extensively been used for establishing swelling pressure-void ratio relationships, the calculated swelling pressures can be treated nearly similar to applied soil suctions (Schanz and Tripathy, 2005). In this study, the void ratios corresponding to the experimental applied suctions of 0.05 to 300 MPa were calculated using Eqs. 9.4 to 9.8. The swelling pressure was treated equivalent to the applied suction. Furthermore, assuming the degree of saturation of the clays remaining constant (S_r = 100%) for all applied suctions considered, the void ratio, e, is equivalent to wG_s. The water content corresponding to any given suction can be calculated using Eq. 9.9. In Eq. 9.9, the total specific surface areas, S, of the clays were considered (see Table 3.1). Thus, the suction-water content SWCCs of the clays were established theoretically.

$$w\,(\%) = \rho_w S d \times 10^6 \times 100$$

<div align="right">Eq. (9.9)</div>

9.3.3 van der Waals attractive pressure theory

van der Waals attractive forces could bond water to clay surfaces (Mitchell, 1993). The osmotic repulsive pressure is much less for bentonites divalent cations than that for Na-bentonite. Montmorillonite particles with divalent cations separated by large distances (>2.5 nm) will collapse together if this force is insufficient to counterbalance the van der Waals attractive forces (Norrish, 1954). At close separation distance between clay platelets, the adsorption potential appears to be dominated by the van der Waals attractive forces, which in turn is related to the specific surface area of the clay particles (Mitchell, 1993; Frydman and Baker, 2009). Equation 9.10 presents the van der Waals-Hamaker equation (Sridharan and Jayadeva, 1982).

$$F_A = \frac{A}{48\pi}\left[\frac{1}{d^3} + \frac{1}{(d+\delta)^3} - \frac{2}{(d+0.5\delta)^3}\right]$$

<div align="right">Eq. (9.10)</div>

where F_A is the attractive pressure in N/m^2, δ is the thickness of the clay platelet (= 1 nm for montmorillonite, and A is the Hamaker constant = 6×10^{-20} J for water as the bulk fluid). The value of A depends upon the clay type, dielectric constant, temperature and the degree of saturation of the clay system (Sridharan and Jayadeva, 1982). In the past, the value of A was shown to vary between 10^{-20} to 10^{-19} J (Sridharan and Jayadeva, 1982; Mitchell, 1993; Frydman and Baker, 2009). F_A can be considered equivalent to an applied suction (Frydman and Baker, 2009). In this study, a single A value of 6×10^{-20} J was considered following the suggestion made by Or and Tuller (1999) and Frydman and Baker (2009).

A simplified version of Eq. 9.10 has been proposed by Verwey and Overbeek (1948) (Eq. 9.11). Equation 9.11 was used for establishing the suction-water content SWCCs of clays based on the attractive pressure theory. In Eq. 9.12, ψ_m, the matric suction of soil in kPa.

$$\psi_m = \frac{A}{6\pi d^3}$$

Eq. (9.11)

By eliminating d in Eq. 9.9 and Eq. 9.11, the suction-water content SWCCs of soils can be determined using Eq. 9.13.

$$\psi_m = \left(\frac{10^{-5}}{\pi}\right)\left(\frac{S}{w}\right)^3$$

Eq. (9.12)

For a known specific surface area of soil and for any given applied suction, the water content can be determined. Similarly, for a known specific surface area and for any given water content, the applied suction can be calculated using Eq. 9.12.

9.3.4 c-axis spacing from micro-macro void ratio relationships

The c-axis spacing is the sum of the distance between two interacting clay platelets, $2d$, and the thickness of the clay platelet, t (0.96 nm for montmorillonite and 0.72 nm for kaolinite) (Mitchell, 1993). Equation 9.9 was used to calculate the changes in the half distance, d, corresponding to the changes in the water contents that were determined experimentally in this study. The equilibrated water contents from the volumetric pressure plate and desiccator tests were considered (see Section 9.2.4). Similarly, the hygroscopic water contents of the clays were also considered. For any given water content, d can be calculated from Eq. 9.9. Thus, the c-axis spacing at each applied suctions can be determined (i.e. $2d + t$). The calculated c–axis spacing at each applied suctions are compared in this chapter with the c-axis spacing determined experimentally using low angle XRD technique (see Section 8.5.2).

9.4 Test results and discussion

9.4.1 Influence of diffusivity on the water uptake capacity

Figures 9.1, 9.2 and 9.3 show the elapsed time versus water content changes (experimental data) for the clays at an applied suction of 3.3 MPa. Equations 9.11 and 9.12 were used to best-fit the experimental data. The values of D (i.e. diffusivity) used to best-fit the experimental data are shown in Figs. 9.1 to 9.3 (i.e. $D = 1.32 \times 10^{-10}$ m^2/s for MX80 bentonite, $= 2.67 \times 10^{-10}$ m^2/s for Yellow bentonite and $= 1.54 \times 10^{-10}$ m^2/s for Speswhite kaolin).

The D values reported by Muurinen et al. (1987) and Nakashima (2004) for MX80 bentonite, by Arcos (2008) for Yellow bentonite and by Sanchez (2007) for a kaolinite (see Table 9.1) were used to establish the elapsed time versus water content relationships for the clays (see Figs. 9.1 to 9.3).

Referring to Figs. 9.1 and 9.2, differences were noted between the experimental results and the calculated elapsed time versus water content relationships based on the D values reported in the literature for the bentonites. The values of D reported by Nakashima (2004) for MX80 bentonite and that by Arcos (2008) for Yellow bentonite were found to be slightly lower than that obtained from the experimental results (see Figs. 9.1 and 9.2). On the other hand, the D
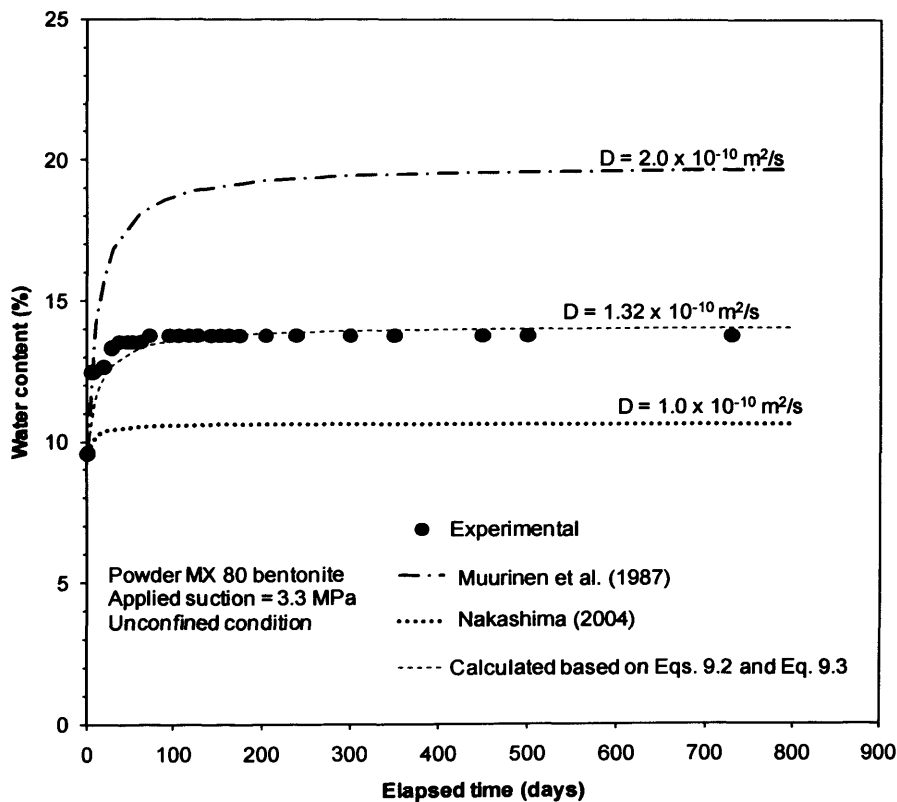
Fig. 9.1: Influence of diffusivity on the water uptake capacity of MX80 bentonite
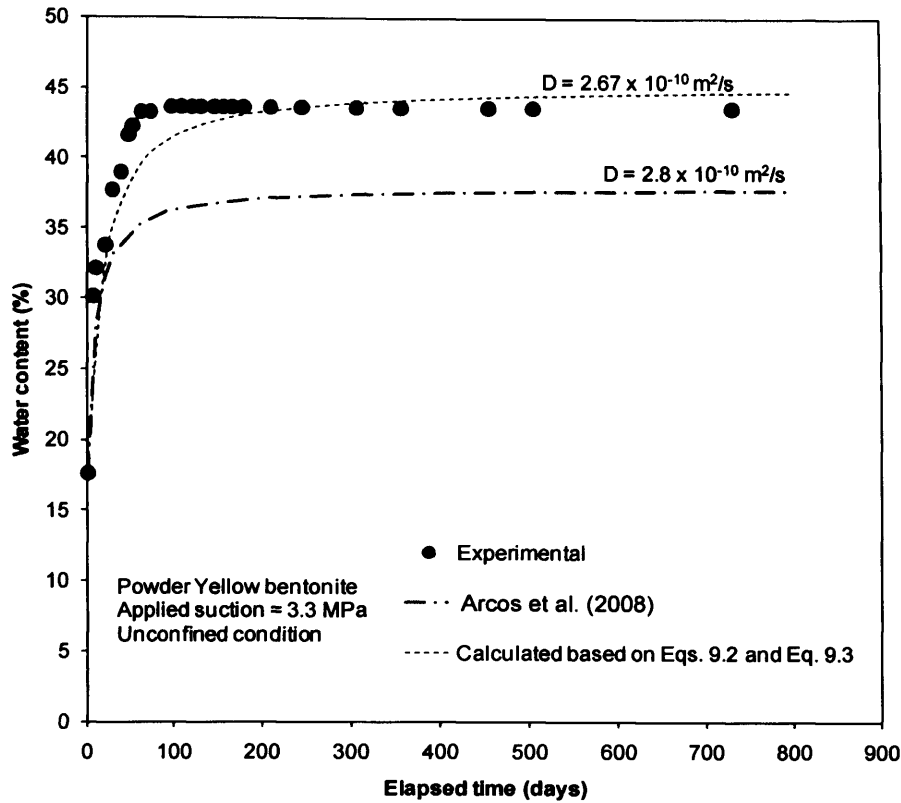
Fig. 9.2: Influence of diffusivity on the water uptake capacity of Yellow bentonite
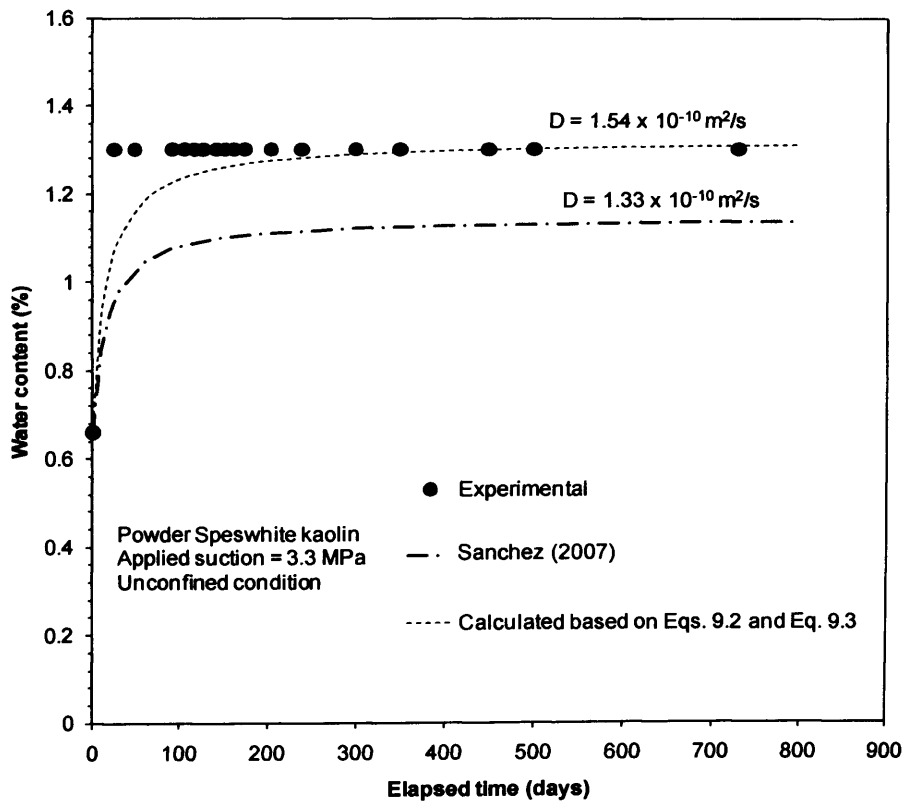
Fig. 9.3: Influence of diffusivity on the water uptake capacity of Speswhite kaolin

value reported by Muurinen et al. (1987) values reported for MX80 bentonite was found to be greater than that obtained from the experimental results. Although the differences between the D values reported in the literature and that were calculated by best-fitting the experimental results are relatively small (i.e. 0.32 x 10^{-10} and 0.68 x 10^{-10} m^2/s for MX80 bentonite and 0.13 x 10^{-10} m^2/s for Yellow bentonite), significant differences were noted for the equilibrium water contents. The differences in the equilibrium water contents were found to vary between 3 to 6% for MX80 bentonite and about 4% for of Yellow bentonite.

In Fig. 9.3, the elapsed time versus water content relationship based on the D value reported by Sanchez (2007) for a kaolinite was found to remain lower than the experimental results for Speswhite kaolin. However, the difference between the experimental and calculated water content for Speswhite kaolin was found to be less than 0.5%.

Figures 9.1, 9.2 and 9.3 show that the D values for the clays in this study are in the order of 10^{-10} m^2/s. Consistent with the experimental data, Richard's equation (Eq. 9.1) replicated the elapsed time versus water content changes of the clays. The results showed that the diffusivity is a sensitive parameter and plays a significant role in the determination of elapsed time versus water content changes for highly plastic clays.

9.4.2 Suction–water content SWCCs from theoretical considerations

9.4.2.1 Drying suction-water content SWCCs

Figures 9.4, 9.5 and 9.6 show the experimental drying suction-water content SWCCs and the calculated suction-water content SWCCs from the Gouy-Chapman diffuse double layer theory and the van der Waals attractive pressure theory for MX80 bentonite, Yellow

bentonite and Speswhite kaolinite, respectively. The calculated suction-water content SWCCs based on the van der Waals attractive pressure theory were found to be similar to that of experimental suction-water content SWCCs of the clays at higher applied suctions (i.e. greater than 1.0 MPa for the bentonites and greater than 20 MPa for Speswhite kaolin). For MX80 bentonite and Speswhite kaolin, the calculated suction-water content SWCCs from the van der Waals attractive pressure theory were found to remain lower than the experimental data points at applied suctions of less than 1.0 MPa, whereas the reverse was the trend in case of Yellow bentonite.

Fig. 9.4: Comparison of theoretical and experimental drying SWCCs for MX80 bentonite

Fig. 9.5: Comparison of theoretical and experimental drying SWCCs for Yellow bentonite

Fig. 9.6: Comparison of theoretical and experimental drying SWCCs Speswhite kaolin

The agreements between the experimental results and the calculated suction-water content SWCC based on the diffuse double layer theory was found to be very good for MX80 bentonite for applied suctions less than 4 MPa. The agreements between the experimental and the calculated suction-water content SWCCs from the diffuse double layer theory for Yellow bentonite and Speswhite kaolin were found to be poor. The disagreements between calculated and experimental results in the case of Speswhite are attributed to thicker kaolinite particles (i.e. several platelet stacked together due to strong hydrogen bonding (Sharma and Reddy, 2004). Physicochemical forces have less influence on the water uptake capacity of kaolinite (Mitchell, 1993).

Referring to Figs. 9.4, 9.5 and 9.6, comparisons of the experimental and the calculated results from the theories indicated that the drying suction-water content SWCC of MX80 bentonite can be calculated based on the diffuse double layer theory, whereas the attractive pressure theory was found to be suitable in establishing the drying SWCCs of the clays at higher applied suctions. The diffuse double layer theory may not be applicable for divalent-rich bentonite at smaller applied suctions due to the fact that the swelling in the case of divalent bentonite is limited and considerably less as compared to Na-bentonite (Murray and Quirk, 1980; Schanz and Tripathy, 2009). Swelling in the case of Speswhite kaolin is relatively small, due to lack of specific surface area and low CEC value. At small interparticle distance, the van der Waals attractive pressures seem to govern the water uptake behaviour of clays (Rao and Sridharan, 1985; Mitchell, 1993).

9.4.2.2 Wetting suction-water content SWCCs

Figures 9.7, 9.8 and 9.9 present the experimental wetting suction-water content SWCCs and the calculated results from the Gouy-Chapman diffuse double layer theory and the van der Waals attractive pressure theory for MX80 bentonite, Yellow bentonite and Speswhite kaolinite, respectively. The calculated suction-water content SWCCs based on the diffuse double layer theory remained higher than the experimental results for suctions less than 2.0 MPa for MX80 bentonite and for suctions less than 1.0 MPa for Yellow bentonite (see Figs. 9.7 and 9.8). At higher applied suctions, the water contents of the bentonites predicted by the theory were far smaller than their experimental counterparts. For Speswhite kaolin, the calculated suction-water content SWCC remained far lower than that of the experimental results for all applied suctions considered (see Fig. 9.9).

The suction-water content SWCC calculated based on the attractive pressure theory was found to agree very well for applied suctions greater than 0.2 MPa for MX80 bentonite (see Fig. 9.7). In this case, the predicted water contents were much lower than the measured water contents at lower applied suctions. The calculated suction-water content SWCC for Yellow bentonite from the attractive pressure theory was found to be in good agreement with the experimental results for applied suctions greater than about 1.0 MPa, whereas at smaller applied suctions, the agreements between the calculated and experimental results were poorer. In the case of Speswhite kaolin, similar to the calculated suction-water content SWCC based on diffuse double layer, the attractive pressure theory predicted lesser water contents as compared to the experimental values for all applied suctions considered.
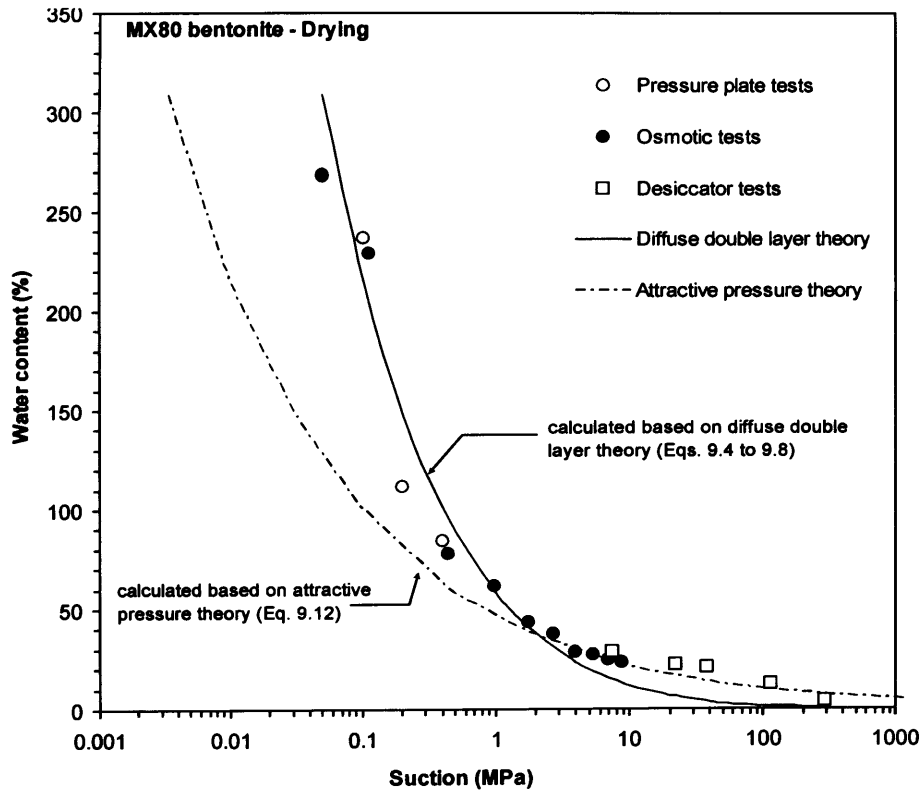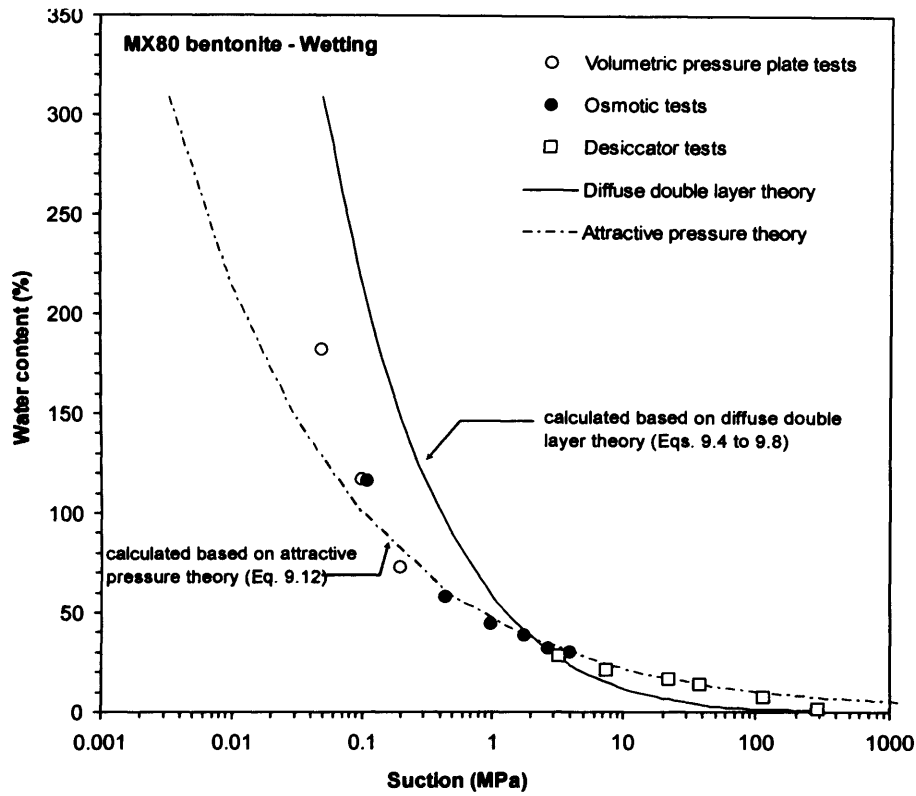
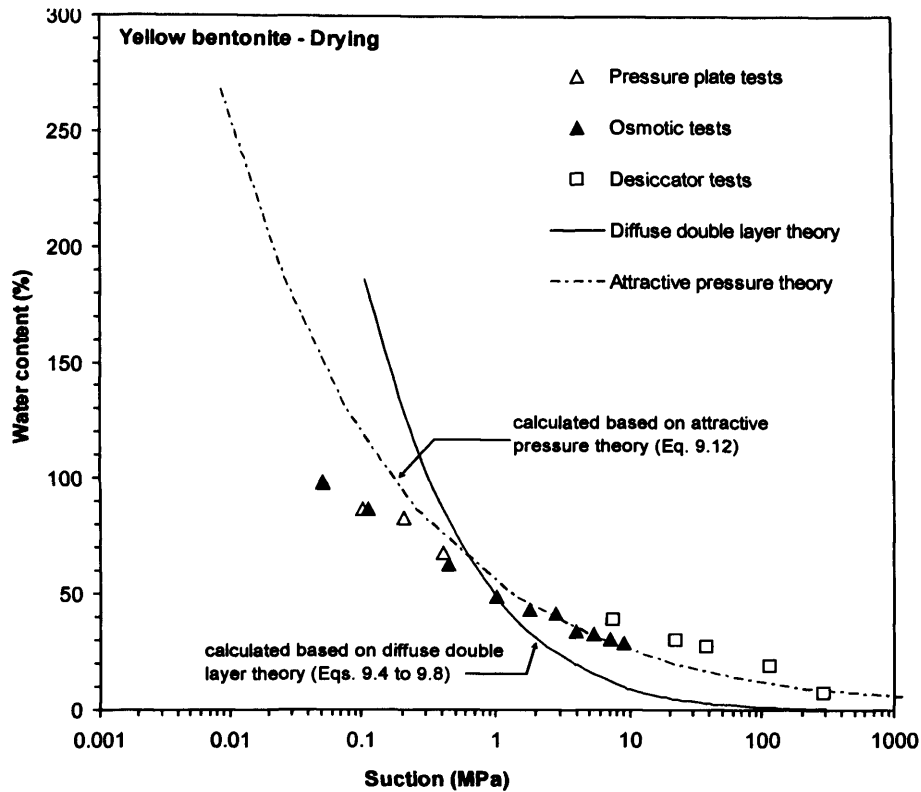Fig. 9.7: Comparison of theoretical and experimental wetting SWCCs for MX80 bentonite
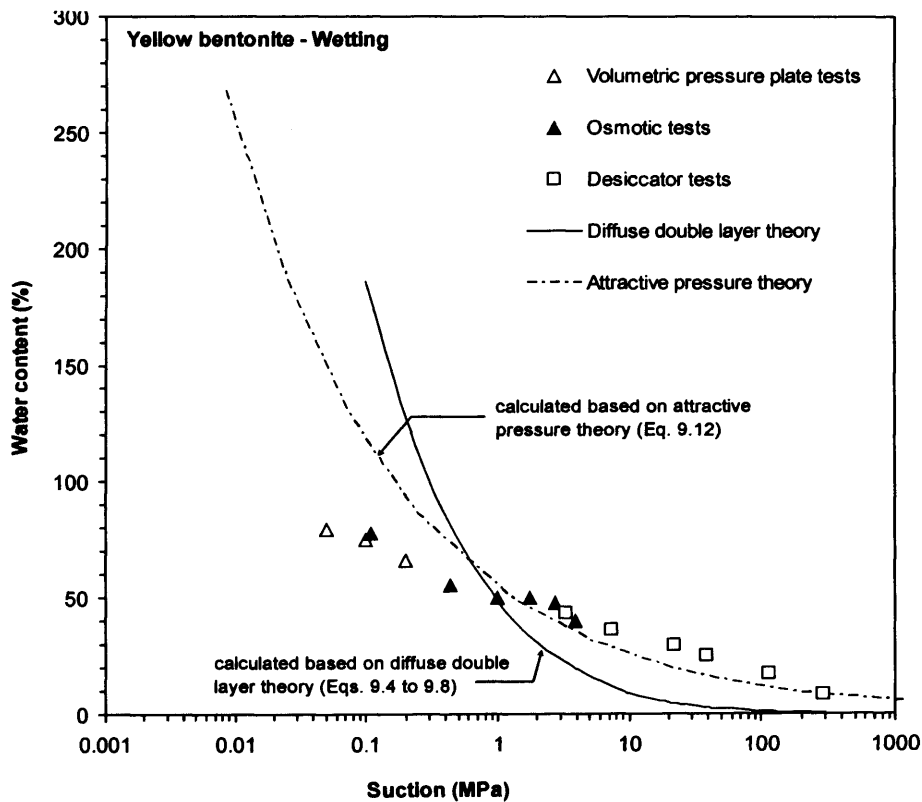
Fig. 9.8: Comparison of theoretical and experimental wetting SWCCs for Yellow bentonite
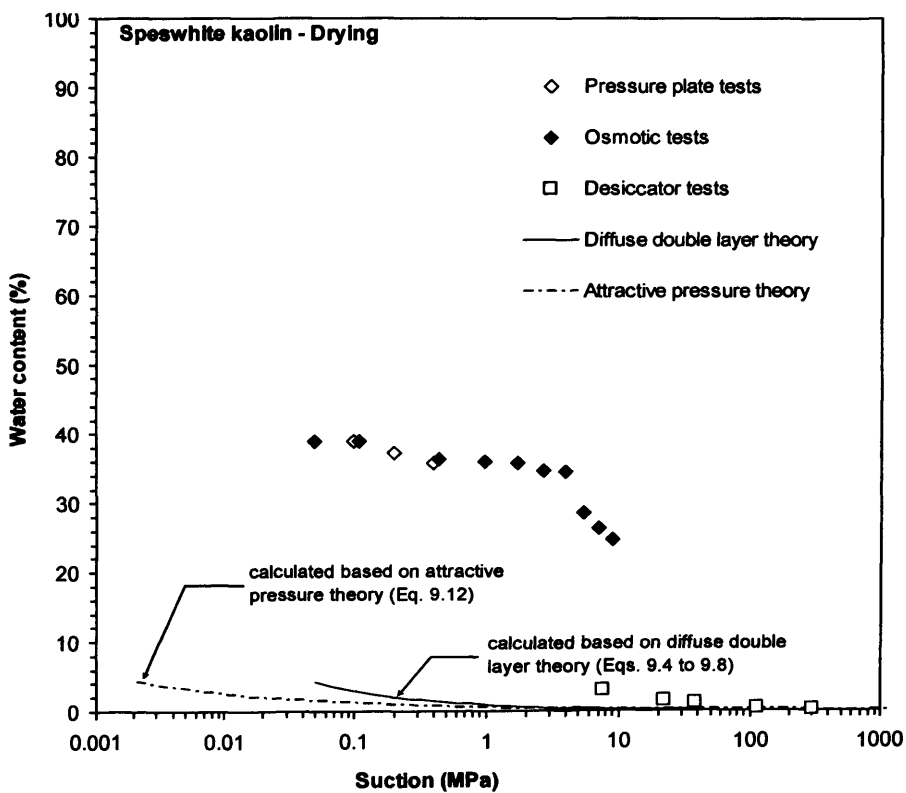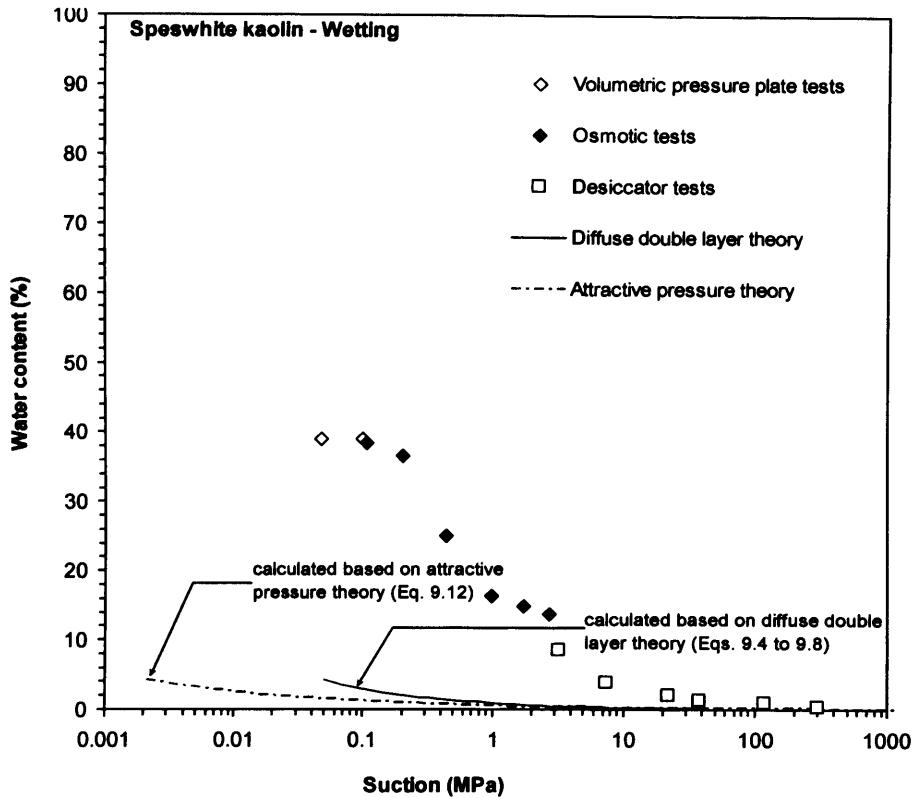
Fig. 9.9: Comparison of theoretical and experimental wetting SWCCs for Speswhite kaolin

The results presented in Figs. 9.7 to 9.9 show that the attractive pressure theory may be used

for establishing the wetting suction-water content SWCCs for the bentonites at higher applied

suctions. Mitchell (1993) stated that van der Waals attractive pressure theory is valid for

particle separation distance of less than 100 nm. At lower suction region, it may be expected

that the diffuse double layer is more dominant; however, comparisons between the calculated

SWCCs from diffuse double layer theory with the experimental results indicated that this

may not necessarily so, particularly during the wetting process. In the case of Speswhite

kaolin, due to a very low specific surface area and a low cation exchange capacity, the

physicochemical forces are less relevant (Mitchell, 1993).

9.4.3 Comparison of theoretical and experimental c-axis spacing

Figures 9.10, 9.11 and 9.12 show the experimental c-axis spacing and the calculated c-axis spacing based on parallel plate consideration (Eq. 9.9) for MX80 bentonite, Yellow bentonite and Speswhite kaolin, respectively. The c-axis spacing corresponding to 1, 2, 3 and 4 layers of adsorbed water for homoionised montmorillonite (Grim, 1968) are also presented in Figs. 9.10 and 9.11. The suction corresponding to the laboratory ambient condition (i.e. temperature = 25 °C and RH = 60%) are also marked in Figs. 9.10 to 9.12.

Figures 9.10 and 9.11 show that the calculated and the measured c-axis spacing increased with a decrease in the applied suction. However, it was noted that the c-axis spacing for Speswhite kaolin remain somewhat unchanged (see Fig. 9.12). For applied suctions of greater than 10 MPa for MX80 bentonite and greater than 30 MPa for Yellow bentonite, the calculated c-axis spacing were found to be smaller than that of the experimental results. On the other hand, at lower applied suctions, the calculated c-axis spacing were found to be greater than that of the experimental results. At an applied suction of 0.05 MPa, the c-axis spacing of Yellow bentonite (about 1.9 nm) was found to be greater than that of MX80 bentonite (about 1.56 nm). In this case, the number of water layers for Yellow bentonite was three as compared to only two number of water layers for MX80 bentonite. Figure 9.12 shows that the experimental results and calculated c-axis spacing for Speswhite kaolin were very similar up to an applied suction of 7.5 MPa.
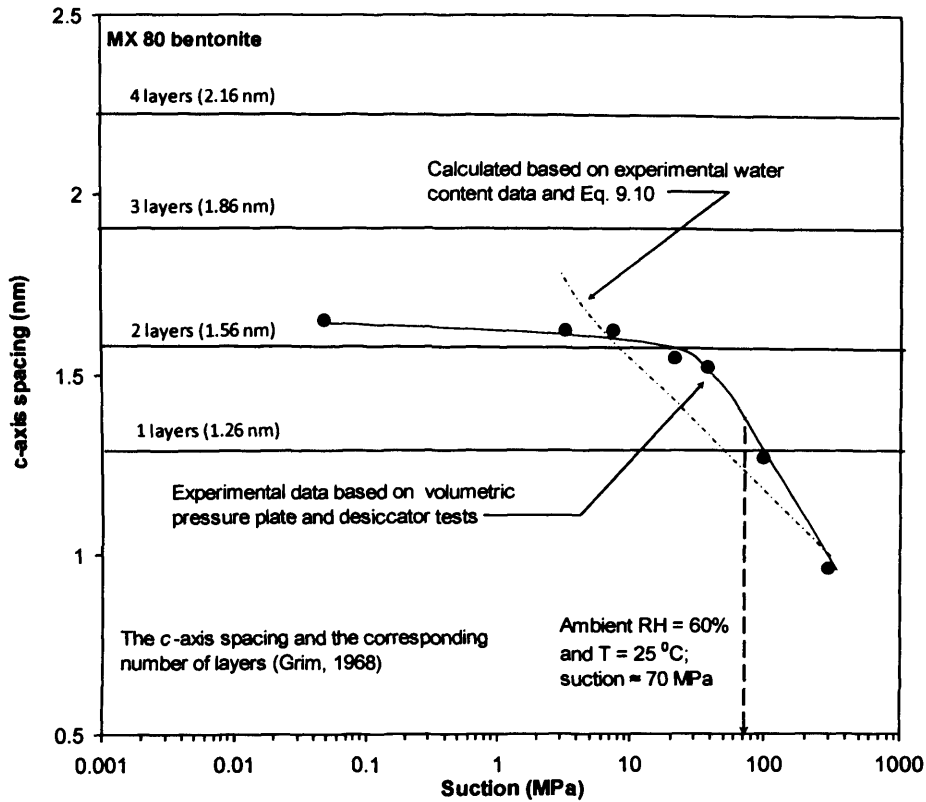
Fig. 9.10: Comparisons theoretical and measured c-axis spacing for MX80 bentonite
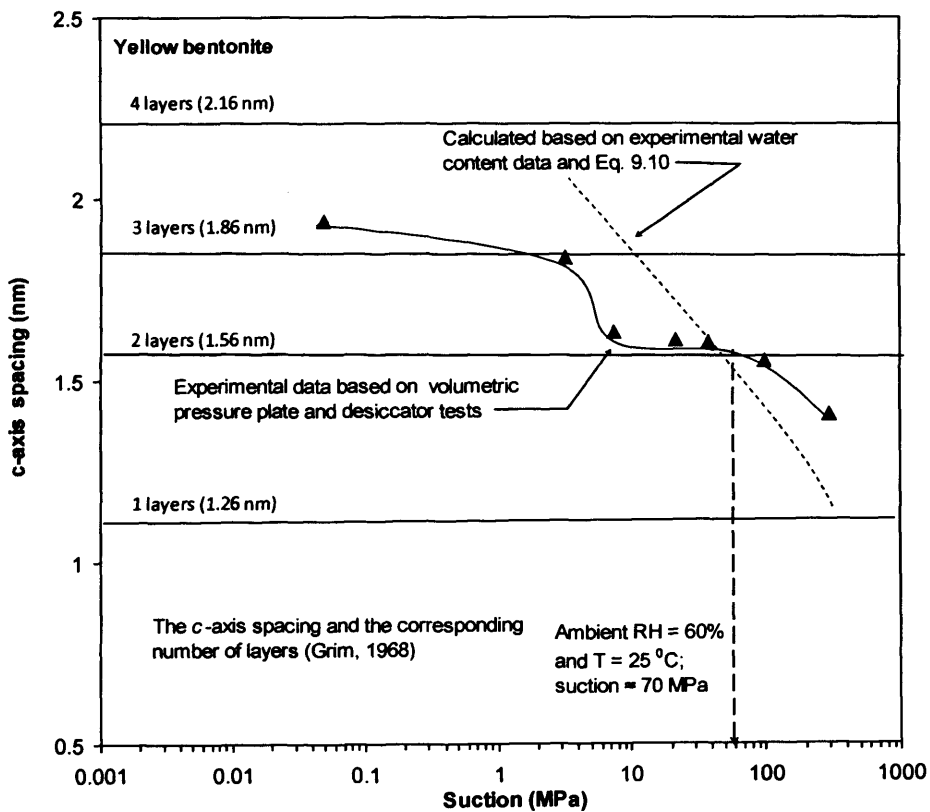
Fig. 9.11: Comparisons theoretical and measured c-axis spacing for Yellow bentonite
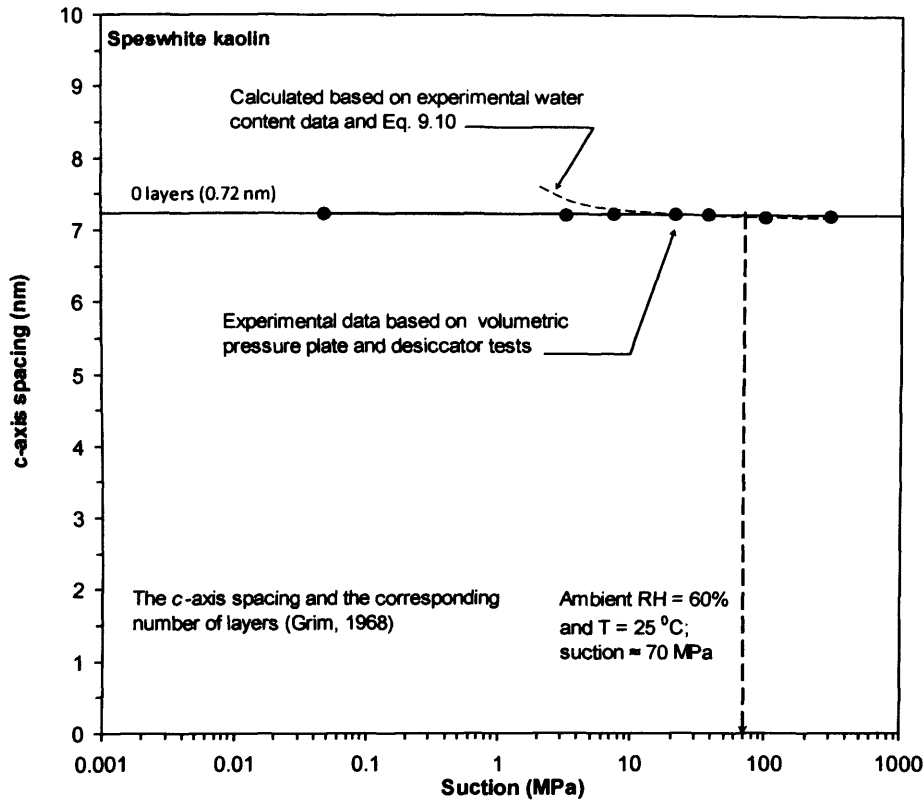
Fig. 9.12: **Comparisons theoretical and measured c-axis spacing Speswhite kaolin**

The measured c-axis spacing for MX80 bentonite and Yellow bentonite in this study were found to be concurrent with the findings reported by Saiyouri et al. (2000) and Likos (2004) (see Section 8.5.2). However, the calculated values of c-axis spacing were found to predict greater c-axis spacing at lower applied suctions than the experimental results due to the fact that the measured c-axis spacing using XRD only accounted for the crystalline swelling of the clays (Grim, 1968). Overall, the agreements between the experimental results and the calculated c-axis spacing based on Eq. 9.9 were found to be very poor.

9.5 Concluding remarks

The findings from the study can be summarised as follows:

i.   The diffusivity is a sensitive parameter that plays a significant role in the determination of elapsed time versus water content changes of clay specimens.

ii. Both the diffuse double layer theory and the van der Waals attractive pressure theory can be used to establish the drying and wetting suction-water content SWCCs of the clays. The diffuse double layer theory was found to provide reasonable results for MX80 bentonite at smaller applied suctions. In this case, the agreements between the experimental and the calculated results were very good for suctions less than 4 MPa. The van der Waals attractive pressure theory provided results that were in very good agreement with the experimental results at large suctions (> 1 MPa for the bentonites and > 10 MPa for Speswhite kaolin).

iii. Severe disagreements were noted between the measured c-axis spacing and the c-axis spacing calculated based on parallel plate considerations.

CHAPTER 10

CONCLUSIONS

The objectives of the thesis were to establish experimentally the drying and wetting soil-water characteristic curves (SWCCs) and shrinkage behaviour of highly plastic clays (MX80 bentonite, Yellow bentonite and Speswhite kaolin) at zero applied stress. An extensive experimental investigation dealing with several testing methods as applicable to unsaturated soil testing was undertaken. The suction-water content SWCCs of the clays were also determined based on physico-chemical considerations. A summary of the research works and the major conclusions drawn from the study are presented in this chapter.

The physical and chemical properties of the clays used were determined following the standard laboratory procedures. The drying suction-water content SWCCs were established by centrifuge, axis-translation, osmotic and vapour equilibrium techniques. Osmotic suction equilibrium on either side of semipermeable membranes in the osmotic tests was investigated via chemical analyses of the Polyethylene glycol (PEG) solutions used at various applied suctions. The factors responsible for intrusion of PEG into the clay specimens in the osmotic tests were investigated by studying the Atomic Force Microscope (AFM) images of the semipermeable membranes used and the Fourier Transform Infrared (FTIR) spectrums of the PEG solutions used. During the drying process, volume measurements of clay specimens by wax method at several applied suctions in the pressure plate and the desiccator tests enabled establishing the suction-void ratio SWCCs and the suction-degree of saturation SWCCs. The drying suction-degree of saturation SWCCs of the clays were also established based on the

224

drying suction-water content SWCCs in conjunction the water content-void ratio shrinkage paths that in turn were established using Clod tests with polyvinyl acetate as an encasement material. The air-entry values (AEVs) of the clays were determined based on two considerations, such as based on the total suction equilibrium on either side of semipermeable membranes in the osmotic tests and based on the suction-degree of saturation SWCCs of the clays. The wetting suction-water content SWCCs of the clay specimens compacted at various dry densities were established for various confining conditions (unconfined, laterally confined, confined) using axis-translation, vapour equilibrium, osmotic and chilled-mirror dew-point techniques. The swelling pressures of compacted bentonites were measured under controlled suctions and using deionised water. Microstructural changes of the clays during the wetting process were studied using Environmental Scanning Electron Microscope (ESEM) and X-ray diffraction (XRD) technique.

The transient water uptake behaviour (i.e. the elapsed time versus water content) of powder clay specimens were determined based on Richard's equation. The Gouy-Chapman diffuse double layer theory and the van der Waal attractive pressure theory were used to establish the suction-water content SWCCs of the clays. The changes in the c-axis spacing of the clays during the wetting process were calculated based on parallel plate consideration. The calculated results were then compared with the experimental results.

Based on the findings reported in this thesis, the following conclusions were drawn.

1. Several techniques, such as centrifuge, axis-translation, osmotic, vapour equilibrium, and chilled-mirror dew-point techniques can be used to determine suction-water content SWCCs of soils. The equilibrium time in these techniques vary quite

considerably from a few minutes in the case of chilled-mirror dew-point technique to several months in the case of vapour equilibrium technique.

2. Comparisons of the pressure plate and the osmotic test results for applied suctions less than 0.44 MPa revealed that equal magnitude of air pressure and osmotic suction of PEG solution brought specimens of the same clay to very similar water contents. Intrusion of PEG into clay specimens in the osmotic tests was very distinct at higher applied suctions. Within a suction range of 2 to 100 MPa, the agreements between the chilled-mirror test results and desiccators test results for the clays were found to be very good.

3. The water uptake capacities of the clays during the wetting process were found to be not influenced by the initial compaction dry density under unconfined condition. At applied suctions greater than 3.0 MPa, the equilibrium water contents of the clays during the wetting process were not affected by the initial compaction dry densities and confining conditions. ESEM observations provided evidence concerning interlayer swelling in compacted bentonites that in turn reduced the larger pores of compacted bentonites during the hydration process.

4. The swelling pressures of compacted bentonites increased with an increase in the compaction dry density and with a reduction in suction. The c-axis spacing of the clays increased with a decrease in the applied suction to a maximum of three mono-layers of water for divalent-rich Yellow bentonite and two mono-layers of water for monovalent-rich MX80 bentonite. Richard's equation was found to replicate the elapsed time versus water content change of the clays wetted under unconfined condition.

The above findings are in conformity with the findings reported in the literature.

5. Significant imbalances were noted between the osmotic suctions due to the expelled and the retained salts (i.e. π_{salt}^1 and π_{salt}^2) on either side of the semipermeable membranes in the osmotic tests. The osmotic efficiencies of the highly plastic clays were held responsible for such inequalities in the osmotic suction. The osmotic suctions corresponding to the expelled salts (π_{salt}^1) were found to be less than 12.0 kPa for the bentonites and less than about 2.0 kPa for Speswhite kaolin for an applied suction range of 0.05 to 8.91 MPa. Therefore, the influence of π_{salt}^1 on the applied suctions in the osmotic tests ($\pi_{PEG} + \pi_{salt}^1$) was found to be insignificant.

6. Differences were noted between the water contents of the clays obtained from the osmotic tests and the desiccator tests in the overlapping suction region of 7.0 to 10.0 MPa. In this overlapping suction region, the water contents obtained from the desiccator tests for the bentonites were distinctly greater than that obtained from the osmotic tests, whereas the reverse was the trend for Speswhite kaolin. The influence of PEG intrusion on the equilibrium water contents of the bentonites at higher suctions was found to be less than 1.5%. Insignificant decrease in the water content of Speswhite kaolin in the osmotic tests for a suction range of 0.4 to 4 MPa clearly indicated that prior to cavitation, the tensile strength of pore-water resisted the applied suction.

7. Based on the physico-chemical considerations as applicable to clay-water systems and the total suction equilibrium on either side of semipermeable membranes in the osmotic tests (i.e. $\pi_{PEG} + \pi_{salt}^1 = \pi_{salt}^2 +$ matric suction), two distinct mechanisms were found to explain well the water content decrease due to applied suctions for highly plastic clays. In mechanism 1, a change in the water content prior to the air-entry is controlled by the osmotic pressure at interparticle level and in mechanism 2; a decrease in the degree of saturation following the air-entry is primarily on account of

227

the matric suction. Based on these two mechanisms, the AEVs of the clays were determined from the chemical analyses of PEG solutions in the osmotic tests. The AEVs of the clays based on the total suction equilibrium in the osmotic tests were found to be about 19.0 MPa for MX80 bentonite, 17.0 MPa for Yellow bentonite and 0.4 MPa for Speswhite kaolin.

8. Clod tests were found to very effective in establishing continuous water content-void ratio shrinkage paths of the clays. The agreements between the void ratios of clays from the wax tests and the Clod tests were found to be good. The Clod test results clearly indicated that the clays desaturated well prior to the corresponding shrinkage limits. Therefore, suctions corresponding to the shrinkage limit water contents may overestimate the AEVs for highly plastic clays.

9. The suction-water content SWCCs in conjunction with the Clod test results that in turn were best fitted with available parametric models enabled establishing smooth suction-degree of saturation SWCCs and further the AEVs of the clays could be determined. Based on the suction-degree of saturation SWCCs, the AEVs of MX80 bentonite and Yellow bentonite and Speswhite kaolin were found to be about 21 MPa, 17 MPa, and 0.4 MPa, respectively. These values were found to be very similar to that of the AEVs of the clays determined from the total suction equilibrium considerations in the osmotic tests.

10. AFM images of the semipermeable membranes with molecular weight cut-off (MWCO) values of 14000 and 35000, both before and after the osmotic tests, clearly revealed that PEG intrusion occurred primarily due to some significant alteration of the membrane pore-size, particularly at higher applied suctions. The maximum pore-size of membrane 14000 that was used for applying a suction of 0.44 MPa increased

from 16.0 to 18.0 nm, whereas it increased from 8.0 to 30.0 nm for membrane 3500 that was used for applying a suction of 7.04 MPa.

11. Fourier Transform Infrared (FTIR) spectrums of PEG solutions showed that PEG 6000 with a greater MW exhibited higher transmittance due to its shorter chain length as compared to that of PEG 20000. Comparisons of FTIR spectrums of freshly prepared PEG solutions of PEG 6000 and 2000 and the solutions aged for 15 days did not provide any evidence of a degradation of PEG molecules with elapsed time.

12. Confinement conditions were found to influence the water uptake behaviour of compacted clays. The equilibrium water contents attained by the clays that were tested under laterally confined and isochoric conditions were far lesser as compared to that occurred for unconfined condition.

13. The diffusivity of clay powders equilibrated at a suction of 3.3 MPa under unconfined conditions were found to be in the order of 10^{-10} m^2/s. The diffusivity was found to be a very sensitive parameter that plays a significant role in assessing the elapsed time versus water content changes of soils.

14. The Gouy-Chapman diffuse double layer theory and the van der Waals attractive pressure theory were found to be useful for establishing the suction-water content SWCCs of the clays. The agreement between the experimental and the calculated drying suction-water content SWCCs for the monovalent-rich MX80 bentonite was very good for suctions less than 4 MPa, whereas the van der Waals attractive pressure theory provided results that were consistent with the experimental SWCCs for suctions greater than 1 MPa for the bentonites and for suctions greater than 10 MPa for Speswhite kaolin. Severe disagreements were noted between the measured c-axis spacing and the c-axis spacing calculated based on parallel plate considerations.

REFERENCES

Abuel-Naga, H. and Bouazza, A. 2010. A novel laboratory techniques to determine the water retention curve of geosynthetic clay liners. Geosynthetics International, Vol. 17, No. 5, : 313-322.

Agus S.S. and Schanz T. 2004. Comparison of four methods for measuring total suction. Vadose Zone Journal. Special section: Soil Water Sensing. Soil Science Society of America, Vol. 4, No. 4 : 1087-1095.

Aitchison, G. D. 1965. Moisture equilibria and moisture changes in soils beneath covered areas/ A symposium in print, G.D. Aitchison, Ed., Butterworths, Australia.

Albrecht, B. and Benson, C. 2001. Effect of desiccation on compacted natural clays. J. Geotech. and Geoenvironmental Eng. Vol. 127, No. 1, : 67-76.

Al-Mukhtar, M., Qi, Y., Alcover, J. F. and Bergaya, F., 1999. Oedometric and water-retention behavior of highly compacted unsaturated smectites. Canadian Geotechnical Journal Vol. 36. : 675-684.

Allen, T. 1974. Particle size measurement. Powder Technology Series. Chapman and Hall 2nd Revised edition.

Alther, G. R. 2004. Some practical observations on the use of bentonite. Environmental and Engineering Geoscience, Vol. 10, No. 4, : 347-359.

Alymore L. A. G, Sills, I. D. and Quirk, J.P. 1969. Surface area of homoionic illite and montmorillonite clay minerals as measured by the sorption of nitrogen. Clays and Clay Minerals, 1970, Vol. 18, : 91-96.

Andersson, C., Barcena, N., Bono, N., Boergesson, L., Cleall, P., Forsmark, T., Gunnarsson, D., Johannesson, L.-E., Ledesma, A., Liedtke, L., Luukkonen, A., Pedersen, K., Puigdomenech, I., Pusch, R., Rhen, I., Rothfuchs, T., Sanden, T., Sineriz, J.-L., Sugita, Y., Svemar, C. and Thomas, H. 2005. Nuclear Science and Technology. Full-scale testing of the KBS-3V concept for the geological disposal of High-level radioactive waste – Prototype repository. Final report.

Archos, D., Grandia, F., Domenech, C., Fernandez A.M., Villar, M.V., Muurinen, A., Carlsson, T., Sellin, P. and Hernan, P. 2008. Long-term geochemical evolution of the near field repository: Insights from reactive transport modelling and experimental evidences. Journal of Contaminant Hydrology. Vol. 102, No. 1-2, : 196-209.

Ariffin, Y. and Schanz, T. 2007. Modified isochoric cell for temperature controlled swelling pressure tests. *In* Experimental Unsaturated Soil Mechanics. Springer Proceedings in Physics, Vol. 112, No. 4 : 229-241.

Arnepalli, D.N., Shanthakumar, S., Hanumantha Rao, B. and Singh, D.N. 2008. Comparisons of methods for determining specific-surface area of fine-grained soils. Geotech Geol Eng. 26: 121-132

ASTM. 2002. D 422-63 Standard test method for particle-size analysis of soils.

ASTM. 2003. D 6836-02 Standard test methods for determination of the soil water characterisitic curve for desorption using hanging column, pressure extractor, chilled mirror hygrometer, and/or centrifuge.

ASTM. 2007. E 104-02 Standard practice for maintaining constant relative humidity by means of aqueous solutions.

ASTM 2010a. D 4943-08 Standard test method for shrinkage factors of soils by wax method.

ASTM. 2010b. D 5298-94 Standard test method for measurement of soil potential (suction) using filter paper.

Bache, B.W. 1976. The measurement of cation exchange capacity of soils. J. Sci. Food Agric. Vol. 27: 273-280.

Barbour, S.L. and Fredlund, D.G. 1989 Mechanisms of osmotic flow and volume change in clay soils, Canadian Geotechnical Journal, 26 : 551–562.

Barbour, S.L., Fredlund, D.G. and Pufahl, D.E. 1991. The osmotic role in the behaviour of swelling clay soils. Proceedings of the NATO Advances Research Workshop, Greece. : 97-139.

Barbour, S.L. 1998. Nineteenth Canadian Geotechnical Colloquium: The Soil–Water Characteristic Curve: A Historical Perspective. Can. Geotech. J. 35:873–894.

Bao, C.G. and Ng, C.W.W. 2000. Some Thoughts and Studies on the Prediction of Slope Stability in Expansive Soils. In Unsaturated Soil for Asia: Proceedings of the Asian Conference UNSAT-Asia 2000, Singapore 10-19 May 2000. Rahardjo, Toll and Leong (eds). Balkema, Rotterdam. : 15-32.

Beamson, G., Pickup, B. T., Li, W. and Mai, S. M. 2000. XPS studies of chain conformation in PEG, PTrMO, and PTMG linear polyethers. J. Phys. Chem. B. 104, No. 12, : 2656-2672.

Beck, Eckardt, C. 1979. The Love Canal tragedy. Environmental Protection Agency History.

Bear, J. 1972. Dynamics of fluids in porous media; Dover Publications, Inc.: New York, NY, : 764.

Benson, C. 2005. Materials stability and applications, in barrier systems for environmental contaminant containment and treatment, C. Chen, H. Inyang, and L. Everett, eds., CRC Press, Boca Raton, FL, : 143-208.

Blatz J.A, Cui Y.J. and Oldecop L., 2008 Vapour equilibrium and osmotic technique for suction control. Geotech. Geol. Eng., Vol. 26, No. 6, : 661–673.

Bolt, G. H. 1956. Physicochemical analysis of compressibility of pure clays. Geotechnique. London: Institution of Civil Engineers. Vol. 6, 86-93.

Bradbury, M. H. and Baeyens, B. 2002. Porewater chemistry in compacted re-saturated MX-80 bentonite: Physico-chemical characterisation and geochemical modelling. PSI Bericht Nr Switzerland.

Bradeau, E., Constantini, J. M., Bellier, G. and Colleuille, H. 1999. New device and method for soil shrinkage curve measurement and characterization. Soil Science Society of America Journal. Vol. 63, No. 3, : 525-535.

Brasher, B.R., Franzmeier, D.P., Valassis, V. and Davidson, S.E., 1966. Use of saran resin to coat natural soil clods for bulk density and water retention measurements. Soil Sci. 101 : 108.

Brindley, G.W. 1966. Ethylene glycol and glycerol complexes of smectite and vermiculites. Clay Minerals, 6, 237-259.

BS 1377-2. 1990. Soils for civil engineering purposes. Part 2: Classification tests. British Standards Institution.

Bouazza, A. and Bowders, J.J. 2010. Geosynthetic clay liners in waste containment facilities. CRC Press/Balkema. : 254

Boivin, P., Garnier, P. and Tessier, D. 2004. Relationship between clay content, clay type, and shrinkage properties of soil samples. Soil Science Society of America Journal. Vol. 68, : 145-1153.

Bourg, I. C., A. C. M. Bourg and G. Sposito 2003. Modeling diffusion and adsorption in compacted bentonite: a critical review. Journal of Contaminant Hydrology. Vol. 61, No. 1-4: 293-302.

Bourg, I. C., A. C. M. Bourg and G. Sposito 2006. Tracer diffusion in compacted, water-saturated bentonite. Clays and Clay Minerals. Vol. 54, No. 3 : 363-374.

Bouyoucos, G.J. 1935. A comparison between the suction method and the centrifuge method for determining the moisture equivalent of soils. Soil Science. Vol. 40, No. 2 : 165-172.

Bulut, R. Lytton, R.L., Wray, W.K. 2001. Soil suction measurements by filter paper. In: Vipulanandan, C., Addison, M.B., Hasen, M. (eds) Expansive clay soils and vegetative influence on shallow foundations, ASCE geotechnical special publication no. 115. Houston, Texas, : 243–261.

Bulut, R., Leong, E. C. 2008. Indirect measurement of suction. Geotech. Geol. Eng., Vol. 26, No.6, 633-644 Cornelis, W. M., Corluy, J., Medina, H., Diaz, J., Hartmann, R., van Meirvenne, M., and Ruiz, M. E.: Measuring and modelling the soil shrinkage characteristic curve, Geoderma, Vol. 137, No. 25, : 179–191.

Burrafato, G. and Miano, F. 1993. Determination of the cation exchange capacity of clays by surface tension measurements. Clay Minerals, Vol. 28 : 475-481.

Campbell, J. 2003. Limitation in the laser particle sizing of soils. In Roach I.C. ed. 2003. Advances in Regolith, : 38-42.

Carlson, L. 2004. Bentonite mineralogy, Part 1: Methods of investigation – a literature review, Part 2: Mineralogical research of selected bentonites, Working report 2004–02, Posiva Oy, Olkiluoto, Finland, : 78.

Carter, M. R. and Gregorich E. G. 2007. Soil sampling and methods of analysis. Canadian Society of Soil Science. Taylor and Francis Group.

Cebula, D.J. Thomas, R.K. and White, J.W. 1981. Diffusion of water in Li-montmorillonite studied by quasielastic neutron scattering. Clays and Clay Minerals, Vol. 29., No. 4, : 241-248.

Celina, M., Ottesen, D. K., Gillen, K. T., and Clough, R. L. 1997. FTIR emission spectroscopy applied to polymer degradation. Polymer Degradation and Stability 58, No. 1, : 15-31.

Cerato, A.B. and Lutenegger, A.J. 2002. Determination of surface area of fine grained soils by the ethylene glycol monoethyl ether (EGME) method. Geotechnical Testing Journal, Vol. 25, No. 3, : 315-321.

Chapman, H.D. 1965. Cation-exchange capacity. In: C. A. Black (ed.) Methods of soil analysis - Chemical and microbiological properties. Agronomy, Vol. 9: 891-901.

Chen, G., Pan, J., Han, B. and Yan, H. 1999. Adsorption of methylene blue on montmorillonite. Journal of Dispersion Science and Technology. Vol. 20, No. 4 : 1179–1187.

Churchman, G.J., Burke, C.M. and Parfitt, R.L., 1991. Comparison of various methods for the determination of specific surfaces of subsoils. Journal of Soil Science, Vol. 42, : 449–461.

Clarke, C.R. and Nevels, J. B. 1996. Shrinkage and suction properties of pledger-roebuck alluvial clay. Transport Research Board. No. 1546, : 162-173.

Cokca, E. 2002. Relationship between methylene blue value, initial soil suction and swell percent of expansive soils. Turkish J. Eng. Env. Sci. Vol. 26 : 521 - 529.

Cornelis, W. M., Corluy, J., Medina, H., Diaz, J., Hartmann, R., van Meirvenne, M., and Ruiz, M. E. 2006. Measuring and modelling the soil shrinkage characteristic curve, Geoderma, Vol.137, No. 25, : 179–191.

Cosgrove, T. 2005. Colloid science: principles, methods and applications. Wiley-Blackwell: Blackwell Publishing Ltd.

Crescimanno, G. and Provenzano, G., 1999. Soil shrinkage characteristic curve in clay soils: measurement and prediction. Soil Sci. Soc. Am. J. Vol. 63, : 25–32.

Cresswell, H.P., Green, T.W. and McKenzie, N.J. 2008. The adequacy of pressure plate a:aratus for determining soil water retention. SSSAJ, Vol. 72, No. 1.

Croney, D. and Coleman, J.D. 1954. Soil structure in relation to soil suction (pF). Soil Science, Vol. 5, No. 1, :. 75-84.

Cruz-Guzmán, M., Celis, R., Hermosín, M.C., Koskinen, W.C., Nacer E.A. and Cornejo, J. 2006. Heavy metal adsorption by montmorillonites modified with natural organic cations, Soil Sci. Soc. Am. J. 70, : 215–221.

Cuisinier, O. and Masrouri, F. 2004. Testing the hydromechanical behavior of a compacted swelling soil. Geotechnical Testing Journal Vol. 26, No. 6.

Cuisinier, O. and Masrouri, F. 2005. Hydromechanical behavior of a compacted swelling soil over a wide suction range. Engineering Geology Vol. 81, : 204-212.

Cui, Y. J. and Delage, P. 1996. Yielding and plastic behavior of unsaturated compacted silt. Géotechnique 46, : 291-311.

Cutoiu, D. 2003. Aspects of Radioactive waste management. Romanian Reports in Physics, Vol. 55, No. 1, : 102-117.

Daniel, D. E. 1993. Geotechnical practice for waste management. Chapman and Hall, London.

Delage, P., Howat, M. and Cui, Y. J. 1998. The relationship between suction and swelling properties in a heavily compacted unsaturated clay. Eng. Geol. Vol. 50, No. 1-2, : 31-48.

Deeds, C. T. and van Olphen, H. 1961. Density Studies in Clay-Liquid Systems, Part II: Application to Core Analysis. Clays and Clay Mineral. (Proc. 10th Natl. Conf., 1961), Vol. 10, : 318–328.

Delage, P., Marcial, D., Cui, Y. J., and Ruiz, X. 2006. Ageing effects in a compacted bentonite: a microstructure approach. Ge´otechnique, Vol. 56, No. 5, : 291–304.

Delage, P. 2006. Some microstructure effects on the behaviour of compacted swelling clays used for engineered barriers. Chinese Journal of Rock Mechanics and Engineering. Vol. 25, No. 4. : 721-732.

Delage, P. and Cui, Y. J. 2008a. An evaluation of the osmotic method of controlling suction. Geomechanics and Geoengineering: An International Journal 3, No. 1, : 1-11.

Delage, P. and Cui, Y. J. 2008b. A novel filtration system for polyethylene glycol solutions used in osmotic method of controlling suction. Can. Geotech. J. 45, 421-424.

Delage, P. Romero, E. and Tarantino, A. 2008. Recent developments in the techniques of controlling and measuring suction in unsaturated soils. In Unsaturated Soils: Advances in Geo-Engineering – Toll et al. (eds). Taylor and Francis Group, London. : 33-52.

Delage P. and Remero R. 2008. Geoenvironmental testing geotechnical and geological engineering, Vol. 26, No. 6, : 729–749.

Dineen, K. and Burland, J. B. 1995. A new approach to osmotically controlled oedometer testing. Proc. 1st Int. Conf. on Unsaturated Soils, Paris, Vol. 2, : 459–465.

Dueck, A. 2008. Laboratory results from hydro-mechanical tests on a water unsaturated bentonite. Engineering Geology. Vol. 97 : 15-24.

Elimelech, M., Zhu, X., Childress, A. E. and Hong, S. 1997. Role of membrane surface morphology in colloidal fouling of cellulose acetate and composite aromatic polyamide reverse osmosis membranes. J. Membrane Science Vol. 127, : 101-109.

Eltantawy, I.N. and Arnold, P.W. 1973. Reappraisal of ethylene glycol mono-ethyl ether (EGME) method for surface area estimation of clays. Soil Sci. Vol. 24, : 232-238.

ENRESA. 2000. FEBEX project — full scale engineered barriers experiments for a deep geological respiratory for high level radioactive waste in crystalline host rock. Final report, Publicación téechnica 1/2000, Empresa Nacional de Residuos Radiactivos SA (ENRESA), Madrid, Spain.

Fam, M.A. and Dusseault, M.B. 1999. Determination of the reactivity of clay-fluid systems using liquid limit data. Canadian Geotechnical Journal, Vol 36, No. 1, : 161 – 165.

Fityus, S.G., Cameron, D.A. and Walsh, P.F. 2003. The shrink swell Test. Geotechnical Testing J. Vol. 28 No. 1.

Fleureau, J. M., Kheirbek Saoud, S., Soemitro, R. and Taibi, S. 1993. Behaviour of clayey soil on drying-wetting paths. Can. Geotech J. Vol.30, : 287-296.

Fleureau, J. M., Verbrugge, J. C., Huergo, P. J., Correia, A. T. and Saoud, S. K. 2002. Aspects of the behavior of compacted clayey soils on drying and wetting paths. Can. Geotech. J. Vol. 39, : 1341-1357.

Folly J.P.W. 2001. Thermo-hydro-mechanical behaviour of unsaturated soil: An experimental study. PhD thesis, School of Engineering, Cardiff University.

Fredlund, D.G. 1964. Comparison of soil suction and one dimensional consolidation characteristics of a highly plastic clay. M.Sc. thesis, University of Alberta, Edmonton, Alta.

Fredlund, D.G., Rahardjo H. 1993. Soil mechanics for unsaturated soils. Wiley-Interscience Publications.

Fredlund, D.G., Rahardjo, H. Leong, E.C. and Ng, C.W.W. (2001). Suggestions and recommendations for the interpretation of soil–water characteristic curves. Proc. 14th Southeast Asian Geotech. Conf., Hong Kong. 1, : 503–508.

Fredlund, D.G. 2002. Use of soil–water characteristic curves in the implementation of unsaturated soil mechanics. Proc. 3rd Int. Conf. Unsat. Soils, Recife, Brazil, Balkema, Rotterdam.

Fredlund, D.G. 2006. Unsaturated Soil Mechanics in Engineering Practice. J. Geotech. Geoenv. Eng., 132, No. 3, : 286-321.

Frydman S. And Baker R. 2009. Theoretical Soil-Water Characteristics Curves Based on adsorption, Cavitation, and Double Porosity Model. International Journal of Geomechanics. ASCE. Vol. 9, No.6 : 250- 256.

Garcia, A. A. 1999. Bioseparation Process Science. Blackwell Science Inc.

Gardner, R. 1937. A method of measuring the capillary tension of soil moisture over a wide moisture range. Soil Science. Vol. 43 : 227–283

Gattermann, J., Wittke, W. and Erichsen, C. 2001. Modelling Water Uptake in Highly Compacted Bentonite in Enviromental Sealing Barriers. Clay Minerals; Vol 36; No. 3; : 435–446.

Gee, G., Campbell, M., Campbell G., and Campbell, J. 1992. Rapid measurement of low soil potentials using a water activity meter. Soil Science Society of American Journal, Vol. 56, : 1068–1070.

Gens, A. and Alonso E. E. 1992. A framework for the behaviour of unsaturated expansive clays. Canadian Geotechnical Journal, Vol. 29 : 1013–1032.

Gens, A., Filippi, M., Vallenjen, B., Weetjens, E., Van Geet., M., Volckaert, G. and Bastiaens, W. 2008. RESEAL II Project – Final report on modelling (WP4). SCK.CEN External Report.

Grim R. E, 1968. Clay Mineralogy. McGraw-Hill, Inc., Second Edition

Griffiths, F. J. and Joshi, R.C. 1989. Changes in pore size distribution due to consolidation of clays. Ge'otechnique Vol 39, No.1, : 159–167

Guan, Y. and Fredlund, D.G. (1997). Use of tensile strength of water for direct measurement of high soil suction. Canadian Geotechnical Journal. Vol. 34, : 604-614.

Haines, W.B., 1923. The volume changes associated with variations of water content in soil. J. Agric. Sci. Cambridge 13, : 293–310.

Han, S., Kim, C. and Kwon, D. 1995. Thermal degradation of poly(ethyleneglycol). Polymer Degradation and Stability 47, No. 2, 203-208.

Hanafy, E.A.D.E. 1991. Swelling/shrinkage characteristic curve of desiccated expansive clays. Geotech. Test. J. Vol. 14, No. 2, : 206–211.

Hang, P. T. and Brindley, 1970, Methylene blue adsorption by clay minerals, determination of surface areas and cation exchange capacities (clay-organic studies XVIII). Clays and Clay Minerals, Vol. 18, : 203-212.

Harris, J. M. 1992. Poly(ethylene glycol) chemistry: biotechnical and biomedical applications. New York: Plenum Press.

Hendershot, W.H. and M. Duquette. 1986. A simple barium chloride method for determining cation exchange capacity and exchangeable cations. Soil Sci. Soc. Am. J. Vol.50 : 605-608.

Hendershot, W.H., Lalande, H. and Duquette, M. 2007. Ion Exchange and Exchangable Cations. In Soil Sampling and Methods of Analysis. Canadian Society of Soil Science. Taylor and Francis Group

Heymann, G. and Clayton, C.R.I. 1999. Block sampling of soil: Some practical considerations. In Geotechnics for Developing Africa. Proceedings of the 12th Regional Conference for Africa on Soil Mechanics and Geotechnical Engineering, Durban, South Africa. A.A Bakema/Rotterdam/Brookefield. : 331-340

Hillel, D. 1982. Introduction to Soil Physics; Academic Press, Inc.: Orlando, FL, : 10.

Himmel, M. E. and Squire, P. G. 1988. Size exclusion parameters. J. Chromatography Library 40, : 3-20.

Houston, S. L., Houston, W. N., and Wagner, A. M. 1994. Laboratory Filter Paper Measurements. Geotechnical Testing Journal, Vol. 17, No. 2, : 185-194.

IAEA 1990. Siting, Design and construction of a deep geological repository for the disposal of high level and alpha bearing wastes. a technical document issued by the International Atomic Energy Agency, Vienna.

Idemitsu, K., Ishiguro, K., Yusa, Y., Sasaki, N. and Tsunoda, N. 1990. Plutonium diffusivity in compacted bentonite. Engineering Geology, No. 28, : 455-462.

Inoue, A., Bouchet, A., Velde, B. and Meunier, A. 1989. Convenient technique for estimating smectite layer percentage in randomly interstratified illite/smectite minerals. Clays and Clay Minerals, 37, 227-234

Iwata, S., Tabuchi, T. and Warkentin, B. P. 1988. Soil-water interactions: mechanisms and applications. New York: Marcel Dekker, Inc.

Johannesson, L.E. and Nilsson, U. 2006. Deep repository – Engineered barrier system. Geotechnical properties of candidate backfill materials. Laboratory tests and calculations for determining performance, SKB R-06-73, SKB, Stockholm, Sweden.

Kassiff, G. and Ben Shalom, A. 1971. Experimental relationship between swell pressure and suction. Géotechnique Vol. 21, : 245-255.

Khanzode, R.M., Vanapalli, S.K. and Fredlund, D.G. 2002. Measurement of soil–water characteristic curve for fine-grained soils using a small centrifuge. Can. Geotech. J. Vol. 39, No. 5 : 1209–1217

Kemper, W. D. and Evans, N. A. 1963. Movement of water as effected by free energy and pressure gradients: III. restriction of solutes by membranes. Soil Sci. Soc Am. Proc. 27, No. 5, : 485-490.

Kemper, W.D. and Quirk, J.P. 1972. Ion mobilities and electric charge of external clay surfaces inferred from potential differences and osmotic flow. Soil Science Society of America, Proceedings, Vol. 36, No. 3 : 426-433.

Kemper, W.D. and Rollins, J.B. 1966. Osmotic efficiency coefficients across compacted clays. Soil Science Society of America Proceedings, Vol., 30, No. 5 : 529-534.

Ke'zdi, A. 1980. Handbook of Soil Mechanics. Soil Testing, Vol. 2. Elsevier Scientific Publishing Company, Amsterdam, Netherlands

Kim, D.J., Vereecken, H., Feyen, J., Boels, D. and Bronswijk, J.J.B., 1992. On the characterization of properties of an unripe marine clay soil. 1. Shrinkage processes of an unripe marine clay soil in relation to physical ripening. Soil Sci. No. 153, : 471–481.

Kim, K. J., Fane, A. G., Ben Aim, R., Liu, M. G., Jonsson, G., Tessaro, I. C., Broek, A. P. and Bargeman, D. 1994. A comparative study of technique used for porous membrane characterization: pore characterization. J. Membrane Science Vol. 87, : 35-46.

Klute, A. 1986. Water retention: Laboratory methods, methods of soil analysis, Part 1, Agronomy, A. Klute. Ed., No. 9, 2nd Ed., American Society of Agronomy and Soil Science Society of America, Madison, WI, : 635 - 662

Koch, D. 2007. European Bentonites as Alternatives to MX-80. International Meeting, September 17-18, 2007, Lille, France. Clays in Natural and Engineered Barriers for Radioactive Waste Confinement, : 23-24

Komine, H. and Ogata, N., 1994. Experimental study on swelling characteristics of compacted bentonite. Canadian Geotechnical Journal Vol. 31, No. 4, : 478–490.

Komine, H. and Ogata, N. 2003. New Equations for Swelling Characteristics of Bentonite-based Buffer Materials. Canadian Geotechnical Journal. Vol. 40, No.2, 460-475.

Komine, H. 2010. Prediciting hydraulic conductivity of sand-bentonite mixture backfill before and after swelling deformation for underground disposal of radioactive wastes. Engineering Geology. Vol. 114, : 123-134.

Kozaki, T., Fujishima, A., Sato, S. and Ohashi, H., 1998. Self-diffusion of sodium ions in compacted sodium montmorillonite. Nuclear Technology, Vol. 121 : 63-69.

Krahn J. and Fredlund D.G. 1972 On total, matric and osmotic suction. Soil Science, Vol. 115, No. 5 : 339-348.

Krosley et al. 2003. Alternative encasement material for Clod test. Geotechnical Testing Journal, Vol. 26, No.4

Kunze, G.W. 1955. Anomalies in the ethylene glycol solvation technique used in X-ray diffraction. Clays and Clay Minerals, 3, : 83-93.

Kutchai, H. 1980. Osmosis – A Self-instructional Package. Department of Molecular Physiology and Biological Physics. School of Medicine, University of Virginia

Lambe, T.W. and Whitman, R.V. 1969 Soil Mechanics. John Wiley and Sons Inc.

Lang, A. R. G. 1967. Osmotic coefficients and water potentials of sodium chloride solutions from 0 to 40 C. Australian Journal of Chemistry Vol. 20, : 2017-2023.

Lauritzen, C.W., 1948. Apparent specific volume and shrinkage characteristics of soil materials. Soil Sci. 65, : 155–179.

Lavkulich, L.M. 1981. Methods Manual, Pedology Laboratory. Department of Soil Science, University of British Columbia, Vancouver, British Columbia, Canada.

Lentsch, S., Aimar, P. and Orozco, J. L. 1993. Separation albumin–peg: transmission of peg through ultrafiltration membranes. Biotechnology and Bioengineering 41, No. 11, 1039-1047.

Leong, E.C., He, L. and Rahardjo, H. 2002. Factors affecting the filter paper method for total and matric suction measurements. Geotechnical Testing Journal. Vol. 25, No. 3 : 322–333

Leong E.C., Tripathy S., and Rahardjo R. 2003. Total suction measurement of unsaturated soils with a device using the chilled-mirror dew-point technique. Géotechnique, Vol. 53, No. 2 : 173-182.

Leong, E.C., Tripathy, S. and Rahardjo, H. 2004. A modified pressure plate apparatus. Geotech Test J. Vol. 27, No. 3 : 322–331

Levitt, D.G. and Young, M.H. 2003. Soils, hygroscopic water content, In Encyclopedia of Water Science, Steward, B.A., Howell, T.A., Marcel Dekker Inc. New York.

Likos, W.J., 2004. Measurement of crystalline swelling in expansive clay. Geotechnical Testing Journal, Vol. 27, No. 6 : 540-546.

Likos, W. J. and Lu, N. 2002. Filter paper technique for measuring total soil suction. Transportation Research Record, 1786, :. 120–128

Likos, W.J., and Lu, N., 2006. Pore scale analysis of bulk volume change from crystalline swelling in Na^+- and Ca^{2+}-smectite. Clays and Clay Minerals. Vol. 54, No. 4, : 516 – 529.

Lourenço, S.D.N., Gallipoli, D., Toll, D.G., Augarde, C.E. and Evans, F. 2011. A new procedure for the determination of the Soil Water Retention Curves by continuous drying using high suction tensiometers. Canadian Geotechnical Journal 48(2): 327-335.

Low, P. F. 1955. The effect of osmotic pressure on the diffusion rate of water. Soil Science No. 80, : 95-100.

Lu, N. and Likos, W.J. 2004. Unsaturated Soil Mechanics. John Wiley and Sons Inc.

Malusis, M.A. and Shackelford, C.D. 2002. Chemico-osmotic efficiency of a geosynthetic clay liner. Journal of Geotechnical and Geoenvironmental Engineering, Vol. 128, No.2 : 97-106.

Malusis, M.A., Shackelford, C.D., and Olsen, H.W. 2003. Flow and transport through clay membrane barriers. Engineering Geology, Vol. 70, No. 2-3 : 235-248.

Marcial, D. Delage, P. and Cui Y. J. 2002. On the high stress compression of bentonites. Canadian Geotechnical Journal Vol. 39, No. 4, 812–820.

Marinho F.A.M. and Oliveira, O.M. 2006. The filter paper method revised. ASTM Geotech Test J, Vol. 29, No. 3 : 250–258.

Mbonimpa, M., Aubertin, M., Maqsoud A. and Bussière B. 2006. Predictive Model for the Water Retention Curve of Deformable Clayey Soils. J. Geotech. Geoenv. Eng., 132, No. 9, 1121-1132.

McKeen, R. G. 1985. validation of procedures for pavement design on expansive soils. program engineering and maintenance service, Federal Aviation Administration,Washington, DC.

Mehlich, A. 1938. Use of triethanolamine acetate-barium hydroxide buffer for the determination of some base exchange properties and lime requirement of soil. Soil Sci. Soc. Am. Proc. Vol. 29 : 374-378.

Metcalf and Eddy. 2002. Wastewater Engineering – Treatment and reuse. 4th Ed. McGraw-Hill Higher Education.

Michel, B. E. and Kaufmann, M. R. 1973. The osmotic potential of polyethylene glycol 6000. Plant Physiology 51, : 914–916.

Minagawa, K., Matsuzawa, Y., Yoshikawa, K., Khokhlov, A. R. and Doi, M. 1994. Direct observation of the coil-globule transition in DNA molecules. Biopolymer Vol. 34, No. 4, : 555-558.

Mitchell, J. K. 1993. Fundamentals of Soil Behavior. 2nd Edition.

Money, N.P. 1989. Osmotic pressure of aqueous polyethylene glycols – relationship between molecular weight and vapour pressure deficits. Plant Physiology. Vol. 91 : 766-769.

Monroy, R., Ridley, A., Dineen, K. and Zdrakovic, L. 2007. The suitability of osmotic technique for the long term testing of partly saturated soils. Geotech. Test. J. 30, No. 3, : 220-226.

Montes-H, G., Geraud, Y., Duplay, J. and Reuschle, T. 2005. ESEM Observations of Compacted Bentonite Submitted to Hydration/Dehydration Conditions. Colloid and Surfaces A: Physicochem. Eng. Aspects, Vol. 262, : 14-22

Morrison, R. T. and Boyd, R. N. 1983. Organic chemistry. Allyn and Bacon Inc. Muller-Vonmoos, M., Kahr, G. and Madsen, F. T. 1994. Intracrystalline swelling of mixed-layer illite-smectite in K-bentonites. Clay Minerals. Vol. 29, No. 2, : 205-213.

Mosser-Ruck, R., Devineal, K., Charpentier, D. and Cathelineau, M. 2005. Effects of glycol saturation protocols on XRD patterns: A critical review and discussion. Clays and Clay Minerals, Vol. 53, No. 6, : 631-638.

Muhammad, N., 2004. Hydraulic, diffusion, and retention characterisitics of inorganic chemical in bentonite. PhD Thesis. University of South Florida.

Muurinen, A. 1987. Diffusion of Uranium in compacted sodium bentonite. Engineering Geology. Vol. 28. : 359-367.

Murray, H. H. 2007. Applied Clay Mineralogy – Occurences, processing and application of kaolins, bentonites, palygorskite-sepiolite and common clays. Development in Clay Science. Elvesier, Amsterdam.

Najaraj, T.S. and Sivapullaiah, P.V. 1981. Plumemet Balance - A Potential Tool for Subsieve Particle Size Analysis. Geotechnical Testing Journal, Vol. 4, No. 1, : 36-40

Nagaraj, T.S. and Miura, N. 2001. Soft clay behaviour analysis and assessment. A.A. Balkema / Rotterdam / Brookfield

Nakashima, Y. 2004. Nuclear Magnetic Resonance properties of water-rich gels of Kunigel-V1 bentonite. Journal of Nuclear Science and Technology. Vol. 41, No. 10, : 981-992.

NDA, 2010. Geological Disposal - Steps towards implementation. Executive summary. Nuclear Decommisioning Authority, UK.

Nelson, J. D. and Miller, D.J. 1992. Expansive soils - problems and practice in foundation and pavement engineering. John Wiley and Sons, Inc., New York.

Newman, A. C. D. 1983. The specific surface of soils determined by water sorption. Journal of Soil Science, Vol. 34, : 23-32.

Ng, C.W.W., Wang, B. and Tung, Y.K. 2001. Three-dimensional numerical investigations of groundwater responses in an unsaturated slope subjected to various rainfall patterns. Can. Geotech. J., Vol. 38 : 1049–1062.

Ng C.W.W. and Menzies, B. 2007. Advanced soil mechanics and engineering. Taylor and Francis

Norrish, K. 1954. "Crystalline Swelling of Montmorillonite: Manner of Swelling of Montmorillonite." Nature 173 : 256-257.

O'Brien. F.E.M. 1948. The control of humidity by saturated salt solutions. Journal of Sci. Instrum. Vol. 25 : 73-76.

Ochs, M., Lothenbach, B., Wanner, H., Sato., H. and Yui, M. 2001. An Integrated sorption-diffusion model for the calculation of consistent distribution and diffusion coefficient in compacted bentonite. Journal of Contaminat Hydrology. Vol. 47, : 283- 296.

Oldecop, L.A. and Alonso, E.E. 2004. Testing rockfill under relative humidity control. Geotech. Test. J. Vol 27, No. 3.

Olsen, H.W. 1969. Simultaneous fluxes of liquid and charge in saturated kaolinite. Soil Science Society of America, Proceedings. Vol. 33 : 338-344.

Or, D. and Tuller, M. 1999. Liquid retention and interfacial area in variably saturated porous media: upscaling from single-pore to sample-scale model. Water Resources Research. Vol. 35 : 3591–3605.

Oweis, I. and Khera, R. 1998. Geotechnology of Waste Management. 2nd Edition. CL-Engineering.

Peavy, H. S., Rowe, D.R. and Tchobanoglous, G. 1987. Environmental Engineering. 7th Edition. McGraw Hill Publishing.

Perkins A.T., Horne, L. and King, H.H. 1937. Humidity and Specific Gravitiy of Soil Particles. Transactions of the Kansas Academy of Science (1903-1937), Vol. 40, : 127-129.

Perko, H.A., Thompson, R.W., and Nelson, J.D. 2000. Suction Compression Index Based on Results from CLOD Tests. Advances in Unsaturated Geotechnics, C.D. Shackelford, S.L. Houston, and N.Y. Chang, Eds., ASCE Press, Reston, VA, :. 393-408.

Peron, H., Hueckel, T. and Laloui, L. 2007. An improved volume measurement for determining soil water retention curves. Geotechnical Testing Journal, Vol. 30, No. 1.

Peron, H., Hueckel, T., Laloui, L. and Hu, L.B. 2009. Fundamentals of dessication cracking of fine-grained soil : Experimental characterisation and mechanisms identification. Can Geotech. J. 46 : 1177-1201.

Pintado, X., Lloret, A. and Romero, E. 2009. Assessment of the use of vapour equilibrium technique in controlled-suction tests. Canadian Geotechnical Journal. Vol. 46 : 411-423.

Plötze, M., Kahr, G., Dohrmann, R. and Weber, H. P. 2007. Hydro-mechanical, geochemical and mineralogical characteristics of the bentonite buffer in a heater experiment: The HE-B Project at the Mont Terri Rock Laboratory – Elsevier, Physics and Chemistry of the Earth Vol. 32, : 730-740.

Pusch R. and Yong R. N. 2005. Microstructure of Smectite Clays and Engineering Performance (Spon Research) (1st Edition). Taylor and Francis, 1st Edition

Pusch, R., 1982. Mineral–water interactions and their influence on the physical behaviour of highly compacted Na bentonite. Canadian Geotechnical Journal Vol. 19, : 381–387.

Pusch R. 2008. Geological Storage of Highly Radioactive Waste Current Concepts and Plans for Radioactive Waste Disposal. Springer-Verlag Berlin Heidelberg.
Quirk, P. 1994. Interparticle forces: A basis for the interpretation of soil physical behaviour. Academic Press Inc.

Quirk, P. 2006. Nuclear Waste Management in Australia- Submission to the Uranium Mining, Processing and Nuclear Energy Review. Institute of Public Affairs.

Rahardjo, H. and Leong, E.C. 2006. Suction measurements. Proc. 4th Int. Conf. on Unsaturated Soils, Carefree, Arizona, Unsaturated Soils. Geotechnical Special Publication 147. G.A. Miller, C.E. Zapata, S.L. Houston and D.G. Fredlund (eds). ASCE, 1: 81–104.

Rao, S. M. and Sridharan, A. 1985. Mechanism controlling the volume change behaviour of kaolinite. Clays and clay minerals, Vol. 33, No. 4, : 323-328.

Rao, S.M. and Shivananda, P. 2005. Role of osmotic suction in Swelling of Salt-amended Clays. Can. Geotech. J. Vol 42, : 307-315.

Reeves, G. M. Sims, I. and Cripps, J. C. 2007. Clay Materials Used in Construction. Geological Society Engineering Geology Special Publications No. 21. Cromwell Press.

Ridley, A. M. and Burland, J. B. (1993). A new instrument for the measurement of soil moisture suction. Ge'otechnique 43, No. 2, : 321–324.

Roberts, J. D. and Caserio, M. C. 1965. Basic principles of organic chemistry, California: W. A. Benjamin, Inc.

Romero, E., 1999. Characterisation and thermo-hydro-mechanical behaviour of Unsaturated Boom Clay: An Experimental Study. PhD thesis, Universitat Polytecnica de Catalunya.

Ross, D.S. 1995. Recommended methods for determining soil cation exchange capacity. in recommended soil testing procedures for The Northeastern United States, 2nd Edition. Northeastern Northeastern Regional Publication No. 493. Agricultural Experiment Stations of Connecticut, Delaware, Maine, Maryland, Massachusetts, New Hampshire, New Jersey, New York, Pennsylvania, Rhode Island, Vermont, And West Virginia.

Rossi, A. M., Hirmas, D. R., Graham, R. C. and Sternberg, P. D. 2008. Bulk density determination by automated three-dimensional laser scanning. Soil Science Society of America Journal. Vol. 72, No. 6, : 1591-1593.

Rowe, R. K. Booker, J.R. and Quigley, R.M. 1997. Clayey barrier systems for waste disposal facilities. Taylor and Francis. 1st Edition.

Rowe R. K. 2005. Long-term performance of contaminant barrier systems. Ge'otechnique Vol. 55, No. 9, : 631–678.

Russell, E. R. and Mickle, J.L. (1970). Liquid limit values of soil moisture tension. Journal of Soil Mechanics and Foundations Division, ASCE., 96, : 967-987.

Saiyouri, N., Hicher, P. Y. and Tessier, D. 2000. Microstructural approach and transfer water modelling in highly compactedunsaturated swelling clays. Mech Cohes Frict Mater 5:41–60.

Saiyouri, N., Tessier, D. and Hicher, P.Y. 2004. Experimental study of swelling in unsaturated compacted clays. Clay Minerals Vol. 39: 469-479.

Salles, F., Beurroies, I., Bildstein, O., Jullien, M., Raylan, J., Denoyel, R., and Van Damme, H. 2008. A calorimetric study of mesoscopic and hydration sequence in solid Na-montmorillonite. Applied Clay Science. Vol. 39 : 186-201.

Sanchez, F. M. 2007. Water diffusion through compacted clays analyzed by neutron scattering and tracer experiments. PhD Thesis. University of Bern

Sato, T., Watanabe, T. and Otsuka, R. 1992. Effects of layer charge, charge location, and energy change on expansion properties of dioctahedral smectites. Clays and Clay Minerals, 40, : 103-113.

Schanz, T. 2007. Theoretical and Numerical Unsaturated Soil Mechanics. Springer.

Schanz, T. and Tripathy, S., 2009. Swelling pressure of a divalent-rich bentonite: diffuse double-layer theory revisited. Water Resources Research Vol. 45, No. 2.

Schiebe, F. R., Welch, N. H. and Cooper, L. R. 1985. Measurement of fine silt and clay size distribution. ASAE Vol. 26, No. 2, : 491-494.

Schofield, R.K. 1935. The pF of the water in soil. Transactions of 3rd Int. Congress of Soil Science, Vol. 2, Plenary Session Papers, Oxford, : 37–48.

Seetharam, S. C. 2003. An investigation of the thermo/hydro/chemical/mechanical behaviour of unsaturated soils. PhD thesis, Cardiff School of Engineering, UK.

Segad, M. Jonsson, Bo Akesson T and Cabane B 2010. Ca/Na Montmorillonite: Structure, Forces and Swelling Properties. Langmuir. Vol. 26, No. 8 : 5782–5790

Sharma, H., Reddy and K. 2004. Geo-Environmental Engineering, Site Remediation, Waste Containment, and Emerging Waste Management Technologies. Wiley.

Simunek, J. Van Genutchen, M.Th. and Sejna, M. 2008. Development and applications of the Hydrus and STANMOD software packages and related codes. Vadose Zone Journal. Vol. 7, No. 2 :. 587-600.

Singer, J.K., Anderson, J.B., Ledbetter, M.T., McCave, I.N., Jones, K.P.N., and Wright, R. 1988. An assessment of analytical techniques for the size analysis of fine-grained sediments. Journal of Sedimentary Petrology, v. 58, : 534–543.

Slager, S. and Koenigs, F.F.R. 1964. Particle Size Analysis of Soils by Means of a Torsion Balance and a Plummet. Sedimentology, 3 : 240-252.

Slatter, E. E., Jungnickel, C. A., Smith, D. W. and Allman, M. A. 2000. Investigation of suction generation in apparatus employing osmotic methods. Unsaturated Soils for Asia, : 297-302.

Soilmoisture Equipment Corporation. 2008a. 1600 5 bar ceramic plate extractor operating manual. Soilmoisture Equipment Corporation, Santa Barbara.

Soilmoisture Equipment Corporation. 2008b. 1250 volumetric pressure plate extractor and hysteresis attachments operating manual. Soilmoisture Equipment Corporation, Santa Barbara.

Spectrum® Laboratories. 2007. Spectra/por® 1, 2, 3, 4, 5, 6, and 7 regenerated cellulose (rc) dialysis membrane. Spectrum product instruction booklet. Spectrum Laboratories, Inc.

Spectrum® Laboratories. 2010. Pore size chart. See. http://www.spectrumlabs.com/dialysis /poresize .html

Sperazza, M., Moore, J.N. and Hendrix, M.S. 2004. High-Resolution Particle Size Analysis of Naturally Occurring Very Fine-Grained Sediment through Laser Diffractometry. Journal of Sedimentary Research, Vol. 74, No. 5, : 736–743.

Squire, P. G. 1985. Hydrodynamic characterization of random coil polymers by size exclusion chromatography. Methods Enzymol 117, 142-153Sposito, G., and Prost, R. 1982. Structure of water adsorbed on smectites. American Chemical Society. Vol. 82, No. 6 : 554-572

Sridharan, A., and Jayadeva, M. S. 1982. Double layer theory and compressibility of clays. Géotechnique, Vol. 32, No.2, 133–144.

Sridharan A., Sreepada Rao A. and Sivapullaiah P.V. 1986. Swelling pressure of clays. Geotechnical Testing Journal, Vol. 9, No. 1 : 24-33.

Stein, R. 1985. Rapid grain-size analyses of clay and silt fraction by Sedigraph 5000D: comparison with Coulter Counter and Atterberg methods. Journal of Sedimentary Petrology, Vol. 55, No. 4 : 590–615.

Tang A.M. and Cui Y.J. 2005. Controlling suction by the vapor equilibrium technique at different temperatures and its application in determining the water retention properties of MX80 clay, Canadian Geotechnical Journal, 42: 287-296.

Tarantino, A. and Mongiovi, L. 2000. A study of the efficiency of semi-permeable membranes in controlling soil matrix suction using the osmotic technique. Unsaturated Soils for Asia, : 303-308.

Tarantino, A., Gallipoli, D., Augarde, C.E., De Gennaro, V., Gomez, R., Laloui, L., Mancuso, C., McCloskey, G., Munoz, J., Pereira, J-M., Peron, H., Pisoni, G., Romero, E., Raveendiraraj, A., Rojas, J.C., Toll, D.G., Tombolato, S. and Wheeler, S. 2011. Benchmark of experimental techniques for measuring and controlling suction. Géotechnique Vol. 61, No. 4: 303–312.

Tchillingarian, G. 1952. Study of Dispersing Agents: Journal of Sedimentary Petrology, Vol. 22,: 229–233.

Terzaghi, K., R., Peck, B. and Mesri, G. 1996. Soil Mechanics in Engineering Practice. John Wiley and Sons, Inc., New York, 549 :

Tessier D., Dardaine M. and Beaumont. 1998. A. Swelling pressure and microstructure of an activated swelling clay with temperature. Clay Minerals, Vol. 33: 255-267.

Tinjum, J.M., Benson, C.H. and Blotz, L.R. 1997. Soil-water characteristic curves for compacted clays. Journal of Geotechnical and Geoenvironmenal Engineering Vol. 11, : 1060–1069.

Thomas, H. R. and He, Y. 1998. Modelling the behaviour of unsaturated soil using an elastoplastic constitutive model. Geotechnique Vol. 48, No. 5, : 339-350.

Thomas, H. R., Cleall, P. J., Chandler, N. A., Dixon, D. A. and Mitchell, H. P. 2003. Water infiltration into a large scale in-situ experiment in an underground research laboratory – physical measurements and numerical simulation. Geotechnique, Vol. 53, No. 2 :207-224.

Thu, T. M., Rahardjo, H., and Leong, E. C. 2007. Soil-water characteristic curve and consolidation behaviour for a compacted silt. Canadian Geotechnical Journal. Vol. 44 : 266-275.

Toll, D. 1995. A conceptual model for the drying and wetting of soil. In 1st International Conference on Unsaturated Soils. Paris

Tripathy, K.S., Subba Rao, K.S. and Fredlund, D.G. 2002. Water content – void ratio swell-shrink paths of compacted expensive soils. Can. Geotech. J. Vol. 39, : 938–959.

Tripathy, S., Sridharan, A., and Schanz, T. 2004. Swelling pressures of compacted bentonites from diffuse double layer theory. Can. Geotech. J. Vol. 41, 437-450.

Tripathy, S. and Schanz, T., 2007. Compressibilty behaviour of clays at large pressures. Canadian Geotechnical Journal 44, : 355–362.

Tuller, M., and D. Or. 2003. Hydraulic functions for swelling soils: Pore scale considerations. J. Hydrol. (Amsterdam) 272:50–71.

Vanapalli, S.K., Fredlund, D.G., Pufahl, D.E. and Clifton, A.W. 1996. Model for the Prediction of Shear Strength with Respect to Soil Suction. Can. Geotech. J. Vol. 33, : 379-392

Vanapalli, S.K., Fredlund, D.G., and Pufahl, D.E. 1998. Unsaturated shear strength behavior of compacted soils in drained and undrained loading conditions. Proceedings of the Second International Conference on Unsaturated Soils, August 27-30, 1998, Beijing, International Academic Publishers, Vol. 1, : 161-166.

Vanapalli, S.K., Fredlund, D.G. and Pufahl, D.E. 1999. The influence of soil structure and stress history on the soil-water characteristics of a compacted till. Geotechnique Vol. 49, No. 2, : 143–159.

van Olphen, H. 1962. Compaction of clay sediments in the range of molecular particle distances. symposium on clay mineral transformation. Clays and Clay Minerals. Vol. 11, No. 1 : 178-187.

van Olphen, H. 1977. An introduction to clay colloid chemistry: for clay technologists, geologists and soil scientists. Interscience, New York.

Verwey, E. J. W., and Overbeek, J. T. G. 1948. Theory of the stability of the lyophobic colloids. Amsterdam: Elsevier.

Villar M.V. 1999. Investigation of the behaviour of bentonite by means of suction-controlled oedometer tests. Engineering Geolology Vol. 54 : 67-73.

Villar, M.V. and Lloret, A. 2004. Influence of temperature on the hydro-mechanical behaviour of a compacted bentonite. Applied Clay Science. Vol. 26, : 337-350.

Villar, M.V. and Gómez-Espina, R. 2008. Effect of temperature on the water retention capacity of FEBEX and MX-80 bentonites, Unsaturated Soils, Advances in Geo-Engineering, London, UK

Vitton S.J., and Sadler L.Y. 1997. Particle Size Analysis of Soils using Laser Light Scattering and X-ray Absorption Technology. Geotechnical Testing Journal, Vol. 20, No 1, : 63-73.

Vitton, S.J., Ott, N.L. and Lehman, M.A. 1999. Automated soil particle-size analysis using x-ray absorption. in nondestructive and automated testing for soil and rock properties, ASTM STP 1350, W.A. Marr and C.E. Fairhurst, Eds., American Society of Testing and Materials, West Conshohocken, PA.

Walker, P. H. and Hutka, J. 1971. Use of the Coulter Counter (Model B) for particle-size analysis of soils. CSIRO, Division of Soils, Technical Paper No.1, 39 .

Walker, P. H., Woodyer, K. D. and Hutka, J. 1974. Particle-size measurements by Coulter Counter of very small deposits and low suspended sediment concentrations in streams. Journal of Sedimentary Petrology, 44, : 673–679.

Wan, A.W., Gray, M.N. and Graham, J. 1995. On the relations of Suction, Moisture Content, and Soil Structure in Compacted Clays. In: Proceedins of the 1st International Conference on Unsaturated Soils. Paris. A.A Balkema : 215-222.

Ward, W. H., Marsland, A. and Samuels, S. G. 1965. Properties of the London Clay at the Ashford Common Shaft: In-situ and undrained Shear Strength. Geotechnique. Vol. 33, : 141-150.

Warr, L. and J. Berger 2007. Hydration of bentonite in natural waters: Application of "confined volume" wet-cell X-ray diffractometry. Physics and Chemistry of the Earth. Vol. 32, No. 1-7 : 247-258.

Williams, J. and Shaykewich, C. F. 1969. An evaluation of polyethylene glycol (P.E.G.) 6000 and P.E.G. 20000 in the osmotic control of soil water matric potential. Can. J. Soil Science 102, No. 6,: 394-398.

Wroth, C.P., and Wood, D.M., 1978. The correlation of index properties with some basic engineering properties of soils, Canadian Geotechnical Journal, Vol, 15 No. 2, : 137-145.

Yahia-Aissa, M., Delage, P. and Cui, Y.J. 2001. Suction-water Relationship in Swelling Clays. In: Adachi, K., Fukue, M. (eds) Clay Science for Engineering, IS-Shizuoka International Symposium on Suction Transport in Soils. Elvesier, Amsterdam, : 327

Yang, N. and Barbour, S.L. 1992. The impact of soil structure and confining stress on the hydraulic conductivity of clays in brine environment. Canadian Geotechnical Journal, Vol. 29, : 730-739.

Ye, W. M., Cui, Y. J., Qian, L.X. and Chen, B. 2010. An experimental study of the water transfer through confined compacted GMZ bentonite. Engineering Geology Vol. 108, : 169-176.

Yong, R.N. and Warkentin B.P. 1966. Introduction to soil behaviour. The Macmillan Company, New York.

Yong, R.N. 2003. Influence of microstructural features on water, ion diffusion and transport in clay soils. Applied Clay Science. Vol. 23, : 3-13.

Zur, B. 1966. Osmotic control the matrix soil water potential: I. Soil-water System. Soil Science. Vol. 102 : 394-398.